NASA CONTRACTOR REPORT

NASA CR-1298

NASA CR-1298

SPACE GEODESY ALTIMETRY STUDY

by Myer Kolker and Ephraim Weiss

Prepared by
RAYTHEON COMPANY
Sudbury, Mass.
for

NATIONAL AERONAUTICS AND SPACE ADMINISTRATION • WASHINGTON, D. C. • MARCH 1969

NASA CR-1298

SPACE GEODESY ALTIMETRY STUDY

By Myer Kolker and Ephraim Weiss

Issued by Originator as Report No. R68-4459

Prepared under Contract No. NASw-1709 by
RAYTHEON COMPANY
Sudbury, Mass.

for

NATIONAL AERONAUTICS AND SPACE ADMINISTRATION

For sale by the Clearinghouse for Federal Scientific and Technical Information
Springfield, Virginia 22151 – CFSTI price $3.00

FOREWORD

This report contains the results of the Space Geodesy Altimetry Study awarded Raytheon Company under Contract No. NASW-1709 by the Geodetic Satellite Program Office, Office of Space Science and Applications, National Aeronautics and Space Administration. The study was conducted by the Space and Information Systems Division of Raytheon Company, under the direction of Myer Kolker as Program Manager with Ephraim Weiss as Technical Director.

Successful implementation of this effort was due largely to Jerome D. Rosenberg, Manager, Geodetic Satellite Programs, NASA, OSSA. Mr. Rosenberg provided the necessary guidance and direction during the study. Dr. Martin J. Swetnick, Chief Scientist, Geodetic Satellite Programs, and Geonautics, Inc. and C & S Inc. in their roles as support contractors to the Geodetic Satellite Programs Office, provided technical advice which contributed significantly to the project.

The primary objective of this study was to perform a tradeoff analysis of radar and laser space altimetry operating in the 1971-1972 time period over the sea surface for providing useful geodetic data.

ABSTRACT

A study was conducted by Raytheon Company, Space and Information Systems Division, for NASA/OSSA, to perform a tradeoff analysis of radar and laser space altimetry systems operating in the 1971-1972 time period over the sea surface for providing useful geodetic data.

User requirements in the field of geodesy are translated into altimetry performance requirements. These are used as requirement specifications for the design of a candidate laser altimeter system and a candidate radar altimeter system. A tradeoff analysis comparing the two candidate systems results in the selection of the candidate radar altimeter system.

ACKNOWLEDGEMENTS

Until recently, altimetry was principally the domain of the barometer. Then the absolute altimeter applied radar ranging devices to altimetry in order to assure terrain clearance. Satellite altimetry is indebted to the pioneers who recognized the measurement capabilities and potential of current technology, and who identified such rewarding applications as geodesy, navigation, and oceanography.

At the risk of committing the sin of omission, we note in particular the relevant contributions of Thomas W. Godbey, Willard J. Pierson, Jr., Elmer J. Frey, William S. von Arx, John V. Harrington, Richard K. Moore, Isadore Katz, and Charles A. Lundquist, and in most cases "et al," whose papers were sources of inspiration and basic reading in preparation for this study.

The multidiscipline requirements of this study were met by a diverse group of contributors.

The geodetic portion was conducted by S.W. Henriksen, of Raytheon's Autometric Operation, Alexandria, Virginia. F. Doyle consulted on and J.H. Tatsch contributed to the geodetic portion of the study.

The laser altimeter portion was performed by the Advanced Electro-Optical Techniques Section of Raytheon's Space and Information Systems Division, managed by A.V. Jelalian, who contributed with helpful discussion and preliminary work, including his experience on an earlier laser altimeter study. The laser altimeter portion was under the technical direction of G. van der Heide, with R.E. Seavey and D.A. Kawachi as chief contributors. W.S. Justice and Dr. W. Keene made significant contributions to the analysis and formation of the computer program regarding the centroid shift due to the sea state.

The radar altimeter portion of the study was conducted by J.D. Morris of the Radar and Communications Department of Raytheon's Space and Information Systems Division, who was also the principal contributor. D.K. Barton, of Raytheon's Equipment Division, Wayland, Mass. provided significant contributions to the radar study as a consultant and a direct contributor. Dr. J.V. Harrington, director of MIT's Center for Space Research, consulted on the design approach. D. Sharpe provided important assistance in the finalization of the radar study.

The systems analysis portion of the study, which consisted principally of the tradeoff analysis between the candidate laser and radar altimetry systems, was conducted by E. Weiss of the Systems Engineering Center of Raytheon's Space and Information Systems Division. J.H. Tatsch made significant contributions to that portion of the study.

Contributions to the study on sea surface effects were made by W. Halvorsen, W. Owen and Dr. H.W. Marsh, all of the Marine Research Department of Raytheon's Submarine Signal Division, New London, Connecticut.

E.F. Hudson maintained essential technical liaison with NASA and others interested in the program.

During the early period of the study, M. Kolker and J.H. Tatsch coordinated the technical activities, and unified the various disciplines to a common purpose. During the latter part of the study, M. Kolker and E. Weiss continued the technical coordination, and directed the technical efforts toward convergence in this final report.

This report was edited by E. Weiss with the capable assistance of J.H. Tatsch and was reviewed by M. Kolker.

CONTENTS

CONTENTS (CONTINUED)

CONTENTS (CONTINUED)

CONTENTS (CONTINUED)

CONTENTS (CONTINUED)

APPENDICES

APPENDICES (CONTINUED)

ILLUSTRATIONS

ILLUSTRATIONS (Continued)

TABLES

SPACE GEODESY ALTIMETRY STUDY

EXECUTIVE SUMMARY

The objective of this six month study was to perform a tradeoff analysis of radar and laser space altimetry operating from a satellite over the sea surface. Designed to provide useful geodetic data, principally measurement of the geoid or mean sea level, the study included:

- Derivation of the quantitative geodetic requirements for altimetry
- Analysis and design of candidate laser and radar altimeter systems
- A tradeoff analysis for selection of the altimeter best qualified to meet the geodetic requirements.

The assumptions included flight capabilities for the time period 1971 - 1972 and an altitude of approximately 1,000 km (540 nmi).

GEODETIC REQUIREMENTS

The geodetic portion of the study examined user requirements; established user needs for oceanography, geodesy, undersea geology, and military applications; and translated them into altimeter performance requirements. This involved examination of the physical nature of the sea surface, the purpose of the user requirements, and the altimetry procedures required to obtain the desired data. Geodetic procedures and data processing were examined to clarify the role of the altimeter in satisfying the requirements.

The altimeter performance requirements generated in this study were for rms error in the range of 0.1 to 7 meters, and measurement densities ranging from 0.1 to 200 measurements per 10,000 km^2. These were used as design objectives for the laser and radar altimeters, and as the principal performance criteria in the tradeoff analysis.

LASER ALTIMETER

The candidate laser altimeter system uses the time interval between transmission and reception of a short duration light pulse from a ruby laser (visible; 6943 Angstroms) to compute the range between the satellite and the sea surface. The transmitter and receiver share the same optics through the use of an optical transmit-receive switch. A range clock is started by the transmitter and stopped when the echo is received. The power centroids of both output and input pulses are detected for precision ranging. A passive cloud sensor is proposed to control operation over cloud cover. The candidate laser system design specifications were established.

RADAR ALTIMETER

The candidate radar altimeter system measures the time interval between the transmission and reception of electromagnetic radiation. The altimeter transmits a train of pulses of radiation at X-band (10 ~~MHz~~ GHz frequency, and compares the return time of the signals reflected from the sea surface with a timing reference controlled by the pulse repetition frequency. The difference between the two is used as an error signal to modify the pulse repetition frequency, which is a measure of the altitude. The center of the leading slope of the radar pulse return is identified and timed for precision ranging. The candidate radar system design specifications were established.

TRADEOFF ANALYSIS

A tradeoff analysis compared the capabilities of the candidate radar and laser altimeter systems to meet the altimeter performance requirements as generated in the geodetic portion of this study. Twenty-three explicit evaluation criteria were established. Quantitative weighting factors were assigned to each for scoring. The complete methodology is presented to permit independent evaluation of the study conclusion.

CONCLUSIONS

The study substantiates that satellite altimeter technology is capable of providing better than 1 meter accuracy for useful geodetic data. Both radar and laser technologies offer promise of meeting ultimate required accuracy in tenths of meters. A radar altimeter system is better able to meet geodetic requirements than a laser altimeter system.

The radar altimeter is selected for the following principal considerations:

- Pointing Data - The laser altimeter system requires very accurate knowledge of attitude (pointing angle), while the radar does not.
- Data Rate - The radar system measurement rate is ten times that of the laser system.
- Accuracy (Data Processing) - The radar altimeter system performs better spatial averaging of the sea surface, and better time averaging over a large number of ranging pulses.
- Volume - The laser system occupies several times the volume of the radar system.
- Weight - The laser altimeter system weighs significantly more than the radar altimeter system.

RECOMMENDATIONS

- Space altimetry should be developed to define the geoid in ocean areas, to support the needs of geodesy, oceanography, submarine geology, and the military.
- Space altimetry development programs should give priority to radar systems, which are better able to meet geodetic requirements than laser systems.

- Experimental programs (aircraft, space) should be implemented to develop the altimeter technology.
- A thorough quantitative space verification experiment design should be developed for the first orbital demonstration of the radar altimeter.
- A continuing program of study, experimentation, and hardware development should be maintained for both radar and laser altimetry in order to achieve an ultimate reliable accuracy of 0.1 meters required by the user with the most stringent requirements of geodesy.
- Ocean impulse response (signature) and reflectivity data should be obtained which are applicable to both radar and laser altimetry, under various sea states and as functions of other parameters.
- Additional study should be conducted to determine the suitability of multi-mission altimetry for simultaneously measuring other phenomena of importance, such as sea state, cloud profile, and atmospheric water content.
- A radar pulse compression study should be added to enhance the scope and depth of this study.
- Space altimetry development programs should monitor the rapid developments in laser research and technology, and assess their implications for satellite altimetry.

SECTION 1

SUMMARY

SECTION 1

SUMMARY

(M. Kolker/E. Weiss)

1.1 STUDY OBJECTIVES

The primary objective of this study was to perform a tradeoff analysis of radar and laser space altimetry operating over the sea surface for providing useful geodetic data; i.e., principally measurement of the geoid or mean sea level. The major work effort concentrated on this primary objective. The major areas of study included the derivation of specific quantitative performance geodetic requirements for altimetry, consideration of the effects of the various ocean surface conditions as a reflective target to altimeter electromagnetic energy, analysis of both radar and laser type altimeter systems, and their tradeoff analysis.

1.2 INITIAL STUDY ASSUMPTIONS

The following initial assumptions were used in connection with the study:

a. Flight capabilities assumed for the approximate time period 1971-1972.

b. Approximate altitude of spacecraft: 500 - 800 n miles.

c. The fundamental mission of geodesy is to measure mean sea level, not to measure ocean sea state conditions. Although the results of this study may be useful to oceanographic sea state research, the primary purpose of the study concerns the specific area of satellite geodesy altimetry related to mean sea level or geoid.

d. No specific mission was defined; e.g., unmanned and manned spacecraft could be considered.

e. The specific geodetic requirements were defined by Raytheon with NASA concurrence. Agreement on these were achieved during the Initial NASA Review.

1.3 ORGANIZATION OF THE STUDY

The general organization of the study is shown in Figure 1-1. The geodesy portion examined user requirements in the field of geodesy, and translated these into altimeter performance requirements, which are a set of specifications to which the altimeter must be designed. The laser and radar specialists designed their respective candidate altimeter systems to meet the altimeter performance requirements, and received inputs on sea surface effects to assist in their tasks. The candidate laser altimeter system and the candidate radar altimeter system were compared in their ability to meet the altimeter performance requirements; the comparison was performed in a tradeoff analysis, which resulted in the selection of the system judged best qualified to meet the altimeter performance requirements.

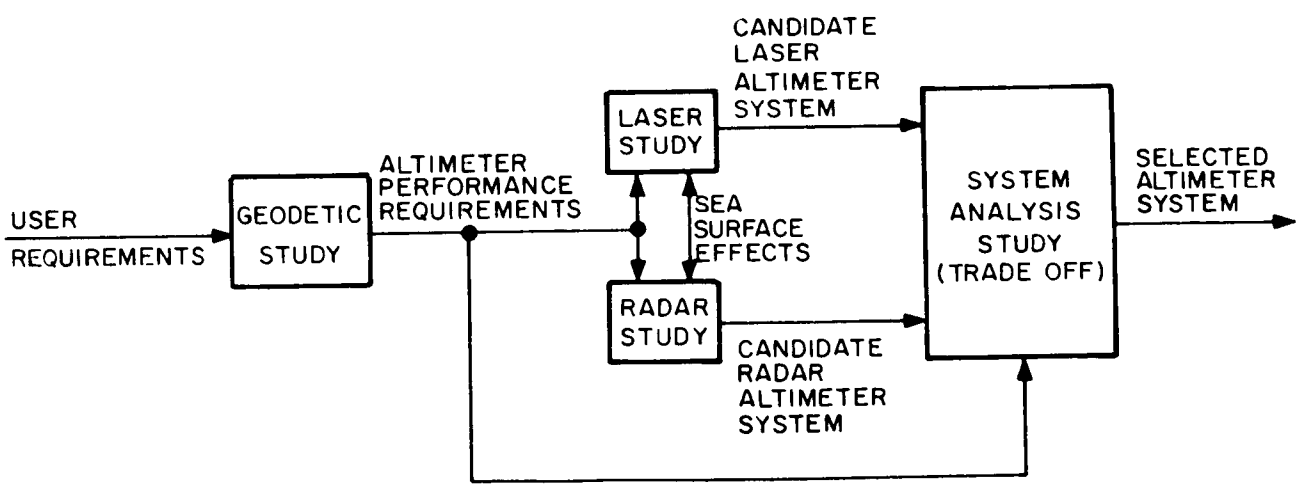

Figure 1-1 Space Geodesdy Altimetry Study Organization

The candidate systems were not completely optimized, but were primarily designed for basic feasibility. The altimeter system design specifications should therefore not be taken literally, since any given parameter could be modified to some extent; this, of course, would affect other system parameters, and perhaps system performance.

Finally, the tradeoff study was performed by comparing the two candidate systems with performance criteria.

1.4 STUDY RESULTS

1.4.1 GEODETIC STUDY

The geodetic portion of the study examined the user requirements (on geodesy), and translated these into altimeter performance requirements (from geodesy). This involved examination of the physical nature and purpose of the requirements, as well as the altimetry procedures necessary to obtain the required data. Geodetic procedures and data conversion and processing were examined in order to clarify the role of the altimeter in satisfying the geodetic requirements.

The altimeter performance requirements generated in this study are summarized in Table 1-1; they were used as the design objectives for the laser and radar portions of this study, and as part of the performance base used in the tradeoff analysis.

1.4.2 LASER STUDY

Figure 1-2 shows the main elements in the laser altimeter system, with the electrical connections drawn in solid lines and the optical paths drawn as dashed lines. The system design specifications are given in Table 1-2. Basically, the system uses the time interval between transmission and reception of a short duration light pulse from a ruby laser to compute the range between the space vehicle and the earth. The transmitter and receiver share the same optics by the use of an optical transmit-receive switch. A range clock is started by the transmitter and stopped when the echo pulse is received. The power centroids

TABLE 1-1

MEASUREMENT DENSITY AND RMS ERROR

Requirement Source	RMS ERROR (m) in Height		Number of Measurements per 10,000 km^2	
	Above Sea	Above Spheroid	w/o Tides	w/ Tides
Mean Sea Level (msl) (Oceanographic)	0.3	0.3	2	4
Submarine Geology				
Static	1	1	200	200
Dynamic	-	-	200	200
Military				
Geometry	7	7	10	20
Gravity	-	-	--	--
Geodesy				
Datum Establishment	1.5	1.5	200	200
Geoid Connection	0.1	0.1	10	20
Geoid Extension	0.5-2	0.5-2	0.1-1	1 - 5

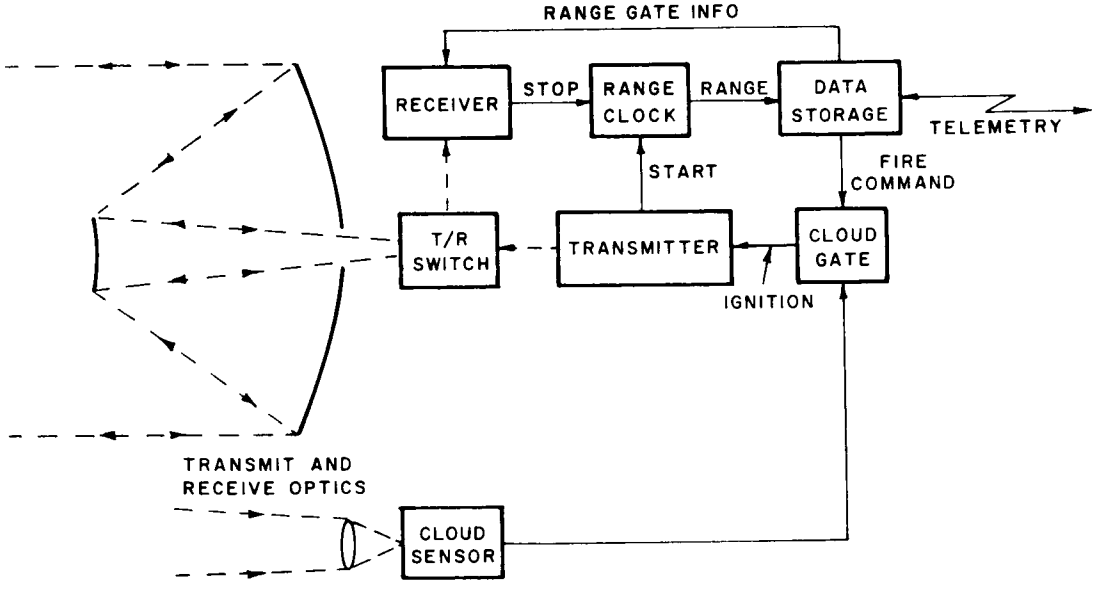

Figure 1-2 System Block Diagram

TABLE 1-2

CANDIDATE LASER ALTIMETER SYSTEM DESIGN SPECIFICATIONS

System weight	33 kg (72 lb)
System volume	74,000 cm^3 (2.6 ft^3)
System power consumption	75 W
Wavelength	6943 Å
Output Energy	500 millijoules
Pulsewidth	<12 ns
Optics diameter	50 cm
Optical filter bandwidth	20 Å
Quantum efficiency of detector	0.12
Computer clock frequency	500 MHz
Transmitter beamwidth	200 microradians (40 arc sec)
Receiver F.O.V.	350 microradians (70 arc sec)
Range gate width	3 μs
Cooling system	Active (liquid)
Electronic bandwidth	50 MHz
Altitude error (accuracy)	<50 cm
Pulse repetition rate	6 per minute
Orbital altitude	1000 km
Total number of pulses	1.6 million
Mission duration	1 year

of both output and input pulses are detected for precision ranging. A cloud gate prevents ignition of the laser if the cloud sensor indicates that clouds obscure the line of sight to the earth surface.

1.4.3 RADAR STUDY

The candidate radar altimeter system is fundamentally a ranging device, which measures the time interval between the transmission and reception of electromagnetic radiation. A block diagram of the system is shown in Figure 1-3, and the system design specifications are given in Table 1-3. The radar altimeter system transmits a train of pulses of radiation at X-band frequency, and compares the return time of the signals reflected from the Earth with a timing reference controlled by the pulse repetition frequency. The difference between the two is used as an error signal to modify the pulse repetition frequency, which is then a measure of the range, or altitude. The center of the leading slope of the radar pulse return is identified and timed for precision ranging. The optional radiometer can be used to reduce refractivity errors.

1.4.4 SYSTEM ANALYSIS STUDY (TRADEOFF)

The system analysis portion of this study consisted mostly of performing a tradeoff analysis between the candidate altimeter systems. For this purpose, the candidate radar and laser altimeter systems, as specified in Figures 1-2 and 1-3 and in Tables 1-2 and 1-3, were compared with each other in their ability to meet the altimeter performance requirements, as generated in the geodetic portion of this study. For purposes of comparison, a set of evaluation criteria was generated, as enumerated in Table 1-4. These were assigned weighting factors for purposes of scoring. Accuracy and data rate were assigned the greatest weights.

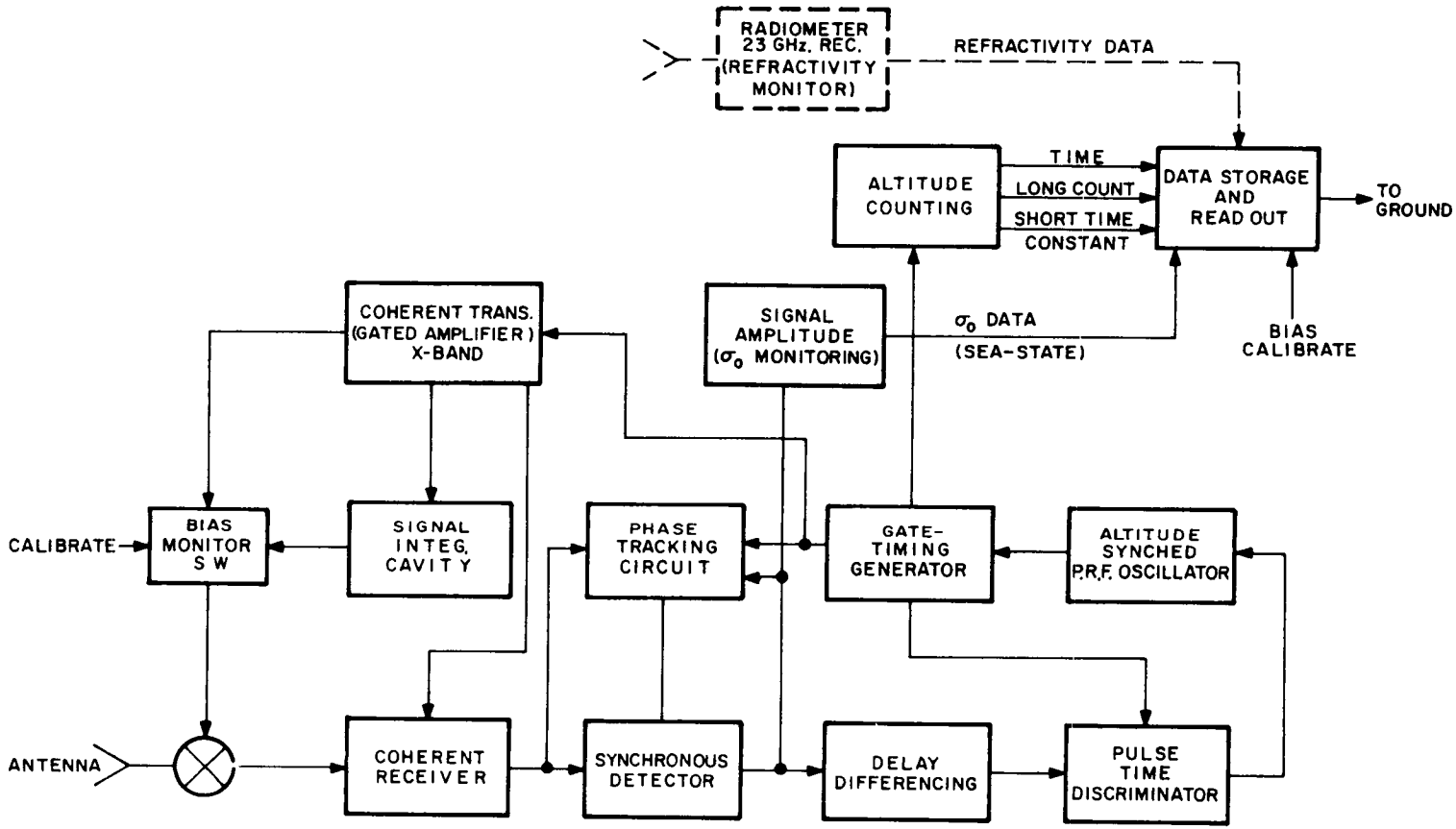

Figure 1-3 Radar Altimeter Block Diagram

TABLE 1-3

CANDIDATE RADAR ALTIMETER SYSTEM DESIGN SPECIFICATIONS

System	
Source Power Required	200 watts dc (see Note below)
Overall System Weight	20 kg (45 lb)
Overall System Volume	10,000 cm^3 (.35 ft^3)
Accuracy	<50 cm
Attitude Stabilization Accuracy	$\pm .3^o$
Antenna	
Diameter	.75 meters (2.5 ft)
Thickness	≈ 1 cm
Aperture Shape	Circular
Aperture Illumination	Uniform
Type	Slotted Array
Beamwidth	2.3^o (40 milliradians)
Gain	38 dB
Weight	2 kg (est.)
Antenna Pattern	$\sin \theta/\theta$
Sidelobe Level	13 dB
Transmitter	
Type	Coherent, Gated Amplifier
Frequency	X-band
Pulse Peak Power	1 kW
Pulse Length	50 ns
Pulse Rise and Fall Times	10 ns
Pulse Repetition Frequency	100 kHz (at 1000 km - altitude dependent)
Receiver	
Noise Figure	8 dB (conservatively)
Bandwidth	20 MHz
Bandpass Characteristic	Synchronous Single Tuned
Receiver Delay	150 ns
Detector	Coherent Synchronous

TABLE 1-3 (Continued)

Processor	
Type	Two-Stage Delay Differencing
Processor Delay	75 ns
Output Waveform	Ramp Doublet (ideal)
Timing Sensor	Pulse-Time Discriminator
Altitude Tracking Circuit	
Type	Phase (altitude) Locked prf Oscillator
Tracking Bandwidth	.157 Hz
Tracking Time Constant	1 second
Altitude Counting Circuit	
Type	Digital Frequency Meter (prf count)
Reference Oscillator Stability	10^{-8}
Reference Oscillator Frequency	10 MHz
Data Storage	Remarks
Altitude Counts	
Time Signals	
Temperature	(Diagnostics)
Voltage	(Diagnostics)
Signal Strength	(Sea-State Indication)
Bias Delay Altitude	(Bias Error Correction)
Radiometer Signal	(Refractivity Correction)
Estimated Stored Data Rate	350 Kilobits per hour

Note: This power rating assumes an overall altimeter system power efficiency of 2.5%, which is conservative. Five percent efficiency (100 W Source Power) is probably achievable, and 10% efficiency (50 W Source Power) has been proposed as achievable. Power rating may also be reduced by other design modifications, such as increasing antenna diameter (see Appendix R-M).

TABLE 1-4

WEIGHTING FACTORS FOR THE EVALUATION CRITERIA

Criterion	Weighting Factor
1. Accuracy	35
2. Data Rate	15
3. Power	4
4. Weight	3
5. Volume	2
6. Life	8
a. Shelf (1) b. Standby (2) c. Operating (5)	
7. Availability	3
8. Performance Potential	3
a. Theoretical (2) b. Probable (1)	
9. Other Capabilities	3
10. Environmental	4
a. Transmission (2) b. Target (2)	
11. Safety	2
12. Calibration	1
13. Requirements on Satellite	17
a. Pointing Angle (2) b. Attitude Data (9) c. Angular Rate (1) d. Thermal (2) e. Telemetry (1) f. Storage (1) g. Supplementary (1)	
	100

The system study indicates:

a. Both candidate altimeter systems are capable of providing useful geodetic data (such as accuracy of 0.5 meters).

b. Neither candidate system is yet capable of meeting all the geodetic requirements (such as 0.1 meter accuracy).

c. The candidate radar altimeter system is better able to meet geodetic requirements than the candidate laser altimeter system.

1.5 STUDY CONCLUSIONS

The tradeoff analysis indicates that the candidate radar altimeter system has a substantially greater prospect of meeting geodetic requirements than does the candidate laser altimeter system; therefore the conclusion of this study is the selection of the radar altimeter.

The principal considerations which enter into this decision are as follows:

a. Pointing data - The laser altimeter system requires knowledge of attitude (pointing angle) to within 10 arc seconds, while the radar altimeter system does not require any attitude information over the same range of attitude angle.

b. Data rate - The radar system data rate is ten times that of the laser system.

c. Accuracy (Data processing) - The radar altimeter system footprint (ground spot size) is about 2500 times the area of the laser altimeter system footprint, resulting in better spatial averaging of sea surface conditions. The radar system also averages about 10^5 pulses (per second) to provide a time average, while the laser system observes one pulse per datum point.

d. Volume - The laser system occupies more than seven times the volume of the radar system; pointing data hardware further increases the ratio.

e. Weight - The laser altimeter system weighs about 1.6 times that of the radar altimeter system; pointing data hardware further increases the ratio.

The differences between the current capabilities of the radar and laser systems may reflect the impact of the large technological investment in microwave electronics during the past several decades vs. the relatively brief development life of laser technology. With laser research and technology evolving at its current rapid rate, significant breakthroughs can be expected. Their implications for satellite altimetry can be determined by monitoring the field, and updating the critical parts of this study.

1.6 STUDY RECOMMENDATIONS

- Space altimetry should be developed to define the geoid in ocean areas, to support the needs of geodesy, oceanography, submarine geology, and the military.
- Space altimetry development programs should give priority to radar systems, which are better able to meet geodetic requirements than laser systems.
- Experimental programs (aircraft, space) should be implemented to develop the altimeter technology.
- A thorough quantitative space verification experiment design should be developed for the first orbital demonstration of the radar altimeter.
- A continuing program of study, experimentation, and hardware development should be maintained for both radar and laser altimetry in order to achieve an ultimate reliable accuracy of 0.1 meters required by the user with the most stringent requirements of geodesy.

- Ocean impulse response (signature) and reflectivity data should be obtained which are applicable to both radar and laser altimetry, under various sea states and as functions of other parameters.
- Additional study should be conducted to determine the suitability of multi-mission altimetry for simultaneously measuring other phenomena of importance, such as sea state, cloud profile, and atmospheric water content.
- A radar pulse compression study should be added to enhance the scope and depth of this study.
- Space altimetry development programs should monitor the rapid developments in laser research and technology, and assess their implications for satellite altimetry.

SECTION 2

GEODETIC REQUIREMENTS

SECTION 2

GEODETIC REQUIREMENTS

(S. W. Henriksen)

2.1 THE ROLE OF GEODESY IN SATELLITE ALTIMETRY

It might seem at first glance as if we should be discussing the role of satellite altimetry in geodesy, since the subject of the study is geodetic requirements for altimetry. Like most first glances, this would give only a partial, and therefore wrong, view of the situation. Altimetry from a satellite has uses in many other fields than geodesy, and especially in ocean areas where altimetry at present gives its best results. Many looks at satellite altimetry from the viewpoints of many different disciplines are needed to give the full perspective and dimensions of the altimeter's role in general. Geodesy is certainly a potential major user of altimetry; at the same time geodesy will not be using the altimetric results for itself but, after dressing them up in geodetic trappings, will hand them over to others for ultimate application.

Geodesy's first role in satellite altimetry is that of a middle man. The orbital height (from tracking data) and the surface depth (from altimetry readings) are combined to give a smoothed section of the surface - a section that, because it is wound over a spherical surface, can be made to run as closely as desired alongside itself and to intersect with itself. In this way the surface eventually is built up from the sections. Once geodesy has constructed the surface from the altimeter samplings it has done its job and hands the surface over to those who will interpret it, correlate it with other data, etc. This role is not very romantic; nor is it satisfying if one wants to stay with the derived surface until all possible use is made. It is very important, however; and it is the geodesist who is uniquely skilled in the best construction of such surfaces.

The second role of geodesy actually precedes in appearance that already discussed. This is to assist in planning the experiment so that the most users will get the best surface for their use. As intermediary between the measurements on the natural surface and the resulting idealization of it, he is in the best position to specify the measurement parameters so that they will yield best surfaces after reduction of the data.

This portion of the study concentrates mainly on the second role of geodesy. It discusses the various disciplines and technologies that have a use for information about the surface of the earth and it looks at the ways that the surface is used. Each way of using the surface leads to different specifications on how accurately it needs to be given and where. These specifications are called requirements on geodesy or user requirements. After interpreting the user's requirements into geodetic terms, geodesy converts them into specifications on when, where, and with what accuracy the altimeter and tracking measurements must be made. These specifications are called requirements from geodesy, instrument specifications, design specifications, etc.

The first role, that of actually constructing an ideal surface from measurements on the real one, cannot be ignored even though we concentrate on the planning role. The way in which the measurements are handled is not arbitrary but is set by many factors such as computational facility characteristics, stage of development of geodetic and astronomic theory, etc., as well as by the nature of the measurements that come in their accuracy, distribution, and frequency. The two roles are therefore related, and a study of one requires attention to the other. Space is therefore given to discussion of data-reduction procedures.

2.2 DEFINITIONS

When people get together for discussion, things go more smoothly if they speak the same language. Even if they start by agreeing to use English, this does not guarantee a common understanding because one

word often has several meanings or may have no meaning at all. It seems best therefore to start by defining the meanings of some words which will be frequently used in what follows and which have acquired imprecise or varied meanings.

2.2.1 REQUIREMENTS

A requirement is defined to be a set of numbers which (1) relates to physical quantities, (2) specifies the allowable range of variation of these quantities, and (3) without which a particular project cannot be correctly carried out. The questions of how important the project may be, how many people support or attack it, how much money is invested in it, etc., are not properly a subject of this study. Nevertheless, some selection of projects has had to be done to avoid losing, among a flood of minor or one-man projects, those projects which are obviously needed. The criteria used in this selection are believed to be reasonable and not severe. They are primarily based on the amount of work that has been put into getting (but by other means) results similar to those provided by the altimeter.

Two different kinds of requirements are recognized. The first kind consists of requirements stated by a non-geodesist as being necessary for doing a particular job. The requirements may or may not be in terms of geodetic quantities; for example, an oceanographer may say that he needs to know the sea height as a function of time to a certain accuracy, or the spacecraft tracker may say that he needs the relative positions of his tracking stations to a certain accuracy. These requirements are called requirements on geodesy, or user (of the altimetric data) requirements. They are levied on the geodesist. He translates them into geodetic language, computes those altimeter characteristics that must be satisfied to meet the user's requirements, and formulates the computation results as requirements from geodesy onto the altimeter designer. These requirements are called performance specifications by the designer and form part of the set of constraints imposed on his design.

2.2.2 DEFINITIONS RELATING TO THE HONESTY OF THE EXPERIMENT

No matter how honest the experimenter may be, nature has a way of presenting her handiwork that can cause him to misinterpret his measurements or to make them improperly in the first place unless he is always careful in his attitude toward the experiment and its results. A number of terms have come into use for describing the way the experimenter relates his measurements to what nature really presents. The more important are mentioned here.

2.2.2.1 Accuracy, Precision, and Error

Accuracy is a numerical indication of how close a measurement or description of a phenomenon comes to the actual value of the phenomenon. The higher the accuracy, the closer the match.

Precision, like accuracy, is a numerical indication of how close a measurement or description comes to some other numerical value. Unlike accuracy, however, this other numerical value is not necessarily the actual value but may be any other arbitrarily chosen number. The one selected is usually some kind of average of the measurements themselves. This has the disadvantage that it will change as the number of measurements increases, but it has the tremendous advantage that the precision can be depended on to increase in almost all cases. Since accuracy values are obtainable very much less often than precision values, and since the goodness of a set of measurements is usually based on one or the other, the advantages of using a number that is sure to improve are obvious.

The error of a measurement is the difference between the measurement and some other number - preferably the true value of the object of the measurement, but otherwise a number which has a high probability of making the error small.

2.2.2.2 Calibration, Testing

Calibration is defined to be that set of procedures in which instrument readings are compared with known and presumably correct values to get a set of numbers which are to be used for correcting all other subsequent instrument readings. Testing is defined to be that set of procedures in which corrected instrument readings (readings from a calibrated instrument) are compared with known and presumably correct values other than those used in calibration to get a set of numbers on the basis of which the instrument's performance is judged.

The distinction between calibration and testing is important not only to make sure that all people involved talk the same language, but also to make certain that when the instrument is being critically evaluated, it will be done on the basis of test results and not on the basis of calibration results. Deliberate falsification of test results is very rare; unintentional use of test results for calibration (and vice versa) is not rare. Such confusion misleads the user into thinking that his instrument has a higher accuracy than it actually has.

2.2.3 SURFACES

The aim of geodesists is to provide, for people who can use them, distances and directions between points on the earth's surface. Since 71 percent of the surface iw water and therefore changing at a rate much more rapid than the geodesists' tools can measure it, extension of the geodetic domain from land into the oceans requires either adoption of new techniques or redefinition of the aims. For present purposes, we shall resolve the difficulty by making the geodesist responsible for (1) positions on the earth's solid surface and (2) for the average position of the water surface.

2.2.3.1 Geon

The solid surface of the earth, including that portion underlying the seas and oceans (with one reservation) is a geon. The small size of man (about 2 meters) compared to the depths of the seas and oceans (5000-6000 meters or more), and the vast areas covered by water, gives him a disproportionate idea of the relation between the oceans and the earth as a whole. In fact, the oceans are no more than a thin sweat covering the low portions of the geon.

One condition that could be placed in the definition of the geon would be that it should not vary because of the gravitational attraction of the sun, moon, etc. Tidal variation would allow the geon and geoid (see following) to be compared directly, since the geoid by definition does not have tidal variations; by doing this we would lose more than we would gain. Tidal movements in the solid earth have been precisely measured in only a few places. Most hypotheses agree that the movements, amounting to 10 - 20 cm, should be about the same everywhere, but this is not an experimental fact. Furthermore, there are solid earth movements of a few centimeters amplitude which are not tidal but are caused by tidal motion. One such movement is the tilt of coastal areas caused by the rising and ebbing of tidal waters. Hence we would have a theoretically convenient definition of the geon but could never locate the geon except in those localities where earth tidal movements were known.

2.2.3.2 Geoid

The geoid is an equipotential surface passing through a defined point usually chosen near msl* The United States geoid, for example, has in the past been given the height of 10 meters at Calais, Maine. If the only forces acting on water were the earth's gravitation and the force arising from the earth's rotation, the connected ocean surfaces would be a single equipotential surface. Passing the geoid through any point at the edge of an ocean would make the geoid fit like shrunken levis over the entire ocean surface. (This is almost true, but not

* mean sea level

quite. If only gravitational and centrifugal forces acted on a water surface and the surface were not already an equipotential surface, water would begin flowing downhill to discard the differences from an equipotential surface. But this flow, in the absence of dissipative forces, would not die out, and the rotation of the earth would eventually convert these flows into currents that piled the water above the geoid at one edge and below it at the other. Dissipation forces would eventually destroy these currents and get everything back to the geoid.)

In an ideal case, where the water was at rest under gravitational and centrifugal forces only, the geoid would be defined in an operational sense everywhere over the ocean surfaces (by operationally defined we mean locatable). Even if the water should be in motion, the geoid might be definable to within a given confidence limit by averaging the motion over a long period of time. This possibility exists only if all water surface motion is a motion above and below the geoid, such that the weighted average of positions is the geoid or the law of motion is known; otherwise the geoid can only approximately be found except at the point of definition.

On land, of course, the geoid cannot be found physically where it lies within the land mass. A surface close to the geoid can be operationally defined on land by stating how it is derived from survey data. This close surface, a quasi-geoid, cannot usually be rigorously demonstrated to be either the geoid or an equipotential surface, but only to be acceptably close to either. It should be obvious from the above that unless the same datum point is used for defining all geoids, these geoids will not coincide except in the zero probability case that the datum points lie on the same equipotential surface. This difficulty could be removed in theory by defining the geoid, not as an equipotential surface through a point, but as an equipotential surface having a certain absolute potential (that surface for which the work needed to move a 1 kg body off to infinity is a given defined amount). Unfortunately it is also obvious that such a definition would introduce more difficulty than it discarded.

2.2.3.3 Mean Sea Level

Water surfaces change position for many reasons i.e., wind, air pressure, earthquakes, temperature changes, etc. The geodesist, looking for a reference surface from which land heights could be measured, adopted the average height of the ocean surface in coastal areas as defining segments of his reference surface. This is not the place in which to discuss the many implications of this choice; it is enough to note that this reference surface, commonly referred to as msl, is almost completely geodetic in concept and use. The oceanographer has little use for the msl of the geodesist. What he is interested in is the deviation of sea surface and sea surface averages of various kinds from the geoid. The geographer is interested in the sea surface as a dynamic object in identifying and assigning measure to the causes of its variation. In satisfying this interest he uses a number of different averages over both time and area.

The geodesist would like to define mean sea level (msl) in such a way that (1) it coincides with the geoid and (2) it is the average of sea level measurements. For many years the ignorant geodesist thought that if average were properly defined, (2) implied (1); hence he was able to define the geoid as a surface coincident with msl over the open ocean. While the surface of stationary water comes close to conforming to an equipotential surface, the surface of moving water can be highly non-conforming. Water moves in the oceans in vast masses both horizontally and vertically as currents. These motions, compounded with the rotation of the earth and maintained by temperature, pressure, and other influences we know little of, make water run uphill and stay that way for very long periods of time. This piling up tilts the surface away from the geoid.

Another influence making the ocean surface different from the geoid is air pressure. Air pressure works in two ways. The first is where the air is more or less stationary but resting with greater pressure on one area of water than on the surrounding area. This has exactly the same effect as putting an invisible plunger into the water; the water follows the contour of the bottom of the plunger. The second way, perhaps not really too different from the first, is for the wind to blow steadily across the surface of the water, piling up the water.

There are other agencies working to displace the water; as long as their effect does not change during the time over which msl is measured, their average effect will be one way only and will not average to zero. In every case water is moved from its ideal position of rest on an equipotential surface and piled up elsewhere, and the msl then includes the pile up.

In Table 2-1 are given some of the more important causes of secular and long period variation in msl, together with their amplitudes and rates. Figure 2-1 shows the total variation in mean sea level. It cannot be too strongly emphasized that most of the data are not experimental but are based on deductions from related fields, theory, and so on. The vertical bars in Figure 2-1 incicate the range of values that have been found for msl.

2.2.3.4 Summary

Geon is the instantaneous surface of the solid earth, including that portion under water. Its determination is the primary objective of geodesy. In this paper it is assumed that tidal vaiations, ets., have not been removed.

Geoid is that equipotential surface which passes through and identifiable point on (or in) the earth and which is the direct result only of the gravitational attraction of the earth and of the earth's rotation. Since water normally flows downhill, and since the geoid datum point is ususally chosen at the coast near msl, a non-moving ocean water surface lies close to the geoid.

Mean sea level is the time-average position of the ocean surface. There are as many different msl's as there are ways of specifying time-average. To the geodesist, however, msl implies that the average is taken is such a way that all periodic and random variations arising from non-terrestrial attraction, meteorlogical factors, and transient disturbances are removed. As an operational (factual) definition, however, msl at a point is the average position on the vertical at that point of water level during the interval over which measurements are made.

2.2.4 DATUM

A datum is a set of numbers completely and uniquely relating a geodetic coordinate system to the surface of the earth.

The position of a rigid body in a coordinate system is completely specified by six numbers - three for specifying the coordinates of a point within the body and three for specifying the rotation of a set of three axes within the body. These would be sufficient for a datum if coordinates were given in a tri-axial coordinate system. Geodetic coordinates, however, are given with respect to the surface of an ellipsoid whose center is the origin and whose axes are the system axes. Three more numbers are needed therefore to specify the lengths of the ellipsoid axes (or only two or one more if two or three of the axes are equal). The datum point is that point on the earth whose coordinates are specified.

These definitions apply ideally. In real life, the datum may be incompletely specified, over-specified, specified by definition of two coordinates at one point and the third (usually height above the ellipsoid) at another, etc. In the past these faults in specifying his datum have not bothered the geodesist as much as have the faults introduced into his networks by inaccurate surveying. We are now coming to the stage where survey errors are no longer large enough to cover up the errors made by the geodesist in defining his coordinate system. Precise definition of datums and datum points is at last becoming necessary.

TABLE 2-1

LONG-TERM AND SECULAR CHANGES IN MEAN SEA LEVEL[15,16,17]

Cause	Amplitude (Meters)	Rate (m/yr)
Tide (nodal)	0.0004	4×10^{-5}
Tide (solar semi-annual)	0.03	2.5×10^{-1} **
Static Air Pressure	2	< 2 *
Land Rise	- - - -	1×10^{-3}
Glacier Formation in Plcistocene (***)	-200	1×10^{-3}
Glacier Melting in Pleistocene	+120	8×10^{-3}
Water Loss (permanent)	-25000	- - - -

* Difficult to separate seasonal and secular variations.

** Period of 0.25 year, approximately.

*** Pleistocene: first epoch of Quaternary period of Cenozoic era, characterized by the rise and recession of continental ice sheets and by the first known appearance of man. Roughly 1 million years ago.

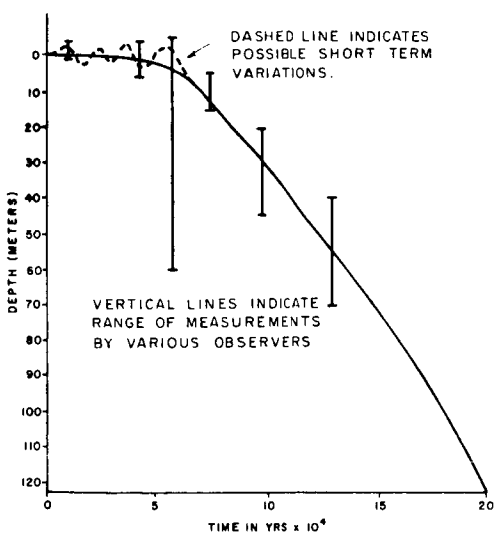

Figure 2-1 Recent Variations in Mean Sea Level[18]

2.2.5 SAMPLE RATE AND SAMPLE DENSITY

The words rate and density are used in reports as equivalent to the terms per unit time and per unit area respectively. This is standard usage, sanctioned also by the Webster's Unabridged (2nd ed.) and the Oxford Dictionary. As far as I know, such usage is followed by every careful writer and use of the word rate to imply number per unit volume (or area or length) is never practiced. Density is sometimes misused, but even then is generally modified by the adjective time or temporal. If, anywhere in my writings, rate is used to mean other than per unit time, I have erred and apologize.

An exact description of an altimeter program would specify (1) the time at which each measurement should be made; (2) the point from which it should be made; and (3) the point to which it should be made. Since we are going to use an altimeter, the third specification is usually implied as a consequence of the first, since an altitude is the perpendicular distance from the altimeter to the surface below. Furthermore, the time specification is not necessary if the surface is time invariant, since an altitude measurement from the given point will give the same number regardless of when it is made. The surface we are actually going to talk about most is, unfortunately, a time-varying surface, the ocean surface. Time must therefore enter into the specifications in some way. How? Well, it is immediately obvious that observation times cannot be specified very long before measurement because we do not know enough about the orbit ahead of time. Furthermore, such specification would be unnecessarily restrictive. There are few ocean features other than tides that are connected with specific times. Most of the ocean features that change are (1) too small to worry about; (2) too slowly changing to be distinguishable from permanent features; or (3) occur in ways and forms that are unpredictable on a mechanical basis. Those features such as waves and air-pressure dimples that are mechanically unpredictable can be described statistically. This is fortunate because these features

are also the most prominent of the time-variant features. Hence our time specification also should be statistical in nature to match the distribution of features that disturb our measurements.

We are not worried about water level changes caused by melting glaciers, leakage of water molecules off into space, minimal hydration, or even precipitation (evaporation cycle variations). These are too small or too gradual. The same is true of polar and long-period tidal variations. We should feel concerned about tidal variations with periods of half a year or less, or about waves (other than tsunamis, which occur unpredictably but infrequently), but as far as waves are concerned, we know sufficiently little about them to assume that we will get the same result by averaging over an area many wave lengths on a side as we would by averaging at a given point over many times. That is, we should get approximately the same value (zero) for average wave height by taking one measurement per square kilometer in a 100 km square area as we would get by averaging over 10,000 measurements at the center of the area. In both cases, we must be careful to space our areal or temporal measurements in such a way that stationary points are avoided. We should avoid a fast sampling rate if we are measuring at a point, since we do not then get a sample of all kinds of wave periods; we should avoid a high sample density in a small area, since we then miss variations in long waves. No harm is done if we have a high sampling rate over a large area or a low sampling rate over an extended period of time in a small area.

We have discussed the relation of sample rate to ocean surface shape with Marine Research Laboratories (MRL) several times. The opinion of MRL is that there is no reason to suppose that the instantaneous average of surface heights over a large enough area will differ from an average of surface height at a point taken over a long enough time. With regard to waves generated directly or indirectly by winds, this means that a set of surface heights measured by a satellite altimeter should, if averaged over time, give the undisturbed surface height. The cognate

conclusion, that the set, averaged over an area, should also give the undisturbed surface height, is not necessarily true. It will be true only if (1) the area is large enough that it contains at least one wavelength of the longest wave of significant height; and (2) it is small enough that undisturbed surface heights are not averaged out. Another way of saying the same thing is that the sea surface variations are ergodic (Kinsman 1965)[1].

The condition that the sampling density and rate be chosen so that useful non-varying-in-time deviations are not distorted must be carefully considered in all cases.

2.2.6 FIX

One way of looking at satellite tracking is to think of each observation as giving one, two, or three coordinates of the satellite in a reference system peculiar to the tracking instrument. Using our knowledge of the instrument calibration constants, orientation, location, and of the atmosphere through which the observation was made, we get one, two, or three relations (functions) between the satellite coordinates in a space-fixed rectangular coordinate system in which lines are not bent by atmospheric or lens refraction. If only one or two relations result, as is the case for most tracking instruments, each observation, therefore, yields one or two equations in the three satellite space-fixed coordinates, and all we can say is that the satellite at the time of observation lay somewhere on a known surface or line in space. But if three relations result, we can solve immediately for the three space-fixed coordinates and know exactly (except for observation errors) the point at which the satellite was when observed. A full set of three space coordinates, and corresponding time, fixes the space position of the satellite at that time and is called a fix in this paper. A partial set of coordinates is also called a fix by some individuals, but such usage is rare.

2.3 REQUIREMENTS

At the start of this discussion we explored and defined the concept of requirement. It was decided that requirements come in two forms (1) those that are placed on us by others and (2) those that we in turn place on others. They come to the geodesist couched in the language of the originating discipline and leave him in the language of the discipline whose job it will be to help satisfy the starting requirement. He is like a translator who is familiar with many languages but is really at home with one, so that in translating from one language to another he always uses his native language as an intermediary. The point of this analogy is that translation through an intermediary loses more than would direct translation. The best way of preventing loss is to close the loop by translating back again and comparing the original with its double translation.

This same procedure of closing the loop to produce feedback from the instrument designer to the originator of the requirement is essential to proper formulation of the requirements on and requirements from geodesy (or, user requirements and design specifications, respectively). There are close relationships between allowable rms error of a point, number, and location of points, extent of surface, etc., and the best results obtained by using these relationships, from the user's point of view, between the variables.

The procedure used in finding the two sets of requirements was a cyclic one. A rough list of requirement sources (users) was drawn up, major requirement categories listed within each category, and tentative values assigned to the categories. Specification requirements were computed from these and labelled Preliminary Requirements from Geodesy. The user requirements and the specifications were then circulated to the oceanographic group, modified, passed through the altimetry design group, and returned to the geodesist for further modification and enlargement. Many such cycles must be gone through before an acceptable

final set of requirements is found. The requirements given below are the product of early stages in the cycling process.

2.3.1 GENERAL INTRODUCTION

Since geodesy is primarily a geometric discipline and is only interested in gravity as a quantity useful in improving the geometric picture, requirements on geodesy are primarily geometric i.e., they concern locations. But while it is clear what we mean by specifying a location on land, we are necessarily ambiguous when talking about the location of a point at sea; either a point on the ocean bottom may be meant, or a point on the surface; in this study points of both kinds will be considered. Even after the ambiguity is removed, a good deal of impreciseness remains if the point is on the surface. This, of course, is because an ocean surface is not invariant in time, but changes from instant to instant and usually changes by considerable amounts; hence, we must in such cases specify not only a location but the exact time for which the location holds.

Many people need the exact specifications of time and location. Specialists in ephemeral events such as wind, waves, tides, tsunamis, seiches, etc., want a picture of the surface as a function of time. Many others, however, are not indifferent to these short-lived events, but actually find them annoying. The geodesist would like, as long as he must deal with sea level as a reference surface, to have the sea as invariant as the land. The oceanologists concerned with mass-transport phenomena (ocean currents, etc.) also find the surface waves a hindrance in defining the geostrophic surface. For such workers, a time-average of the height is much better. Such an average, if carried out over a period of time long enough that the quantity

$$\frac{1}{t_2 - t_1} \int_{t_1}^{t_2} h(\lambda, \phi_o\ t)\ dt$$

converges, is called msl.

What is a long enough time? Unfortunately, the answer is far from clear. The changes in sea level, studied as functions of time, are found to be sums not only of periodic and of random functions, but also of a linear and perhaps quadratic function of t. Consequently, a short averaging interval will be unsatisfactory because it does not outlive variations, while a long averaging interval fails to show the secular variation.

The list of requirements was compiled from a survey of official government reports, scientific publications, and unofficial communications and publications of various types. The bibliography at the end of this report contains the sources of most of these requirements. Those requirement sources not cited in the bibliography were, as explained elsewhere, inferred from unknown requirements in other fields. Table 2-2 is the list of requirement sources and associated requirements. For each source the phenomena of main interest are given, together with the extent of the phenomena's effect at msl (width between 50% of minimum height points) and the height at 50% of maximum.

2.3.2 OCEANOGRAPHIC REQUIREMENTS

Oceanography is taken to include all studies having to do with the fluid oceans and seas but to exclude studies of ocean bottom topography (which is placed under geodesy) and ocean bottom geology (which is placed under geology). In other words, oceanography is to the hydrosphere what meteorology is to the atmosphere and geology to the lithosphere.

TABLE 2-2

REQUIREMENTS ON GEODESY REFERENCES 19 THROUGH 29

User	Area(s) Involved	Requirements (m) Vertical RMS Error	Requirements (m) Horizontal RMS Error	Width x 10^{-3} (3dB) (m)	Comments
Oceanography					
Static	Open Ocean	0.2	>10,000-	200-1000	
Dynamic	Open Ocean	0.2	>10,000-	>1000-	
Geology					
Structure	Entire Ocean	1-3	1000	20-100	
Seismic	Oceanic Ridge, Other Seismic Areas	<0.1-	1000	20	
Military					
Geodetic	Launch Area	10	-	Not Applicable	-
Gravimetric	Along Flight Path Zone	-	100	Not Applicable	Gravity Equivalent
Industry	Continental Shelf	Not Defined	50	Half the Shelf Width	
Tracking	Neighborhood of Tracking Stations Near Ocean	0.5-7.	1000-10,000	Not Applicable	
Geodesy					
Validation	Marshalls, Azores, Ascension	5	1000-5000	20	
Connection	Caribbean, Indian, China Sea	0.3	-	-	
Marine	Entire Ocean	-	-	-	
Navigation	Open Ocean	Classified or Not Defined	Classified or 1000	Not Applicable	

I divide oceanography arbitrarily into two parts - static oceanography which is concerned with reasonably timeless phenomena such as water salinity, composition, density, and mean surface shape; and dynamic oceanography which covers comparatively fast-changing events such as tsunamis, seiches, wind waves, tides, mass transport, heat flow, etc.

Only the static phenomena are considered here as "required"-connected. The dynamic phenomena, while extremely interesting, are barred by the conditions of the study from being investigated for their own sake. Of course, waves, tides, and seasonal level variations must be given some consideration to make sure that they will have negligible effect on the estimates of static phenomena, but otherwise all information gathered on the ocean's momentary surface is incidental only. Table 2-3 lists the major static oceanographical phenomena for which requirements can be set up, while Table 2-4 lists some of the major (in this study) disturbing dynamic phenomena.

TABLE 2-3

STATIC OCEANOLOGICAL PHENOMENA[30,31,32]

Type	Maximum Dimensions	
	Height (m)	Width (km)
Geostrophic Current	2	500
Air Pressure (Static)	2	2000
Air Pressure (Wind)	1	2000
Geoid	50	10,0000

TABLE 2-4

DYNAMIC OCEANOLOGICAL PHENOMENA

Type	Height (m)	Width (km)	Period (Seconds)
Wind Waves	20	1.6	30
Swells	10	1.6	30
Seiches	1	-	3×10^4
Tsunamis			
Open Ocean	1	200	9×10^2
Coast	30	-	9×10^2
Swashes	600	-	-
Tides (Open Ocean)			
M_2	0.5	-	4.3×10^4
S_2	0.	-	4.3×10^4
M_f	0.06	-	1.2×10^6
M_m	0.03	-	2.4×10^6
S_{sa}	0.03	-	8×10^6
Pole Wandering	0.005	-	34×10^6

The optimum project would be one that measured msl over the entire hydrosphere to the ultimate with the smallest variance of which the altimeter system is capable. This is set as the first goal, with the provision that the variance will be less than 100 m^2.

Should later study of altimeter capability, satellite characteristics, and data processing limitations show that a complete hydrosphere survey is not practicable, then we must limit our aspirations. The extent of and regions to which they are limited depend on what caused the limitation - weather or altimeter life (in terms of number of measurements); altimeter accuracy. Table 2-5 lists five of the regions which are important enough to warrant independent survey. Rms error (absolute value) is estimated.

TABLE 2-5

SPECIFIC REGIONS [17,22,33,34]

Regions	Subject	Rms Error of Measurement (m)
Central Pacific	California Current	0.2 - 0.5
N.E. Atlantic	Satellite Geoid	5 - 10
Caribbean	Astro-Geodetic Geoid	0.1 - 1.0
S.W. Pacific	Satellite Geoid	5 - 10
South Central Pacific	Geoid	1 - 10

2.3.3 GEOLOGICAL REQUIREMENTS

While geology is defined in almost as many different ways as there are definers, the present study considers it as the sum of two different but related subjects - the shape and structure of solid earth, and the changes in shape and structure. The shape of the solid earth is the province of geodesy; under the oceans it is marine geodesy or hydrography. The gross features of the bottom topography are imaged in the geoid and could be roughly mapped with an altimeter. Such mapping could be crude and, in view of the existence of programs for relatively accurate measurement of bottom topography, futile. Structural investigations (investigation of the density distribution) require at least some independent information on topography but are reasonable and useful.

Study of changes in bottom structure and topography by actual measurement of the changes is not considered practicable for a satellite altimeter project. The time scale is either too long or, in the case of catastrophic changes, too short in relation to the size of detectable shifts. The most promising approach is through the precise measurement of those structures which are directly related to the changes i.e., faults and cryptovolcanic features.

There does not appear to be any geological reason for restricting structural geology investigations to any particular ocean region. The ESSA program for mapping the bottom of the Pacific Ocean at 18 km (10 nm) intervals will provide a suitable source of topographic information if the altimetric sampling density is of the same order of magnitude.

For investigation of seismic (dynamic geology) regions there is no need for coverage of the entire ocean. Those regions which are seismically active are well known and are indicated in Figures I.43, I.48, and I.49 of Scheidegger (1962)[2].

The rms error allowed for useful work in structural geology is taken as that which will permit differentiating between topographic and density contributions to the geoid. This error tolerance has been set at 1 - 3 meters.

The principal problem in using satellite altimetry for satisfying oceanographic requirements is of course that of separating msl, measured by the altimeter, from the geoid, which is not measurable but can be computed or approximated by an observable variable. This problem has been discussed in the preceding section on oceanographic requirements. In trying to satisfy geological requirements the same problem arises but here the geoid, and not the msl-geoid difference, is important. A standard method for finding the geoid is to integrate the gravity anomalies using Stokes's formula. To construct the geoid near large mass inhomogeneities requires detailed knowledge of the gravity variations in the area and a less detailed knowledge of variations everywhere else, if the geoid is constructed in the usual manner. In Figure 2-2 is shown a typical sea mount profile (outline of shaded portion) with accompanying variation of gravity anomaly along the profile (interrupted curve). Above this are shown the curves gotten by computing the effect of the topography itself on the gravity, assuming four different densities for the solid material. If the anomaly could be attributed to the charted topography only, the indicated curves would indicate the

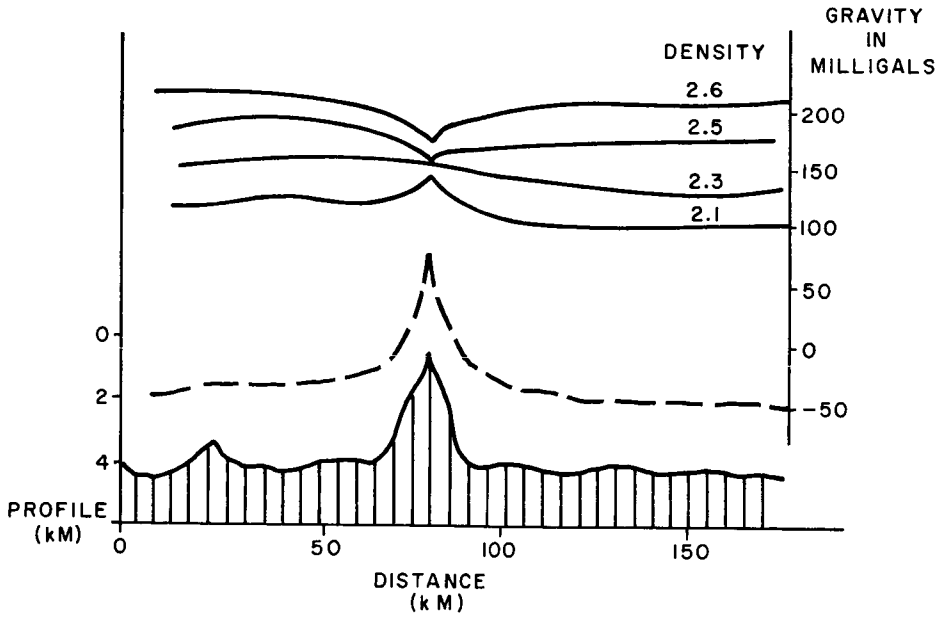

Figure 2-2 Typical Seamount Gravity Profiles

presence of a density anomaly, since we would have to assign a different density to the seamount material than to surrounding solid material to account for the observed gravity anomaly. We know that such a simple assumption does not hold for many situations on land by checking gravity against seismic data. It would therefore be dangerous to make such an assumption in sea areas without more data. In particular, isostatic compensation leads to dips or rises in the curve which should not be removed through density variation.

Gravity values will of course not be given directly by altimeter measurements. Instead, it is the geoid (actually msl) variations that will be gotten. Table 2-6 gives representative values of geoid variations resulting from typical submarine features. They were computed from gravity profiles taken from various sources (Von Arx 1966[3]; Menard 1964[4]; Shepard 1963[5]; Schimke and Bufe 1968[6]).

TABLE 2-6

EFFECTS OF SUBMARINE TOPOGRAPHY
ON THE GEOID

Feature	Geoidal	
	Height (m)	Width (km)
Seamount	3	15
Guyot	4	20
Fault	5	100
Trench	8	100

2.3.4 MILITARY REQUIREMENTS

There are a vast number of military geodetic requirements. Of these, the only ones with strong relations to the oceanic geoid are derived from long or medium-range ballistic missile technology.

A major source of information on military requirements in this area is the list of specifications for Department of Defense World Geodetic Systems 1960 et seq. Since these specifications are related to long-range missile characteristics, they are very restricted in distribution and will not be considered here. The types of requirements considered are (1) geometric, relating to the coordinates of launch and target points, and (2) dynamic, relating to the trajectory. We cannot associate exact numbers with specific missile requirements since this would involve classified information. Nominal values can be assigned, however, on the basis of unclassified information. The principal sources for this information are (1) rms error estimates for the ESSA geodetic program and (2) simple calculations of accumulated rms error over a 90^{o} arc.

Geoid or msl measurements can satisfy geometric requirements only in the neighborhood of launch points, and then only for those launch points close to sea level or easily related to msl and the geoid.

The geoid profile can also be used by taking the gradient along a trajectory, for precisely determining the gravity perturbations.

In talking about the effects of gravity anomalies on trajectories, we must always remember that gravity anomalies, by definition, are the difference between gravity as measured (and reduced to a standard surface) and gravity computed from a standard formula - usually the International Gravity Formula (IGF). There are no such animals as higher-order anomalies or short-wavelength anomalies. They are useful in trajectory computation if the trajectory is computed using the anomalies as perturbing forces added to the ICF force. They become less useful if the unperturbed acceleration is not computed from the IGF.

We should also exercise care in evaluating the effects of "short-wavelength" undulations on the trajectory. While the effect of the n-th term on the potential decreases as $(a_o/r)^{n+1}$ (where a_o is the Earth reference sphere radius, and r is the geocentric satellite distance), the effect on the acceleration decreases as $(n+1)(a_o/r)^{n+2}$. When normalized with respect to the C_{oo} term (excluding the C_n^m coefficients), the n-th term of the acceleration is $(n+1)\left(\frac{a_o}{r}\right)^n$. Table 2-7 shows the effects of higher degree harmonics on acceleration at various altitudes, without the factor (n+1) (upper number, in parentheses), and with the factor (n+1) (lower number); this emphasizes the role of the factor (n+1). Note that at a height of 500 km the 48th term is still 150% as effective as the reference term, but the 1000 km height the 48th term is negligible.

2.3.5 INDUSTRIAL REQUIREMENTS

The principal industrial requirements considered are those of the mining and petroleum industries. These probably will be the major users of marine geodesy in the future, and official government policy emphasizes the importance of these industries (Science Advisory Committee 1966, 1968)[7]. None of these industries, however, has stated any need for precise geoid or msl data. There are definite requirements for horizontal position data (see Table 2-8), but these do not correlate particularly with msl or geoid determinations.

TABLE 2-7

EFFECTS OF HIGHER-DEGREE HARMONICS ON ACCELERATION

Distance r (km)	Ratio (A,B)*			
	(n+2): 5	10	20	50
200	(0.91)	(0.78)	(0.57)	(0.26)
	3.6	7.0	11.4	13.0
500	(0.80)	(0.55)	(0.26)	(0.03)
	3.2	5.0	5.2	1.5
1000	(0.32)	(0.05)	(0.001)	-
	1.3	0.45	0.02	-
1500	(0.18)	(0.01)	-	-
	0.7	0.09	-	-

* Upper item of each pair is ratio $(a_o/r)^4$ A dash indicates a value smaller than 0.001

and lower item is $(n + 1)\ (a_0/r)^n$.

where n is the degree of the term

r = geocentric distance to satellite = a_o+h

h = altitude

a_o = Earth's radius = 6400 km

TABLE 2-8

INDUSTRIAL POSITIONING REQUIREMENTS

Industrial Source	Type	Error Bounds	
		Vertical	Horizontal
Minerals	Under way	-	10 m
	Stationary ship		
	in sight of land	-	10 m
	in open ocean	-	50 m
Petroleum	Drilling and construction	-	3 m

Documents already referred to give the areas of concern to industrial users and the order of their importance to United States of America users. This order is as follows:

1st priority - Shelf areas of the U.S.A.
2nd priority - Shelf areas of other countries
3rd priority - Deep ocean areas off the U.S.A.
4th priority - Other ocean areas

The 1968 paper (Marine Science Affairs)[7] mentions a need for bathymetric maps of the shelf areas at a scale of 1:250,000. According to customary standards this would imply approximately a 230 m 3σ error horizontally. The vertical error at the 3σ level would be about 470 m if a 500 m contour interval is used. At present, the rationale behind the 1:250,000 value is not known.

2.3.6 TRACKING REQUIREMENTS

The tracking category covers those user groups who are concerned with the tracking, for whatever purpose, of objects whose trajectories extend over the domain of more than one datum or into regions not governed by a datum. It therefore includes such users as the Atlantic Missile Range, most of the NASA satellite and deep-space tracking groups, and COMSAT. In all cases, concomitant requirements are for the use of a common coordinate system for all portions of the orbit or trajectory.

Areas involved by the requirements are (1) those within immediate neighborhood of the tracking stations, and (2) those traversed by the trajectory of orbit projection on the earth if the area has an appreciable gravitational effect on the object. Only those tracking stations in the immediate neighborhood of the sea need be considered here. Furthermore, not all of these require the small geoidal height rms error available from satellite altimetry.

The rms error estimates are related to the rms errors of the tracking instruments involved. A complete analysis of this would take a dis-

proportionate amount of time, and preliminary values of ±0.5 to ±5 meters have been assigned as covering the performance of most tracking installations that can use geoidal height or msl information.

The concept of feature width or wavelength has no immediate meaning in this context, although a lively imagination could create one. Note that the military requirements noted previously are very closely related to the tracking requirements discussed here. Some of the tracking requirements are of course military; they are included here because there is more of a family resemblance among the tracking requirements than among the members of a general military requirements category.

2.3.7 GEODETIC REQUIREMENTS

Geodesy is a tool, not an end. Hence, it cannot properly levy requirements on itself but must wait for users of geodesy to state them. Nevertheless, geodesy has here been elevated to user status so that it can serve as a catch-all for the requirements of many legitimate users whose justifications do not seem to have been definitely or strongly expressed. Such users as boundary commissions, mapping or geographical organizations, etc., are included here. It could really be argued that geodesists do in a sense create requirements since it is common practice, when planning future work, to guess at what will be needed by all major classes of users 10, 20, or 30 years ahead and to justify geodetic programs and goals on this basis. To separate such requirements from those with more solid justification would be difficult, and geodesy is therefore to be taken as a polite equivalent of miscellaneous users. Accordingly, the geodetic requirements are on the basis of the following three assumptions:

a. Requirements exist in those areas where previous surveys of questionable accuracy exist, as around Ascension Island and Bikini. These surveys were made gravimetrically and the data run through Stokes' formula. Since Stokes' formula is known to give erroneous results, all sea surveys whose final results were obtained through Stokes' formula can be considered suspect and independent validation required.

b. Requirements exist where the variance of present (land) geoid heights can be reduced to the minimum existing variance. The variance of geoidal heights increases approximately in proportion to distances from the datum point. The rate of increase of variance changes also with distance, but irregularly and unpredictably since it depends not only on the topography and geology but also on the spacing and variance of the measurements. Considerably higher uniformity of geoidal height variance can be gotten by using msl and ocean geoid data for connecting geoidal profiles, as in the Caribbean and the Indian Ocean.

c. Eventually, a worldwide geodetic network covering not only the land surface but also the sea floors will be needed. Already much need exists in limited areas for military applications. The variance specification of horizontal and vertical control are assumed to be the same as those for the same control on land.

The areas where requirements can be reasonably imposed are, from the foregoing, either those where geoidal heights already exist but are doubtful, and must be verified, or those where heights do not exist. In the first category are included all oceanic areas where the geoidal heights have been found by gravimetric survey. Among these are the previously-mentioned Ascension Island and the Eniwetok-Bikini areas.

The rms requirement depends on the application. Three applications were referred to: (1) refinement/validation of existing surveys; (2) connection of existing surveys; and (3) extension of present surveys. Preliminary values for the allowable rms errors corresponding to each of these applications is given in Table 2-2.

Since at present the spherical harmonic series is a common way of representing gross features of the geoid, the dimension of such features could be given by specifying the wavelength implied by the spherical harmonic term of largest amplitude that the feature generates. However, such specification is natural only in applications where (1) the harmonic series expansion itself is useful, as in trajectory computation, and (2) where high degree harmonics (for example, degree higher than 20)

are not of importance. Less than a fourth of the user requirements involve the geoid in its harmonic expansion form as a natural mode. The other requirements find a specification in terms of the 3 dB width more natural, and this type of specification is therefore used almost exclusively.

2.3.8 NAVIGATION REQUIREMENTS

Navigation requirements are singled out from the miscellaneous category in which they would otherwise be placed. This is done to emphasize its dual role in industry and defense. No navigational requirements are known to exist for msl in the industrial field. There are, however, definite requirements for msl (or geoid) in defense applications where ship or submarine long-range missiles are involved.

All ocean areas of the world are involved when navigation requirements are discussed, even arctic waters. Requirements near land are better satisfied through non-satellites methods, while requirements in the Arctic Ocean cannot at present be satisfied at all by satellite altimetry.

Exact values for the requirements both in altitudes and in horizontal coordinates cannot be given without getting into military security problems. If military navigation requirements are omitted, the existence of other navigation requirements for msl cannot be shown.

2.4 REQUIREMENTS FROM GEODESY

As suggested earlier, the geodesist often plays the role of middle man between the people who use geodetic information and those who design geodetic instruments. In the present case of the satellite altimeter, he translates the needs of potential users into geodetic language and then this again into language understood by the radio or optics designer. We have covered, in Section 2.3, the translation of oceanographic, geologic, military, etc., needs into geodetic quantities such as geoid height, horizontal, and vertical coordinates, etc. In the present section we translate the geodetic quantities into such satellite system

quantities as satellite orbital parameters, measurement frequency, rate, and rms error, meteorological variables to be measured, and so on. The translation process is shown as a flow diagram in Figure 2-3.

2.4.1 INTRODUCTION

Once the requirements of the user have been clearly stated, the geodesist transforms them into requirements that he can place on the instrument designer and which are intelligible to the latter. In the present case the requirement comes to the geodesist as specifications on the regions where measurements are to be made and the rms error allowable in the quantities of interest to the user. Because of the nature of the problem, these quantities must be either the coordinates of msl (or the geoid) with respect to the spheroid, or gravitational acceleration at certain points on the surface. The quantities that must be provided the designer are, correspondingly, the places along the satellite path at which measurements must be made, the times at which they must be made if this is important, and the allowable rms error in measurement and place of measurement.

In saying that the allowable rms error in measurement must be specified, we must be clear about what measurements we are talking about. The geodesist would like to have the altimeter measure the distance along the vertical from the altimeter to the instantaneous surface. He can then specify that the altimeter measure this distance with a certain maximum variance. To avoid misunderstanding and to get an agreement with the designer on what will be measured, he should start with enough understanding of altimeter design that he can also specify requirements in terms more readily useable by the designer. That is, the geodesist should be able to say: either measure the distance to sea level along the vertical, with rms error of $\pm\sigma_h$, or measure a distance from the altimeter to the sea's surface along some line and give both the distance and deviation from the vertical to within limits $\pm\sigma_d$, and $\pm\sigma_\xi$, σ_η. As Figure 2-4 shows, the desired quantity h (normal to the geoid) may not be available because the altimeter actually measures h_1, h_2, or both simultaneously (i.e., normal to sea level).

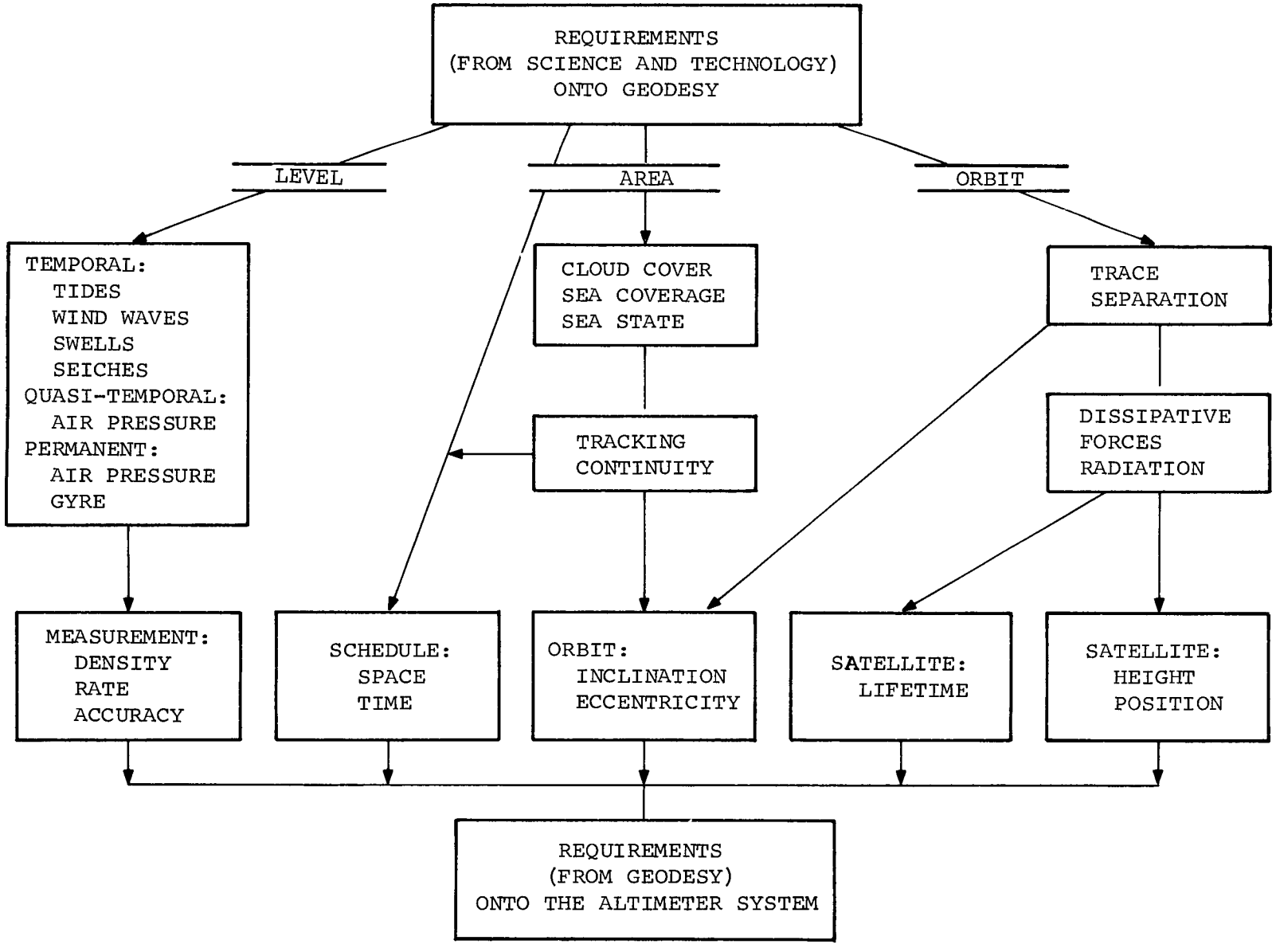

Figure 2-3 Translation of Requirements ON Geodesy into Requirements FROM Geodesy

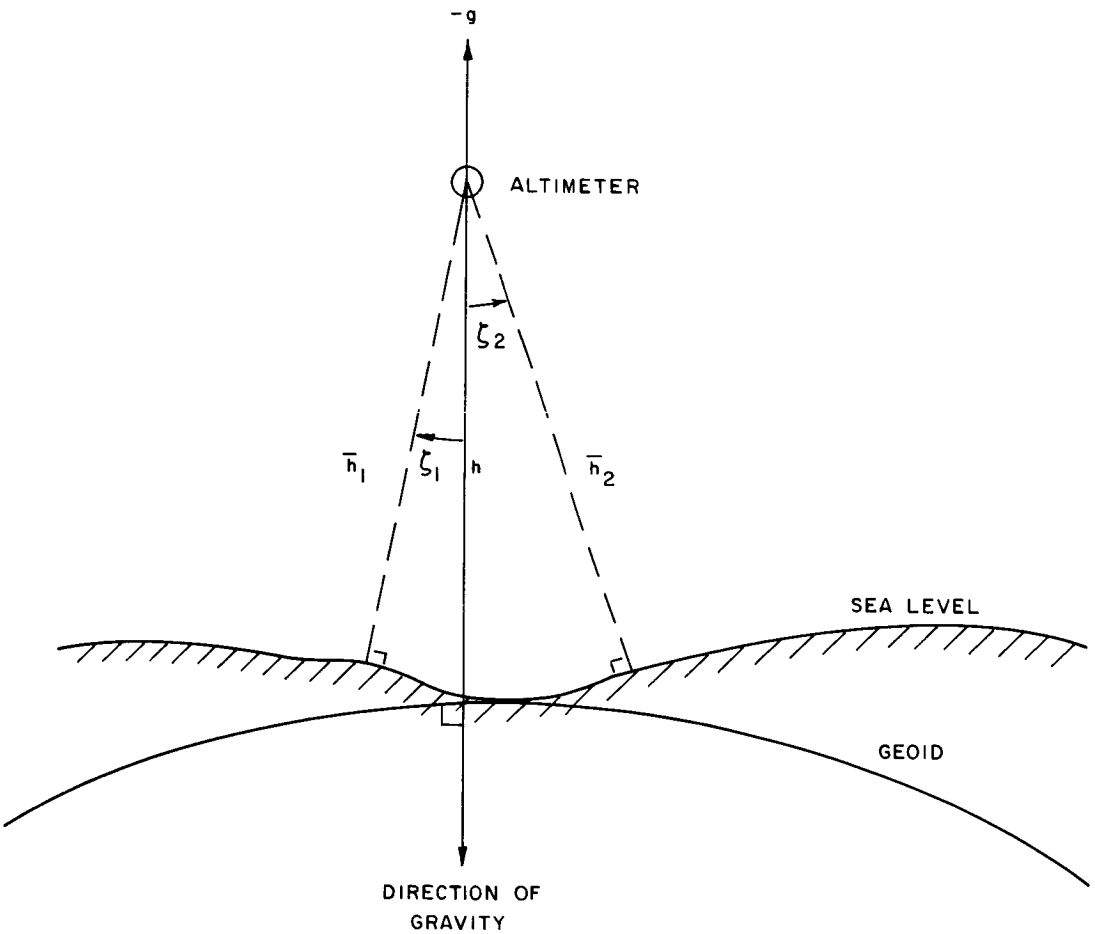

Figure 2-4 Relation of Mean Sea Level to Altitude

2.4.2 LIST OF PRELIMINARY REQUIREMENTS FROM GEODESY (DESIGN SPECIFICATIONS)

In Table 2-9 are given the requirements from geodesy or specifications to be used for beginning the altimeter design. The geodesist's requirements to the designer are of course determined by the users' requirements to the geodesist and the same categories therefore are used for both kinds of requirements. The regions in which measurements are to be made were listed in Table 2-5 and are not repeated. Certain satellite orbit parameters are related to the regions to be surveyed; values for these parameters are therefore given. The values are not

TABLE 2-9

REQUIREMENTS FROM GEODESY

USER	Satellite Life Yrs.	Satellite Height km.	Inclination °	Eccentricity	Measurement Density (1)	Measurement Accuracy (2)	COMMENT
Oceanography							
Static	2	> 500	80	Low	5	0.1	-------
Dynamic	1	"	60	"	-	-	No Requirement
Geology							
Structural	NA	"	-	"	200	1	------
Seismic	NA	"	70	"	200	1	------
Military							
Geodetic	-	"	60	"	25	5	------
Gravimetric	NA	"	60	"	-	-	(3)
Industrial	NA	< 300	60	High	NA	NA	No vertical accuracy defined
Tracking	NA	"	60	"	20	1	------
Geodesy	NA	"	75	"	20	1	------

NOTES: (1) Density in number/10^4 km^2
(2) Accuracy in meters
(3) Requirements for altimeter measurements for gravimetry not considered at present
NA - Not applicable

determined by the regions alone, however. Other factors such as weather, the ratio of land to sea area, required accuracy of measurement of altitude (not range), and so on, must also be considered. Some of these factors, again, are related to instrument design, e.g., weather will be less important if a radio frequency altimeter is to be used than if a visual wavelength altimeter is to be used. The orbital inclination i, the orbital eccentricity e, the altitudes at perigee, and the functioning lifetime of the altimeter, are therefore at this stage assigned nominal values only.

The inclination i was in each case selected to give the maximum number of passes over the area of interest while avoiding areas of no interest and staying out of areas with high percentage of cloud cover the year round. Clouds should have little effect on rf altimeter data but until more information on performance and design of a laser altimeter is available, persistently overclouded areas should be avoided, at least in planning. There is some correlation between cloudiness and sea state; until more information is also gotten on the effect of sea state on altimeter accuracy, avoidance of cloudy areas should reduce problems with sea state. Cloud cover data obtained from the USAF Space Planner's Guide (1966) were adequate for setting orbital constraints in Table 2-9. A similar but more detailed analysis has been done by G. van der Heide as part of the laser altimeter study.

Altimeter lifetimes for all user requirements except the oceanographic are irrelevant so long as the measurements can be satisfied. For study of oceanographic phenomena the lifetime must be long enough that (1) temporal variations not removed by theory can be averaged out; and (2) those temporal variations which are of interest are detected.

Satellite lifetime is a factor in altimeter lifetime and is decided by the perigee and apogee radii, or, equivalently, by perigee and apogee heights. Perigee heights were chosen greater than 500 km for all user requirements except industrial. This height together with near zero eccentricity gives a daily rate of height decay considerably less than 1 meter. (Personal Memorandum of March 1968)[32].

Measurement density was computed on the assumption of a time-constant surface height, and represents the number of samples needed to assure, with 66 percent probability, that the computed surface does not deviate by more than the indicated rms error from the true surface. The density increases if sampling is random.

2.4.3 LIST OF SECOND-CYCLE REQUIREMENTS FROM GEODESY

After a first estimate of "Geodetic" design specifications had been made and discussed with the instrument design teams, a closer look was taken at some of the specifications. This review resulted in the numbers given in Table 2-10. The height of msl with respect to the spheroid is determined by the difference between an orbital measurement and an altitude measurement. Consequently, the measurement of the satellite orbit height with respect to the spheroid should be made to the same accuracy as the measurement of altitude from the satellite. Hence, the rms error in height of sea surface above spheroid is approximately $\sqrt{2}$ times the value given in either half of the rms error column. The density estimates are given both for a stationary and for a tide-affected surface. Note that only low densities require a significant addition to take care of tidal variations. The increase cannot be handled as a pure density increase, of course, but must be properly spread out in time. It cannot be handled by extending the range of measurement over one or two wavelengths, since this could result in contamination by natural geoid undulations and would in any case be inefficient. The extra observations should be spread out in time, as explained elsewhere.

TABLE 2-10

MEASUREMENT DENSITY AND RMS ERROR

	RMS ERROR (m) in Height		Number of Measurements per 10,000 km^2	
Requirement Source	Above Sea	Above Spheroid	w/o Tides	w/ Tides
Mean Sea Level (Oceanographic)	0.3	0.3	2	4
Submarine Geology				
Static	1	1	200	200
Dynamic	-	-	200	200
Military				
Geometry	7	7	10	20
Gravity	-	-	--	--
Geodesy				
Datum Establishment	1.5	1.5	200	200
Geoid Connection	0.1	0.1	10	20
Geoid Extension	0.5-2	0.5-2	0.1-1	1 - 5

2.5 GEODETIC PROCEDURES INVOLVED IN SATISFYING REQUIREMENTS

As explained at the beginning of this chapter, geodesy plays two roles: that of converting altimetric measurements into surface coordinates; and that of interpreting the needs of potential customers for surface coordinates into specifications on the measurements. The second role was discussed in Sections 2.3 and 2.4. In Section 2.5 we discuss briefly the first role. Much of what would ordinarily be covered in

this section has already been covered in preceding sections. The factors that enter into converting msl to the geoid were considered in the discussion on oceanographic requirements, for instance. This is because anything that the geodesist considers a correction brought in to change msl to geoid or altimetry measurement to msl is sure to be considered in some other discipline as an important and beautiful subject of investigation. I therefore, merely mention such factors in this section, referring to previous sections for fuller discussion.

Because the satellite altimeter data relate directly to the instantaneous sea surface, through averaging to the mean sea surface, and indirectly by introduction of other data to the geoid, the data reduction processes required are shown, first for getting instantaneous and msl (see Figure 2-5), and then for getting the geoid (see Figure 2-6). Equations used are for the most part well known; furthermore, their detailed listing would require six or seven pages of closely-packed formulae without much resultant edification. They are, therefore, merely referred to in what follows.

2.5.1 MEAN SEA LEVEL

In finding sea level and mean sea level the input data are: measured distances, corresponding times, and instrument calibration constants: satellite coordinate(s) observed by tracking stations; times of observation; instrument calibration data; and station coordinates. Also available may be auxiliary data such as sea state in area of altimetric observation, surface reflectivity, cloud cover, atmospheric propagation characteristics, and altimeter orientation. All data will of course be accompanied by variance estimates.

Tracking station data together with atmospheric data are analyzed and processed as they come in. Satellite altimeter measurements, together with atmospheric propagation data and calibration data are likewise analyzed and processed. Tracking and altimetry data are combined in two different ways, as indicated on the following page:

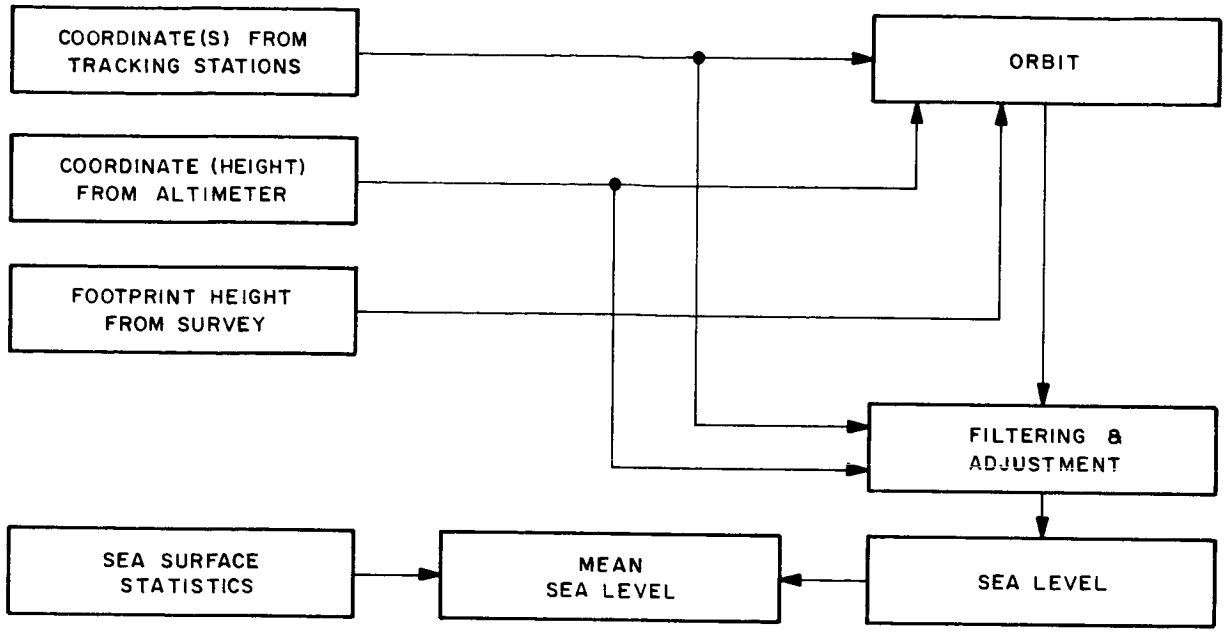

Figure 2-5 Data Reduction Processes Required for Mean Sea Level

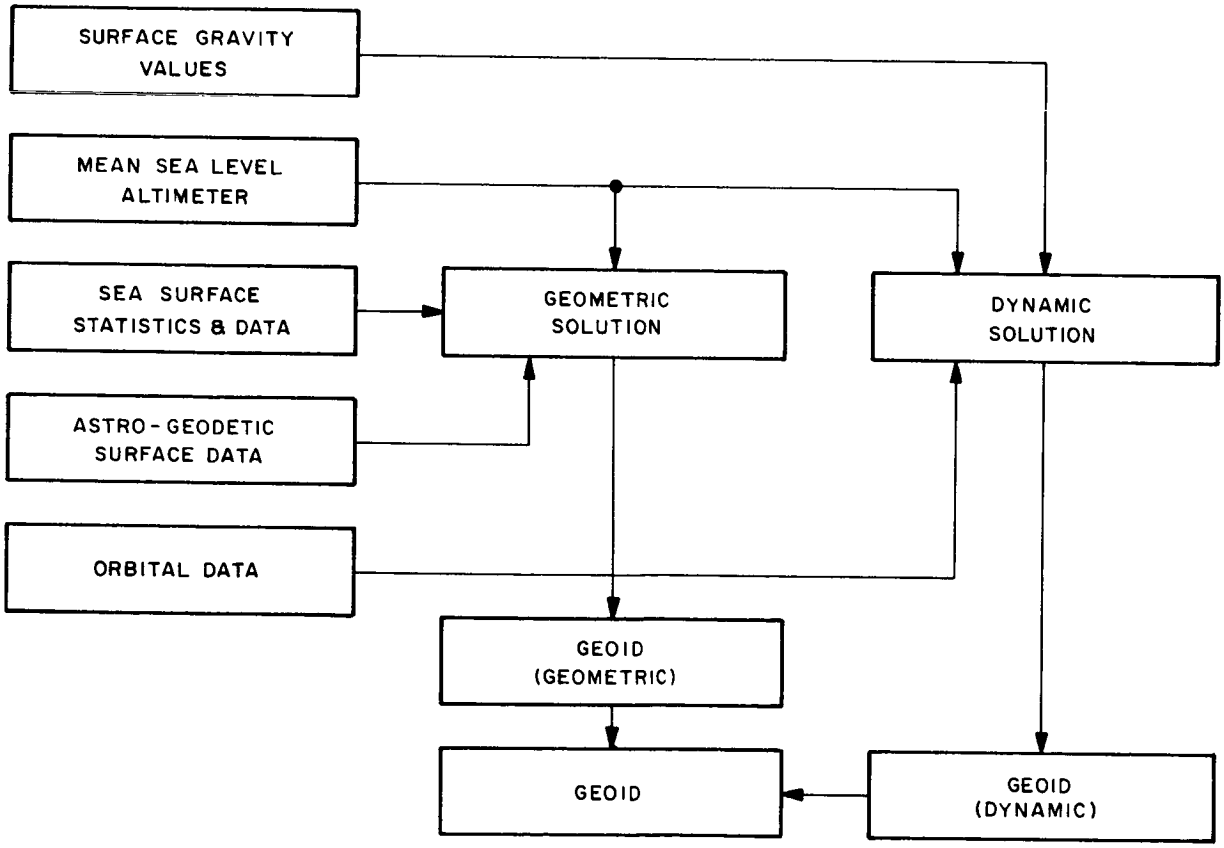

Figure 2-6 Data Reduction Processes Required for Geoid

a. Tracking and altimeter data, after being prepared by correction for calibration differences, atmospheric propagation effects, etc., are introduced as observations into the equations for the satellite motion (orbit) and the geoid. Residuals are computed, variances and confidence limits estimated, and the data filtered. An adjustment is made and then residuals, variances, and sampling parameters recomputed to verify randomness of the errors, normality of the distribution, and absence of non-observational errors. (Wherever possible, independent data giving separation between sea level and the geoid are introduced; otherwise msl is equated with geoid).

b. Tracking and altimetry data are processed as in (a) above except that the altimetry data are not used in the orbit but are used (without the outside data on foot print height above spheroid) for derivation of the msl, not the geoid. Thus (a) provides a check of the results of each procedure and (b) effectively separates msl from the geoid. More precisely, since it is not really the geoid that is derived, the double processing provides a check on the extent to which the msl is contaminated by correlation with the C_n^m, S_n^m coefficients and vice versa. The complexity of the situation (sea state, measurement discontinuity, etc.) makes separation of factors relating msl to the geoid through the covariance matrix alone very risky.

In either case the sea level surface is synthesized sequentially. Solution for the surface (and coefficients) could be done in batches, but is undesirable for two reasons. First, sequential synthesis (that is, construction of results from data as they arrive by modification of existing results in accordance with new data) effects a very considerable shortening in the length of time spent in data processing, with final results following on the heels of the arrival of the final data. Secondly, as long as there is any control of the measurement times, the progress of the experiment can be changed, as indicated by current computations, to strengthen the results. This is a method of steepest descent procedure for optimizing the experiment as far as results are concerned.

That is, the experiment is continually steered in a direction such that the final derived surface is the most accurate that could have been found with the given number of measurements. One does not get this result for nothing, of course. Sequential procedures are usually less efficient than batch procedures in that the number of steps of computation is greater. This is not an important consideration in most cases.

Since the altimeter has done some mechanical averaging of heights already, the sea level resulting is not a true instantaneous sea level but an area-and-short-time average level. Such information as is available on sea state and sea state statistics is fed in both to give corrections from measured height to mean height and to filter out some of the sea state noise by using the sea state statistics as weighting function. This surface is then run through auto correlations and cross-correlation analysis to produce a true msl as closely as possible.

2.5.1.1 Mean Sea Level and Sampling

The relation of sample density and sample rate to requirements for msl is complicated in theory but simple in practice. This inversion of the usual rule holds because the differences between what the altimeter calls area-average sea level, msl, and geoid-related msl are at present small compared to the expected rms errors of altimetric measurements. Also, fortunately, tidal variations in msl can be well computed in many areas. The hierarchy of measurement-rate, measurement-density relations is organized as follows.

2.5.1.1.1 Measurements to the Geoid

If the geoid could be measured, sample rate would be irrelevant except for noting cataclysmic effects such as accompany volcanism and earthquakes, and very slow effects such as (if it exists) continental drift. Note that the geoid is the result of only two effects: the rotation of the earth and the time-averaged mass distribution. No clear definition of the length of the time interval has ever been given, but neither have geoid measurements to date been sufficiently accurate that a precise definition was needed.

2.5.1.1.2 Measurements to Mean Sea Level

Such measurements require that enough samples be taken to (1) allow definition of what the sea level would be in the absence of temporal variations and (2) average out the temporal variations. A difficulty may occur here because the altimeter will take a weighted average of distances to various parts of the uia (used irradiation area), call this the measured altitude to the area-averaged surface, and equate this to a time average at the subsatellite point. But the area average must therefore smooth out that part of the msl which varies within the uia, whereas a true temporal average would not.

2.5.1.1.3 Measurements to the Sea Surface

These do not permit time averaging. Therefore, either the sample rate must be high enough that the instantaneous surface is gotten, or the density and rate must be high enough within the sampled area that all wavelengths of importance are deducible.

2.5.2.3 Geodetic Reference System of Mean Sea Level

Almost any reference system may be used in calculating msl. If msl is measured only in a few non-contiguous and small areas, the natural systems to use are those of the nearest geodetic datums. The Carribbean surface would thus be referred to North America 1927 datum, the Timor sea area to New Australian or Malaysian datum, Indian ocean measurements to Indian datum, etc. If a major portion of the ocean surface is mapped, an intrinsic satellite datum would be indicated; thus the current could easily be transformed into DoD WGS or other geocentric reference system. (Note that no satellite-derived reference system is truly geocentric, and the various geocentric datums can vary as widely in their origin as can absolute systems.) I would recommend giving msl and the derived geoid in a number of reference systems. The computation is not difficult and many of the users will be interested in the behavior of the geoid in their datum-governed area.

2.5.2 GEOID

In describing the procedure for deriving msl from altimeter measurements, we noted that the C_n^m, S_n^m coefficients in the Legendre series description of the geopotential were derived. These coefficients define an equipotential surface once the value of V_0 in

$$V_0 = \frac{k^2 M}{a_0} \sum \left(\frac{a_0}{n} \right)^{n+1} \sum P_n^m (\sin \phi) * Y_n^m ,$$

$$Y \equiv C_n^m \cos m\lambda + S_n^m \sin m\lambda ,$$

has been decided on. The surface is an approximation to the geoid in sea areas if V_0 is properly chosen. It is not the geoid nor is it a geoid. There are too many terms missing and it is also contaminated by the confusion of msl with equipotential surface. Nevertheless it does approximate what is sought and it is therefore called, in the figure, the dynamic geoid. It should of course, be strengthened by including in the solution surface- or airborne-gravimeter values. One way of incorporating these values would be to extrapolate them to satellite altitude. A better way as far as reliability of final results is concerned is to determine the dynamic geoid in such a way that the weighted equations give the best least squares fit to tracking observations, altimeter measurements (corrected where possible) and gravity values at the surface. There are certain theoretical difficulties in this approach but the improved results should warrant the extra effort.

The geoid can also be derived as a geometric object (slightly damaged, perhaps, by use of orbit theory based on tracking observations). This is feasible, however, only if independent information is available on geoid-sea level separation. Where such information is available, the necessary corrections are applied to the msl discussed in the preceding section.

We could of course throw all the mean-sea level, gravity, astro-geodetic, etc., information together into one pot, to make geodetic bouillabaise. As sometimes happens with such all-in-ones, however, the result may contain too many ingredients of doubtful ancestry to be safely digestible. Recent work by Bjerhammer 1967[9] has shown the need for care in preparing such soups.

Other instruments could be used in addition to the altimeter to give independent information on the gravity field. These extra data would help separate geoid from msl. Unfortunately the scope of this study does not include such instruments as subject matter.

2.5.3 ERROR ANALYSIS

The following paragraphs present in highly condensed form the equations governing the error analysis for satellite altimetry. They are presented here because they will play the primary role in deciding the usefulness of the experiment, and also to point out the relationship between the dynamic and geometric geoids. This relationship is sometimes referred to as "bootstrapping."

The basic equation relating the variance of the altimetry measurements (satellite to msl), $\Sigma^2(h)$, to the variance of the height of msl with reference to the spheroid, $\Sigma^2(\bar{H})$, and the variance of the satellite location (in geocentric coordinates), $\Sigma^2(\bar{L})$ can be written:

$$\Sigma^2(h) = B_1 \Sigma^2(\bar{H}) B_1^T + B_2 \Sigma^2(\bar{L}) B_2^T \qquad (2\text{-}1)$$

which is the inverted form of the equation for $\Sigma^2(\bar{H})$. Figure 2-7 illustrates the geometric relationships. Note that in this presentation h is assumed to be a scalar. The tensors $\Sigma^2(\bar{H})$ and $\Sigma^2(\bar{L})$ are converted to quadratic form by the vectors

$$B_1 = \frac{\partial h}{\partial H_i} \quad \text{and} \quad B_2 = \frac{\partial h}{\partial L_i} \qquad (2\text{-}2)$$

It can be shown that two tensor equations exist relating h to $\bar{H}$ and $\bar{L}$ (through the envelope equations) so that h and $\bar{L}$ do uniquely determine $\bar{H}$. The Equations (2-1) and (2-2) can therefore be used in determining $\Sigma^2(\bar{H})$.

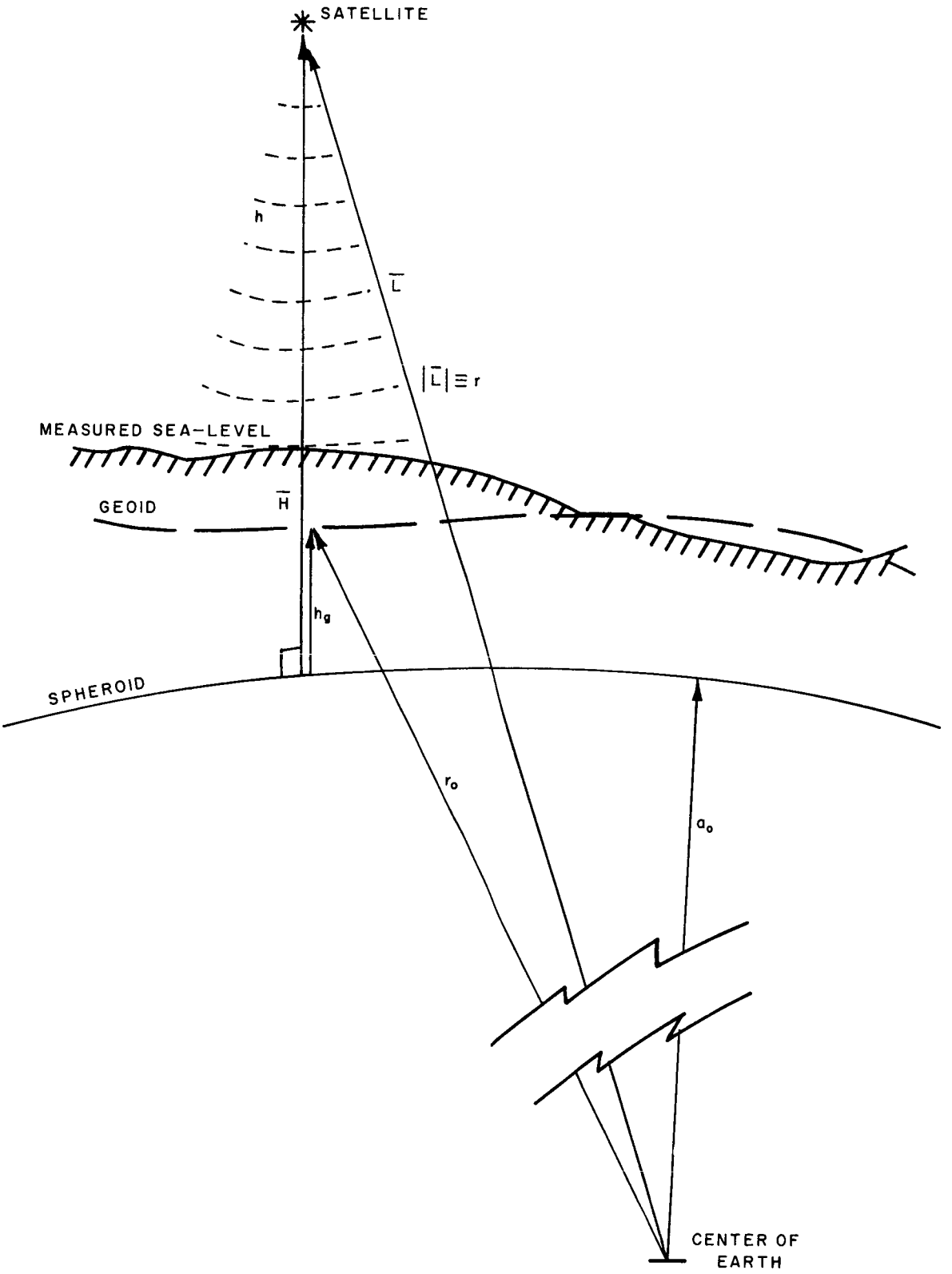

Figure 2-7 Geometric Relationships for Error Analysis

There exists one additional equation which provides a relation between $\bar{H}$ and $\bar{L}$. This relation is obtained through the equation:

$$h_g = f(\bar{H}, t) \tag{2-3}$$

where h_g is the geoid height (with reference to the spheroid), and t is the time. Ideally, t does not appear; in practice, it is present; furthermore, the form of and parameters in f will be very poorly known. Experience shows that the difference between the true value of h_g and the value obtained through Equation (2-3) will be less than 2 meters almost everywhere. If this difference is acceptable, then the gravitational potential, U_o, at mean sea level can be written:

$$U_o = \frac{k^2 M}{a_o} \sum_n \left(\frac{a_o}{r_o}\right)^{n+1} \sum_m P_n^m (\phi') D_n^m e^{-im\lambda} \tag{2-4}$$

(using complex numbers, and taking the obvious measures to retain the real portion).

The variable r_o (geocentric distance to point at msl where U_o is being expressed) is a function of $\bar{h}_g$, so that we have the required relation on solving the differential equations of motion:

$$d^2\bar{L}/dt^2 = \nabla U + \bar{F} \tag{2-5}$$

for $\bar{L}$, where $\bar{F}$ is the nongravitational perturbing force. Then $\Sigma^2(\bar{L})$ contains not only the contributions from the tracking instruments but also the contributions from the variances of the D_n^m and of the parameters present in $\bar{F}$, as these are propagated through the integrated equations of motion.

A simpler and better procedure, but one which has not yet been fully exploited, is to use U, not in Equation (2-4), but in equation

$$U(\bar{r}) = \frac{1}{2\pi} \iint_S \frac{(\partial U_o / \partial H)}{\left|\bar{r}_s - \bar{r}'\right|} dS \tag{2-6}$$

where $\bar{r}_s$ is the vector of points on the geoid surface and $\bar{H}$ is the normal thereto. U_o is then given in tabular form and we can forget all about the D_n^m, which, after all, have no physical significance. The variance of the vector $\bar{L}$ is then related to the surface specified by U_o through numerical and not algebraic relations.

Deriving the formulae for the elements of B_1 and B_2 of Equations (2-2) and for the transformation tensors used in putting all coordinates into a common system is straightforward but laborious. Since their general form can be seen from inspection of the variance tensors involved, their explicit formulation here does not seem useful. For practical purposes, a computer program for calculating U, D_n^m, $\bar{L}$ and $\bar{H}$ can easily be made to compute the B_1, B_2, etc. Most of the equations and programs needed for computation of the variance $\Sigma^2(\bar{H})$, etc., have been developed at Raytheon for use on the IBM 360 computer.

2.6 CONCLUSIONS

Out of the rich variety of information in the preceding sections, only a few conclusions are drawn and given here. These are as follows:

a. Of the various requirements on geodesy, those for providing continuity between astro-geodetic geoid segments, for improving gravity-field parameters used in orbit computation, and for getting msl variations appear to be most important as far as immediate use of results is concerned.

b. While a few requirements can tolerate rms errors in a range of plus or minus 15 meters in msl, most requirements imply that the rms errors should be within a plus or minus 1 meter range or less, and many are best satisfied if the range is plus or minus 0.2 meters or less. But those requirements which involve small rms error ranges for the msl also invariably imply similar ranges for the geoid. This means that to make full use of the altimeter measurements we should have geoid determination of comparable rms error range. Altimeter measurement and geoid determination can be done as completely separate projects. Some

separation is inevitable since geoid determination will involve use of data in addition to what comes from the altimeter. A very high degree of coordination is desirable, though, because altimeter location and altitude will be important ingredients in the geoid determination and because we would expect to minimize the msl versus geoid errors by closely matching the points where msl is measured to the points at which the geoid is determined. We can conclude, therefore, that the more exacting requirements will be best satisfied by (1) including geoid determination in the altimeter data reduction procedure and (2) designing the altimeter instrument and system (in which the tracking network is included) for geoid as well as msl measurement.

c. It is certain that because of technological and operational factors the entire set of the requirements from geodesy (Table 2-10) cannot be satisfied for even one user application. A thorough preflight analysis of each user application should be made using linear (or non-linear as required) programming techniques, and used together with the altimeter system analysis to optimize the experiment as a whole. That is, the experiment should be planned so as to get the most useful information at minimum cost in a reasonable length of time.

SECTION 3

LASER ALTIMETER

SECTION 3

LASER ALTIMETER

(G. van der Heide)

3.1 INTRODUCTION AND SUMMARY

3.1.1 INTRODUCTION

The purpose of this study was to compare the application of lasers versus radars in a spaceborne altimeter system. The end results of these measurements was to obtain a better definition of the geoid. This portion of the report contains the results of the laser studies.

3.1.2 SUMMARY

Specific system recommendations without specification of an actual space vehicle must be done on the basis of accuracy, weight, power and volume considerations. Based upon the study conducted, the recommended system for a laser altimeter is a ruby type laser system operating at 6943Å. Preliminary system design specifications are as follows:

Wavelength	6943 Å
Output Energy	500 millijoules
Pulsewidth	<12 ns
Optics diameter	50 cm.
Optical filter bandwidth	20 Å
Quantum efficiency of detector	0.12
Computer clock frequency	500 MHz
Transmitter beamwidth	200 microradians (40 arc sec)
Receiver F.O.V.	350 microradians (70 arc sec)
Range gate width	3 μs
Cooling system	Active (liquid)
Electronic bandwidth	50 MHz
Altitude error (Accuracy)	<50 cm
Pulse repetition rate	6 per minute
Orbital altitude	1000 km

Total number of pulses	1.6 million
Mission duration	1 year
System weight	33 kg (72 lb)
System volume	74,000 cm^3 (2.6 ft^3)
System power consumption	75 W

The specifications listed above can be met except for the total number of pulses with hardware available at the present time. It is our opinion that an altimeter satisfying all the above mentioned parameters can be built by 1971.

3.2 OPERATIONAL SYSTEM REQUIREMENTS

3.2.1 GEODETIC REQUIREMENTS

At the beginning of the study, preliminary geodetic requirements were assumed as an accuracy requirement of 1 meter to mean sea level and a data rate as high as practically feasible. The orbital altitude was assumed to be 1000 kilometers. The satellite was supposed to operate over ocean surfaces only.

During the course of the study the geodetic requirements became firm with an accuracy requirement of .1 to 7 meters and a required measuring density of 5 to 200 points per 10,000 km^2, depending on the mission. The orbital altitude remained unchanged. The duration of the mission has been assumed to be one year during the period 1971 to 1973.

The ability of the proposed system to meet the geodetic requirements is discussed in Section 3.4.6.

3.2.2 TRANSMISSION REQUIREMENTS

The study assumed a requirement for continuous operation by day and night and under all types of weather conditions. No prior knowledge of those conditions was assumed. It quickly became apparent that transmission through clouds is an impossiblity for any laser system and therefore, the all weather requirements had to be relaxed. Because no prior knowledge was assumed concerning cloud cover, the incorporation of

a satellite borne cloud sensor was necessary in order to increase flash lamp life and prevent unnecessary power drain.

The uncertainty of the sea state and the error that could be introduced by a very rough sea made it desirable to measure return pulse shape or return pulse length which is expected to be a function of the sea state. This provides us with the added advantage that information is obtained about the sea state on a global scale. In addition it may reduce the error in the range measurement if the relationship between the pulse shape and the sea state is known.

3.2.3 ENVIRONMENTAL REQUIREMENTS

During the system design phase, an environment of large accelerations has been assumed. Temperature variations within the system once in orbit are assumed not to vary more than $\pm 50^{o}C$.

The system is not designed to be subjected to salt spray or high humidity tests.

If stored in a dust free, dry and reasonable temperature controlled environment, the shelf life of the system is expected to be two years without loss of calibration.

3.3 SYSTEM DESCRIPTION

3.3.1 INTRODUCTION

The following section describes the design concept of a laser altimeter system. The output power and pulse length requirements are based on the analysis of error sources, while pulse repetition rate is selected on the basis of the geodetic, electrical power and cooling considerations.

A transmitter field-of-view (Ω_t) of 200 meters at 1000 km altitude on the ocean surface was selected on the basis of ocean wavelengths and the range error from beam size at offset angles of incidence. The receiver field-of-view (Ω_r) is made somewhat larger to allow for optical

misalignment and to collect nearly all the energy in the beam since the 200-meter width refers only to the half intensity points. A field-of-view of 350 meters is considered sufficient.

3.3.2 SYSTEM BLOCK DIAGRAM

A simplified version of the system block diagram is described in this subsection while the following subsections treat the separate functions in more detail. Figure 3-1 shows the important elements in the system with the electrical connections drawn in solid lines and the optical paths drawn as dashed lines. Basically, the system uses the time interval between transmission and reception of a short duration light pulse to compute the range between the space vehicle and the earth. Therefore a transmitter and receiver are needed which can share the same optics. The function of the optics can be changed from a transmit optics to a receiving optics by the use of an optical Transmit-Receive switch. The operation of the transmitter is controlled by ignition commands which are stored in the data bank via the uplink channels. In addition, a cloud gate will prevent ignition of the laser if the cloud sensor indicates that clouds obscure the line of sight to the earth surface.

The operation of the receiver is controlled by the range gate setting which is also programmed in the data bank. This gate opens the receiver input only during the time that the return pulse is expected, thereby decreasing the amount of random noise that can be accumulated during the time interval between the pulses. The random noise could cause false alarm readings in the receiver. A more detailed analysis of this effect is given in section 3.4.2.2.

A start signal is transmitted to the range clock when the transmitter generates the output pulse. When the echo pulse is received by the system, a stop signal is sent to the range clock, stopping the range count. The information contained in the clock is then transferred to the data storage bank for telemetry to the ground station and the clock register is cleared for the next reading.

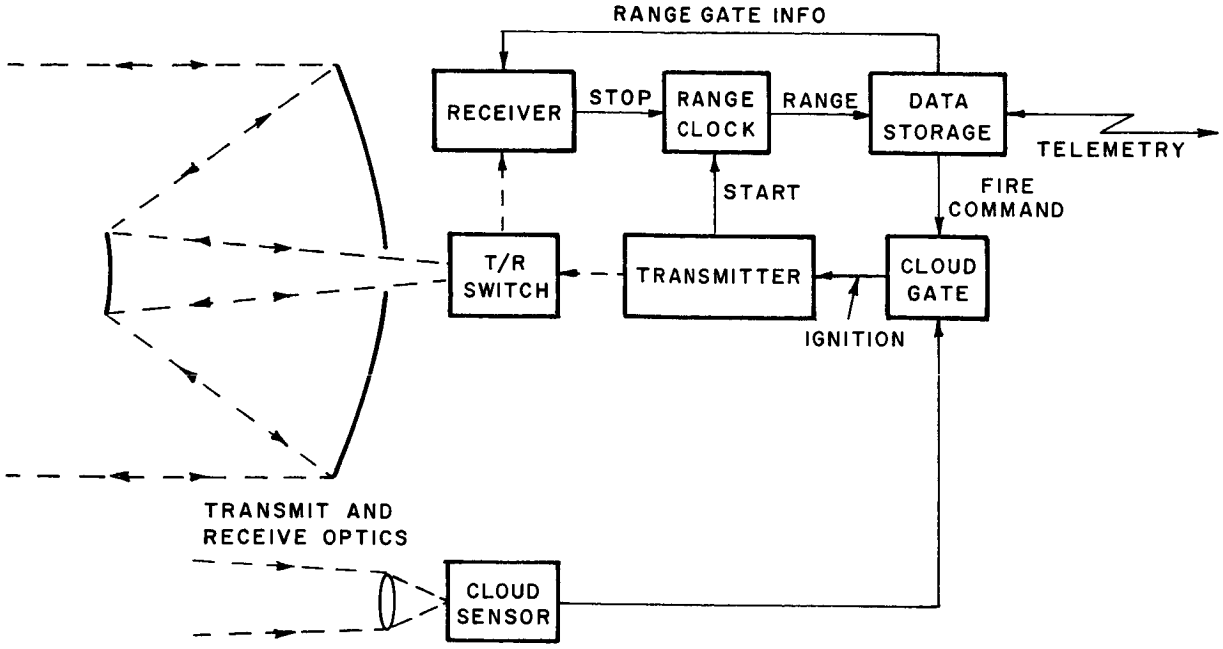

Figure 3-1 System Block Diagram

3.3.3 TRANSMITTER

3.3.3.1 Block Diagram

A functional block diagram of the transmitter is given in Figure 3-2. From the data storage bank,a command is given to initiate the charging of the laser energy storage bank. After the charging is completed a fire command is given via the cloud gate to ignite the laser flashlamp. The cloud gate will be closed to prevent ignition of the flashlamp if the output of the cloud sensor indicates that the path of vision to the earth surface is obscured by clouds.

If the gate is open, the flashlamp will be ignited and a pulse is sent to the Q switch pulser. At the end of the optical pumping cycle, or about 600 microseconds after ignition of the flashlamp, the Q switch will open and an optical output pulse will be generated in the laser. A photodetector placed behind the laser is used to detect this output pulse and the electrical circuitry following this detector determines

the centroid of the output pulse. The concept of this circuit is identical to that used with the receiver and is described in detail later in Section 3.3.8.

Upon location of the output pulse centroid, a clock start pulse is generated that starts the range clock. The laser ruby is cooled by a liquid that is pumped by a coolant pump through a satellite heat exchanger. From the heat exchanger the heat is dissipated by the satellite heat dump. Cooling requirements are given in more detail in section 3.3.3.2.

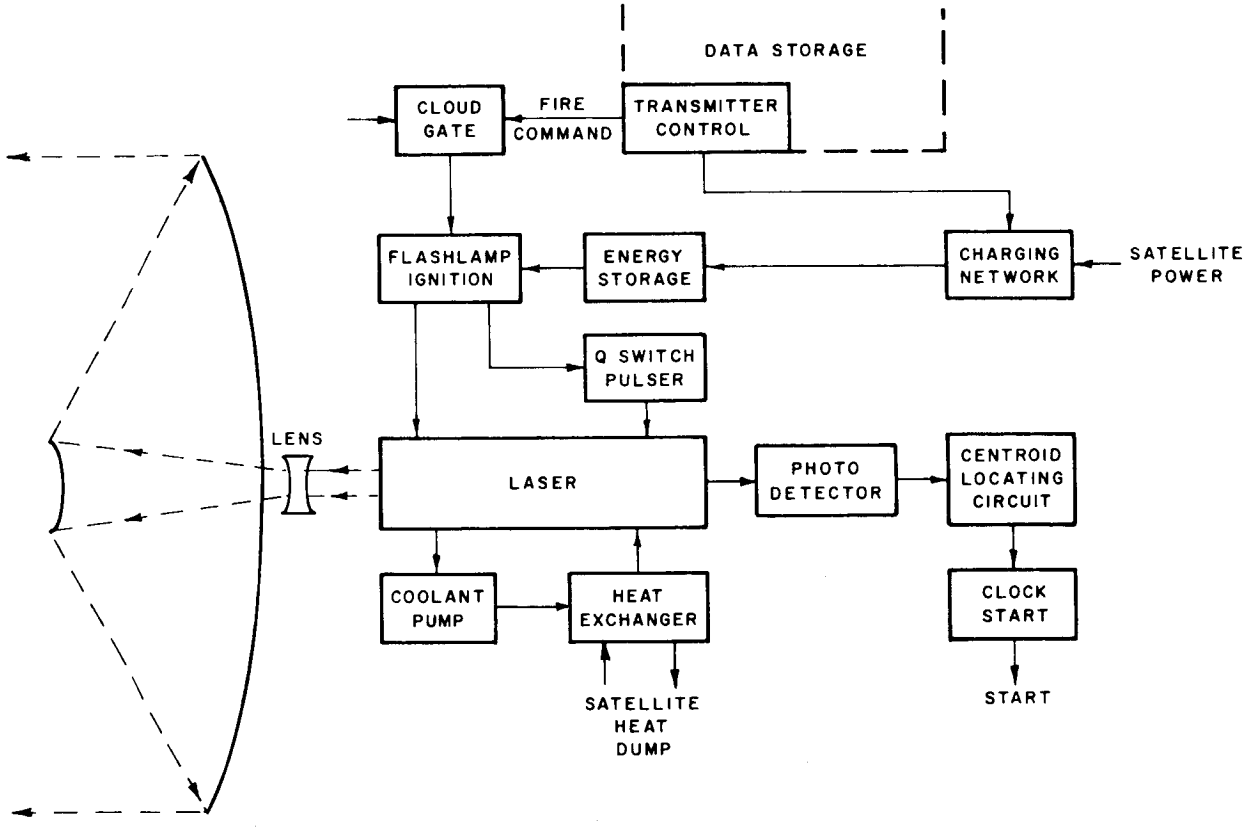

Figure 3-2 Transmitter Block Diagram

3.3.3.2 Laser Design

The design requirements based on the accuracy analysis are an output pulse energy of 500 millijoules in a length of less than 12 nanoseconds and a repetition rate of one pulse every 10 seconds.

Using an empirical power output of .1 joule per cc of ruby material, we derive a volume for the ruby crystal of 5 cm^3. Because the pulse length of the laser is strongly influenced by the physical length of the laser crystal,[1] we would use a short but practical size. We have therefore selected a ruby rod 80 mm long and 10 mm diameter, which is a readily available size and will match the source when pumped with a linear flashlamp. Figure 3-3 is a schematic of the laser transmitter. The ruby crystal and flashlamp are surrounded by an elliptical cavity with a small ellipticity so that crystal and flashlamp are closely coupled. The crystal will be kept at 275 degrees K $^{+5}_{-20}$ by a liquid that flows over the ruby surface by means of a pyrex flow tube. In addition, the pyrex will also prevent the U.V. output of the flashlamp from reaching the ruby material. The U.V. radiation has been in the past a major source of the surface damage effect observed in many Q switched lasers.

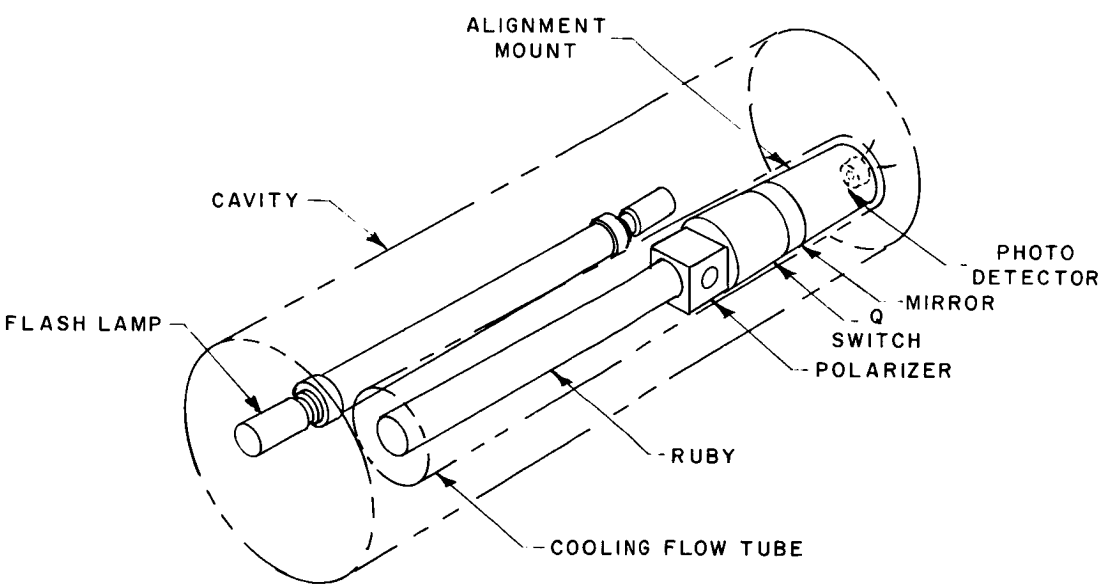

Figure 3-3 Laser Design

Measurements in our laboratory have indicated that the ruby generally absorbs about 25 percent of the energy emitted by the flashlamp. In our case, therefore, 125 joules are dissipated as heat by the ruby. For a repetition rate of 6 pulses per minute, the heat exchanger has to remove an average of 12.5 watts of heat. The lamp will be cooled by heat conduction through its electrode fittings. The ruby ends should be finished to a flatness of $\frac{\lambda}{20}$ with a parallelism of 2 seconds of arc or better. No coatings are applied to the ruby, but to prevent lasing action before the Q switch is opened, the reflectivity of the back end of the ruby is practically eliminated by optical contact between the ruby and the polarizer. The polarizer in turn is contacted to a Pockels' cell type switch, whose rear face is coated for maximum reflection at the laser wavelength. The ruby, polarizer and Q switch will be preassembled and aligned in the optics shop before installation in the laser head.

This procedure facilitates quick and easy replacement during the testing phase and results in a rugged assembly of the parts which have to be maintained in precise alignment. Using these construction techniques, a total optical path length of 200 mm can be achieved between output face and end mirror. With an optical path length of 50 cm, a pulse length of 22 nanosecond has been obtained in the laboratory during previous tests on a Q switched system. Because the pulse length of a Q switched laser is strongly dependent on the optical path length, we feel confident that a 20 cm optical path will deliver a less than 12 nanosecond pulse.

3.3.3.3 Flashlamp Life

If the mission time of the system is one year, and the earth is covered with clouds for 50 percent of the time, 1.5×10^6 flashes are required from the laser. The required number of flashes from the laser cannot be achieved by a single flashlamp at the present time. Using today's techniques it can be predicted that even in the period of 1970 to 1975 no flashlamps will be available to deliver that number of

flashes. We therefore propose a cavity design with a drum holding 9 or 10 flashlamps. The drum will rotate a new flashlamp in the cavity upon command of a ground station or after a predetermined number of shots.

To prevent light leakage and subsequent loss of efficiency a part of the elliptical cavity is duplicated for each flashlamp and is part of the drum. A sketch of the design concept of the flashlamp drum is given in Figure 3-4. To prevent waste of space, the ruby half of the cavity and some of the circuitry can be located inside the drum.

Electrical contact to the flashlamps will be made by hard silver contact points penetrating into a soft silver alloy in the flashlamp fittings as shown in Figure 3-5. Because the soft silver will flow around the surface of the contact points a good electrical contact is assured.

The flashlamp will be a Xenon filled quartz envelope of conventional design with a length of 80 mm and a diameter around the electrodes of 13 mm. To obtain a uniform discharge across the diameter with the currents involved, the portion between the electrodes is reduced to an inside diameter of 8 mm. The oversized electrodes will make it possible to obtain about 200,000 shots from one such lamp, so that a drum with 8 flashlamps could give us a sufficient number of shots to obtain a one-year operation of the altimeter.

3.3.4 LASER POWER SUPPLY

3.3.4.1 Energy Storage Network

The energy storage network stores and delivers the power needed to drive the flashlamp. A practical design is a capacitor bank storage network coupled through one or more coils to the flashlamp in the form of a lumped component pulse forming network. This assures a fast rise time of the current through the flashlamp, a uniform pumping rate and no current reversal through the lamp. Current reversal or ringing is one of the major reasons for premature flashlamp failure. To get an output

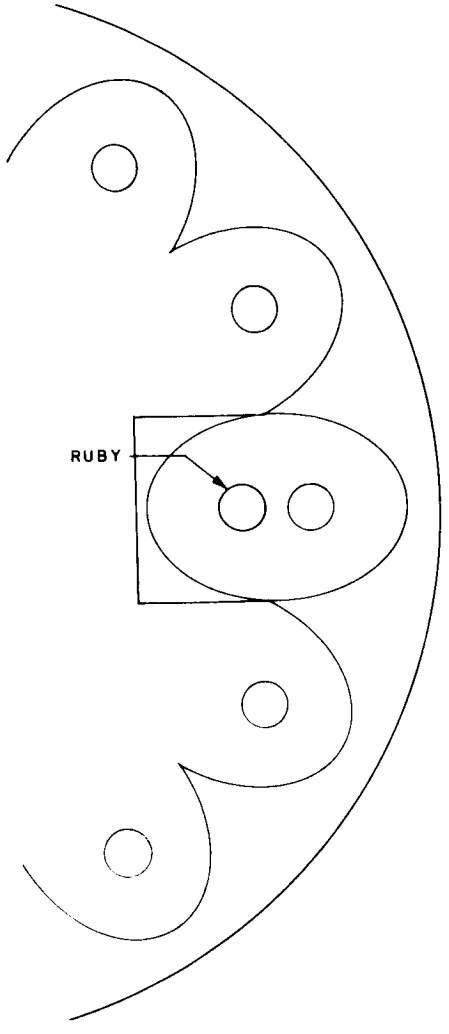

Figure 3-4 Flashlamp Drum Design

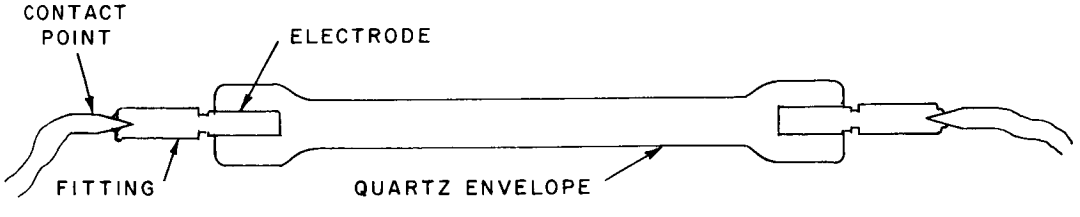

Figure 3-5 Flashlamp Contact

energy of .5 joules from the ruby, an input energy of 500 joules must be supplied to the flashlamp. We have freedom in selecting the voltage on the flashlamp, between the minimum operating voltage of the lamp and the maximum holdoff voltage of the lamp. For the type of lamp intended for this application, the minimum operating voltage is 1200 volts and the holdoff voltage is 2000 volts. We have selected an operating voltage of 1300 volts, so that a capacitor bank of 600 microfarads is needed to store 500 joules of electrical energy. Dividing this capacitor bank into three sections of 200 microfarads each and using metalized paper capacitors, the storage bank can be built with a total weight of 35 pounds.

The flashlamp ignition will be accomplished by series injection. In this technique, which has been used in our laboratories for several years, a saturable core inductor forms the last coil in the pulse forming network. A current sent through a primary winding of this inductor will generate a voltage over the flashlamp higher than the hold off voltage. After ignition the current through the secondary winding saturates the core, and causes the coil to act as a normal part of the pulse forming energy storage network.

3.3.4.2 Charging Network

A dc to dc converter will be used to transform the satellite power to the power used by the altimeter. Some of this power is utilized by the electrical circuitry of the receiver, the data storage bank and the transmitter control circuits, but the major portion of the energy is consumed by the laser transmitter. Using modern solid state circuit techniques the total power drain by the converter can be estimated to be 70 watts from the satellite batteries, for a 6 pulses per minute repetition rate. A linear charge network will be used to supply the power for the capacitor bank, so that the power drain on the satellite power station is constant in time. The coolant pump requires an additional 5 watts from the satellite power supply so that the complete altimeter power drain is 75 watts during operation.

3.3.5 TRANSMIT AND RECEIVE OPTICS

In designing the transmitter and receiver optics the choice must be made between a coaxial system and a spaced elements system. This choice must be made based upon weight, volume, difficulty of alignment, cost and proven reliability. In the spaced elements system, the transmitter and receiver each have their own optics but boresighting of the two systems is critical and, of course, volume is greater than that of a coaxial system. In the coaxial system the transmitter and receiver share the same primary optical system but a transmit-receive switch is required. The function of this switch and its configuration is described in detail in Section 3.3.6.

Because the time interval between transmission and reception of the ranging pulse is about 6 milliseconds, fast switching times are not required. This makes a T-R switch more attractive and the development of electro-optic switches is far enough advanced that a selection of a coaxial system with a T-R switch can be made with confidence.

The second choice one has to make is the selection of a reflective versus a refractive system. Refractive systems have the advantage that they lend themselves more easily to a rugged and relatively temperature insensitive construction but suffer from a weight problem. Our optics requirements prescribe a 50 cm aperture and this size makes a glass lens impractical. A second disadvantage of a refractive system is the dependence of the focal length on the refractive index of the surrounding medium. This immersion problem[2] has been studied before and is responsible for a large amount of energy loss in the receiver for low f-number systems.

Reflective systems are not dependent on the surrounding medium and are therefore more attractive. However, a disadvantage of a reflective system is the need for a secondary mirror which is partially blocking the effective aperture or the utilization of off-axis components which must be carefully corrected for off-axis aberrations. This last method is very expensive and its reliability is questionable.

Based on the considerations mentioned above, our selection has been a reflective system in the form of a Schwarzchild telescope (see Figure 3-6). In this type of telescope a cone of light with one apex angle (divergence) is converted into a cone with a different angle. This applies to transmission as well as to reception. The cone conversion should be done in such a way that spherical aberration, coma and astigmatism are zero. The mirrors in the system are therefore not simple paraboloids or hyperboloids but are corrected and more difficult to fabricate.

The diffraction limit of a 50 cm diameter mirror can be calculated from the formula

$$\delta = 1.22 \frac{\lambda}{D}$$

so that

δ = 17.1 microradians.

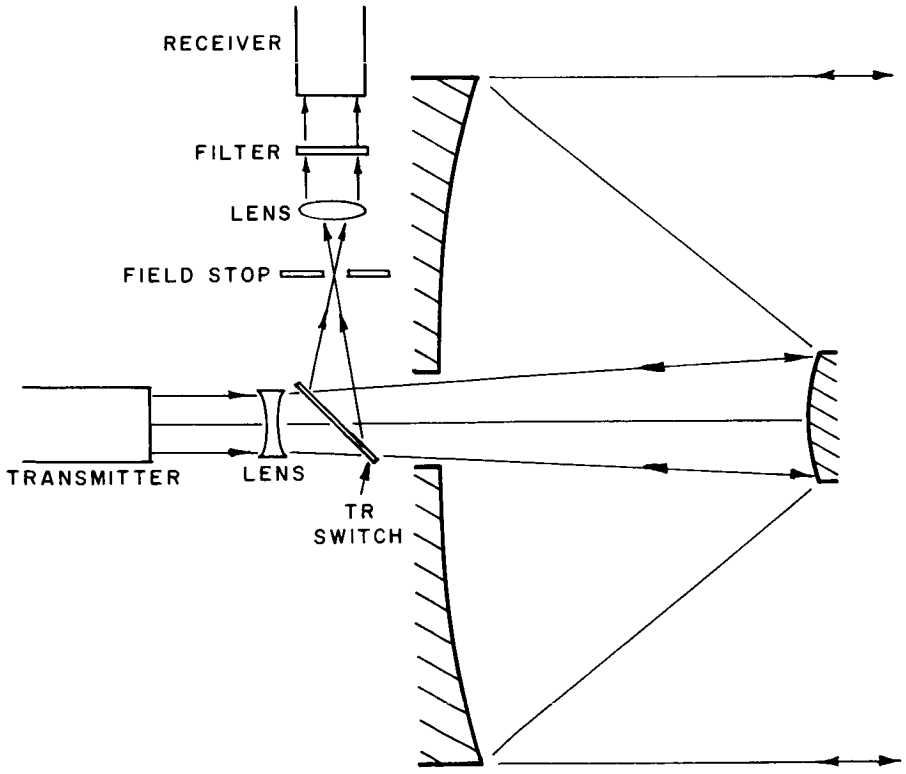

Figure 3-6 Schwarzchild Telescope

The transmitter beam in our system is required to illuminate a 200 meter spot size on the ocean surface, so that the divergence of the beam is 200 microradians, for an altitude of 1000 kilometers. Because the system does not have to meet the diffraction limit we have designed a primary mirror with a speed of 0.9.

The surface finish required on the mirror is therefore only 1/12 of the finish required to obtain the diffraction limit. This would keep the mirror well within fabrication tolerances. The secondary mirror is in the form of a hyperboloid with a diameter of 80 mm. The collecting efficiency of the system using 98% reflectivity for the mirrors is roughly 87 percent including the loss in the T-R switch.

A small negative lens is used between the transmitter ruby and the telescope so that the divergence of the output beam is 200 microradians. The field of view of the receiver using the same telescope is held to 350 microradians by a field stop placed in the focal plane of the telescope. This assures that the illuminated spot is within the field of view of the receiver. A collimating lens and a bandpass filter with a width of 20 $\mathring{A}$ placed in front of the receiver completes the optical system.

The bandwidth of this filter is selected to accomodate the shifts in temperature of the laser and the filter. The collimating lens is needed to bring the cone angle of the beam down to the acceptance angle of the filter which is about 50 milliradians for an average 20 $\mathring{A}$ wide filter.

3.3.6 TRANSMIT AND RECEIVE SWITCH

3.3.6.1 Mechanical Switch

The time interval between transmission and reception of the ranging pulse is about 6 milliseconds so that a mechanical solenoid operated transmit-receive switch can be used. Such a switch would take the form of a diagonal mirror placed behind the primary mirror as in Figure 3-6. During transmission the mirror is pulled out of the way of the transmitter beam by a solenoid. After transmission the mirror is released by

the solenoid and rests against three points of a support fixture. This insures that it is in the correct position for reception. Solenoids with a release time of 1 millisecond are now available, so that the mirror has enough time to come to rest on its three points support. The mirror is used for reception rather than for transmission, because the high power density of the transmitter beam could damage the silver surface of the mirror. A mechanical T-R switch is simple in concept and inexpensive to construct.

3.3.6.2 Electro-Optical Switch

If moving parts are not acceptable in the space environment in which the satellite operates, an electro-optical T-R switch can be used. This switch does not have any moving parts but depends on the routing of the light as a function of polarization. Change of polarization from a state of transmission to a state of reception is accomplished by a Pockels' cell in the same way as the operation of a Q switch. Because the return pulse is not necessarily linearly polarized a dual switch must be used to account for the two planes of polarization. Such a switch has been designed with an expected transmission efficiency of 90 percent.

3.3.7 RECEIVER

3.3.7.1 Block Diagram

The receiver block diagram is shown in Figure 3-7. After passing through the receiving optics the light pulse is converted to a pulse of electrical energy by a photomultiplier. A range gate is used to activate the photomultiplier during reception of the light pulse. This technique reduces the effect of random arrival of noise type signals, thereby increasing the signal-to-noise ratio. The range gate setting has to be programmed in the data storage bank via the uplink channel. It is expected that the range can be predicted with an accuracy of ±200 meters so that a gate time of 3 microseconds should allow ample time for reception of the return pulse.

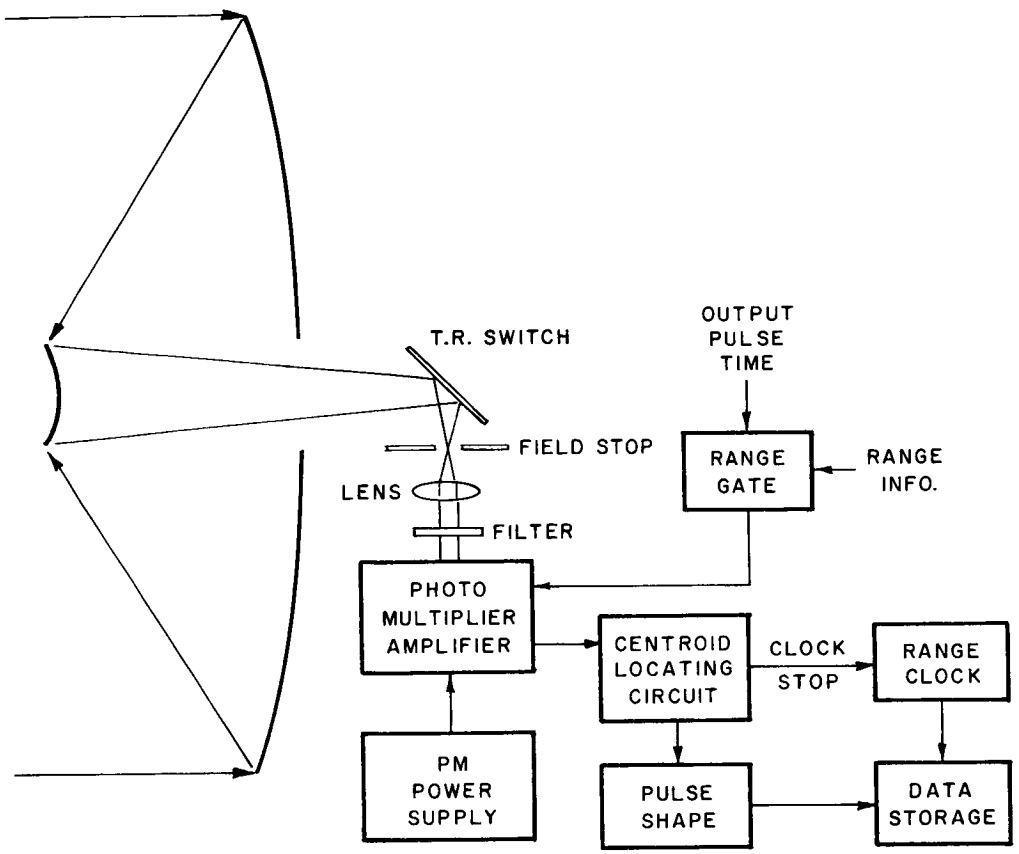

Figure 3-7 Receiver Block Diagram

After suitable amplification, the electrical signal is fed into a centroid locating circuit. The location of the centroid is the most accurate way of measuring the range as is justified in Section 3.4.4. The elements of the circuit and its operation are discussed in Section 3.8 on data processing. After the centroid of the return pulse is located, a stop signal is sent to the range clock. The reading of the clock is then transferred to the data storage bank for telemetry to the ground station.

In addition the signal is fed into a circuit that determines the pulse shape. This information is important in the determination of the sea state and the visibility just above the ocean surface, for oceanographic and meteorological purposes.

3.3.7.2 Photo Detector

A photomultiplier is used to convert the optical signal return to an electrical signal. At present this conversion efficiency is about 3 percent, but in private conversations with the manufacturers of these tubes, it was indicated that an efficiency of 12 percent may be expected in the years 1970, 1971. The increase in efficiency is due to a new photocathode material combined with a multiple reflection technique.

This technique uses a series of reflections between the cathode material and the face plate of the tube to convert more of the optical energy into photoelectrons.

3.3.8 DATA PROCESSOR

The data processor or centroid detection circuit is shown in Figure 3-8. The circuit used to determine the centroid of the transmitter pulse is almost identical to that used by the receiver except it does not include the matched filter and the pulse form processor. As shown in Figure 3-8, the output of the photomultiplier-amplifier combination enters a matched filter (integration time t_i of 20 nanoseconds) and threshold circuit to identify the signal from the noise background. The integration time is based on the following: A pulse of 12 nanoseconds width between the half intensity points is emitted by the laser. This length is enlarged before it reaches the matched filter in the receiver by the irregular sea surface, the oblique angle of incidence and the receiver. The contribution from the sea surface is about 4 nanoseconds, from the oblique incidence 2 nanoseconds and from the receiver about 3 nanoseconds, for a total enlargement of 9 nanoseconds. Thus, the pulse length at the input of the matched filter is about 20 nanoseconds which should also be the integration time of the filter.

The photomultiplier output also enters a delay line so that the entire pulse may be re-examined after it is detected. When threshold is exceeded, a gate following the delay line is closed. The signal is sent to an integrator. Since the time at which the integral reaches

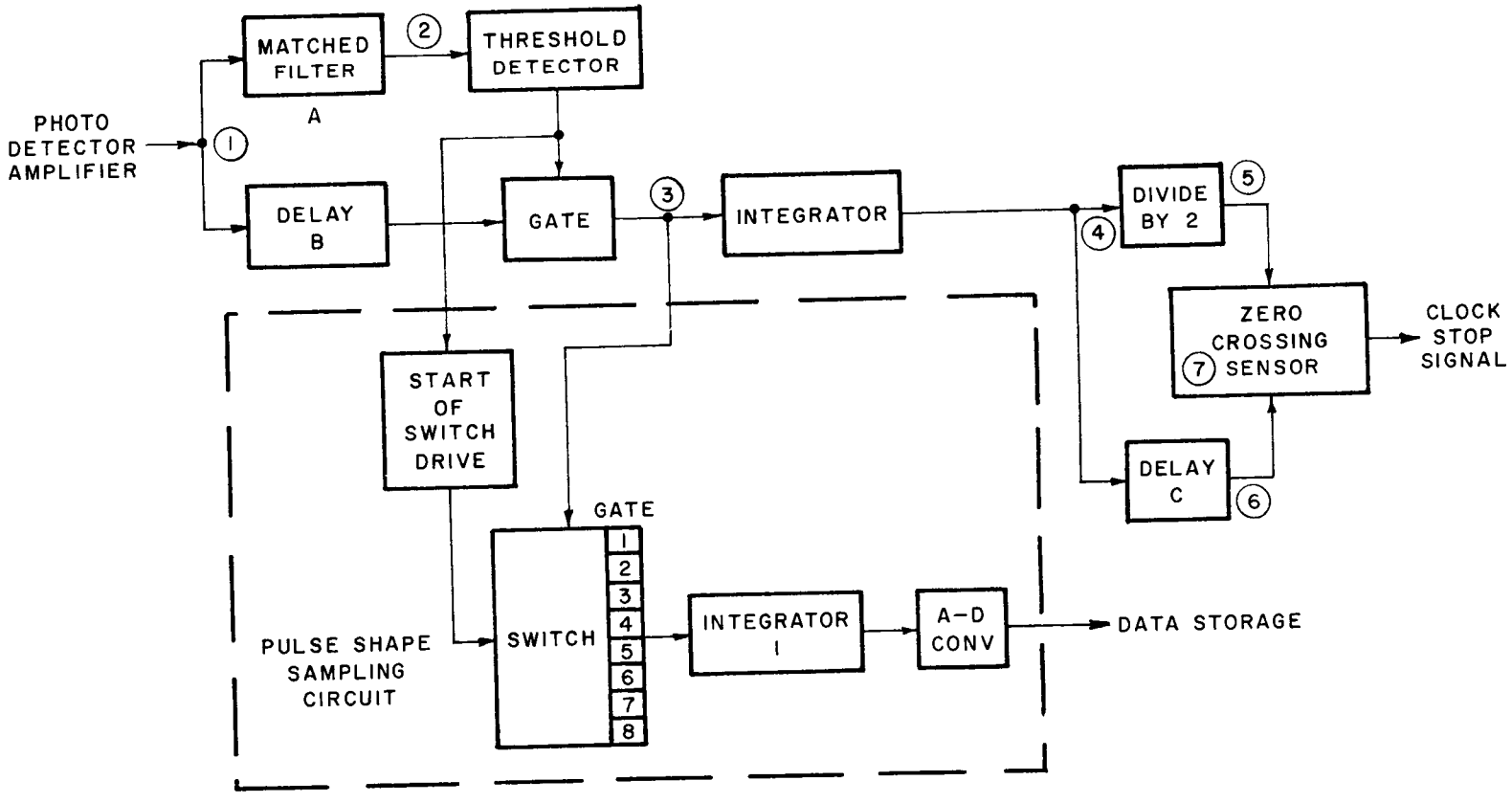

Figure 3-8 Block Diagram of Data Processor

half its final value is desired for locating the pulse centroid, the half amplitude is subtracted from the delayed output of the integrator as illustrated in the block diagram. When the difference crosses zero the centroid is located and the range clock is stopped. A correction is applied to the range reading to compensate for the delays in the circuit. A signal vs time diagram is given in Figure 3-9. The expected delays are the time constant of the matched filter A (10 nanoseconds), the delay in circuit B (25 nanoseconds) and the delay in circuit C (40 nanoseconds).

The additional parameter of echo pulse length may be desired for evaluation of the sea state. The rougher the sea the longer the pulse will be. One method of determining pulse length is to divide the time period containing the signal into several intervals and counting the number of intervals containing the signal.

The sampling of the pulse shape takes place after the gate by switching the signal at 5 nanosecond intervals into integrators. The switchdrive starts when the presence of a pulse is indicated by the threshold circuit. Eight intervals of five nanoseconds each will yield the pulse length to a total accuracy of about five nanoseconds for large signal returns. The pulse shape sampling circuit is not needed to provide the altimeter reading but is an option that can be used to determine sea state.

3.3.9 CLOUD DETECTOR

The detection of the presence of clouds in the path of the laser altimeter is of value in preventing unnecessary pulses. By preventing the laser from firing, flashlamp lifetime will be increased and power consumption will be reduced.

Clouds can be detected by monitoring the sunlight reflected from the target below in the daytime or by using a radiometer to determine the background temperature for operation at night. A combination of

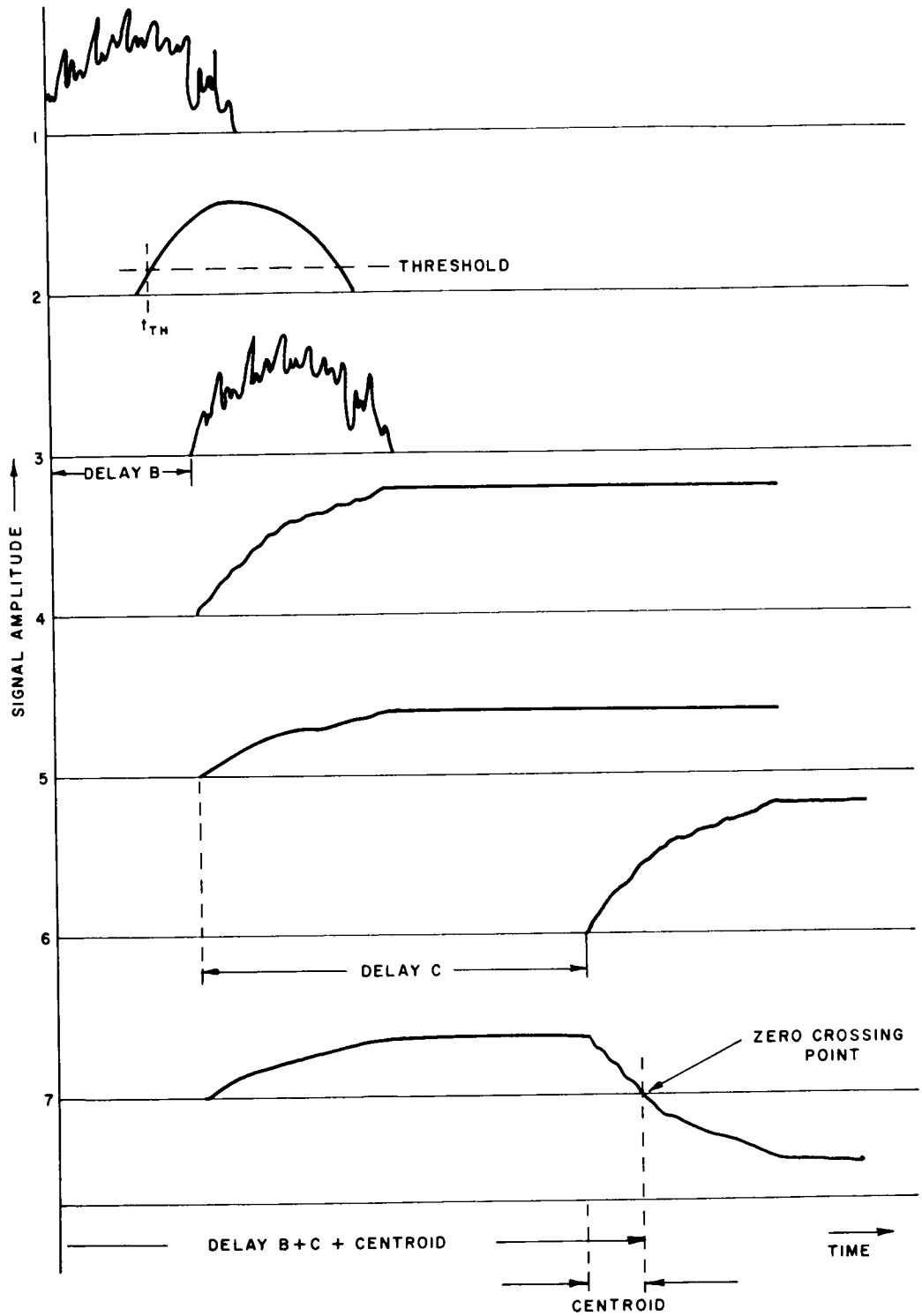

Figure 3-9 Signal vs Time Diagram of the Signal Processor

both can be used, thereby increasing reliability. The application of a radiometer for this purpose is well developed and is being used in cloud mapping by the Nimbus satellite.

The detector used to measure the sunlight reflected from clouds is simpler in approach and construction. Its utilization is based on the fact that clouds are good reflectors for sunlight and water surfaces are not.

The device consists of a telescope with a one-inch aperture, an S-20 photomultiplier, power supply, and a current threshold circuit. The device could be designed so that a signal higher than a given threshold would indicate the presence of a cloud. It would work during the day when the sun is at least 20^{o} above the horizon. With the sun high in the sky, a field-of-view on the sea of one kilometer, an aperture size of one inch, and a photomultiplier gain of 10^{5}, a current of about 0.2 milliampere can be expected at the output of the photomultiplier in the presence of a cloud. The return when there is no cloud can be as high as about 0.04 milliampere, a factor of five less. If threshold is set at 0.06 milliampere, clouds are detected whenever the sun is more than 20^{o} above the horizon, since the return varies with the sine of the elevation angle.

This cloud presence indicator would be operable a maximum of 40% of the time for positions of the sun close to the plane of the satellite orbit and a minimum of zero hours when the orbital plane is nearly perpendicular to the direction of the sun, unless the threshold is made adjustable.

3.3.10 SYSTEM WEIGHT

Weight of the altimeter package excluding fixtures necessary to mount it in the satellite is 33 kilograms (72.5 lbs.). A breakdown of the weight of the individual elements that make up the system is given in Table 3-1.

TABLE 3-1

WEIGHT DISTRIBUTION

DC-DC converter	0.9 kg	2.0 lb.
Energy storage network	15.9	35.0
Charging network	1.8	4.0
Laser head	2.0	4.5
Photodetector	0.5	1.0
Optics	2.7	6.0
T-R switch	0.2	0.5
Receiver electronics	2.7	6.0
Mechanical parts	2.9	6.5
Pump heat exchanger	2.7	6.0
Cloud detector	0.5	1.0
Total weight	32.8 kg	72.5 lb.

As the table shows, the capacitor bank contributes quite significantly to the system's weight and if a breakthrough in laser technology results in a higher efficiency than can be obtained at present, a substantial reduction in weight can be realized.

3.3.11 SYSTEM VOLUME

The system volume can be derived from Table 3-2 to be about 73,500 cc (2.6 cubic ft.) contained mainly in a cylindrical shape of about 50 cm in diameter and 50 cm in length.

The major portion of the volume requirements is determined by the size of the telescope. Unless a laser with more output power is used, adding weight and power consumption, no reduction in optics size can be expected during the next few years.

TABLE 3-2

VOLUME

Optics	56,000 cc
Receiver	2,000
Laser Transmitter	9,000
Laser Power supply	4,000
Pump, heat exchanger	600
Receiver and electronics	1,700
Cloud detector	200
Total	73,500 cc or 2.6 cu.ft.

TABLE 3-3

POWER CONSUMPTION

Laser transmitter	65 watts
Receiver and data processor	3.5
T-R switch	0.5
Cloud detector	1.0
Cooling pump	5
Total	75 watts

During standby due to cloud cover, the power drain drops to 1 watt and when the system is on standby over land areas or on command of the ground station, the power consumption can be as low as .25 watts with only the telemetry receiver operating.

Significant reduction of the power drain can be expected if the laser efficiency can be increased by more selective pumping.

3.3.13 DATA STORAGE AND TELEMETRY

The data storage and telemetry functions are graphically illustrated in Figure 3-10.

The uplink command transmits a pulse number and a time of firing into the data bank. Also, an estimated range value is recorded for each pulse for the range gate setting. The spacecraft carries its own time clock so that the data bank starts the transmitter charge cycle about 10 seconds before ignition time. At the time that the measurement has to be made ignition commands are given to the transmitter and the range gate is set. Range clock readings are recorded in the data storage bank upon return of the range pulse. Amplitude information relating to the pulse shape, attitude angle information and output energy readings are also simultaneously recorded in the data bank. When the satellite comes within reach of a ground tracking station the pulse number is transmitted together with the range clock reading, attitude angle reading, pulse shape and output energy readings. Data reduction is avoided in the satellite in an attempt to keep the system as simple and reliable as possible.

Telemetry requirements have been computed on a per pulse basis. The mission time between telemetry ground stations and the pulse repetition rate can then be used to compute the total storage and telemetry requirements.

The downlink information per measurement can be broken down as follows:

Pulse number	:	12 binary bits
Clock reading, centroid	:	10 binary bits
Pulse amplitude readings	:	32 binary bits
Pointing angle	:	32 binary bits
Laser energy	:	4 binary bits
Downlink total	:	90 binary bits

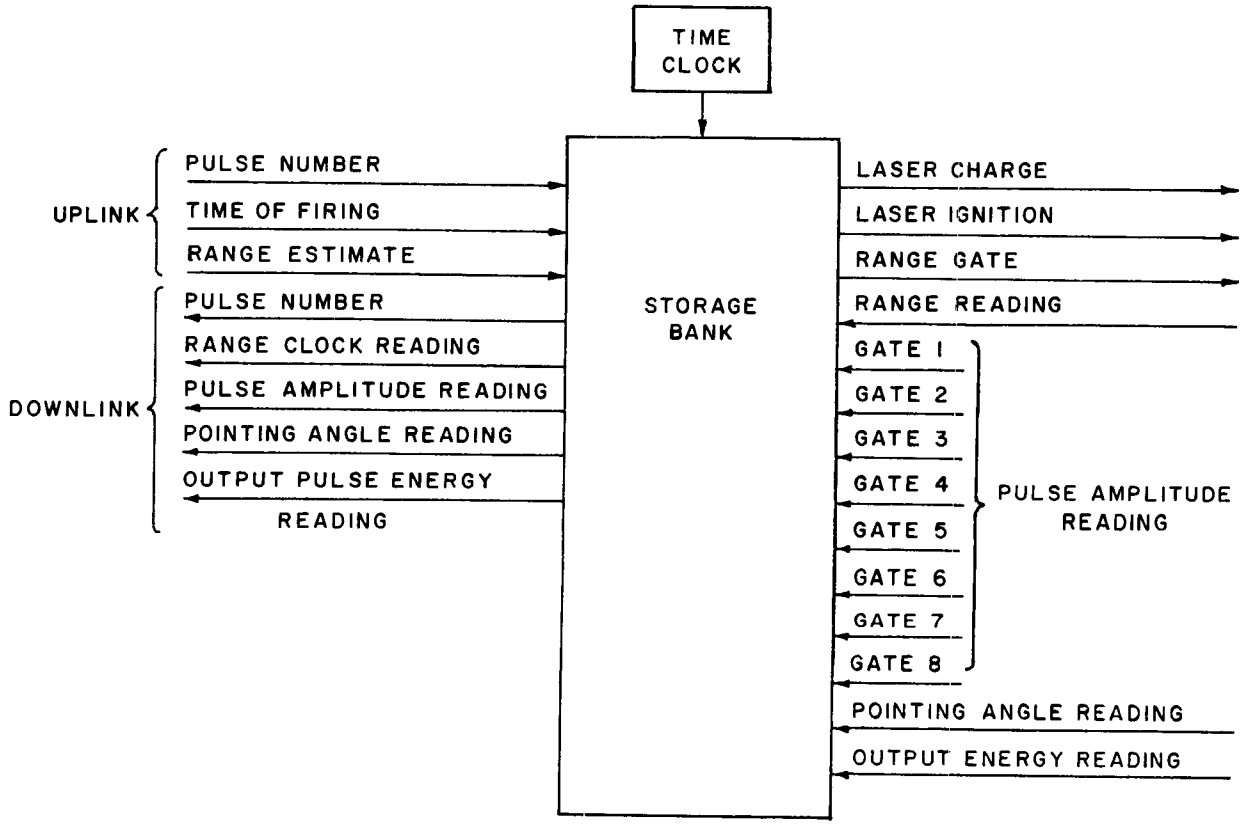

Figure 3-10 Telemetry and Data Storage

For the uplink we have per measurement:

Pulse number	:	12 binary bits
Firing time	:	20 binary bits
Range gate position	:	8 binary bits
	:	40 binary bits

In addition, several housekeeping functions may be monitored and uplink commands such as lamp change or switch "off" and "on" may be required but their use may be infrequent and would not add significantly to the data storage or telemetry requirements.

3.3.14 REQUIREMENTS IMPOSED BY ALTIMETER ON SATELLITE

a. The pointing angle within which the satellite must be oriented for suitable altimeter operation is .25 degrees.

b. Accuracy within which the pointing angle must be known by the altimeter for suitable operation is 15 arc seconds. These requirements weigh heavily in the accuracy of the altimetry system and reduction of the numbers given would increase the accuracy of the altimeter.

c. There is no constraint on the rate of rotation of the satellite around its vertical axis for altimetry over the ocean. If the instrument is operated over land masses, there may be an uncertainty as to where the actual measurement is being made.

d. Thermal constraints are mainly on the ruby crystal which should be kept at about 275 degrees $K\ ^{+5}_{-20}$. The rest of the system could vary as much as $\pm 50^{o}C$ before losing accuracy.

e. Telemetry - About 130 binary bits of information have to be transmitted between satellite and ground station for every 10 seconds of flight time between readouts.

f. Storage - Data storage has to be provided for an equal number of binary bits for each 10 seconds flight time between readouts.

g. A prediction has to be provided for the altitude of the spacecraft versus time and switch "on" and "off" times have to be transmitted to indicate land masses.

3.4 SYSTEM CONSIDERATIONS

3.4.1 INTRODUCTION

The following section describes the analysis that has led to the selection of the altimeter system described in the previous section. It deals with the level of confidence of making a true detection of the return pulse, the probability of false alarm signals and the accuracy that can be obtained in the range reading. One of the major areas of concern in the accuracy analysis is the error introduced by the sea state uncertainty. This is treated in great detail in Section 3.4.4.9. In addition, Section 3.4.5,6 describes the system's limitations and its ability to meet the geodetic requirements. Capabilities of the system over land areas are discussed in Section 3.4.7.3.

3.4.2 LASER ENERGY ANALYSIS

In the operation of the laser radar, the optical pulse is transmitted to the target and its echo detected by opening the receiver gate and waiting for a signal greater than the threshold level. The threshold is designed to shut out the noise. The energy of the laser must be sufficient to return a signal consistently larger than the threshold. The noise, false alarm and detection probabilities determine the minimum signal amplitude to insure detection.

3.4.2.1 Probability of False Alarm

To obtain the probability of false alarm, a certain number of steps have to be taken in the proper sequence. These are:

a. Calculation of the noise from:

1. Dark current

2. Atmospheric backscatter of the transmitted signal

3. Scatter from the atmosphere and ocean surface due to sunlight illumination

b. Calculation of the probability of false alarm. This factor depends on the total noise received, the gate width and the receiver integration time.

3.4.2.1.1 Noise Due to Receiver Dark Current

To get sufficient gain in the first stage of the receiver, a photomultiplier type detector has to be used. These detectors exhibit a random emission of photoelectrons from the photocathode resulting in a dark current. For most commercially uncooled photomultipliers with a photosensitive surface suitable for operation in the wavelength region of interest, the amount $\bar{n}_{d.c.}$ of photoelectrons which can be attributed to dark current is about 10^4 photoelectrons/second. This means that during the integration time t_i the average total number of dark current photoelectrons is:

$$n_{d.c.} = 10^4 \, t_i \tag{3-1}$$

The integration time t_i is related to the matched filter bandwidth and thus $t_i \approx 20 \times 10^{-9}$ seconds.

3.4.2.1.2 Laser Backscatter

The amount of photoelectrons which are emitted by the photocathode as a result of the received signal due to laser backscatter may be written as:

$$n_{B.S.} = \frac{E_T \, \eta_o \, \eta_Q \, C \, t_i \, \pi \, D_R^2 \, \Gamma_A \, \sigma \, e^{-2\bar{R}\sigma}}{8h \, \nu \, R^2} \tag{3-2}$$

where:

E_T = transmitter output power in joules

η_o = overall optical transmission efficiency 40%

η_Q = quantum efficiency of the photocathode 12%

C = speed of light 3×10^5 km/sec

D_R = effective diameter of the receiving optics

Γ_A = atmospheric backscatter anisotropy parameter $\frac{1}{8\pi}$

σ = extinction coefficient (km^{-1})

$\bar{R}$ = effective thickness of the atmosphere 1.5 km

h = Planck's constant 6.62×10^{-34} joules sec

ν = frequency of the laser radiation 4.3×10^{14} Hz

R = spacecraft altitude 1000 km

Because the atmosphere changes optical density and therefore σ as a function of altitude, we have taken σ at sea level and an effective thickness of the atmosphere of 1.5 km. From formula (3-2)

$$n_{B.S.} = (8.15 \times 10^{8})\, E_T\, t_i\, D_R^{\,2}\, \sigma\, e^{-3\sigma} \text{ photoelectrons.}$$

3.4.2.1.3 Noise Due to Backscatter from Atmosphere and Ocean Surface Due to Sunlight Illumination

During daylight operation, the sun causes backscatter noise to be received by the system from the atmosphere and the ocean surface. This return may be related to be albedo of the earth so that the amount of photoelectrons due to solar backscatter becomes

$$n_{S.B.S.} = \frac{I_s(\theta,\lambda)\,\Omega_R\,\Delta\lambda\,\pi\,D_R^{\,2}\,\eta_Q\,\eta_{o\,x}}{4\,h\,\nu}\left[\Gamma_A(1-e^{-\bar{R}\sigma}) + (\rho.G)\,e^{-2\bar{R}\sigma}\right] t_i \qquad (3\text{-}3)$$

$I_s(\theta,\lambda)$ = the solar power in watts/m^2 Angstrom and is a function of the angle θ with the normal to surface of the earth and the center frequency related to λ. I_s (0, 7000) ~ .15 watts/m^2 $\mathring{A}$

$\Delta\lambda$ = the optical filter bandwidth 20 $\mathring{A}$

Ω_R = solid angle subtended by the receiver field of view

$\rho.G$ = the ocean effective reflectivity at vertical incidence .025.

The term Γ_A $(1-e^{-\bar{R}\sigma})$ is due to the backscatter from the atmosphere and the term $(\rho.G)$ $e^{-2R\sigma}$ is due to the backscatter of the ocean surface. Using the above mentioned parameters the formula (3-3) becomes

$$n_{S.B.S.} = (4x10^{17})\ t_i\ D_R^2\ \Omega_R \left[\frac{1}{8\pi}\ (1-e^{-1.5\sigma}) + .025e^{-3\sigma}\right] \qquad (3-4)$$

Clouds may also produce solar backscatter, but in the envisioned system concept, a cloud detector will prevent operation of the ranging system if illuminated clouds are in the field of view of the receiver.

3.4.2.1.4 Total Receiver Noise

The amount of photoelectrons due to all noise sources during daytime operation can now be written as:

$$n_{(day)} = t_i \left[10^4 + \left\{8.15 \times 10^8\ E_T\ \sigma\ e^{-3\sigma} + 4.0 \times 10^{17}\ \Omega_R \left[\frac{1}{8\pi}\ (1 - e^{-1.5\sigma}) + .025e^{-3\sigma}\right]\right\}\ D_R^2\right] \qquad (3-5)$$

For night time operation the third term equals zero so that we get

$$n_{(night)} = t_i \left[10^4 + 8.15 \times 10^8\ E_T\ D_R^2\ \sigma\ e^{-3\sigma}\right] \qquad (3-6)$$

For daytime operation the third term of formula (3-5) varies from .024 for clear air (σ = .14) to .03 for $\sigma > 1$. Since the variation is small, we consider the worst case, which is σ = 0.1 and the third term becomes $1.2 \times 10^{16}\ \Omega_R$. Differentiating the second term in formula (3-5) shows that it reaches a maximum for σ = .33, so if we use this value the second term becomes

$1.0 \times 10^8\ E_T$ as a worst case.

The first term in (3-6) is therefore always much less than the other terms so that we may write

$$n_{(day)} = \left[1.0 \times 10^{8} E_T + 1.2 \times 10^{16} \Omega_R\right] t_i D_R^2 \quad (3\text{-}7)$$

$$n_{(night)} = \left[1.0 \times 10^{8} E_T\right] t_i D_R^2 . \quad (3\text{-}8)$$

3.4.2.1.5 False Alarm Probability

Taking a field of view of 10^{-7} steradians, corresponding to a 350 meter spot size, we find from equation 3-7 that

$$n_{day} = (1.2 \times 10^{9}) t_i D_R^2 \quad (3\text{-}9)$$

The probability of false alarm can now be found from

$$P'_{fa} = \frac{P_{fa} t_i}{t_g} \quad (3\text{-}10)$$

P'_{fa} = probability that more photoelectrons are received from the noise sources during the integration time than allowed by a predetermined threshold level

t_g = gate time or the time that the photomultiplier is operative

P_{fa} = total probability that more photoelectrons are received from the noise sources than allowed by the threshold setting during the range gate time t_g.

For a P_{fa} of 1%

$$P'_{fa} = \frac{2.0 \times 10^{-10}}{t_g}$$

and for a P_{fa} of .1%

$$P'_{fa} = \frac{2.0 \times 10^{-11}}{t_g}$$

In both cases we can derive n from formula (3-8) and (3-9) to be

$$n_{(day)} \simeq 24\ D_R^2 \quad \text{and}$$

$$n_{(night)} \simeq 2\ D_R^2$$

Using Poisson's statistics, we can now determine the threshold level necessary for such P'_{fa} via

$$P'_{fa} \geq \sum_{K=n_t}^{\infty} \frac{n^K e^{-n}}{K!} \tag{3-11}$$

Taking $t_g = 3 \times 10^{-6}$ seconds we solve for n_t and find that a threshold level $n_t = 19$ photoelectrons is sufficient to guarantee a probability of false alarm smaller than .1% during daytime operation and 5 photoelectrons for operation at night for 50 cm receiving optics.

3.4.2.2 Probability of Detection

The probability of detection is defined by

$$P_D = \sum_{K=n_t}^{\infty} \frac{n_s^K e^{-n_s}}{K!} \tag{3-12}$$

n_s = the amount of photoelectrons which can be attributed to the signal input.

If we wish $P_D = 99\%$ we will find $n_s = 30$ photoelectrons or $n_s = 25$ photoelectrons for $P_D = 90\%$ using 50 cm diameter optics and daytime operation. For night time operation $n_s = 10$ photoelectrons for $P_D = 99\%$ and 8 photoelectrons for $P_D = 90\%$.

3.4.2.3 Calculation of Transmitter Energy for Detection

We can obtain the required transmitter energy for detection from

$$n_s = \frac{E_T D_R^2 \eta_o \eta_Q (\rho G) e^{-2\sigma \bar{R}} \pi}{4 h \nu R^2} \qquad (3\text{-}13)$$

or,

$$E_T = (3.0 \times 10^{-4}) \frac{e^{3\sigma} n_s}{D_R^2}$$

The results of this calculation are presented in Figure 3-11 for different atmospheric conditions during day and night operation. In meteorological terms, very clear atmosphere corresponds to a visibility of 28 kilometers, clear to 7 kilometers and light haze to 3.5 kilometers. For a 50 cm optics diameter one can see that a 500-millijoule system can still satisfactorily operate if the visibility is slightly less than 7 km with a probability of detection of 90% and a probability of false alarm of .1%.

The curves also show that increase in power above the .5 joule level does not cause a significant increase in detectability. The power requirements derived above insure that the return signal is detected. However, the accuracy that is needed for the altimeter measurements may impose more severe requirements on the system pulse power. This requirement is discussed in Section 3.4.4.2.

3.4.3 OCEAN REFLECTIVITY

In Section 4.1.1.3 an ocean effective reflectivity ρG of 2.5 percent was used in the calculation of the noise due to solar backscatter. The same value also applies to the reflectivity encountered by the laser signal for the purpose of the energy analysis. The factor ρ is the reflectivity (ratio of reflected power to incident power) of a flat water surface at normal incidence and can be calculated with Fresnel's law to be .02 for wavelengths in the visible spectrum. The gain G is

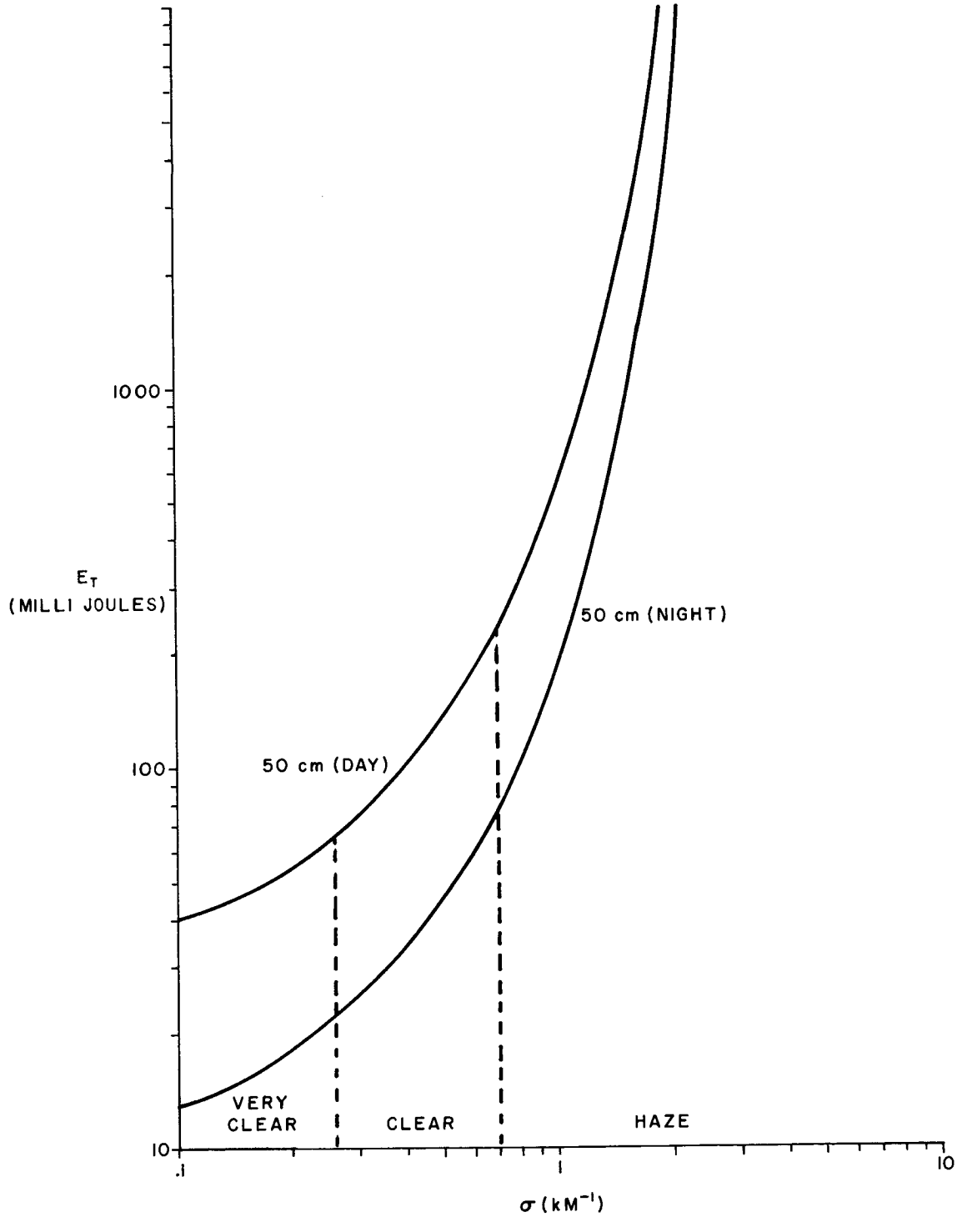

Figure 3-11 Required Energy for Detection: P_D = 90%; P_{fa} = .1%

the factor describing the relationship between the returned energy and the angle between the normal and the point of observation with respect to a source radiating into a one steradian solid angle.

The energy returned from the ocean surface is, however, dependent upon spot diameter, the structure and shape of the ocean surface and wavelength. No measurements have been made under the conditions with which the altimeter system operates and therefore an estimate of ρG has to be made based on measurements taken by different systems and under different conditions. The information we have available is obtained with small spot size laser systems with spot diameters of 30 feet and one foot operating at a wavelength of 1.06 and 10 micron and from measurements of the sun glitter patterns.[3,4,5]

G can be calculated from the measurements at 1.06 micron to be 0.6 while from the measurements at 10 microns, G can be calculated to be 1.25. The gain that can be calculated from the sun glitter pattern is about 60. The spread between the gain based on different observations indicates that no fixed number can be used for the effective reflectivity until a program of testing has been performed.

3.4.4 ERROR ANALYSIS

Many parameters in the measuring system are sources of error and influence the accuracy of the measurements. The following sections describe the different sources of error, their order of magnitude and how they influence the design requirements of the altimeter system.

3.4.4.1 Pulse Length

The finite length of the pulse introduces an error since precise location within the received pulse is ambiguous. The absence of clean rectangular shapes on the transmitted and received pulses renders the leading edge an inaccurate reference. A more accurate reference is the center of the pulse. The accuracy is a function of the pulse length and amplitude.

The shape of the output pulse is a function of the photon gain in the laser crystal and cannot be altered at will. In general the pulse shape of a Q-switched ruby laser is close to a Gaussian curve. The variation in the received signal amplitude, which for the low photon levels of laser echos, can be considerable in relation to the signal, causes a variation in the time at which the threshold for signal detection is exceeded, thereby creating a range error. The error could be substantial if the "leading edge" mode of measurement is relied upon. The accuracy is improved by locating the centroid of the pulse and perhaps also the trailing edge, a technique utilized in radar to improve accuracy with low signal-to-noise ratios. The centroid detection technique consists of finding the centroid of the pulse by integrating it and locating the point at which the integral reaches half its final value.

The equation for the range error with centroid detection is derived by determining the apparent offset caused by noise. The noise causes a fractional variation in each half given by the reciprocal of the signal-to-noise ratio. Since the half signal is approximately half the total signal but the noise in each half is the noise for the whole signal divided by the square root of two from statistical considerations, the fractional variation in each half signal is given by

$$\frac{\Delta(S/2)}{S/2} = \frac{N/\sqrt{2}}{S/2} = \frac{\sqrt{2}}{S/N} \qquad (3\text{-}14)$$

where S/N is the signal-to-noise energy ratio for the whole echo. Since this variation can occur in each half, the total fractional difference between the signals is larger by the square root of two:

$$f_s = \sqrt{2} \times \frac{\sqrt{2}}{S/N} = \frac{2}{S/N} \qquad (3\text{-}15)$$

A fractional difference in signal is related to the error in time by the formula

$$\delta\tau \approx \frac{f_s \tau_p}{4} \tag{3-16}$$

for a rectangular pulse, where f_s is the fractional difference in signal and τ_p the pulse length. By substitution,

$$\delta\tau \approx \frac{\tau_p}{4} \times \frac{2}{S/N} = \frac{\tau_p}{2\,(S/N)} \tag{3-17}$$

To account for the irregular shape of the pulse, especially after reflection from a sea surface, the factor of two is arbitrarily removed:

$$\delta\tau \approx \frac{\tau_p}{S/N} \tag{3-18}$$

and,

$$\delta R = \frac{c\delta\tau}{2} = \frac{c\tau}{2\,(S/N)} \tag{3-19}$$

Centroid detection is not seriously affected by large variations in signal amplitude caused by changes in atmospheric transmission and sea reflectivity, since both pulse halves are equally altered. It is the statistical variations in the generation of photoelectrons which degrade the accuracy. The effect of these variations is taken into account through the signal-to-noise ratio in the above formula.

The 1 σ noise-in-signal is given by the square root of the average number of photoelectrons, n_s, (except for very low signal levels). Thus,

$$S/N = \sqrt{n_s} = \sqrt{50 \text{ photoelectrons}} = 7$$

for an average clear day. Noise from other sources is overshadowed by the statistical variations. By substituting this value in the above equation the range error is calculated to be:

$$\delta R = 1.5 \times \frac{1}{7} = \underline{0.21 \text{ meter}}$$

In marginal weather the signal may be as small as the threshold level of 19 photoelectrons in which case the 1 σ error may be as large as 0.5 meter.

3.4.4.2 Pulse Energy

The pulse energy must be considered in the error analysis because it influences the signal-to-noise ratio and thereby the accuracy of the range measurement. In the previous section a signal requirement n_s of 50 photoelectrons is selected based upon range accuracy requirements. The laser energy is calculated from this with the equation,

$$E_T = \frac{n_s \, 4h\nu \, R^2 \, e^{2 \, \sigma \bar{R}}}{\pi \, \eta_o \, \eta_Q \, (\rho \, G) \, D_R^2} \qquad (3\text{-}20)$$

where the symbols are defined in previous sections.

Using an extinction coefficient $\sigma = .70$ we get

$E_T = 500$ millijoules

for

$D_R = 50$ cm

A signal of 50 photoelectrons is much greater than the signal contributed by the daytime background noise. Therefore, night operation does not offer any advantage over operation during daytime.

Other parameters influence the signal-to-noise ratio, the atmospheric transmission and the receiver aperture diameter. Using a pulse length of 10 nanoseconds and a transmitter power of .5 joule the range error has been computed for various atmospheric transmissions and an aperture size of 50 cm. The resulting range error has been plotted in Figure 3-12.

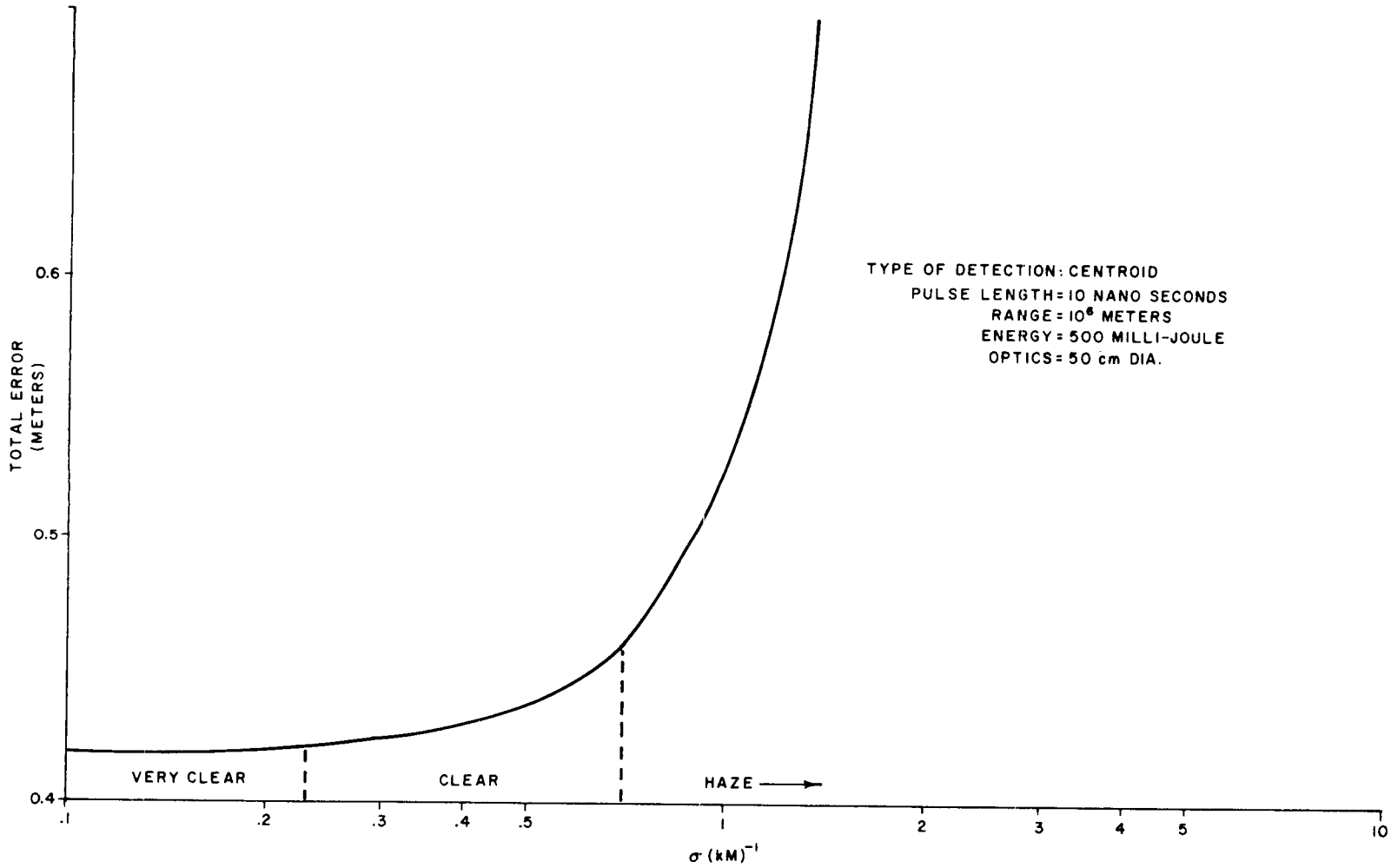

Figure 3-12 Range Error vs Atmospheric Transmission

3.4.4.3 Angular Uncertainty

Although the satellite will be directionally stabilized, an offset from the normal to the ocean surface is likely to occur (see Figure 3-13). If this offset is not measured precisely, an error in altitude could result. The formula for the error can be shown, for the worst case of the offset error in the same direction as the offset, to be:

$$\delta R_{\theta} \approx H\ \theta\ \delta\theta \qquad (3\text{-}21)$$

where:

δR_{θ} = range error from angular uncertainty

H = altitude

θ = offset angle

$\delta\theta$ = error in measuring the offset angle

Star trackers deliver a measurement accuracy of about 10 arc-seconds in each angle. With an offset of 0.25 degree and an altitude of 1000 kilometers, the range error is 0.2 meter. The error is plotted as a

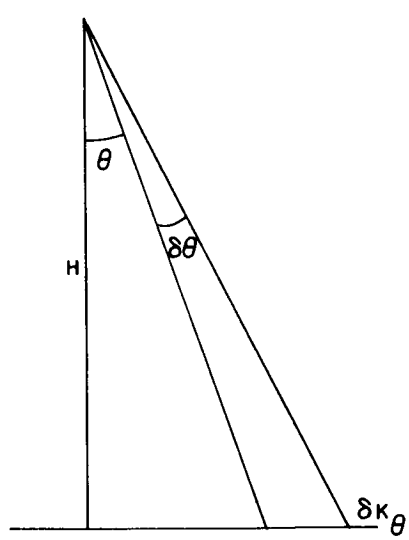

Figure 3-13 Angular Uncertainty

function of angular uncertainty and offset angle in Figure 3-14. If no angle measuring device is utilized and the satellite is assumed vertical, the offset must be restricted to one milliradian (0.05°) to prevent the range error from exceeding 0.2 meter.

3.4.4.4 Beam Width

The angular offset contributes an additional error through the elongation of the pulse at oblique angles of incidence to a flat target. The pulse elongation is given in terms of range as,

$$\delta R' \approx D\ \theta \qquad (3\text{-}22)$$

where:

$\delta R'$ = pulse elongation in range from oblique angles

θ = offset angle

D = diameter of the illuminated spot on the sea surface

The error is smaller than the elongation by roughly a factor of 4 if leading edge detection is utilized, and is smaller yet with pulse centroid detection. Thus the error is estimated to be

$$\delta R_b \approx 0.1\ D\ \theta$$

where δR_b is the range error from pulse elongation at oblique angles of incidence. To confine the error to 0.1 meter, the beam size should not exceed 200 meters, assuming a 0.25 degree maximum offset.

3.4.4.5 Atmosphere

The atmosphere extends the length of the optical path by about two meters through its refractive index. This enlargement is a function of temperature, pressure and water vapor content. However, since these parameters are not measured but must be estimated, based upon location and time of year, the accuracy with which the path enlargement is determined is limited to about ±0.1 meter at 6943Å. Therefore,

$$\delta R_a \approx 0.15 \text{ meter}$$

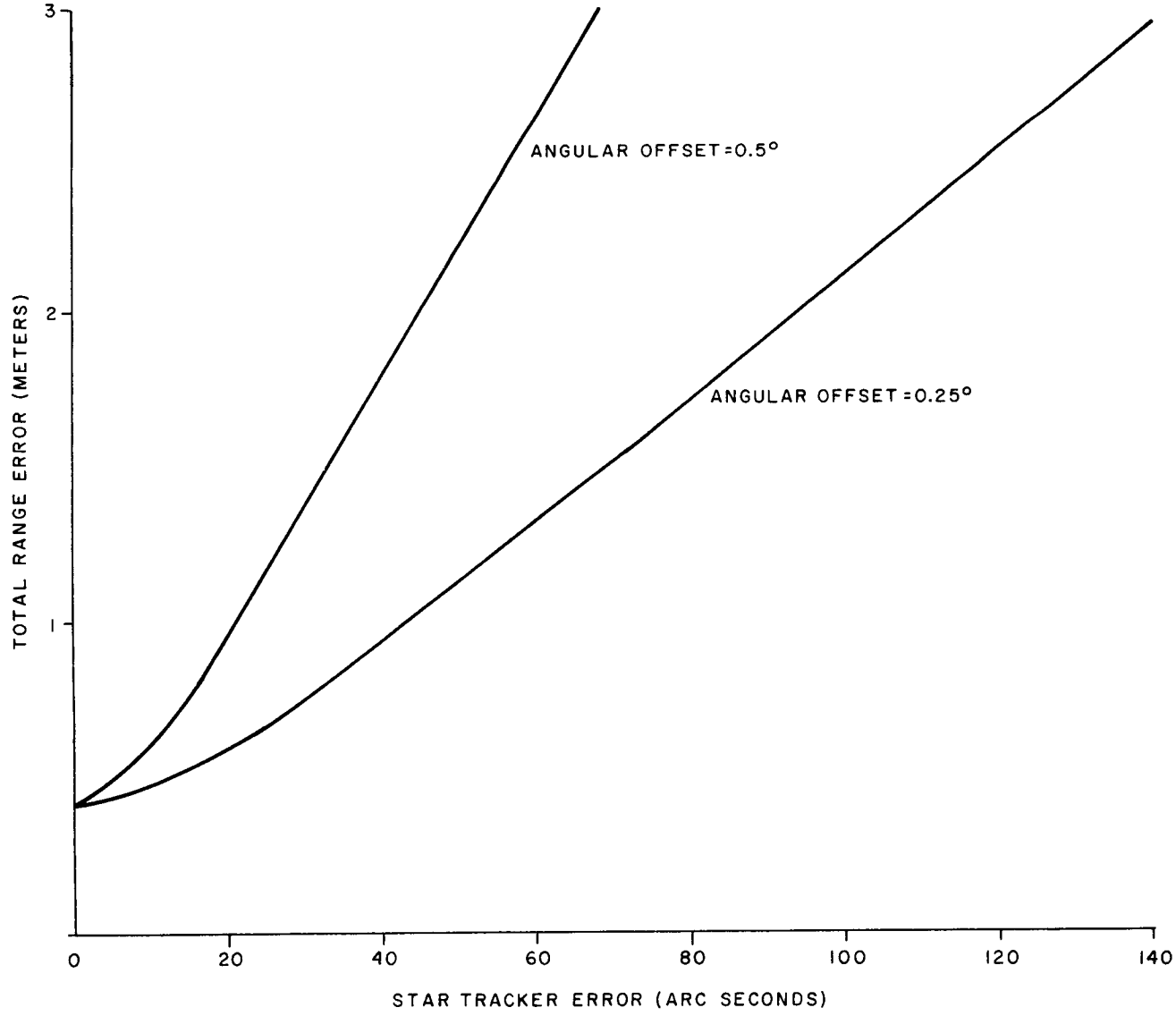

Figure 3-14 Total Range Error vs Angular Uncertainty

where δR_a is the range error due to the atmosphere. Appendix L-A treats the atmospheric fluctuation in greater detail.

3.4.4.6 Receiver

The receiver introduces errors in several ways. It elongates the pulse in the photomultiplier and the matched filter, and it various the amplitude due to the variation in gain for each photoelectron. There are long term errors stemming from variations in the characteristics of the receiver, temperature variations and changes in the threshold level. Most of these errors should be minimized by using centroid detection rather than the leading edge technique alone, but some residual error is to be expected.

The major portion of the error is contributed by the limited accuracy of the receiver in locating the apparent centroid. Sophisticated techniques may be utilized, but a residual error of one-twentieth the received pulse length (of about 20 nanoseconds) is assumed. Combining the individual errors by root-sum-square the error contributed by the receiver is calculated to be 0.2 meter.

For a breakdown of the error introduced by the individual elements of the receiver see Figure 3-15.

3.4.4.7 Clock

The clock introduces errors in two ways, through the instability during the pulse transit time and the digital readout. The clock should maintain a stability of one part in 10^8 during the transit time of about 6 milliseconds. This results in a range error of 0.01 meter which is negligible.

The digital readout rounds off the elapsed time to some integral number of nanoseconds. If the resolution is two nanoseconds, the maximum error is ± one nanosecond or ± 0.15 meter in range. Since 1 σ error values are of interest an error of 0.1 meter is assumed, which corresponds to the 67% probability level. For a two nanosecond resolution a

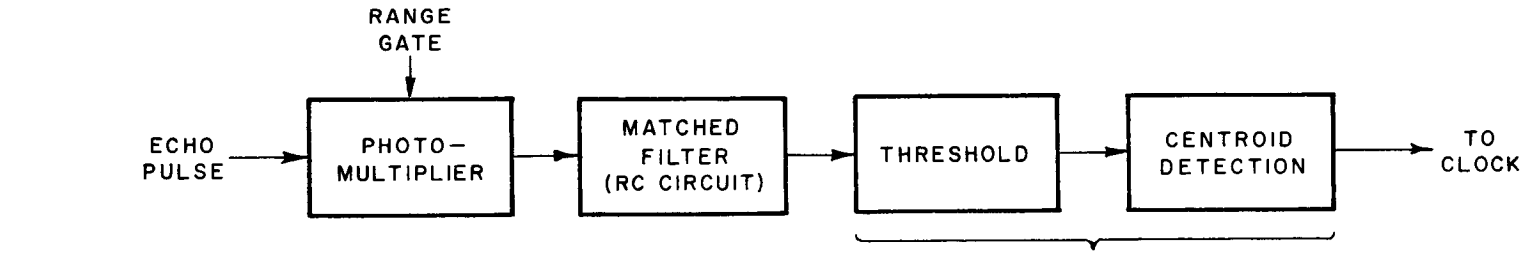

EFFECTS:	PULSE ELONGATION ≈2 NSEC	AMPLITUDE VARIATION ≈10% FOR EACH HALF OF PULSE	PULSE ELONGATION ≈4 NSEC	ACCURACY IN LOCATING APPARENT CENTROID ≈1 NSEC
CONTRIBUTION TO RANGE ERROR:	0.03	0.1	0.06	0.15 METER

ROOT-SUM-SQUARE = 0.2 METER

Figure 3-15 Receiver Error Tabulation

clock frequency of 500 megacycles/sec is required. The counter should be free of mistakes in counting, specifically, no pulse should be missed. The readout need only have the last three or four digits because the initial ambiguity in altitude is limited to about ± 1000 nanoseconds (150 meters). Since the digital readout error is encountered on both the start and stop pulses, the total error is $\sqrt{2} \times 0.1$ or about 0.15 meter.

3.4.4.8 Calibration

The measured distance differs from the true optical path length due to factors which are present for all measurements. These include the delay in the receiver, in particular the photomultiplier, the difference in path length through the optics, and the separation of the triggering time for the transmitted pulse from the pulse centroid, detected upon return. These differences are calibrated either experimentally or analytically, and the resultant error is small. If the range-finder is experimentally calibrated over, say, a one-kilometer path which is independently measured to better than one part in 10^5, the residual calibration error should be limited only by the resolution of the digital readout, which amounts to about 0.15 meter (δR_{cb}). Variations in the receiver characteristics with time and temperature may alter the calibration correction so that periodic recalibration and temperature measurement may be necessary. In principle, at least, these can be satisfactorily performed periodically in orbit.

3.4.4.9 Sea State

3.4.4.9.1 Computed Error

Since the distance from the satellite to mean sea level must be measured with a high degree of accuracy, the nonuniform sea surface caused by wind waves must be accounted for in the signal processing.

One method of obtaining an estimate of mean sea level is to illuminate a large area of sea surface, and hence, average over many waves. Because of beam attitude offset from the vertical, the laser illuminated

spot must be less than about 200 meters in diameter. (See section 3.4.4.4.) Since this is on the order of a wavelength for ocean waves, significant fluctuations in the measured mean sea level might be expected.

For reasons discussed earlier, the processing of the returns for maximum signal accuracy will include finding the centroid of the received pulse. In order to obtain some idea of how the centroid of the return pulse differs from the actual mean sea level, a simplified model of the ocean surface and transmitted beam was assumed and a computer program was written to compute the difference between the mean sea level and the centroid of the return signal. This difference could then be examined under varying conditions of sea surface, to provide some idea of the random error generated.

The ocean surface was assumed to consist of a one-dimensional sinusoid of arbitrary phase. The laser beam was assumed to be a one-dimensional Gaussian in space and Gaussian in time. The transmitted pulse was allowed to strike the model sea surface normally and the centroid of the return signal was computed. The ocean wave was represented by the relation

$$y = A \cos\left(\frac{2\pi x}{L} - \phi\right) \tag{3-23}$$

Then the slope is

$$\frac{dy}{dx} = \tan\theta = -\frac{2\pi A}{L} \sin\left(\frac{2\pi x}{L} - \phi\right) \tag{3-24}$$

where

A = 1/2 peak-to-trough amplitude of the wave

L = the spatial wavelength

ϕ = phase of wave

$\tan\theta$ = slope of wave

y = vertical distance from mean sea level

x = horizontal distance from the center of the illuminated spot

The energy returned from a point "x" along the wave is

$$\Delta E_R(x) = \frac{\rho_o \ \Delta E_o}{2\pi \ \sigma_1 \ \sigma_2} e^{-\frac{x^2}{2\sigma_2^2}} e^{-\frac{1}{2}\left(\frac{2\pi A}{L\sigma_1}\right)^2 \sin^2\left(\frac{2\pi x}{L} - \phi\right)} \tag{3-25}$$

where

ρ_o = reflectivity of water for normal incidence

ΔE_o = incident energy per unit length

$\Delta E_R(x)$ = the energy received per unit length at a position "x"

σ_1^2 = variance of the beam pattern reflected from the sea surface

σ_2^2 = variance of intensity in the transmitted beam

E_o = total incident energy

Let,

$$k = \frac{\rho_o \ E_o}{2\pi \ \sigma_1 \ \sigma_2}, \quad \alpha = \frac{1}{2}\left(\frac{2\pi A}{L\sigma_1}\right)^2 \tag{3-26}$$

The total energy received at a particular time is

$$E_R(t) = k \sum_{n = 0, \pm 1, \pm 2 \ldots} e^{-\frac{x^2}{2\sigma_2^2} - \alpha \sin^2\left(\frac{2\pi x}{L} - \phi\right)} \tag{3-27}$$

where

$$x = (+ \text{ and } -) \frac{L}{2\pi}\left[\cos^{-1}\left(-\frac{ct}{2A} + 1\right) + \phi\right] + nL \tag{3-28}$$

The above result is the received waveform for a transmitted pulse which is a delta function in time. Thc actual pulse is Gaussian in time so that the resultant received pulse is given by the convolution of the two functions, i.e.,

$$\bar{E}_R(t) = \int_{-\infty}^{\infty} \left[\frac{e^{-\tau^2/2\,\sigma_3^2}}{\sqrt{2\pi\,\sigma_3^2}} \right] E_R(t - \tau)\, d\tau \qquad (3\text{-}29)$$

and the centroid is

$$C = \frac{\int_{-\infty}^{\infty} t\, \bar{E}_R(t)\, dt}{\int_{-\infty}^{\infty} \bar{E}_R(t)\, dt} \qquad (3\text{-}30)$$

By appropriate mathematical transforms (see Appendix L-B), it can be shown that the centroid is independent of the transmitted Gaussian pulse; thus,

$$C = \frac{\int_{-T}^{T} t\, E_R(t)\, dt}{\int_{-T}^{T} E_R(t)\, dt} \qquad (3\text{-}31)$$

A computer program was written to perform the necessary summations and integrations. The parameters were varied and the difference between the centroid and the mean was tabulated. In the computer program run, the laser spot size was taken to be 200 meters, and the variance in the reflected energy from small patches of ocean assumed to be that which would yield a beamwidth or $\pm 25^{\circ}$ at the 3 dB points which is based on the literature and is in agreement with experimental results obtained by Raytheon Company. The parameters which could then be varied were the wavelength, wave height and phase.

The results show that for the worst case which could occur, the phase would be zero, the wavelength greater than 250 meters and the wave height "2A" would be 3 meters or more. For this bounding case, the centroid shift was .25 meter. Available data tabulated in Section 3.4.5.2 shows that ocean waves higher or longer than that occur less than 10% of the time,[6] thus the computed error is a worst case. In general the phase will not be zero so that the average occurring error due to the sea state may be taken as .15 meter.

3.4.4.9.2 Sea State Model Justification

The ocean surface is a two-dimensional continuum of sinusoids with irrational periods and arbitrary phases. This is considerably more complex and of a more random nature than our simplified model. Measured centroid of returns can be expected to average period and phase effects over the randomly associated sinusoids both temporarily and spatially, resulting in smaller average deviation from the mean value (mean sea level) than that calculated from our single frequency (wavelength) model. Thus, the errors calculated from our monochromatic model can be considered an upper bound on the expected error in measurement.

In the preceding analysis it was assumed that the centroid of the received signal was a good approximation to mean sea level. This assumption was based on the results obtained by other researchers and from results of a study done by Raytheon Marine Research. The interaction of light with the ocean surface is described by what is called a "tolerance ellipse". This is an area on the sea surface which has the proper slope to reflect the light back to the receiving optics on the satellite. Since the receiving optics present a finite solid angle to the reflected light, the area over which light will be reflected has a slope of $z_x \pm \delta_x$, $z_y \pm \delta_y$. Thus, any positions on the wave which have the required slope within a "small" tolerance will reflect light back into the receiver. Since the laser illumination will strike the sea surface at normal incidence, returns will occur for points of zero slope. Since there is a complete spectrum of wavelengths from

millimeters to hundreds of meters, the returned signal comes from many small individual "glitters". Thus, for the centroid of the return signal to be at mean sea level, we must have the centroid of the number of points where the slope is zero versus the vertical displacement of the points be equal to the mean level. Marine Research Labs generated, by computer, a sample ocean surface from dynamic ocean records. At particular distances from the mean of this sample ocean surface, they found the number of points of zero slope, as shown in the histogram, Figure 3-16. This is the model used in the radar study (Appendix R-J).

If we take the centroid of this curve, it turns out to be located at the mean sea level. Thus, the justification for using the centroid of the return signal to find the mean sea level. The model of ocean surface used by Marine Research Labs is not strictly valid since the spatial resolution is only a few feet, but given that any particular square foot patch of sea surface is similar to any other patch, the model will provide useful results.

In conclusion, we may say that measuring the centroid of the returned signal will provide a good measurement of mean sea level within the errors described by the simplified sea model assumed in the study.

3.4.4.10 Total Error

The errors sources are listed in Table 3-4. Although not all of the individual errors are Gaussian in their amplitude distributions, they may be combined as root-sum-square as a rough approximation. The resultant error of each individual measurement is calculated to be:

Laser Range Measurement Error = 0.46 meter

This is approximately the 1 σ error, which corresponds to about a 70% probability. The total error is based on a system that uses components within the present state of the art. It can be assumed that angular uncertainty can be decreased if better star trackers become available. The atmospheric error can be neglected if a two-frequency system is used,

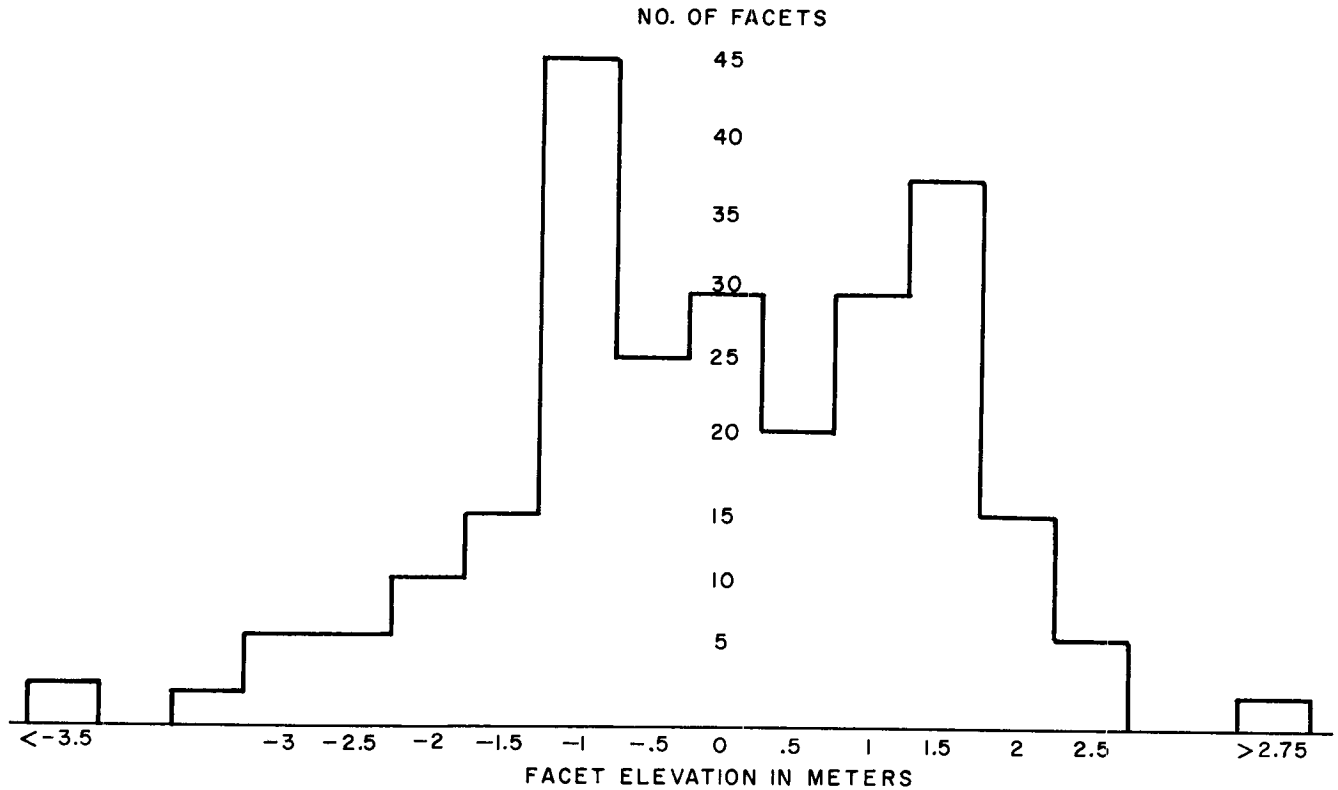

Figure 3-16 Elevation and Number of Facets with Zero Slope

TABLE 3-4

ERROR CONTRIBUTION

Error Source	Parametric Values	Contribution
Pulse Length	Length = 10 nsec Average Clear Weather	0.21 meter
Sea State	Maximum Wave Height approximately 3 m	0.15
Angular Uncertainty	Offset = 0.25^{o} Error in Offset = 10 arc sec	0.2
Beamwidth	Offset = 0.25^{o} Beamwidth = 200 m	0.1
Receiver		0.2
Clock Inaccuracy	Clock Inaccuracy = 10^{-8}	0.01
Clock Readout	Digital Readout: next even nanosecond	0.15
Calibration	Digital Readout: same as above	0.15
Atmosphere	Index of Refraction	0.15
	Root-Sum-Square = ±0.49 meter	

and receiver and clock accuracies can be improved when the state of the art of electronics engineering advances during the coming years. It is therefore safe to predict that the accuracy potential for a laser altimeter system is about .35 meter for each measurement.

3.4.5 SYSTEM LIMITATIONS

The operation of the system depends on the availability of a clear line of sight between the spacecraft and the ocean surface. If heavy clouds obscure this line of sight the system is unable to make a measurement.

A rough sea surface with waves over 3 feet in height allows measurements to be made with an accuracy of less than .5 meter. The extent of the occurring of cloud cover and a rough sea surface on a global scale is discussed in the next sections.

3.4.5.1 Cloud Cover

3.4.5.1.1 Transmission Through Clouds

To determine if and to what degree various types of clouds transmit laser light, we have tabulated the types of clouds, their minimum base height, their typical thickness X and the extinction coefficient σ per km for a one-way transmission path. Using the formula

$$I_T = I_o \, e^{-\sigma X} \tag{3-32}$$

we can calculate the total transmission for a one-way path.[7] The results are listed in Column 5 of Table 3-5.

The results shown that no transmission can be expected through clouds consisting of aerosol particles. The high altitude clouds which consist of ice crystals form no obstacle to laser light transmission. The one-way transmission in percent for all types of atmospheric conditions is graphically indicated in Figure 3-17.

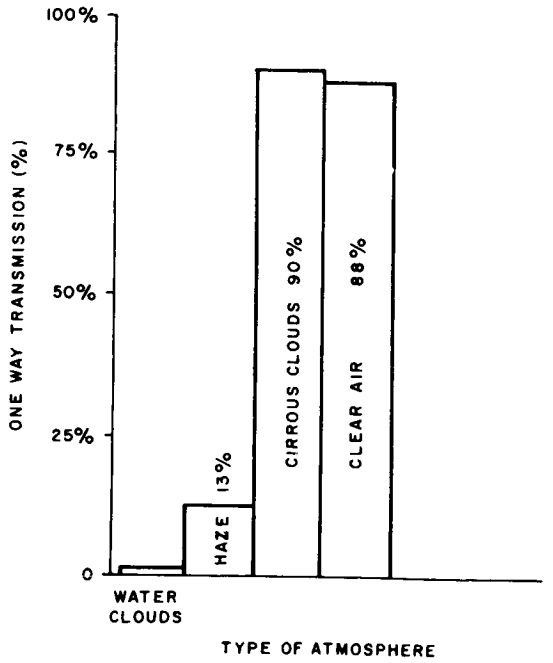

Figure 3-17 Transmission vs Atmosphere

TABLE 3-5

ATMOSPHERIC TRANSMISSION

Cloud Type	Minimum[7] Base Height	Typical[7] Thickness (km)	Extinction[7] Coefficient σ (km^{-1})	One-Way Total Transmission
Stratus	0.3	0.9	23-95	0
Strato-Cumulus	0.3	1.8	40	0
Cumulus	0.3	1.8	10-100	0
Cumulus-Congestus	0.3	3.0	50-200	0
Cumulo-Nimbus	0.3	6.0	150	0
Nimbo-Stratus	0.0	3.0	150	0
Alto-Stratus	3.0	0.9	95	0
Cirrus	7.7	0.03	.6	.98
Cirro-Stratus	7.7	0.15	.6	.91
Cirro-Cumulus	7.7	0.3	.6	.83
Haze	0.0	1 km	2	.13
Clear Air	0.0	1-2 km	0.13	.88

3.4.5.1.2 Probability of Cloud Cover

Because range measurements from the satellite are impossible when the area of interest is covered with clouds, it is important to obtain a factor indicating the probability of cloud cover. This factor will, during the tradeoff analysis, determine the mission time that is needed to obtain a required amount of data points for a given sampling rate.

For the purpose of this study we have divided the world's oceans into four distinct parts:

a. The Artic Ocean north of the 65^{o} parallel.

b. The North Atlantic and North Pacific Ocean between 25^{o}N and 65^{o}N.

c. The Middle Atlantic, Middle Pacific, and Middle Indian Ocean, between 25^{o}S and 25^{o}N.

d. The South Atlantic, South Pacific, and South Indian Ocean, south of 25^{o}S.

The probability of cloud cover over these areas is based on an annual cycle as follows:[8]

Arctic Ocean	68%
North Atlantic Ocean	62%
Middle Atlantic Ocean	50%
South Atlantic Ocean	67%
North Pacific Ocean	60%
Middle Pacific Ocean	52%
South Pacific Ocean	65%
Middle Indian Ocean	50%
South Indian Ocean	68%

The data shows an increase in cloudiness with increasing latitude from about 50% along the equator to about 70-80% above the poles. Especially South of the 60^{o}S parallel the cloudiness increases rapidly near the coast of Antarctica.

Data taken at two-month intervals shows an increase in cloudiness over all oceans North of 25^{o}N and South of 25^{o}S during the last half of the year. For the regions along the equator the variations are nil. The results are graphically indicated in Figure 3-18 showing the annual mean transmission probability in percent for each area of the oceans. From this study one can conclude that the average mean probability for successful transmission is 40% for a mission with a duration of at least one year covering all the oceans of the world.

3.4.5.2 Sea State

3.4.5.2.1 Error Versus Sea State

When the ocean surface increases in roughness, the average wave height will increase. The influence of the wave height variations can be studied with our computer program. Also the change in wave period, related to wavelength, can be handled by the computer, but in addition the reflectivity of the ocean surface can change.

This change in reflectivity is due to the formation of breaking crests and foam streaks. These changes are difficult to work into the computer program so that for the purpose of our analysis we have assumed the reflectivity to depend only on the slope of the ocean surface. The maximum error ($\Phi = 0$) caused by the ocean surface for different heights of the waves and different wavelengths was calculated on the computer and the results are plotted in Figure 3-19.

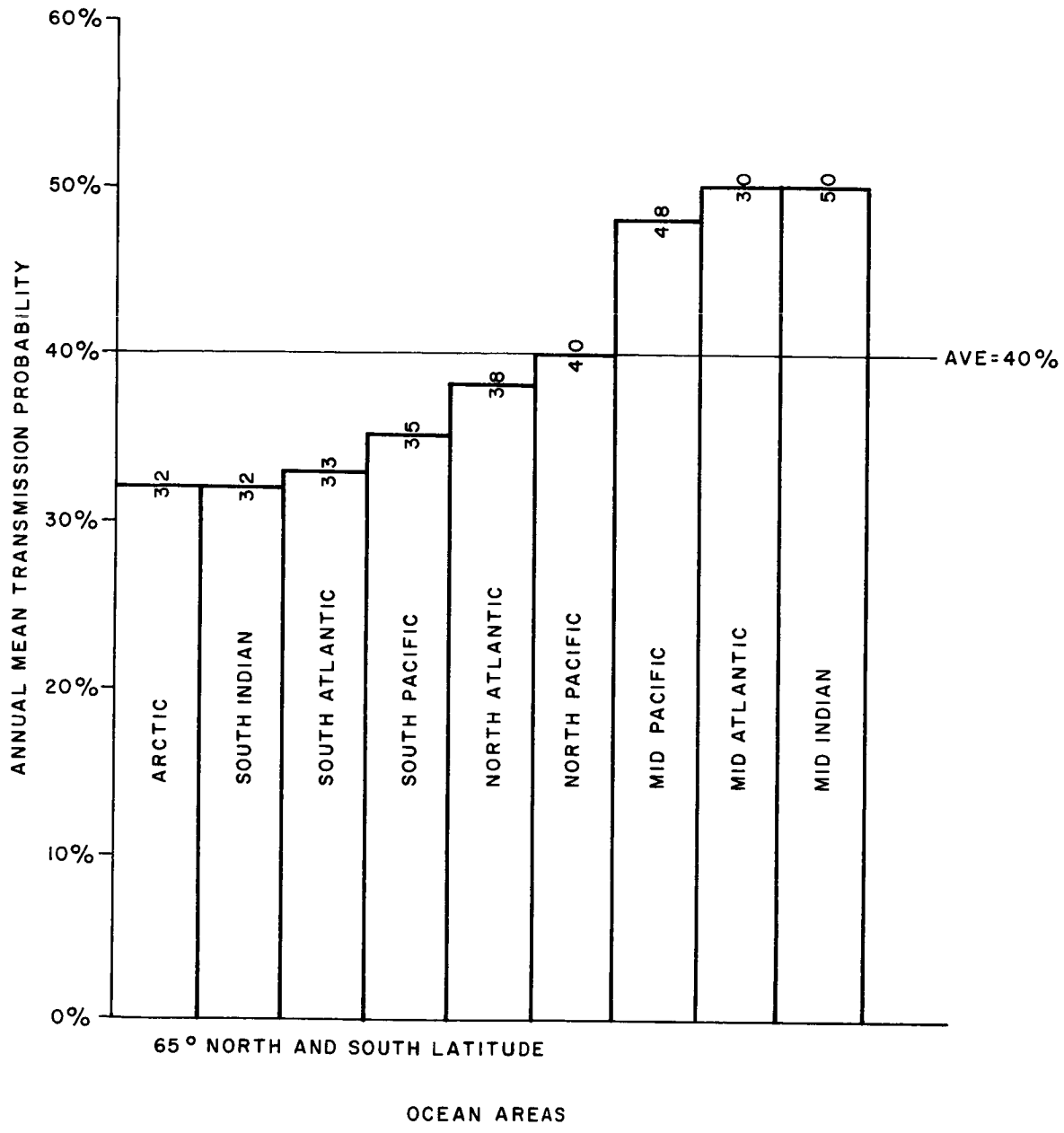

Figure 3-18 Transmission Probability over the Oceans

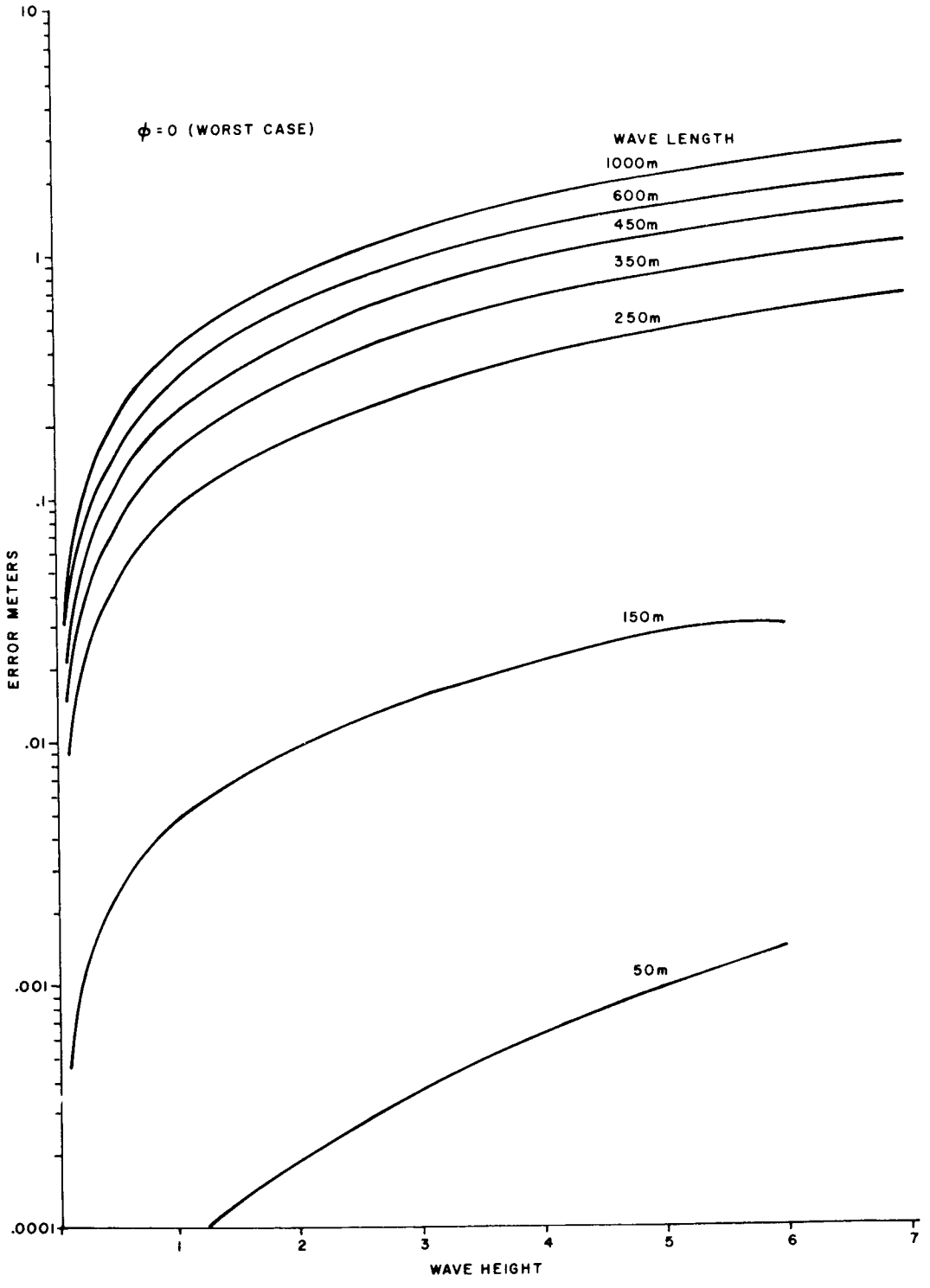

Figure 3-19 Range Error vs Wave Length and Wave Height

3.4.5.2.2 Probability of Occurrence of Rough Seas

We have studied wave records taken over a period of several years and in several parts of the world.[6] The results of these studies are tabulated in Table 3-6 and indicate that on a global scale the wave heights do not exceed 3 meters for 90% of the time.

In addition, wave periods shorter than 11 seconds corresponding to wavelengths shorter than 200 meters occur in the world's oceans more than 90% of the time.

TABLE 3-6

SEA STATE OCCURRENCE

South Indian Ocean	Period < 12-13 sec	95%
	Height < 3.5 m	91%
South Pacific Ocean	Period < 10-11 sec	90%
	Height < 3.5 m	89%
North Atlantic Ocean	Period < 12 sec	95%
	Height < 4.0 m	88%
Mid Atlantic Ocean	Period < 8-9 sec	90%
	Height < 2.5 m	95%
Mid Pacific Ocean	Period < 8-9 sec	95%
	Height < 2.5 m	95%
Mid Indian Ocean	Period < 10 sec	90%
	Height < 2.5 m	90%

3.4.6 ABILITY TO MEET GEODETIC REQUIREMENTS

3.4.6.1 Accuracy

Accuracy requirements for the altimeter system have resulted from the geodetic requirements study. The results of this study are tabulated in Table 3-7 showing accuracy and data rate requirements to resolve certain features in the geoid of the earth for the benefit of the mentioned fields of technology.

From the analysis performed on the laser altimeter system we can conclude that the only requirement that cannot be easily met is the accuracy required to establish a geoid connection. Other requirements concerning accuracy can be met either by the individual measurement or by the reduction of a greater than needed amount of measurement samples.

3.4.6.2 Data Rate

The data rate requirements can be derived from the measurements density mentioned in Table 3-7. The velocity of the satellite is about 7 kilometers per second for an altitude of 1000 kilometers. Therefore, it passes in 14 seconds over a ground path of 100 kilometers, meaning that a maximum of two measurements can be made with our data rate over this distance. If 200 measurements have to be made in an area of 100 by 100 kilometers, we may assume that 14 measurements have to be made along each 100 kilometer path length. It can be concluded that a minimum of seven to ten passes have to be made along the same trajectory during the time of the mission to meet the geodetic requirements of 200 measurements per 10,000 km^2. Whether this requirement can be met, depends on the time duration of the mission and the total surface area to be covered. The lower density requirements mentioned in the table can be met without difficulty.

TABLE 3-7

GEODETIC REQUIREMENTS

Requirement Source	RMS Error (m) in Height Above Sea/Spheroid		Number of Measurements per 10,000 km^2	
			w/o Tides	w/ Tides
Mean Sea Level (Oceanogr.)	0.3	0.3	2	4
Submarine Geology				
Static	1	1	200	200
Dynamic	----------		200	200
Military				
Geometry	7	7	10	20
Gravity	----------		--	--
Geodesy				
Datum Establishment	1.5	1.5	200	200
Geoid Connection	0.1	0.1	10	20
Geoid Extension	0.5-2	0.5-2	0.1-1	1 - 5

3.4.7 OTHER SYSTEM CAPABILITIES

3.4.7.1 Measurements of Sea State

In addition to improving the accuracy of the measurements, the pulse shape detector also could possibly provide information about the sea state. This information can be used by meteorologists and oceanographers to obtain records about the sea state condition on a global scale. Information like this is helpful in predicting a sea state condition in certain parts of the ocean for the benefit of shipping. Ships must decrease their speed thereby lengthening the duration of the voyage when an area with high seas is encountered. Many ships could reach their destination sooner by taking alternate routes if sea states along the shipping routes could be predicted in advance.

3.4.7.2 Measurements of Maximum Cloud Height

Because clouds are good reflectors for laser radiation, the altimeter system may be used to measure the maximum altitude of clouds. This would involve deactivating the cloud detector and making the range-gate-time longer.

Information about cloud height could, combined with the observations by the NIMBUS satellite, be helpful in predicting meteorological phenomena and the development thereof.

3.4.7.3 Measurements Over Land

Land targets have generally a higher reflectivity than the ocean surface, so that the return pulse is stronger. This in turn results in an increase in accuracy of the altitude measurement. In addition the pulse shape information can be used to provide information on variations in height within the beam spot size.

3.4.7.4 Measurements of Tracking Station Location

Explorer XXIX (the Geodetic Explorer) carries a set of optical beacons so that its position can be photographed by telescopic cameras against a background of stars. The satellite is usually photographed simultaneously by three camera stations, two at known locations and the third at an unknown location. Using star charts, one can use the obtained information to define the position of the third station relative to the positions of the other two stations.

The optical beacons used on EXPLORER XXIX are xenon flash lamps quite similar to the ones used for the laser. Therefore, the power supply for the laser may be used to power the optical beacons if the altimeter is not active.

3.5 SYSTEM TRADEOFFS

3.5.1 LASER SELECTION

In general, the mode of operation can be divided into incoherent operation or coherent operation. In the incoherent mode of operation the range is determined by measuring the time difference between the transmission and reception of a pulse. Noise entering the receiver in a random process may introduce range errors as explained in the error analysis. Pulses have to be fairly short in order to make an accurate estimate of range.

The coherent mode of operation uses a frequency- or amplitude-modulated signal and performs phase tracking as a means of measuring range. Its advantage is that random noise does not contribute to the signal; therefore operation at lower energy levels is possible. An evaluation of the available lasers operating in the incoherent or coherent mode is given in the following sections.

3.5.1.1 Incoherent Lasers

For application in a pulsed system we may consider the optically pumped solid state lasers: Ruby, YAG, Nd-doped glass and doubled YAG, the electrically excited solid state lasers such as Gallium Arsenide and pulsed gas lasers, such as Argon, HeNe, CO_2 and Nitrogen.

Most of these lasers do not have sufficient output power to be considered for this application and only Ruby, YAG, Nd-doped glass and doubled YAG are likely candidates. In satellite-borne applications, the input power requirement is one of the prime parameters.

For Ruby and Nd-doped glass systems the requirements on the input power are much higher per joule output power than for YAG systems, but the quantum efficiency of the receiver is much higher for Ruby than for YAG and Nd-doped glass systems. Therefore, Ruby and doubled YAG remain the only two possible laser systems.

Doubled YAG would take less input power per joule output power than Ruby, and the receiver sensitivity would also increase by a factor of two, but this requires 250 millijoules from the doubled YAG system and only 40 millijoules have been obtained so far. For these reasons only a ruby laser can be considered a practical system for the altimeter.

3.5.1.2 Coherent Lasers

In the coherent mode of operation the output signal is amplitude - or frequency - modulated and after demodulation of the received signal a phase comparison is made with the transmitted signal. The output power requirements are less than in the incoherent mode but are still too high to be satisfied by the He-Ne or Argon Laser. Only the CO_2 laser seems possible of generating enough power for this application. However, some disadvantages for using this laser need to be considered before it can become a prime system candidate. These disadvantages are:

a. Detectors operating at 10.6 micron require cooling to about 70^{o} Kelvin.

b. The optical alignment of the local oscillator signal and the reflected signal from the target is very critical.

c. Most CO_2 laser systems built today are not able to satisfy the environmental requirements imposed on a satellite-borne altimeter. Therefore, an extensive effort in packaging would be required.

d. Frequency stability and operation at one single frequency is required to obtain accurate measurements. This requirement is still not fully satisfied at the present time.

Although the disadvantages are serious, they may be overcome during the next few years. Therefore the CO_2 laser cannot be completely disregarded. Hence, a preliminary investigation has been made of the use of a coherent CO_2 laser system for the measurement of the range to mean sea level. The method of measuring range with a CW system has the advantage of a long "time on target" which helps to smooth out errors

due to sea state conditions. However, the analysis of the signal processing runs into problems of cross-correlation techniques and involves information processing theory. Also the method and mode of modulation of the CW signal requires an intensive study effort which is beyond the scope of this study. We must conclude therefore that the use of CO_2 lasers for an altimeter satellite may be possible, but that an analysis of such a technique justifies a separate study.

3.5.2 FABRICATION FEASIBILITY

The system as described can be built without major difficulty. The flashlamp drum has not been attempted before but its construction is mechanically feasible. Of course, if other pumping schemes such as surface spark discharge pumps or plasma pinched pumps prove to provide the required number of pulses or if a major breakthrough provides us with a conventional flashlamp with a life of 1.6 million flashes, the rotating flashlamp drum can be discarded. This would result in a simplified system taking less volume and reducing its weight. Assembling the critically aligned optical parts in the laboratory and sealing them in place as a separate unit omits duplication of expensive optical alignment tools at the assembly sight and prevents dust from settling in the optical path. It also results in a more rugged package and prevents misalignment under environmental strains. Tolerances on the telescope mirrors are not critical due to the fact that the beam size is several times the diffraction limit for the optics size used. Power supplies like the one required for the laser transmitter have been built and have qualified for space environment.

3.5.3 AVAILABILITY

All parts except the flashlamps are presently available or can be manufactured. If a short time and limited mission were contemplated, even present day flashlamps could be used up to a total of 5000 flashes per lamp. For the system we have analyzed, however, flashlamps with more lifetime are needed. They could be developed and space qualified before 1971 if the manufacturers are actively stimulated.

3.6 RECOMMENDATIONS

3.6.1 UNRESOLVED DATA

The relationship between the return pulse shape and the state of the sea surface is at present still unknown. Our efforts to find such a relationship by investigating the data obtained by various flight test programs have not produced any usable information. For the purpose of our analysis of the interaction of the pulse and the sea surface we have therefore constructed our own model. This model treats the ocean surface as a smooth, one-dimensional sinusoid and studies its effect on an impulse which is both gaussian in cross-section and in time. The reflectivity of an element of ocean surface was assumed to be partially diffuse and partially specular with a gaussian intensity fall off away from the normal direction. The model provides us with a first order estimate of the dependence of the centroid on the sea state.

In reality the ocean surface is vastly more complex and more data is needed to show how close our estimate of the centroid shift is to that of the real world.

The data should be a two dimensional mathematical representation of the ocean surface.

The probability of certain sea state conditions are tabulated for certain parts of ocean. In particular the areas bordering the coast lines are well studied. However, large areas of the oceans such as the polar regions are not documented and more information about the probable sea state on a global scale would be helpful.

3.6.2 PROPOSED PROGRAMS

3.6.2.1 Sea State Study

3.6.2.1.1 Ocean Signature

As mentioned above more data is needed relating the received pulse waveform to the sea state. These data can be obtained by flying a laser system in a high altitude aircraft over the open ocean. The

laser system should have the same characteristics as the altimeter system regarding pulse length and beam spot size. No data processing is needed during the testing phase other than an oscilloscope equipped with a photographic camera. For comparison a stereo camera on the same aircraft should be used to record the ocean surface within the footprint of the beam. Changes in reflectivity of the ocean surface can be measured by a CW helium neon laser which is close enough in wavelength to the ruby laser so that the reflectivity of the water is similar.

3.6.2.1.2 Ocean Reflectivity

The reflectivity of the ocean surface (ρG) is a relatively unknown quantity which depends on beamwidth, sea state and wavelength. No data has been taken using the conditions under which the altimeter operates. At best we can take the data that has been obtained by other researchers and derive from this an approximation for the ocean reflectivity. Because the reflectivity used in our calculation is still only an approximation, a flight test with the purpose of obtaining this information is recommended. During the flight test the equipment should be outfitted in such a way that an identical area is illuminated on the ocean as in the case of the altimeter. The equipment used is identical to that mentioned in Section 3.6.2.1.1 and the tests can be performed simultaneously.

3.6.2.2 Laser Pumping Development Program

3.6.2.2.1 Flashlamp Development

The flashlamp is the major cause of failure and inefficiency of ruby lasers.

During our discussions with leading flashtube manufacturers, it has been pointed out that because the use of flashbulbs for lasers represents only a small part of the flash tube market, no interest exists on their part to develop a more efficient and durable flash tube. Unfortunately, most laser manufacturers lack the background and facilities to undertake such development programs on their own.

According to the scientists working in the field, flash tubes with a life of 200,000 flashes can be produced. We would suggest therefore that such a development program be stimulated.

3.6.2.2.2 Other Pumping Methods

Pumping a solid state laser with a standard flashlamp is the reason for low efficiency in ruby lasers. Much of the energy emitted by the flashlamp falls outside the frequency region (the pumping band) that corresponds to the energy gap between the ground state and the excited state of the ruby material. If a source can be developed that emits only in the pumping band,a significant increase in efficiency may be expected. The source can be an improved version of the currently available lamps or could have a completely different configuration. Presently surface spark discharge pumps and plasma pinch pumps are under development. To stimulate more activity in these areas of development we suggest a program aimed at improving the efficiency of laser systems intended for space applications.

3.6.2.3 Photon Collector Development

An increase in the amount of photons received results in an increase in the signal-to-noise ratio. This, in turn, reduces the error of the range measurement. A larger antenna or collector would capture more photons returning from the target but systems with a high quality optical collector of 50 cm seem at the present not feasible for space applications. For the altimeter system a larger antenna would be attractive because the surface quality does not have to perform to the diffraction limit. It seems therefore possible to develop an erectable optical collector outside the spacecraft. We suggest that such a program be stimulated.

3.6.2.4 Coherent Ranging Study

A preliminary study has been made of the use of coherent laser systems for measuring range to mean sea level. This has the advantage of a higher data rate and a smoothing out of the sea state around mean

sea level. The study is a complicated one and could not be completed within the scope of our current work. However, we must conclude that without such study the use of coherent techniques cannot be ruled out and therefore a study effort about coherent ranging techniques is suggested.

3.6.2.5 Pointing Requirements and Reduction

As can be seen from the error analysis, the pointing inaccuracy is an important contribution to the total range error. We propose a program aimed at the development of techniques that could be used to reduce the pointing requirements. Such techniques would include three beam ranging systems, wide beam ranging and the use of horizon trackers and stabilizers.

SECTION 4

RADAR ALTIMETER

SECTION 4

RADAR ALTIMETER

(J. Morris)

4.1 INTRODUCTION AND SUMMARY

4.1.1 PRIMARY OBJECTIVES

This study has been conducted for the purpose of defining a radar system capable of being used as a satellite altimeter over ocean areas of the Earth. The altitude information obtained will be used to determine the Earth's geoid, i.e., the equal gravity potential surface closely corresponding to mean sea level. This geodetic requirement demands the highest possible altitude accuracy commensurate with satellite constraints as to size, weight, power, and attitude stabilization.

The study has been conducted to aid in analyzing the problems incurred and for suggesting techniques for accomplishing the desired accuracy objectives. It also permits evaluation of the radar approach as compared to the laser approach for accomplishing the same objective.

By way of summary, it can be stated that altitude accuracies approaching 0.3 meters seem attainable even under some unfavorable conditions of sea state and from satellite altitudes in the vicinity of 1000 km.

4.1.2 SUMMARY OF TECHNIQUES

Some of the techniques proposed are as follows:

a. The use of a small antenna that can be mounted integrally with the satellite. The corresponding relatively large antenna beamwidth demands only moderate vertical attitude stabilization accuracy.

b. The use of a gated amplifier (coherent) type transmitter. Compared to the magnetron, this provides good waveform control as to pulse shape, and is relatively free from jitter or pulsewidth modulation that could otherwise seriously degrade accuracy.

c. The use of coherent or synchronous detection. This gives a linear output relatively free from waveform changes as a function of signal-to-noise variations. Sizeable errors would result from the use of non-coherent detection.

d. The use of a nearly sea-state immune processor. This provides sea level altitude readings corresponding to that of a calm sea, even in the presence of sea-states as high as those corresponding to 20 knot winds (3 meter waves peak-to-peak). Some reduction in accuracy is expected at higher sea-state conditions, but the use of a sea-state monitoring circuit has been proposed that may permit sea-state corrections to be inserted, or may permit readings to be discarded in the event of seriously degrading sea-state conditions.

e. The use of a highly redundant prf. The prf used is high but not beyond the limit that permits the range ambiguity to be resolved by relatively coarse ground station tracking information.

f. The use of a system bias error monitoring circuit. This may permit the monitoring of receiver and processor delay variations so that corrections may be introduced for preserving high accuracy, even in the event of changes in equipment delays.

g. The use of an auxiliary radiometry type receiver for providing atmospheric water vapor readings (not included in present system). Such readings would permit corrections to be introduced with respect to troposphere refractivity variations and thereby reduce this error by a factor of two.

4.1.3 RECOMMENDED SYSTEM

The recommended system can be specified as follows:

System	
Source Power Required	200 watts dc (see Note below)
Overall System Weight	20 Kg (45 lbs)
Overall System Volume	10,000 cm^3 (600 in^3)

Note: This power rating assumes an overall altimeter system power efficiency of 2.5%, which is conservative. Five percent efficiency (100 W Source Power) is probably achievable, and 10% efficiency (50 W Source Power) has been proposed as achievable. Power rating may also be reduced by other design modifications, such as increasing antenna diameter (see Appendix R-M).

System (Continued)	
Accuracy	< 50 cm
Attitude Stabilization Accuracy	0.3^{o}
Antenna	
Diameter	.75 meters (2.5 ft)
Thickness	≈ 1 cm
Aperture Shape	Circular
Aperture Illumination	Uniform
Type	Slotted Array
Beamwidth	2.3^{o} (40 milliradians)
Gain	38 dB
Weight	2 Kg (est.)
Antenna Pattern	$\sin\theta/\theta$
Sidelobe Level	13 dB
Transmitter	
Type	Coherent, Gated Amplifier
Frequency	X-band
Pulse Peak Power	1 kW
Pulse Length	50 ns
Pulse Rise and Fall Times	10 ns
Pulse Repetition Frequency	100 kHz (at 1000 km - altitude dependent)
Receiver	
Noise Figure	8 dB (conservative)
Bandwidth	20 MHz
Bandpass Characteristic	Synchronous Single Tuned
Receiver Delay	150 ns
Detector	Coherent Synchronous
Processor	
Type	Two-Stage Delay Differencing
Processor Delay	75 ns
Output Waveform	Ramp Doublet (ideal)
Timing Sensor	Pulse-Time Discriminator

Altitude Tracking Circuit	
Type	Phase (altitude) Locked prf Oscillator
Tracking Bandwidth	.157 Hz
Tracking Time Constant	1 second
Altitude Counting Circuit	
Type	Digital Frequency Meter (prf count)
Reference Oscillator Stability	10^{-8}
Reference Oscillator Frequency	10 MHz
Data Storage	**Remarks**
Altitude Counts	
Time Signals	
Temperature	(Diagnostics)
Voltage	(Diagnostics)
Signal Strength	(Sea-State Indication)
Bias Delay Altitude	(Bias Error Correction)
Radiometer Signal	(Refractivity Correction)
Estimated Stored Data Rate	350 Kilobits per hour

4.2 SYSTEM REQUIREMENTS

4.2.1 GEODETIC REQUIREMENTS

System requirements have been specified by the geodesists. The more detailed geodesy specifications are contained in a separate section.

The usefulness of the data obtained from the altimeter increases rapidly with the accuracy attained. An accuracy of 1 meter or better is considered to be of prime value. Accuracies of about 0.3 meter appear to be attainable in early models and should have great geodetic interest.

Data densities of 200 readings per 10,000 sq km have been specified. This density is presumably intended to have uniform distribution, giving one reading per 50 sq km having point-to-point spacings of about 7 km for a rectangular area.

The radar altimeter generates essentially continuous data along the flight path of the satellite. Lateral coverage between ground paths is

limited by orbital parameters and equipment life. On the assumption of 90 minute orbits and 1 year equipment life, the ground tracks will have about 3.5 km spacing intervals, or enough to give some data redundancy to permit selection of the most favorable data while eliminating suspect data obtained during intervals where signal strength might be so low as to be suspect, or where some conditions relating to refractivity or satellite altitude may have resulted in poor data.

Since a 90 minute satellite orbit transverses 16 orbits per day, the approximate 2000 hours (80 days) of expected operating life for first systems without redundancy gives an average of about 15 km spacing intervals at the equator, and appears to provide enough data to establish the geoid while providing good information on tides and other surface disturbances. Longer equipment life can be expected in later equipment provided that development programs are directed toward that end. An ultimate 10,000 hours (about 400 days) of life appears to be in the not too distant future.

For this study, altimetry requirements are for sea areas only. The horizontal resolution is comparable to the rather large ground spot or footprint size (about 7 km diameter for 50 ns pulses), indicating that some changes in system concepts are required for altimetry over land. Smaller spot sizes can be obtained either by using a narrow beam such as with a laser, by using extrmely short pulses, or by using extremely large antennas. Further study is required for the land altimetry problem.

This study is the first phase of a continuing program culminating in satellite flights during 1971 and beyond. This preliminary study is devoted primarily to the conceptual aspects of the system for purposes of examining problems and techniques and for making laser-radar tradeoffs. Further studies will be needed for hardware design details.

4.2.2 SATELLITE CONSTRAINTS

It has been sated that the satellite used for the altimetry mission will be designed to accommodate the equipment within reasonable satellite constraints. However, since both radar and satellite together

determine overall system cost, the optimum design must consider the interface of each system with the other. For example, large antennas increase vehicle diameter requirements, increase the attitude stabilization requirement, and reduce transmitter power requirements. A rather intricate analysis beyond the scope of the present study is needed to determine the exact antenna diameter that maximizes performance and minimizes costs. The .75 meter antenna proposed was somewhat intuitively chosen and has not resulted from extensive studies of stabilization systems and various possible vehicle configurations.

Satellite operational altitudes in the vicinity of 1000 km have been suggested as being nearly optimum for altimetry. As a processing convenience and to minimize the corrections required for vertical velocity components, a nearly circular orbit is recommended. Individual satellite altitudes may vary from approximately 800 to 1300 km, provided each meets the circular orbit recommendation. Transmitter power adequate for 1300 km orbits should be provided.

Data storage and telemetry equipment are to be provided, including the necessary command equipment for establishing control of read-in and read-out commands from ground stations. Stored data will be coded for the purpose of minimizing data storage, read-out bandwidth, and power requirements.

No constraints on system power have so far been established. In the interest of high accuracy as a primary objective, rather large prime power levels have been indicated. Power reductions may be contingent on engaging in rather long range development projects on transmitter design or on establishing performance compromises in altitude accuracy. More specific data on estimated system powers, together with other pertinent data, is contained in Section 3.

4.2.3 AUXILIARY DATA

The altimeter can be used for collecting information which is useful for other interests besides geodesy. Some indication of sea-state may be available from signal strength information and may be stored and read out for the benefit of related services.

Some information on atmospheric water vapor content may be made available by the use of a radiometer operating at water vapor emission frequencies. Provisions for this type of equipment have been considered in Section 3.

Some thought has been given to the possibility of obtaining cloud profile data from the altimeter. However, clouds are weak radar targets and require power levels beyond that which could be considered in this equipment. Specialized equipment operating at more appropriate frequencies would be better suited for cloud profilometry.

4.3 SYSTEM DESCRIPTION

The system described has been configured to meet the geodetic requirements with the highest possible altitude accuracy consistent with reasonable satellite constraints. It may also provide auxiliary data such as sea-state and atmospheric water vapor parameters that may have value beyond the primary altimetry function.

The system design is to be considered as conceptual for the purposes of facilitating radar-laser trade-off studies, for describing techniques which appear to have advantages, and for indicating the performance objectives that are being proposed.

No attempt has been made to finalize hardware details or to generate precise circuit configurations. These detail aspects are left for future study directed more specifically to these tasks.

4.3.1 BLOCK DIAGRAM

The radar altimeter block diagram is shown in Figure 4-1. This diagram is shown in sufficient detail to indicate the subcircuits which are to be described in more detail in the following pages. These subcircuits include:

a. Transmitter-Modulator
b. Antenna
c. Receiver-Detector
d. Phase Tracking Circuit
e. Processor

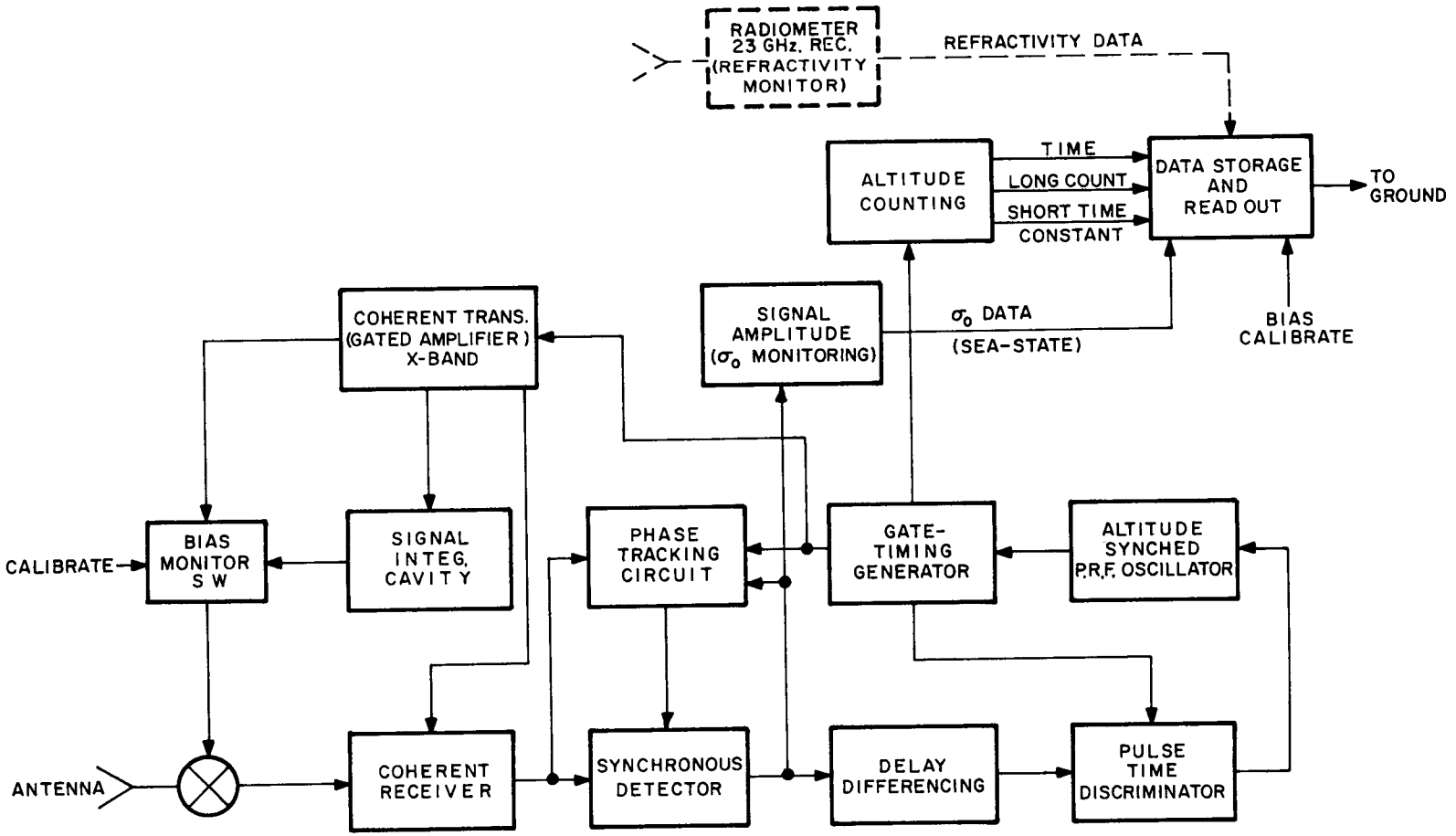

Figure 4-1 Radar Altimeter Block Diagram

f. Altitude Tracking Circuit

g. Altitude Counting Circuit

h. Auxiliary Data Circuits

i. Data Storage and Telemetry.

4.3.1.1 Transmitter-Modulator Circuits

4.3.1.1.1 General Considerations

The primary accuracy considerations imposed by the transmitter are concerned with obtaining precise waveform control at power levels that assure large S/N ratios at the output. Consideration must also be given to phase tracking and altitude tracking performance to be described later.

Waveform control implies the generation of stable pulses subject to minimum jitter, minimum width modulation, and freedom from moding which may produce serious changes in pulse envelope waveforms with resulting timing errors.

The waveform control required for best accuracy stresses the need for a gated-amplifier form of transmitter giving output pulses that have rapid rise and fall times and negligible timing uncertainties such as jitter and misfire. Magnetron transmitters have been ruled out because of their inherently poor waveform control.

A low-level, coherent, rf source oscillator can be used, switched on or gated into the transmitter amplifier at low levels by a broadband microwave diode switch. A TWT type transmitter having a 40 dB gain at a fixed X-band frequency is suggested. Some tube development could make possible the availability of more efficient, more reliable, cold cathode amplitron type transmitters. These tubes are presently unavailable with the required gain at X-band. Solid state transmitters for this service are some years away and would most likely be complex multiple elements for the power levels being presently considered. In the near future, hybrid systems may be developed which meet the requirements of peak power, high prf, high reliability, and efficiency.

The following transmitter specifications are presently recommended:

Type	Coherent, Gated-Amplifier
Frequency	X-band
Pulse Length	50 ns
Pulse Rise and Fall Times	10 ns
Pulse Peak Power	1 kW
Pulse Repetition Frequency	100 kHz (at 1000 km altitude).

Coherent operation is recommended to obtain linear receiver detection. It ties in well with the gated-amplifier transmitter configuration, since both the gated amplifier and the coherent detector require the use of a low level cw source oscillator.

The X-band frequency specification results from trade-offs between ionospheric refraction, which becomes troublesome at lower frequency, and atmospheric attenuation, which becomes a problem above X-band. X-band also makes possible the use of a reasonably small, structurally mounted antenna, and also the use of microwave components of convenient size and weight that have received considerable development effort because of their frequent use in other systems.

The 50 ns pulse length represents a trade-off with respect to sea-state on the one hand, which requires pulse lengths of about 3 times or more greater than expected wave heights, and on the other hand, accuracy considerations such as relative immunity to noise, clutter, and waveform variations that favor short pulses. The 50 ns compromise meets the accuracy requirements of all these limiting factors.

The 1 kW pulse peak power specification is somewhat higher than is necessary from a S/N standpoint for altitude tracking, but is required for S/N for the phase tracking circuit. Power estimates given in Appendix R-M show the relationships involved. (See Appendix R-M for power vs antenna.)

The pulse repetition frequency (described in Section 4.3.1.6 and Appendix R-F) is altitude dependent because of the altitude-locked prf oscillator that is used for providing basic altitude information. Although

prf varies with altitude, a frequency of 100,000 pps can be assumed at 1000 km altitude, varying as the inverse of altitude about this point. This prf is about the highest that can be used without excessive interference between successive pulses.

4.3.1.1.2 Pulse Compression Considerations

Pulse compression is discussed briefly in Appendices R-A and R-L. (A detailed analysis of pulse compression is beyond the scope of the present study.) The conclusions are briefly summarized below.

Advantages of pulse compression for this application are:

a. Reduction in transmitter pulse peak power requirements. Alternatively, pulse compression might be used to increase resolution with no increase in pulse peak power. In our system, the reduction in pulse peak power would be the primary advantage, especially if the reduction were great enough to permit the use of solid state transmitters.

b. A smaller, lighter system. The use of solid state transmitters could possibly reduce system size and weight by 50 percent or more. Presumably, the pulse compression system would be compatible with the presently conceived system. No overall system redesign would be required except for introduction of the pulse compression equipment.

Coherent processing is assumed with no power limitations imposed for phase tracking. With the phase tracking power limitation removed, and with duty cycles increased to between 25 and 50 percent by pulse compression, solid state becomes sufficiently attractive to warrant very thorough study as a possibility.

c. Improved reliability and extended equipment life. When ordinary microwave tubes such as magnetrons or traveling-wave tubes are used, equipment life is limited by these tubes that have life expectancies of 2000 hours or less. In the event that the use of solid state transmitters were practical, the life of the transmitters could approach that of the remaining circuits. The prospects for a one-year operational life would be greatly enhanced.

Disadvantages to pulse compression are:

a. Complexity. Circuits must be added for dispersing the transmitter signal and compressing it again when received.

b. Waveform degradation. Every pulse compression circuit introduces some sidelobes that distort the processed waveform to some extent. Consideration must be given to the effects of the sidelobes on accuracy. Provided that the sidelobe pattern is fixed and not random, the effects on altitude measurements may be predictable. In this case, corrections may be introduced to provide accuracies comparable to those without pulse compression.

If pulse compression cannot be used so as to make possible the use of solid state transmitters, then negligible advantage in equipment size, weight, or reliability could be expected. In that case, the complexities and degradations introduced would appear to outweigh the advantages. Prospects for a completely solid state altimeter appear good; however, they should be studied further in an attempt to reduce pulse-peak power requirements.

4.3.1.2 Antenna

The system has been configured about the small antenna or large beamwidth approach in which the first return from vertical is inferred from the received waveform, instead of being measured directly from a narrow beam that excludes all but the vertical return signal.

Advantages of the small antenna approach are:

a. A simple, readily feasible antenna structure, which can be mounted integrally with the satellite structure. The large antenna approach requires furlable arrays that require hitherto impractical mechanical tolerances, introduce feedline problems, and associate altitude delay errors resulting from equipment separation distances from the antenna.

b. The absence of attitude stabilization problem introduced by the use of large antennas may require that the beam be oriented with

respect to the vertical within a milliradian or less. This orientation accuracy is difficult at best.

c. The consistency of the beam pattern relative to the substantial beam distortions associated with large, unfurlable type antennas.

The antenna specifications are as follows:

Diameter	.75 m (2.5 ft)
Antenna Shape	Circular
Type	Slotted Array
Thickness	$\approx$ 1 cm
Estimated Weight	2 kg (4.4 lbs)
Aperture Illumination	Uniform
Antenna Pattern	$\sin\theta/\theta$ (13 dB sidelobe level)
Approximate 3 dB Beamwidth	2.3^{o}
Approximate Antenna Gain	38 dB

The slotted array having .75 meter diameter can be structurally mounted and requires a vehicle vertical attitude stabilization accuracy of only about 0.3^{o} to give accurate altitude operation without excessive waveform degradation. A less exacting array from a fabrication standpoint is the horn-fed reflector array; this type construction requires greater total volume but may be lighter in weight and is generally much less expensive. (See Appendix R-M.)

Uniform aperture illumination is readily obtained with the slotted array and gives better antenna gain than do shaped illuminations. Sidelobe levels are higher, but are of little significance for this type radar.

4.3.1.3 Receiver-Detectors

The receiver-detector specifications are as follows:

Receiver Noise Figure	8 dB
Bandwidth	20 MHz
Bandpass Characteristic	Synchronous Single Tuned
Receiver Delay	$\approx$150 ns

The 8 dB noise figure is reasonably conservative for a good X-band receiver, nonparametric. The 20 MHz bandwidth closely matches the spectrum of the 50 ns transmitted pulse taken to be approximately gaussian and measured at about half amplitude level. The synchronous single-tuned bandpass characteristic is also approximately gaussian to match the signal spectra. The match is close enough to give negligible signal-to-noise loss and will give small waveform distortion.

The receiver delay of about 150 ns is approximately 3 times the reciprocal bandwidth and is standard for receivers. This receiver delay corresponds to a range (altitude) delay of 23 meters and would represent an error if it were uncalibrated and uncorrected. The use of a bias calibration circuit permits this delay, together with any variation that might occur as a function of temperature or aging, to be corrected and will leave only a negligibly small residual error.

The dynamic range of the receiver should be large enough to handle the largest changes in signal strength with negligible compression or change in wave shape. The inclusion of 30 dB of agc capability with a 0.1 second time constant, fast enough to follow expected changes in reflection coefficient σ_o (effective target cross-section per unit area) versus sea-state, should provide extra assurance of linear performance.

A synchronous or linear type detector is considered to be necessary to assure unchanging waveshapes in the detector as the signal-to-noise ratio changes. The output waveform of envelope or square-law detectors changes rather extremely as S/N changes, giving faster rise times and corresponding apparent altitude shifts upward when S/N increases, independent of agc action which still leaves the S/N ratio unchanged. The effect of S/N ratios on rise times is analyzed in Appendix R-C.

4.3.1.4 Phase-Tracking Circuit

The rf or i-f phase of the received signal is doppler shifted with respect to the transmitted signal by any vertical components of vehicle velocity which may be present, by the off-vertical angular locations of

target elements, or by vertical components of sea-state velocity. Because of these various doppler shifts, the phase of the received signal must be tracked and a reference oscillator capable of voltage controlled phase shift must be provided for referencing the synchronous detector.

This phase tracking circuit must be broad-banded to follow the most rapid doppler frequency bandwidths within the ramp-step region of the received waveform. Bandwidths somewhat in excess of 1 kHz are required for phase tracking and are broad enough to place a lower limit on transmitter power to provide good signal-to-clutter ratios over this rather broad bandwidth.

Other techniques besides synchronous detection for eliminating this detector nonlinearity error have been considered. Agc is not effective here, since it controls signal strength only without controlling the S/N ratio which is the error generating parameter.

Another possible technique is to accurately monitor S/N so that continuous timing corrections as functions of S/N can be made. However, such devices seem somewhat imprecise and complex.

The best assurance of accuracy appears to lie in providing sufficient transmitter power to give good phase tracking accuracy so that synchronous or linear (superposition-wise) detection can be employed.

A technical point with regard to synchronous detection arises over the ability of the detector to generate a ramp step output as desired, in the presence of Rayleigh noise clutter. The analysis requires the examination of the cross-correlation or coherence function between the clutter waveform (bandpass Rayleigh noise) and the reference oscillator (stable sine wave relative to the coherence duration). The analysis is shown in Appendix R-H, and indicates a coherence interval adequate for the required processor waveform generation.

4.3.1.5 Processor

The function of the processor is to operate on the received waveform in a manner suitable for extracting sea-level altitude relatively independently of sea-state, clutter, and receiver noise.

The technique used has been rather thoroughly discussed in Appendix R-A which demonstrates the use of two stages of delay-differencing to generate a doublet type, zero axis crossing type waveform. The axis crossing point provides good accuracy by virtue of its relative immunity to amplitude changes and sea-state, and by virtue of its slope-doubling characteristic.

The timing point provided by the processed doublet waveform is delayed approximately 1.5 pulse lengths with respect to the ranging return that would have been obtained from a calm sea level. (See Appendix R-F.) The processing delay is compensated for in the process of calibration and should remain stable (within circuit stability limits) once calibration has been performed.

The output from the processor is fed to a pulse-time discriminator for precise altitude tracking. Individual pulse return waveforms are, of course, contaminated by receiver noise and Rayleigh clutter. Use of long-time (1 second) smoothing permits accurate averaging or mean altitude determination from a large number of sampled values.

The technique of obtaining sea-state immunity is contingent on having a return waveform ramp length (pulse width) somewhat in excess of the range increment corresponding to expected wave heights, and on using a pulse time discrimination (P.T.D.) gate, short enough to exclude the sea-state generated waveform curvatures that occur near the beginning and end of the return waveform ramp. More elaborate explanation is contained in Appendix R-A.

4.3.1.6 Altitude Tracking Circuit

The altitude tracking circuit can be regarded as essentially a phase-locked prf oscillator in which the phase of the locking waveform is dependent on altitude delay. In this sense, the radar signal is part of a feedback path for frequency and phase locking the prf oscillator. With all delay parameters of the feedback path known or calibrated, then the process of measuring altitude becomes a matter of measuring the

prf over a convenient measuring interval. The exact relationship between altitude and prf is given by:

$$h = \frac{c}{2}\left(\frac{n_a + \frac{1}{2}}{f_r}\right) - \frac{c}{2}(t_a + t_r + t_p) \qquad \text{(See Appendix R-F)}$$

where n_a is the range ambiguity factor obtained from coarse altitude information available from ground tracking stations, f_r is the prf measured over an interval long enough to give good accuracy, and t_a, t_r, and t_p are the respective atmospheric refractivity, the receiver, and the processing delays. The receiver and processor delays are so complex as to be unamenable to accurate calculations, but can be calibrated on a ground test range. In-flight calibration may be performed against a fixed delay corresponding to a fixed altitude.

The phase-locking circuit for establishing the frequency and phase of the prf oscillator will use a pulse-time discriminator that samples the timing of the processed waveform doublet (zero axis crossing point) with respect to a prf generated pulse. (See Appendix R-F.) Small changes in altitude result in corresponding changes in echo delay and waveform timing. The pulse time discriminator senses the timing error and generates a voltage that adjusts the prf oscillator frequency in the required direction for maintaining exact phase (altitude) tracking. Since altitude changes are relatively slow (permitting narrow band filtering), then very good smoothing (to reduce the effects of receiver noise and sea clutter) is obtained. Bandwidths of 1 Hz give nearly noise-free tracking with small altitude tracking errors from filtering delays. (See Integration Error in the accuracy analysis, Section 4.4.1.)

4.3.1.7 Altitude Counting Circuit

It was discussed in paragraph 4.3.1.6 that the altitude tracking circuit converts altitude information into prf information. The altitude counting circuit is in effect a frequency meter in which prf is measured in units conveniently related to altitude. Altitude may be

measured as accurately as prf can be measured. Accuracy consideration must be given to quantization errors and to reference oscillator instability errors.

The frequency of the prf oscillator can be measured against a stable frequency standard by counting N_c pulses from the high frequency standard during an interval, while N_r pulses are being counted from the prf oscillator. Prf quantization error is made negligibly small by starting the count coincident with the first prf pulse and ending on the N_rth count, and by having the clock frequency much higher than the prf frequency. The corresponding clock count from the standard will be related to prf frequency by:

$$\frac{N_c}{N_r} = \frac{f_c}{f_r} \quad .$$

Selection of clock frequency f_c and prf count N_r can be made so that N_c numerically represents the altitude, h. This selection could be convenient for measuring altitude directly, but is not necessary and is subject to change in the event that the ambiguity integer (n_a) changes. Corrections must also be introduced for delay errors which further complicate the problem of obtaining simple relationships between N_c and h, and exact altitude is obtained from the relationship:

$$h = N_c \times \frac{c}{2} \left(\frac{n_a + \frac{1}{2}}{f_c N_r} \right) - \Delta h_d = k_1 N_c - \Delta h_d$$

which shows that altitude is proportional to clock count after corrections for miscellaneous delays (Δh_d) have been introduced.

Several options are possible for processing altitude data. It may become possible to transmit prf pulses directly to ground stations for precise monitoring, thereby eliminating a sizeable amount of frequency measuring and data storage equipment aboard the satellite. The prf signals may be transmitted to ground in the form of narrow band sine wave signals for high sensitivity. This option is contingent on having

ground stations equipped with frequency standards for frequency metering. Corrections must be introduced to take into account doppler shift versus vehicle velocity. Estimates have been made in Appendix R-J which indicate that two significant figure accuracy in vehicle velocity relative to ground station is required for making doppler corrections. Variation in atmospheric refractivity may also introduce errors (see Section 4.4.1.4). Further study of this point is indicated.

4.3.1.8 Data Storage and Telemetry

Satellite-borne data reduction requires storage of data for readout at convenient intervals near ground based receiving stations. Data storage and telemetry equipment have not been extensively studied. Some estimates have been made to indicate the magnitude of data to be handled.

Altitude data readings must be referenced to a corresponding time scale. Time markers should occur at 1 second intervals, supplemented by double marks at 5 second intervals, and with other codings at minute and hour intervals. Altitude readings need not store all significant digits but only the last four that are subject to change between successive readings. Large reductions in storage capacity are possible by use of digital coding techniques that can constitute a separate study for specialists in this field of data handling.

In addition to time and altitude data, it is expedient in the interest of accuracy to store and telemeter other pertinent data relating to altitude accuracy. Equipment temperatures and voltages may be monitored at rather infrequent intervals without requiring a large amount of data storage capacity. Also signal strength data for inferring sea-state, and water vapor radiometry data for inferring tropospheric refractivity delays could and probably should be recorded.

Some consideration has been given to the possibility of obtaining continuous readout of altitude variations with respect to the intermittent altitude counts as obtained from the altitude counting circuit.

A very simple detector circuit could be employed to register short time-constant variations in prf in the form of a varying prf dependent voltage. This continuous data may contain information not present in the intermittent counts and may be useful for terrain variation studies. Storage of continuous data of this form, however, may call for special processing which may not be convenient. Further investigation of this point will be made later.

Other useful data for transmission to ground includes the bias delay calibrating output, the circuit of which is described in Section 4.3.1.9. It is assumed that at convenient intervals, perhaps once per hour, an output will be obtained showing any change in receiver and processor delay constants. This delay reading will be in the form of an altitude reading versus a calibrated delay, and will not affect data storage requirements to any significant degree since normal readings will be interrupted while calibration readings are being stored. Calibration can occur over land to avoid interference with altimetry operation over ocean areas.

4.3.1.9 Auxiliary Data Circuits

Three circuits for obtaining auxiliary data have been considered. These circuits are (1) a bias delay calibrating circuit, (2) a signal amplitude monitoring circuit, and (3) a troposphere water vapor monitoring circuit.

The bias delay calibrating circuit consists of a signal switching circuit, including a calibrated range delay plus a signal integrating element. The integrating element may consist of a high-Q microwave cavity to simulate the integrating characteristic of the sea surface and give a waveform having the characteristics of the actual received waveform. The calibrating delay incorporated need not correspond to the entire satellite altitude delay, but need only represent the unambiguous range with the ambiguity term (n_a) replaced by zero. A delay in the order of 1000 times shorter than altitude delay will thus be provided with a corresponding relaxation in accuracy requirements.

This calibration signal can be routed through the receiver and processor to give an altitude count which can then be compared with the original calibrated count. Any changes from the calibrated altitude indicate variations in receiver and processor delays which can be used for updating delay error corrections.

The second auxiliary circuit is the signal amplitude monitoring circuit, which samples the agc voltage. The agc sample will be gated near the peak of the required waveform on a pulse-to-pulse basis and will be smoothed in about a 0.1 second bandwidth filter before use for gain control. The agc bias signal obtained will be related to input signal strength and may be used for inferring sea-state.

The third circuit, the tropospheric water vapor circuit, may consist of a radiometry receiver operating at about 23 GHz frequency where water vapor absorption and reradiation coefficients are high. Output values from the receiver will vary with water vapor content and temperature, and should permit first order corrections for refractivity variations to be introduced. Further study is obviously required to determine the relationship between radiometer readings and refractivity corrections. This circuit is offered as one possible means of handling the refractivity problem. The circuit may be unnecessary, in the event that adequate weather data becomes available via ground stations, ships at sea, aircraft, or weather satellites. However, the satellite-borne radiometer may provide data that can be used to supplement data obtained from other sources.

4.4 SYSTEM PERFORMANCE

4.4.1 ACCURACY ANALYSIS

Major altitude error contributing factors are analyzed in this section, and estimates of the error magnitudes are obtained for each item. A summary gives the combined error to be expected for the overall system.

4.4.1.1 Receiver Noise Error

The received pulses are processed to generate a doublet waveform whose zero axis crossing point is used as a timing reference. When the idealized waveform is perturbed by receiver noise, some timing uncertainty results in the axis-crossing instant of the timing waveform. This timing uncertainty corresponds to an altitude uncertainty which can be estimated as follows. (Receiver noise in the presence of the axis-crossing ramp is shown in Figure 4-2 below.)

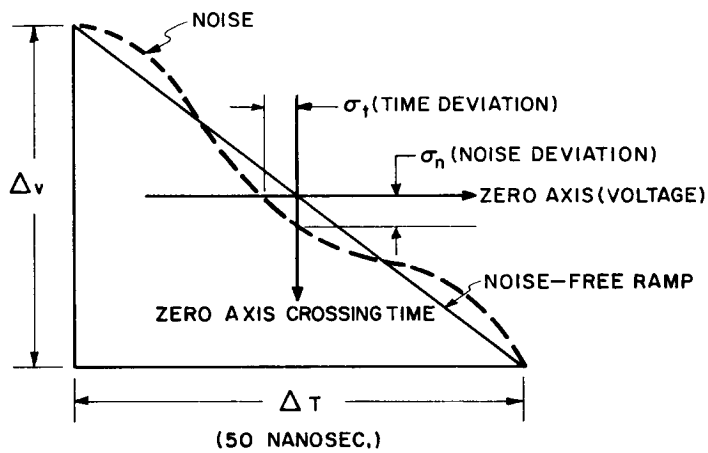

Figure 4-2 Receiver Noise in Presence of Axis-Crossing Strip

From the figure above, the following proportion is apparent:

$$\frac{\Delta v}{\Delta T} = \frac{\sigma_n}{\sigma_t} \tag{4-1}$$

Solving for the time uncertainty (σ_t) due to noise gives:

$$\sigma_t = \sigma_n \frac{\Delta T}{\Delta v} = \frac{\Delta T}{\Delta v/\sigma_n} = \frac{\Delta T}{\sqrt{S/N}} \tag{4-2}$$

The corresponding altitude uncertainty due to noise is:

$$\sigma_{hn} = \frac{c\sigma_t}{2} = \frac{c\Delta T}{2\sqrt{S/N}} \qquad (4\text{-}3)$$

From the doublet waveform diagram (Figure A-6 of Appendix R-A) it can be seen that:

ΔT = 50 ns = pulse length of transmitter,

and from Appendix R-B,

$\sqrt{S/N} = 2\sqrt{(S/N)_i}$ = peak-to-peak signal to rms noise amplitude ratio after integration (subscript i). (4-4)

The range equation analysis (see Appendix R-B, Section B.1) for the worst case parameters in Table B-1 results in an altitude uncertainty of:

σ_{hn} = .0086 m (.028 ft) altitude uncertainty versus noise.

4.4.1.2 Clutter Error

Clutter results from the vector addition of random return from independent target points. When the number of point scatterers is large, the detected amplitude of the reflected signals has a Rayleigh distribution and its bandwidth is the reciprocal of the transmitted pulse length. If the transmitted pulse is rectangular with length $\hat{t}$, its bandwidth is about $1/\hat{t}$ (cps) and the clutter waveform will have not more than about 1/2 cycle of clutter per signal pulse length or over the rise time of the received signal. This waveform will be somewhat coherent from pulse to pulse, but the phase will change at the doppler frequency rate, i.e., many times slower than the clutter signal frequency or pulse signal frequency.

Clutter introduces an altitude uncertainty similar to receiver noise error, and the altitude uncertainty can be reduced by integration. The altitude uncertainty due to clutter can be written as:

$$\sigma_{hc} = \frac{\frac{c\hat{t}}{2}}{2\sqrt{(S/C)_i}} \tag{4-6}$$

where $c\hat{t}/2$ is the pulse time base (meters), and the factor of 2 in the denominator results from slope doubling by the delay-differencing circuits in the processor.

The signal-to-clutter term $(S/C)_i$ is the power ratio after integration, and can be estimated as follows:

$$(S/C)_i = (S/C)_1 \, n_i \quad \text{(assuming nearly matched filter processing)}, \tag{4-7}$$

where $(S/C)_1$ is the signal to clutter ratio of signal waveform samples and is given as:

$$(S/C)_1 = \frac{\text{mean}^2}{\text{rms}^2 - \text{mean}^2} = \frac{\pi}{4 - \pi}, \text{ for Rayleigh distribution.} \tag{4-8}$$

The number of clutter samples (n_i) integrated is given by:

$$n_i = \frac{f_d}{2B_n} \tag{4-9}$$

where

$f_d = \frac{2v}{\lambda} \times \theta = \frac{2v}{\lambda} \times \sqrt{c\hat{t}/h}$ = maximum doppler frequency (at end of 50 ns pulse)

$\approx$ 1500 Hz

v = vehicle velocity

λ = radar signal wavelength

θ = attitude angle with respect to vertical

h = altitude

also, $B_n \cong .16$ Hz (noise bandwidth of tracking filter). (See Figures A-1 and A-2 of Appendix R-A.

The analysis in Appendix R-B, Section B.2, results in a clutter error of:

$$\sigma_{hc} = .036 \text{ m } (.12 \text{ ft})$$

4.4.1.3 Sea-State

In Appendix R-A , it is pointed out that the effect of sea-state is (1) to round out the waveform somewhat in the vicinity of break points, and (2) to shift the ramp crossover point by an amount equal to the shift of the centroid of the sea-state impulse response. (See also Appendix R-G.) Since the timing point, which is chosen as the zero axis crossing point in the processed doublet, is instrumented to be centered between breakpoints, the error of principal importance is the shift in centroid due to sea-state.

Elaborate theoretical analysis of the electromagnetic response of the sea surface at vertical incidence, under widely varying sea-state conditions, and backed up by extensive experimental data, is singularly lacking. However, computer-generated simulations obtained from Raytheon's Submarine Signal Division (see Appendix R-G) allows preliminary estimates of shift in centroid versus sea-state to be made. These data ignore possible effects of whitecaps and spray, which are probably negligible for sea-states with winds of less than 20 knots.

The data in the table of centroid shifts shown below indicate that for the processor assumed, (which Appendix R-A shows are the same magnitude as centroid shift due to impulse response), sea state errors are negligible for winds of less than 20 knots.

Wind (Knots)	Approximate Shift in Centroid of Impulse Response
10	.01 m
20	.03 m
30	.07 m
40	.12 m
50	.20 m

The shifts indicated are too small to be significant for purposes of this study, and may well be the result of sampling errors because of limited empirical data. The shifts shown were downwards, toward wave troughs, which may seem paradoxical in light of the higher elevations in the crest direction. This elevation effect appears to be more than compensated for by the occurrence of a larger number of troughs and fewer high crests.

More study on this subject appears to be needed. It can be anticipated that with adequate data that may eventually become available, corrections for sea-state may be introduced as a function of known wind or wave heights.

4.4.1.4 Changes in Atmospheric Refractivity

Changes in refractivity (propagation velocity) in both the ionosphere and the troposphere have been considered. Frey, Harrington, and Von Arx[3] show that for the ionosphere at X-band, day to night variations in range "error" (delays) of 2 to 10 cm. can be expected. Since a portion of this delay is predictable, it appears that at X-band, uncorrected ionospheric residual errors can be made negligibly small.

Troposphere data are taken from Barton[2], Chapter 15, and from the Handbook of Geophysics[4], Chapter 9. Mean delay through the troposphere corresponding to a refractivity (N) of approximately 300 amounts to a range delay at vertical relative to that in vacuum of about 2 meters, which can be used as a corrective factor. Extreme variations in N at sea level amount to about ±50 and represent altitude errors (uncorrected) of about 0.3 meters (see Appendix R-I).

Corrections for variations in N require information on weather conditions including water vapor content, temperature, and pressure. Some data on water vapor and temperature (the most significant parameters) can be obtained by the use of a satellite-borne radiometer operating at about 23 GHz, where moisture absorption and reradiation is prominent. Relationships between radiometer signal strengths and N have not been determined in this study, but can probably be obtained by further study. Further weather information may be obtained from ships at sea, weather satellites, and from ground weather stations where they exist.

Assuming probable operation at much less than the extremes of ±50 in N, and with at least partial corrections being possible with use of weather data, it seems reasonable to estimate troposphere altitude errors in the vicinity of 0.1 meter:

$\sigma_{hr} \approx .1$ m (.3 ft) .

4.4.1.5 Integration Errors

Since low-pass filtering or signal integration is necessary for reducing receiver noise and sea clutter effects, it follows that some attenuation and lag errors are introduced in the process. The altitude tracking servo can be represented, for analysis purposes, by a low-pass filter having a transfer function determined by the circuit parameters. Altitude changes can then be represented by voltage changes at the filter input, with the smoothing or filtering effect introducing errors in the signal readout.

The use of an anticipated 1 Hz bandwidth in the servo integrator permits all but the most abrupt geoid surfaces to be tracked with negligible filtering error. As a worst-case example, assume a sea-mount producing a gaussian-like depression of the sea surface. Let this depression be about 20 km across the half-amplitude dimension, and assume a vehicle velocity of 7 km/sec. For this time function input, the filtered output will show a time lag with respect to the input of about 0.16 seconds (corresponding to the filter time constant), and an attenuation in

depression amplitude of about 1.5%. The 0.16 second lag corresponds to about 0.11 km displacement in the apparent location of the depression, and the 1.5% attenuation corresponds to about 0.15 meter altitude error for a 10 meter depression.

Integration errors thus are not constant, but depend on the magnitude and bandwidths of the terrain contour. However, since the servo transfer characteristics will be known, it becomes possible to correct sufficiently so that negligible uncorrected error should result even for worst cases.

4.4.1.6 Bias Errors

Bias errors can be defined as errors resulting from uncorrected, slowly-varying or fixed signal delays such as receiver delays, processor delays, transmitter and modulator delays, plus other miscellaneous variable delays which may be temperature, voltage, or aging dependent. Delays tend to increase the apparent altitude and may represent one of the largest error sources unless corrections are provided.

Corrections may be made on the basis of test range calibrations performed on an accurate ground-based range under controlled conditions. Ground tests will generate data not only on receiver and processor delays using actual transmitter waveforms, but will also yield information on such factors as temperature, voltage, and possibly even aging variables.

A bias calibrating circuit is planned as part of the operational radar. This circuit consists of a signal simulator with a delay corresponding to a known fixed altitude. At appropriate intervals such as once per hour, a check of the calibrated delay can be processed, and changes in output reading may be used to provide calibration corrections to the altitude readings.

With careful design, selection of best quality components, adequate ground range testing and use of the operational calibration circuit, it should be possible to control bias errors within an estimated 0.2 meters.

This does not represent a high confidence estimate, pending the study of experimental test data which will be available only after breadboard equipment has been constructed and operated.

Present bias estimates (50% confidence level) are placed at:

$$\sigma_{h\beta} \approx 0.2 \text{ meters} .$$

4.4.1.7 Received Waveform Variations

The received signal waveforms are derived from the impulse response represented by a decaying exponential having a time constant (t_c) which varies with altitude, with σ_o angular variations, and with beam vertical pointing errors. Estimates have been made of the altitude error resulting from these changes in time constant.

The error relationship (see Appendix R-D) is:

$$\sigma_{hw} = \frac{ct_1}{2} \times \frac{3t_1}{t_c} \times \frac{dt_c}{t_c} .$$

Assuming a worst case 10% variation in time constant and a 50 μs pulse ($t_1 = t/2 = 25$ μs) and a 5 μs time constant gives:

$$\sigma_{hw} \approx .006 \text{ meters (negligible)} .$$

4.4.1.8 Signal Amplitude Variations

Rather serious altitude errors can result from waveform variations resulting from signal-to-noise or amplitude variations in circuits, which are non-linear over the dynamic range of the signals. Receiver or processor saturation or the use of envelope or square-law (non-coherent) detectors can result in errors of this description.

Non-coherent detectors can cause rather large errors when signal changes occur through the $S/N \approx 1$ region. At lower signal levels, the detector operates nearly quadratically, so that a ramp input results in a slowly rising output. At higher signal levels, the start rises more and more abruptly giving the output waveform an appearance equivalent to that of a shift in time or reduced altitude. An analysis (see Appendix

R-C) was performed on a 50 ns transmitted waveform which indicated that the altitude error may amount to 1.5 meters or more as an extreme case. With signal variations of 15 to 20 dB anticipated versus σ_o sea-state, the probability of a prohibitively large error is high. For this reason, the use of coherent detection which is linear, i.e., independent of signal amplitude, was studied. With the use of a coherent or synchronous detector, this error source is effectively eliminated.

Other sources of signal compression effects in the receiver and processor can be removed by providing adequate dynamic range with agc. With signal levels near or below noise, dynamic range requirements are nominal. The narrow-band tracking circuits increase the S/N ratio to desired levels where dynamic compression effects will be of no concern.

With these considerations in mind, this error source may be taken to be negligibly small:

$$\sigma_{hA} \approx 0 \ .$$

4.4.1.9 Altitude Counting Errors

Altitude counting, referenced to a secondary frequency standard, is subject to three error sources: (1) that resulting from inaccuracy or instability in the reference oscillator, (2) that resulting from quantization, and (3) that resulting from vehicle altitude changes during the counting interval.

The reference oscillator stability requirements are related to altitude accuracy requirements by the error form:

$$\frac{dh}{h} = \frac{df_c}{f_c} \quad \text{(counting oscillator stability error)}.$$

Requirement for less than 1 meter error in 1000 km therefore, dictates a frequency stability of the same ratio, or better than 1 part in 10^6. To eliminate this error source entirely requires that stabilities of at least 10^{-7} and preferably 10^{-8} be attained. Good crystal oscillators with oven controlled crystals are presently capable of this

accuracy. Methods for cross checking against ground based oscillators are discussed in Appendix R-J.

Quantization errors result from digitizing the count and can amount to the range (altitude) equivalent of one cycle over the counting interval (T_c). Since the altitude (h) is proportional to the clock count (N_c) (see Section 4.3.1.7),

$$\frac{dh}{dN_c} = \frac{h}{N_c} .$$

For a count of unity, $dN_c = 1$ and $N_c = f_c T_c$. The quantization error is then given by:

$$\sigma_{hQ} = dh = h \frac{dN_c}{N_c} = \frac{h}{f_c T_c} \quad \text{(quantization error)}.$$

Solving for the required clock frequency (f_c) for .1 meter quantization error (σ_{hQ}) and assuming a count interval of 1 second (T_c) and 10^6 meters altitude (h), gives:

$$f_c = 10 \text{ MHz} \quad (\text{for } \sigma_{hQ} = .1 \text{ meters}).$$

If the vehicle changes altitude during the counting interval, the final altitude count corresponds to some previous altitude because of counting lag. The correction for this effect is simplified by the fact that orbital velocities are essentially constant over the 1-second counting intervals. On the basis of constant velocity, analysis (see Appendix R-E) shows that the actual altitude at the end of the count is given by:

$$h_v = h_c + \frac{\Delta h_c}{2} \quad \text{(altitude with climb correction)}.$$

That is, altitude at the end of the count is the indicated altitude (h_c), plus half the altitude change during the count (or between successive counts). With this correction introduced, negligible residual error may be attained as a function of vehicle vertical motion.

Combining these three counting errors, an error of

$\sigma_{hc} \approx$ .1 meter (expected counting error)

should be attainable.

4.4.1.10 Multipath Errors

Inhomogeneities in the atmosphere introduce the possibility that several signal paths of different lengths to the sea-surface and retrun may exist. Some smearing of signal waveforms with resulting altitude uncertainty may therefore result. Investigation indicates, however, that multipath errors are minimum over vertically directed beams and are much worse for communication links beamed along the horizontal[5]. Smearing of a few nanoseconds is found to be about the maximum in worst cases over horizontal communication links. Vertically positioned beams then, which are much less severe, should have negligible smearing. This error source can be neglected thus:

$\sigma_{hM} \approx 0$.

4.4.2 ACCURACY SUMMARY

An error summary, contained in Table 4-1, shows estimated errors for itemized error factors before/after ground based data corrections.

4.4.3 LAND CAPABILITY

Highly precise altimetry over land is limited by beam spot size or horizontal resolution defined by spot illuminated area. Since the radar altimeter using a 50 ns pulsewidth generates about 7 km spot diameter; horizontal resoltuion to better than spot diameter cannot be expected.

If precise altitude data at precise points on land is required, then techniques for obtaining small beamwidths must be considered. Lasers appear to have a great advantage for this case. Radar may be considered only if very large antennas at high operating frequencies can be employed. Special techniques for radar altimetry over land using aircraft with doppler-navigator-type vertical sensors have been considered. Satellite radar altimetry does not appear attractive for precise measurements over land.

TABLE 4-1

ERROR SUMMARY

Error Item	Estimated (Uncorrected)	Estimated with Data Corrections	Present Confidence Level (Corrected)	Remarks
1. Receiver Noise	.009 m	.009 m	>90%	
2. Sea Clutter	.04 m	.04 m	>90%	
3. Sea State	.03 m	.01 m	50%	At 20 knots wind. (See Note 1.)
4. Refractivity	.3 m	.1 m	75%	See Note 2.
5. Integration	Variable	0	95%	See Note 3.
6. Bias	.3 m	.2 m	50%	Gated amplifier-low jitter, fast rise time. (See Note 4.)
7. Waveform Variations	.1 m	.1 m	90%	
8. Amplitude Variation	.05 m	.05 m	90%	Assumes coherent detector. Much larger error for non-coherent.
9. Digital Counting	.3 m	.1 m	90%	See Note 5.
10. Multipath	0		>95%	
Total σ (rss)	.53 m	.26 m	50%	Bias error limited at present; much higher confidence possible after testing.

(See following two pages for Notes concerning this table.)

TABLE 4-1 (Continued)

NOTES

Note 1. Based on Marine Research Lab impulse response data (see Appendix R-G). As a function of wind, the following uncorrected errors are obtained:

Wind (knots)	Centroid Error	Remarks
10	.01 m	These values assume that error increases as square of wind velocity. No correction for whitecaps, spray, etc. is assumed. Based on limited theoretical data; has not been verified experimentally.
20	.03 m	
30	.07 m	
40	.12 m	
50	.20 m	

Note 2. The 0.3 m assumes variation in N(refractivity) of about 100 (or ±50) for extreme weather (see Barton[2] Figure 15.9). With weather data available from ships at sea, weather satellites, or by radiometry, improved data may be expected. It seems likely that at least a 2 to 1 improvement in N data should be possible for ground processing corrections.

Note 3. The processing filter introduces lag and attenuation errors which depend on terrain contours. For contour variations of 1 Hz or slower, the errors are small and can be removed entirely by ground based computers.

Note 4. Bias errors require calibration data for accurate estimation. Errors include estimated calibration error on a test range, plus expected aging and environmental variables over the life of the vehicle.

A built-in bias measuring circuit is contemplated; it would provide correction information and raise confidence that bias errors have not built up during operation.

TABLE 4-1 (Continued)

NOTES

Note 5. Counting errors include clock stability, quantization, and vehicle vertical velocity errors. If raw prf data were transmitted to ground on a CW basis for ground based processing, then much improved accuracy would be expected.

4.4.4 ABILITY TO MEET GEODETIC REQUIREMENTS

Geodetic requirements were originally stated with respect to the rms altitude accuracies for several geodetic uses, and also for the corresponding data reading densities for each use.

The most stringent accuracy requirement given was that of making "geoid connections" where accuracies of 0.1 meters were specified. This accuracy appears to be marginally possible with first flyable models. Not more than about 10% confidence level should be expected in meeting this requirement. It might be expected that with 5 to 10 years of development time, and with experience in reducing data to introduce all necessary corrections, the confidence level might be increased to 50% or better.

The next most stringent accuracy requirement is the oceanographers' need for accuracy of about 0.3 meters, for establishing mean sea level. This accuracy has been taken as a reasonable design objective for first models. A confidence level of 50% is given for first models and should increase to 75% or higher for developmental models, which should be available in 5 to 10 years.

Other requirements such as submarine geology and military geometry, which are less stringent, are more easily met and should be attainable with confidence levels approaching 100%.

Measurement densities have been specified in terms of the number of measurements obtained per 10,000 sq. km of sea surface area. This specification implies intermittent readings. It puts no constraint, however, on the radar which generates quasi-continuous measurements along the ground track.

It is presumed that reasonably uniform density of measurements over the 10,000 sq. km area is desired and may be more explicitly stated as at least one measurement per 50 sq. km (200 per 10,000 sq. km). The density distribution is then determined to some extent at least, by satellite orbit parameters and by equipment life.

A coarse estimate of ground track spacings can be made by assuming uniform coverage. A ninety-minute orbit gives sixteen orbits or 32 crossings per day. For an average of 7 km spacings then, about 6000 crossings must be made, requiring about 6 months equipment life.

This equipment life requirement cannot be met with the transmitter equipment which is presently available. For gated-amplifier types at X-band, life maximums of 2000 hours (3 months) are being quoted. Prospects are good that longer life can be obtained after developments extending over the next few years. The availability of solid state type transmitters in the not too distant future may also increase reliability and make possible the ground coverage density being sought.

4.5 SYSTEM TRADE-OFFS

This section reviews some of the more important techniques and parameter-selection trade-offs. Most of the items covered here have been mentioned in other sections, but are compiled and summarized here for ease of review.

4.5.1 ANTENNA SIZE

Two basically different altimeter techniques are possible depending on the use of either a large or a small antenna. The large antenna approach implies the use of an antenna large enough to remove nearly all beam and earth curvature effects at the sea surface intercept so that

the received waveform is then a good replica of the transmitted waveform with negligible waveform stretching which otherwise results from intercept time differences over the target area.

The small antenna approach accepts the presence of wavefront curvature over the antenna beam area, but considers the resulting waveform distortion to be analytic, such that high quality altitude information can be extracted from it.

The small antenna approach which has been selected for this system yields a received waveform which is very nearly an integral of the transmitted waveform over the target area, in which case processing is complicated by the need for an extra processing stage simulating differentiation to compensate for the integrating characteristic of the target.

Even with this complexity, the small antenna approach has been considered to be the more feasible of the two possibilities. The large antenna approach requires a furlable antenna configuration necessitating hitherto impractical mechanical tolerances. In addition, the vertical attitude stabilization accuracy required would call for precision difficult to attain in satellite-borne equipment. The furlable antenna would most probably employ a horn-feed having long transmission lines running from the transmitter to the horn. Delays in the line, in the ray paths, and in the rather uncertain reflector position (if remote from the vehicle) may introduce sizeable errors.

Some sources[3] contend that ultimate altimeter accuracy in the presence of sea-state is to be obtained by using an extremely small beam capable of analyzing the microscopic structure of the intercepted surface. The fine grain advantage is lost, however, in the uncertainty of any given sample with respect to msl. Msl may be inferred on the basis of large statistical samples which then permit reconstruction of the mean data from the many bits of microscopic data. The small antenna approach handles enough data over the width of single processed wavefronts to allow good averaging on each pulse, and gives nearly ideal averaging after reasonably long smoothing intervals.

4.5.2 PROCESSING TECHNIQUES

A number of processing alternatives are possible which have relative advantages and disadvantages. Nearly all good processors attempt to maximize signal-to-noise ratios and derive an amplitude-independent axis-crossing timing point by using some form of differencing such as early-late gating, split gating, differentiation, or delay-differencing.

The two-stage delay differencing method of processing has been selected because it provides the desired doublet type of time discriminator waveform with good axis-crossing characteristics. These characteristics include relative immunity to amplitude changes, good immunity to drift with respect to voltage, aging, etc., and relative immunity to sea state. Delay differencing is reasonably easy to instrument, and has good stability. Most of these characteristics are shared by the gating method described by Barton (see Appendix R-L).

4.5.3 TRANSMITTER FREQUENCY

An X-band transmitter was chosen for the operating frequency because it represents the best compromise between ionospheric delay errors which become prohibitively large at lower frequencies, and weather problems such as atmospheric attenuation and rain backscatter which become troublesome at higher frequencies. X-band permits the use of a conveniently small antenna while retaining reasonably good gain. Microwave components are readily available here because of common usage in a wide range of equipment.

4.5.4 PULSE LENGTH

Transmitter pulse length was placed at 50 ns as a compromise between strong signal amplitude and relative immunity to sea state, which favor long pulses, as against waveform timing errors, which favor short pulses. Short pulses are nearly immune to small attitude stabilization errors and errors resulting from changes in waveform time constants. The doppler bandwidth for phase tracking would also be reduced by using short pulses. The 50 ns compromise appears to meet all accuracy requirements.

4.5.5 PULSE REPETITION FREQUENCY

The transmitter prf was selected to be as high as possible, but without incurring range ambiguity problems which cannot be readily resolved from coarse altitude information available from other sources, and without incurring phase tracking problems resulting from overlap of successive pulses in too-rapid succession. The 100,000 prf at 1000 km altitude falls within these limits and seems the simplest means of obtaining high duty cycle and of reducing pulse peak power requirements. Phase tracking becomes impossible at prf's which are low compared to the bandwidth of the signal being tracked. The high prf also aids altitude tracking performance and gives much improved accuracy because of the short time period per prf interval. Percentage errors over the short time base are a much smaller percentage of ranging time than the same percentage errors over the entire unambiguous range which is some 1000 times greater.

4.5.6 TRANSMITTER WAVEFORM

Transmitter waveforms can be classed as either simple pulse or pulse compression waveforms. Unless pulse compression with extremely high duty cycles between 25% and 50% can be used, making possible the use of solid state transmitters, then little would be gained from pulse compression. Pending further study of pulse compression possibilities, a simple pulse system has been selected.

The simple pulse system is capable of meeting accuracy requirements but requires high pulse peak power and has shorter life than is desired. Eventual use of solid state transmitters, possibly with pulse compression, is envisioned.

4.5.7 DETECTOR TYPE

The selection of coherent detection as opposed to the simpler envelope or square-law detection is based on considerations of the rather large timing shift error in the detected waveform where signal-to-noise changes occur in the noncoherent detector input. Coherent detectors on

the other hand are linear with respect to superposition, meaning that no change in signal waveform occurs as the accompanying noise amplitude, or signal-to-noise ratio, is varied. Altitude errors well in excess of the 1 meter requirement could be expected in the event of 15 to 20 dB changes in σ_o (reflection coefficient of the ocean) values if noncoherent detection is employed.

4.6 RECOMMENDATIONS

Additional investigations leading to the eventual construction of an operational altimeter are being considered.

The following tasks are recommended for consideration to promote the development of the radar altimeter.

4.6.1 SPECIFIC CIRCUIT DESIGN AND HARDWARE DEVELOPMENT

It has already been pointed out that studies to date have been directed toward conceptual designs only, for the purposes of examining the major problems and for exploring techniques for meeting these problems.

The following phase of the work would cover the detailed design of circuits, firming of concepts, and selection of hardware components. This phase should include interface with satellite design so that the most reasonable compromises (trade-offs) between radar needs and vehicle constraints can be arrived at. Antenna size, attitude stabilization, and source power typify parameters that warrant thorough investigation.

4.6.2 BREADBOARD TEST OF CONCEPTUAL DESIGNS

In the course of the present study, techniques have been suggested that can be considered as advancements in the state-of-art and require operational verification and evaluation. Such concepts include the phase tracking circuit intended to operate in doppler clutter, the two-stage delay-differencing processor of waveforms obtained from a synchronous detector, the altitude-locked prf oscillator for altitude tracking

and coherent, gated-amplifier transmitter circuits. While analysis indicates high expectation of satisfactory performance, experimental work can be valuable for indicating problem areas and for evaluating performance.

4.6.3 PULSE COMPRESSION STUDIES

The possibility exists that transmitter-modulator pulse peak power requirements and also equipment size and weight may be reduced by the use of pulse compression. A conclusive evaluation cannot be presented without a careful study of a number of pulse compression techniques including fm swept (chirp) types over a range of compression ratios and examination of several types of compression circuits. The characteristics to be studied include equipment complexity and size, possible performance degradation, and transmitter advantages. Miscellaneous waveform coding and phase shift keying techniques should also be studied.

4.6.4 BIAS ERROR EXPERIMENTS

One of the largest potential error sources in the altimeter is bias error due to receiver-processor delay. This delay must be precisely known and calibrated against long time variations from a variety of causes in order to assure high accuracy.

Techniques must be developed for measuring bias in operational circuits against targets that simulate the sea surface; these must be tested over accurately measured test ranges. It appears that the integrating characteristic of the sea surface may be simulated by the use of high-Q microwave cavities. Techniques for introducing clutter or doppler simulation can probably be developed for more realistically simulating sea return signals.

4.6.5 REFRACTIVITY MONITORING STUDIES

Radiometry at 23 GHz where water vapor absorption and reradiation are maximized, affords a means for measuring water vapor content of the troposphere and for deriving corrections in refractivity associated with water vapor. A potentially large source of altitude error may be

eliminated if suitable radiometry equipment can be developed and if relationships between readings and refractivity can be derived.

4.6.6 NEW TECHNOLOGY IN SOLID STATE POWER SOURCES

Quite significant improvements in system size, weight, and power may be expected when solid state microwave technology permits the generation of 100 watt pulses at X-band or higher frequencies.

4.6.7 IMPULSE RESPONSE OF SEA STATE

The present study indicates that no extensive investigation of the electromagnetic impulse response of the sea surface at vertical incidence from high altitude over a wide range of sea state conditions has been conducted to date. The work done by Raytheon's Marine Research Laboratory is the only known analysis* (see Appendix R-G) and is not extensive enough to be of great value.

A study of electromagnetic models is indicated, covering the return from waves as functions of wave slopes and facet curvatures or dimensions. The models used by MRL were based on optical analogy, considering each wave maxima or minima as an equally weighted facet. Consideration should be given to facet weighting versus radius of curvature at crests and troughs and on capillary wave reflections along wave slopes. Computer programs for simulating waves and for generating statistically smoothed data (not histograms) versus wave elevation would be highly desirable. The radar reflections from whitecaps and spray and their weighting effect as a function of wind speed are also of interest.

Experimental verifications of theoretical and computer simulation studies are indicated. These data can be obtained by airborne radar using sub-nanosecond pulse techniques at very high prf rates.

*Rather extensive data on sea clutter and backscatter at shallow angles is available[12,13,14], and on reflection coefficients at vertical incidence[12,13] is available and has been reviewed. None of these documents contains information on impulse response at vertical incidence, and they are of no value for determining centroid shift of the electromagnetic response with respect to sea state.

It would be highly desirable to have a mean sea level reference reflector located at some convenient point at sea. This reflector may be a tower-mounted corner reflector, or alternatively a sea wave damping circular structure large enough to give a strong return from a smooth surface at calm sea level.

Flights could be made over these reference targets under varying sea state conditions, using the references as bench marks or range marks against which wave impulse response returns could be compared. Subsequently, the actual altimeter radar proposed for the satellite might be flown over the reference targets to determine any change in altitude readings versus reference target levels under varying sea state conditions.

4.6.8 WAVEFORM ANALYSIS VS DETECTOR TYPES

For this study, processor waveform analysis has been simplified by assuming square-law detectors whose output signal (amplitude) is proportional to the input power. Linear detectors are somewhat more cumbersome to analyze, since the output signal (amplitude) is proportional to the input signal amplitude, and the square-root of the input power. A general analysis of the performance of detectors, including the effects of changes in S/N ratios, is beyond the scope of the present study. Such an analysis would be helpful in determining which type of detector would be most suitable for meeting system requirements.

It is recommended that a study be conducted to investigate detector output waveforms, including the effects of wide variations in S/N ratios and the effects on altitude accuracy, for the following:

a. Square-law detectors, defined as detectors which perform instantaneous squaring of the input waveform amplitude. This type of detector gives the linear ramp which has been treated in the idealized waveforms. Waveforms from this type detector are probably the simplest to analyze, as mentioned above.

b. Square-law detectors, defined as envelope detectors which operate on the non-linear or knee region of diodes such as vacuum tubes with extended cutoff, or solid state devices operated near the cutoff point.

c. Linear-law envelope detectors or peak detectors, defined as detectors which switch instantly and act as ideal half-wave or full-wave detectors. Effects of non-ideal switching should be investigated.

d. Linear detectors, defined as network-linear or coherent type detectors, such as synchronous detectors. This type detector has been recommended in this study because of its immunity to waveform changes versus S/N, and because of its high efficiency in cases where $S/N \ll 1$.

However, this detector gives a square-root type waveform for a linear power input to the detector, which rises very abruptly and non-linearly at the leading edge. Furthermore, the coherence function in narrow band (bandpass) noise affects the resulting detector output waveform, and requires further study for the case of phase tracking in the presence of clutter and varying doppler.

SECTION 5

SYSTEMS ANALYSIS

SECTION 5

SYSTEMS ANALYSIS

(J. Tatsch/E. Weiss)

5.1 TRADEOFF METHODOLOGY

The principal purpose of the tradeoff study is to make a selection between the proposed geodetic satellite altimeters. The basic criterion is how well system specifications are met. System specifications were developed from geodetic requirements, which consist of a set of rms errors and measurement densities for each set of geodetic requirements, summarized in Table 5-1.

For purposes of the tradeoff, it is necessary to compare how well the proposed systems are expected to perform tasks under the same ground rules. The ground rules are conditions under which the measurements will be performed, including assumptions as to the nature of the surface viewed, such as sea-state, and conditions affecting transmission. The assumptions include the best available useful data, but in any event must be the same for both radar and laser. The data may be probabilistic in nature, and include information on the topography and/or reflective characteristics of the sea surface during the measurements. In the absence of adequate real data, assumptions must be judiciously made; in any event, greater validity is expected for the comparison between the performances of the two candidate systems than for the performance of either system alone.

For purposes of this study, it is necessary to reconsider and possibly modify the error analyses prepared in developing the candidate systems, in order to compare their performance in attempting to satisfy the specific task under consideration. This should provide performance data and include a description of the rms error in the measurement, and the measurement density, as well as other performance characteristics.

TABLE 5-1

MEASUREMENT DENSITY AND RMS ERROR

REQUIREMENT SOURCE	RMS ERROR (m) in Height Above Sea/Spheroid		Number of Measurements per 10,000 km^2 without Tides	with Tides
Mean Sea Level (Oceanography)	0.3	0.3	2	4
Submarine Geology				
Static	1	1	200	200
Dynamic	----------		200	200
Military				
Geometry	7	7	10	20
Gravity	----------		--	--
Geodesy				
Datum Establishment	1.5	1.5	200	200
Geoid Connection	0.1	0.1	10	20
Geoid Extension	0.5-2	0.5-2	0.1-1	1 - 5

The tradeoff criteria are selected and weighted in advance for each task. The weighting factors consist of the number of points (out of 100) assigned to each criterion. The performance for one candidate system is judged for each criterion against that of the competitive system and scored differentially, using the weighting factor assigned to that parameter. In differential scoring, points are awarded to one or the other of the candidate systems, or to neither. Any number of points can be awarded, as long as it is not in excess of the weighting factor assigned to the criterion under evaluation. The fraction of the total weighting factor that is allocated to one system is a measure of the difference in performance between the two systems (a small fraction indicates less difference than a large fraction). Differential scoring is much less difficult than absolute scoring (or independent scoring), especially of dissimilar candidate systems, and addresses the problem of comparison directly rather than indirectly. The partial scores for each parameter are added to form the total score for each candidate system. This scoring table is examined to evaluate how the candidate systems compare with each other as geodetic satellite altimeters.

A tradeoff study such as this one is a rather complex dynamic process, partly because of the problem of obtaining a common denominator for comparing two dissimilar systems, and partly because of the difficulty in quantitatively weighting and scoring the individual criteria. Sound technical judgment and experience play a major role, and the decision-making process cannot be completely prescribed a priori. An attempt is made to specify the procedure and decision-making pursued during the tradeoff process itself in sufficient detail so that the reader is able to decide for himself where the various judgments enter into the process, and so that the reader can modify those aspects of the decisions with which he may have reservations, or which suit his modified needs.

The principal attributes of this tradeoff methodology are summarized as follows:

a. It is based on first order effects. This does not involve detailed parametric comparison of variables, inasmuch as these systems are in the preliminary design stage.

b. The assumptions and methodology are explicitly stated wherever practicable, thereby providing the opportunity for the reader to take issue with the various features of the study. An important aspect of any study is the choice of proper assumptions.

c. In the absence of real data, reasonable assumptions are made regarding the data. Such assumptions must avoid unwarranted preference for one candidate system over another, and must be applicable to both candidate systems, and therefore useful for comparison of performance.

d. The critical decisions, such as weighting and scoring are performed in a quantitatively visible manner, so that while experience and technical skill are involved, the reader can take issue with specific judgments and determine for himself the effect of modifying these judgments to suit his particular needs.

5.2 CANDIDATE ALTIMETER SYSTEMS

For purposes of this study, the candidate radar altimeter system and the candidate laser altimeter system were designed in order to compete with each other in meeting geodetic requirements. Some feedback during the design of the competing altimeter systems, and between the altimeter systems and the geodetic requirements, served to enrich the study and improve the competitive altimeter designs. Still, it must be emphasized that the altimeter designs themselves were not optimized, but were primarily designed for basic feasibility.

One may be tempted to accept the altimeter system design specifications literally, and to make hard judgments based on those specifications. It is helpful to recognize the degree of flexibility of each parametric value, and to be aware to some extent of the penalties (or gains) which might occur in other parameters as a consequence of changing these values.

In allocating relative points to the altimeter systems, one must recognize that although the parametric values may not be optimized, it is necessary to rate them as given in the candidate system design specifications, even while recognizing the consequences of flexibility. Otherwise, one is likely to optimize individual parameters independently, which is contrary to the nature and design of actual systems.

In summary, there are two aspects of the candidate altimeter systems which should be borne in mind. First, the candidate systems are not completely optimized, but are reasonable baseline systems. Second, despite the fact that the candidate altimeter system designs are not optimized, the tradeoff (comparison) must be made between these candidate systems as designed by the radar and laser study teams respectively, not as the systems analyst would like to see them designed, even though there exists the latter temptation.

5.3 EVALUATION CRITERIA

Descriptors, including evaluation criteria, are by no means unique. The list of evaluation criteria which evolved appears to be sufficiently inclusive to adequately characterize and compare the performance of the laser and radar altimeters systems. Overlap and redundancy are to some extent unavoidable, and an attempt is made to clarify criteria relationships in the evaluation description.

The evaluation criteria used in the study are the following:

- Accuracy

  rms error (meters) expected as a result of errors from all sources

- Data Rate

number of measurements per 10,000 km^2 which the system can perform (the inverse is the area over which measurements are averaged)

- Power

average continuous power (watts) required of satellite power supply during the mission

- Weight

weight (kgm) of entire altimeter, exclusive of power source, and exclusive of specified requirements on the satellite

- Volume

volume (cubic cm) of packaged altimeter, when loaded for takeoff, exclusive of power supply and exclusive of specified requirements on the satellite (also, any unusual dimensions)

- Life

a. shelf life - time (days) system can remain after assembly (including calibration) prior to launch, without degradation during subsequent use

b. standby life - time (days) in orbit during which system can remain available for use either intermittently or continuously, without degradation

c. operating life - total/time (days) during which system can take data, either continuously, or as integral of intermittent operation (not to be confused with pulsed vs cw transmission

- Availability

probability of candidate system hardware components being fully developed (space qualified) in time for space operation in 1971-72. (This is subjective judgment, but a necessary consideration)

- Performance Potential

a. theoretical potential accuracy and data rate (Criteria 1 and 2) of the candidate system

b. probable accuracy and data rate (Criteria 1 and 2) available within a specified time (such as 5 to 10 years)

- Other Capabilities

a. other functions which candidate altimeter system can perform with little or no modification; ditto, with modifications

b. capability over the ground

- Environmental Constraints

a. transmission constraints - specify those environmental conditions between the satellite and the target (Earth) which limit accuracy, and the extent of the limitation.

b. target constraints - specify the extent to which target conditions (sea state, reflectivity, etc.) limit accuracy

- Safety

is there a potential radiation hazard to a person or object on the ground due to the ranging beam from the altimeter? Is radiation interference a problem?

- Calibration

a. time required for calibration after complete assembly and testing, but prior to launch. (Holding of calibration should be included in life)

b. can calibration be performed (upon command, or pre-programmed) in orbit? If so, time required for calibration; time interval recommended for re-calibration

- Requirements Imposed by Altimeter on Satellite

a. satellite stabilization, or pointing angle within which satellite must be oriented for suitable altimeter operation

b. attitude data, or accuracy within which pointing angle must be known by altimeter for suitable operation

c. angular rate (angle per unit time) which satellite should not exceed for suitable altimeter operation

d. thermal constraints - temperature range within which satellite environment must be maintained for altimeter. Heat load which must be dissipated (and schedule of such dissipation)

e. telemetry - amount of data (bits) and time schedule for transmission (bit rate) in both directions between ground stations and satellite in order to meet system specifications.

f. storage - on-board storage and data processing requirements (if any) not included in altimeter package

g. supplementary information requirements - what additional information does the candidate system require from outside itself (from satellite and/or ground station) in order to fulfill its function? Are any supplementary sensors necessary?

5.4 WEIGHTING FACTORS FOR THE EVALUATION CRITERIA

The determination of weighting factors for the evaluation criteria is a relatively subjective process, in which the experience and judgment of the analyst play dominant roles. The weighting factors are by no means unique, and reflect the relative importance assigned to the various characteristics of the system. It is easy to fall into the trap of over-compartmentalization, wherein separate detailed consideration of the elements is made without consideration of the system as a whole. Our experience indicates that despite the necessity for compartmentalization for purposes of discussion, there must be

sufficient adaptability in the tradeoff process to modify the weighting factors after the fact; the list of initial weighting factors given in Table 5-2 should therefore be considered as the base for the tradeoff study, with subsequent adaptability implicit.

As it turned out, attitude data is of greater importance than originally expected, and had to be reconsidered separately.

5.5 SCORING THE CANDIDATE ALTIMETER SYSTEMS

5.5.1 ACCURACY

The laser altimeter is accurate to about 1/3 meter under ideal no-sea-state conditions. With waves not in excess of 3 meters, accuracy is about 1/2 meter. The principal contributor to inaccuracy is the angular uncertainty; angle with respect to vertical should not exceed $.25^{o}$, and should be known to 10 arc sec, in order to maintain a contribution to the error of not more than .3 meter.

The radar altimeter has accuracy of .53 meters uncorrected, of which .3 meters are due to receiver bias, .3 meters due to refractivity, and .3 meters due to digital counting errors. With corrections that are feasible, these three error contributors may be reduced to .2, .15 and .1 meters, respectively, contributing to a total error (rms) of .26 meters. Sea state is not considered a problem for winds of less than 20 knots.

Geodetic requirements vary from about .1 meter to 7 meters. Both radar and laser altimeters are designed to fall well within this range, and have comparable accuracy, at least in principle.

In comparing laser altimeter accuracy with that of a radar altimeter it is obvious that a simple statement of accuracy is inadequate; accuracy is dependent on the values of other parameters, such as power, attitude, life, and other criteria such as environmental constraints.

TABLE 5-2

INITIAL WEIGHTING FACTORS FOR THE EVALUATION CRITERIA

Criterion	Initial Weighting Factor
1. Accuracy	35
2. Data Rate	15
3. Power	4
4. Weight	3
5. Volume	2
6. Life	8
a. Shelf (1) b. Standby (2) c. Operating (5)	
7. Availability	3
8. Performance Potential	3
a. Theoretical (2) b. Probable (1)	
9. Other Capabilities	3
10. Environmental	4
a. Transmission (2) b. Target (2)	
11. Safety	2
12. Calibration	1
13. Requirements on Satellite	17
a. Pointing Angle (2) b. Attitude Data (9) c. Angular Rate (1) d. Thermal (2) e. Telemetry (1) f. Storage (1) g. Supplementary (1)	
	100

Therefore, the rating of accuracy emphasizes consideration of the altitude measurement process.

5.5.1.1 The Altitude Measurement Process

The measurement of altitude is performed by transmitting an electromagnetic signal from the satellite to the Earth, then receiving and processing the returns.

The laser beam is relatively narrow (.2 milliradian, or 40 arc sec.), with a 200 meter diameter circular footprint (half-power point where it hits the Earth). The reflected radiation is collected from a 350 meter diameter circular area, and the centroid (half-power point of the integral) of the return pulse is considered the time reference for the return signal. A single such measurement represents one datum point.

The radar beam is relatively wide (40 milliradians, or 2.3^{o}). The ground area which contributes to the altitude measurement is determined primarily by the pulse width (50 nanoseconds), which corresponds to a 7 km diameter circle at the point of closest approach on the Earth. The radar footprint covers about twice as large an area as the pulse, since (1) the processing of the return signal is significant up to about 1.5 times the pulsewidth, so that a 10.5 km circle is relevant; and (2) the sub-satellite track moves about 7 km during the one second time constant over which the radar signal is being averaged. (The ratio of radar to laser footprint areas is thus about 2500.)

The contribution from various parts of the radar footprint are weighted in a rather complicated manner in the processing of the radiation return, due to the combination of the reflection of the incident radiation from the target area (including the geometric time delays) and the signal processing technique itself. The size of the footprint thus represents a general boundary incorporating the major portion of the surface area which contributes to a single measurement of height, and a weighted averaging takes place over the footprint.

The radar processor has a time constant of about 1 second, during which time about 100,000 pulses are averaged, and the output represents one datum point. (The sub-satellite point moves about 7 km during one second).

Thus, whereas the laser sees a small spot for a relatively brief instant, the radar smears (averages) its radiation over a large spot during the time the spot moves about one diameter along the track. The averaging which is performed by the radar is particularly helpful in suppressing short-term and high frequency surface effects, and in determining an average height to the local mean sea level. This smoothing is desirable for altimetry over the ocean, as long as variations in altitude over the footprint area do not degrade the resolution and accuracy expected of the altimeter, which is generally the case. The radar smoothing time (and averaging area), which is slightly adjustable, was in fact designed to meet the geodetic requirements of measurement density (numbers of measurements per unit area). The laser footprint is sufficiently small that there is very little averaging either in time or in space, and its measurement is more direct; on the other hand, the laser encounters a sampling uncertainty in that its quick look may not be sufficiently representative of the average conditions (in time, or almost equivalently, in space) at the target location.

For purposes of scoring accuracy, the requirements are considered to be reasonably met in principle by both altimeters. The radar altimeter is considered to be somewhat superior in its measurement processing, including averaging and continuously available data, particularly when considering the goal of measuring altitude to mean sea level for geodetic purposes. Accordingly, the radar altimeter is allocated five points (out of 35) for measurement accuracy.

5.5.2 DATA RATE

The requirement of 200 measurement per 10,000 km^2 corresponds to 7.2 million measurements over the 361 million km^2 ocean surface area of the Earth, or one measurement per 50 km^2. This is the most stringent geodetic requirement listed.

For the satellite altitude under consideration, a ground track speed of about 7 km/sec is indicated. For maximum use of data, the radar would space its crossings about 7 to 7.5 km apart laterally at the equator. (This results in denser data collection at the higher latitudes, which is unavoidable.) Since the circumference of the Earth is about 40,000 km, about 5,500 crossings are necessary to cover the entire Earth just once. With two crossings per orbit, this requires about 2,750 orbits. At 14 orbits per day, about 200 days are needed to cover the entire ocean surface of the Earth once. (This does not include other problems, such as sea state or heavy rain, which necessitate redundancy of coverage.)

The laser altimeter is limited in data rate to one reading every 10 seconds, or every 70 km of ground track. Assuming ideal programming of data points for each orbit, the orbits would then be spaced about .7 km apart at the equator in order to average the necessary measurement density (per unit area); this would require 10 times the number of crossings and orbits as radar, so that 2,000 days (or 5.5 years) would be necessary to ensure complete coverage of the entire ocean surface of the Earth once. (This does not include other problems such as sea state or cloud cover, which necessitate redundancy of coverage.)

It is clear that data rate is intimately related to lifetime. Data rate in itself is important, primarily in programming the satellite orbits, although it may be of concern in the measurement of time-dependent variations in apparent altitude. With regard to lifetime, data rate imposes different lifetime requirements on the two altimeters, the laser altimeter requiring at least 10 times the lifetimes of the radar altimeter due to its slower rate of measurement of altitude.

The foregoing lifetime discussion is for worst cases; i.e., assuming that coverage of the entire Earth were necessary, and that the density of samples must meet the specifications at the equator, where the spacing between successive orbits is greatest. (More detailed discussion of sampling appears in Geodetic Appendices B and C.)

It may be noted that both the laser and the radar altimeters have shelf and standby lifetimes of one year or more. The laser altimeter claims operating life of the order of one year, while the radar claims 2,000 hours (.23 years) of operating life at ten times the data rate.

The data rate requirement is that the altimeter can take the data at a rate consistent with system requirements, including the implied number of data points and the satellite lifetime of the order of one year. Due to its relatively slow data rate, the laser altimeter could not take data covering the entire Earth (oceans) in one year, even assuming continuous operating were feasible. It would need 5.5 years. The radar could do the job in 200 days (if it lived so long), which is well within the satellite lifetime.

Other factors have been considered, but do not strongly affect the results here. For example, not all geodetic requirements are for the maximum measurement density, and the others are much more readily managed by both systems. Also, geodetic requirements do not necessarily require mapping the entire Earth, as presumed for this discussion. Part of the Earth is land; some parts of the water surface may not be as important as others. And in particular, it may be reasonable to relax the density of data near the equator in order to improve overall coverage. Also, the inclination of the orbit (possibly to 70° or less) relaxes the crossing separation by the sine of the angle of inclination, which may be a substantial effect. On the other hand, cloud cover, precipitation and sea state make redundancy in coverage necessary if complete mapping is desired.

All things considered, the fact that the radar can take data ten times as rapidly (about twenty times as rapidly, considering the average cloud cover), even though its lifetime is one fourth as long, is considered substantial enough to allocate four points (out of 15) to radar over laser.

5.5.3 POWER

The laser altimeter requires about 75 watts. The radar altimeter requires about 200 watts. These are average system power requirements during continuous operation; standby power is much less for both systems.

The laser power is proportional to data rate, which means that it cannot be substantially reduced without serious penalties elsewhere. Laser power affects cooling requirements, and includes a 5-watt cooling pump. On standby, laser only uses about 1 watt or less.

The radar power requirement may be significantly reduced by improving the overall altimeter system power efficiency from the conservatively assumed value of 2.5% and/or by increasing the antenna diameter, as discussed in Appendix R-M. Also, reduction in pulse peak power or in PRF may be acceptable.

On balance, the laser altimeter is judged to have maintained a closer check on power, and inasmuch as reducing the 200 watt level of the radar would have had other effects, the laser altimeter is allocated four points (out of 8) for purposes of this trade-off.

5.5.4 WEIGHT

The proposed laser altimeter system weighs about 33 kgm (72 lb) including its thermal system but excluding telemetry and an attitude (pointing) system. The proposed radar altimeter system weighs about 20 kgm (45 lb). While the difference is considered substantial, laser weight does not appear to be excessive, and system weight does not appear to be a limiting factor in the altimeter design. Due to the large factor (which could otherwise be used to relax other parameters), radar is allocated two points (out of 5) for purposes of this trade-off.

5.5.5 VOLUME

The candidate laser altimeter system has a volume of approximately 73,500 cm^3 (2.6 cubic feet), contained mainly in a cylindrical shape of about 50 cm in diameter and 50 cm in length. This is largely determined

by the size of the telescope, which in turn is a function of the laser output power.

The candidate radar altimeter system has a volume of about 10,000 cm^3 (.35 cubic feet), of which the most cumbersome dimension is that of the 75 cm (2.5 feet) diameter antenna. The antenna size is largely determined by power considerations.

Note that for both candidate systems the critical dimensions as well as the volume are determined primarily by power considerations. Neither candidate system is of itself excessive with regard to volume or critical dimensions, but these parameters do have value in trading off against other parameters. Since the laser system requires more than seven times the volume of the radar system, the radar is allocated two points (out of 3).

5.5.6 LIFE

Both radar and laser altimeters indicate relatively long shelf lives, in excess of one year and possibly indefinite. In orbit, standby life is about the same (one year) for both laser and radar altimeter.

The operating lifetime of the laser system is limited by the total number of flashes, (1.6 million) which is the current stumbling block. With continuous use at one flash every 10 seconds, laser operating lifetime is about one year.

The operating lifetime of the radar system is about 2000 hours (83 days) for about 7 million data points with off-the-shelf components, under continuous operation. This is a significant limitation to the current radar capability, particularly since the satellite is currently expected to have a lifetime in excess of one year.

Consideration of life did not include such necessary design parameters as radiation vulnerability and protection, built-in test equipment (BITE) or repair capability in orbit.

Both altimeter systems have limitations, and neither is judged to be substantially advantageous with regard to life.

5.5.7 AVAILABILITY

Laser items are all within the current state-of-the-art, except flashtubes, which are expected to be capable of development conservatively for operational use by 1971. Radar components are all within the current state-of-the-art, and improvements are probable in some areas. The radar system is judged to have a slight advantage, but not enough to warrant allocation of trade-off points.

5.5.8 PERFORMANCE POTENTIAL

The theoretical potential for the laser altimeter is an estimated accuracy of 25 cm, and data rate of 1 measurement every 5 seconds. It is conceivable that these can eventually be reduced to 10 cm and one per second, respectively. The theoretical potential of the radar altimeter is estimated at 10 to 20 cm; data rate improvement may be possible, but requires further analysis. These limitations, on both laser and radar altimeter system, are principally due to signal-to-noise consideration of the signal returns. The laser appears to be most limited in its potential data rate, and the radar in its large footprint size, or averaging area. The long-range potential of the two systems does not appear to offer a substantial advantage of one system over the other.

5.5.9 OTHER CAPABILITIES

The laser altimeter system may measure sea state, determine the presence of clouds, and perhaps measure the altitude and density of clouds; these are possible capabilities. The laser altimeter as designed has the capability of making some meaningful measurements over land (at least in many cases), and may measure average height and perhaps some ground contours. The radar altimeter system may measure sea state. The inclusion of an auxiliary radiometer could measure atmospheric refractivity and sense clouds. It may also be possible to obtain cloud profile data, but this may require additional power.

On balance, the laser system appears to have greater capabilities, particularly over land terrain, and is accorded one point (out of 3).

5.5.10 ENVIRONMENTAL CONSTRAINTS

Most transmission constraints are rather straightforwardly manageable by the radar altimeter, since they do not contribute excessively to the error budget, and are further reducible by supplementary equipment. Sea spray and heavy precipitation do present accuracy problems, which the system can be made aware of.

The laser altimeter is exceedingly vulnerable to transmission problems, and is completely inoperative in the presence of clouds. In practice, the seriousness depends on the specific mission. If the mission specifies a maximized duty cycle (i.e., a large number of measurements per unit area), if time is a critical limitation (i.e., short allowable standby time, or short satellite lifetime), or if the target area has an unusually small number of clear days, then the laser altimeter is in serious trouble. On the average, however, cloud cover is not a serious problem, providing the region under investigation is covered more than once during the measuring period of interest; i.e., the probability of obtaining measurements during the total experiment must be reasonable high.

Waves attributable to sea state were originally believed to be a major problem area in this study. As it turns out, waves due to sea state are indeed of importance in accuracy of measurements, but are not as dominant for purposes of comparison as originally expected. In the case of radar, the sea state effect is expected to be averaged out to the point where it is negligible for wave heights of less than 3 meters (crest to trough). For the laser altimeter, the sea state assumes greater importance, especially for those effects which do not average out over the relatively small footprint. Sufficient analysis has been performed to indicate a subordinate effect on the laser altimeter due to sea state for waves of less than 3 meters (crest to trough) in height. Although for some areas of the ocean it is not uncommon to encounter larger waves (higher winds, rougher seas) than those considered, the percentage of time during which these conditions prevail is relatively

small, and the need for useful data from all target areas encountered is not considered an absolute requirement. (Based on data available in Hogben and Lumb, it has been determined that on an oceanwide basis, averaged over all seasons, the probability of encountering waves higher than 3m is less than 5%). In terms of focussing attention on the primary study purpose, waves attributable to sea state are considered a relatively unimportant aspect. Thus, while the radar altimeter can handle sea state effects more readily it is not considered of great enough significance to penalize consideration of the laser altimeter.

On balance, environmental constraints may present a problem, but they aren't necessarily overwhelming; and if they do, then the radar system is favored. (Score radar two points out of four.)

5.5.11 SAFETY

The radar radiation is substantially harmless, although it may be a technological nuisance from the point of view of radio frequency interference (RFI) with rf systems on the Earth's surface. The laser radiation presents a hazard only in the unlikely event that an observer on the ground is within the small footprint, is pointed directly at the laser, and is sighting through a telescope with sufficient collecting power to collect sufficient radiation to do eye damage. Since the laser altimeter transmits .5 joules of radiation over a 200 meter diameter footprint, and the maximum radiation level for the eye has been set at about 10 microjoules, an optical instrument with a 90 cm diameter aperture would be the minimum with which an observer could exceed the safety standard. From a technical point of view, this would require a highly unprobable situation in order to cause injury. However, nontechnical considerations may impose constraints, and this threat leads to an award of one point preference to radar over laser (out of two).

5.5.12 CALIBRATION

The types of problems involved in calibration are comparable to a first order for both altimeter systems. Such items as built-in test

equipment (BITE) were not considered in this study. No preference is offered.

5.5.13 REQUIREMENTS ON THE SATELLITE

5.5.13.1 Pointing Angle

The radar altimeter functions well when attitude is maintained with respect to the vertical to within $.3^{\circ}$, and some tolerable degradation is experienced for larger angles, perhaps up to $.75^{\circ}$. The laser altimeter has a relatively rigorous requirement that the pointing angle should not exceed $.25^{\circ}$. The reason for this requirement is that the laser beam pointing direction is well-defined, whereas the radar has a broad beam, and the radar system is mainly concerned with the flatness (uniform amplitude) of the beam over the region of concern. On balance, the radar is allocated one point (out of 2).

5.5.13.2 Attitude Data

The radar does not require attitude information at all if the pointing angle is less than $.3^{\circ}$. For larger angles, the radar could improve accuracy somewhat by knowledge of the attitude to within about 0.1°. The laser altimeter system requires attitude information to within 10 arc seconds. This is because the laser system is fundamentally a ranging device, and its narrow beam does not assure that it will strike the Earth at the point of closest approach. The 10 arc second requirement is a serious one, which is not included in power, weight, volume, or accuracy (which is dependent on this information) considerations. Due to the impact of this requirement on the trade-off study, it is considered in paragraph 5.5.14 as a separate item. (Subsequently, the weighting factors are reassigned to reflect this impact.)

5.5.13.3 Angular Rate

For the angular rates normally encountered in satellites, no problem is expected for either laser or radar altimeter system.

5.5.13.4 Thermal

The laser system requires thermal control at normal temperatures to $\pm 20^{\circ}C$, except for the ruby crystal, which should be kept at about $275^{\circ}K$ $\pm 2^{\circ}K$, and generates about 12.5 watts of heat. These requirements, while not too formidable, necessitate careful thermal design considerations.

Most of the radar system has adequate control at normal temperature to $\pm 30^{\circ}C$, with critical timing circuits requiring $\pm 10^{\circ}C$. Additionally, the radar system requires a small (less than 16 cm^3) self-contained oven for thermal control of the stable clock oscillator crystal.

Both sets of thermal requirements appear reasonable and although the laser requirement is somewhat more severe, it is not considered significant for purposes of this study.

5.5.13.5 Telemetry

More than 99% of the radar data is involved in altitude measurement (counting) and the timing signal upon which it depends. The total telemetry requirement for radar (including monitors) is about 135,000 bits per hour, with data reduction performed on the ground.

The laser system requires about 47,000 bits per hour for telemetry. Laser data is reduced on the ground.

Although it appears that less telemetry may be required of laser, the factor of three is not considered significant for these preliminary considerations.

5.5.13.6 Storage

Data storage is proportional to telemetry buildup for both systems, and is similarly not significantly different.

5.5.13.7 Supplementary

The laser system requires on-off switching information (either programmed or telemetered) to enable it to cease operation and conserve pulses (for longer useful life) when it can be determined in advance

that the information received will not be useful (due to cloud, fog, presence of land, etc.).

The radar operating life may be similarly extended by shutting it off over land. For some missions, this may be necessary.

Switching on and off will probably be mandatory, in the case of radar due primarily to RFI (radio frequency interference) considerations relative to the ground, and in the case of laser due primarily to potential radiation (safety) considerations.

No unusual supplementary information is required for either system. No preference is awarded to either system for this aspect of the trade-off.

5.5.14 ATTITUDE DATA RE-EXAMINED

The laser altimeter requirement on the satellite for pointing angle information to within 10 seconds of arc is quite stringent. Satellite attitude stability is easily obtained to within a few degrees, and with some instrumentation may be controlled to a fraction of a degree. As a minimum requirement for proper operation of the laser altimeter, one angle must be measured, between the line-of-sight of the laser beam and the normal to the surface of the Earth. This involves knowledge of the local geometry to an accuracy of better than 10 arc seconds, which is not normally available. Horizon sensors (such as the IR type) are off-the-shelf items, with measuring accuracy reputed to be about 0.1 degree. Measurement of the local normal, or the local vertical, to the required accuracy requires relatively high precision instrumentation, including an inertial platform. One way to meet the problem is to employ a pair of star-trackers, and measure the angles between the bore-sights of the star-trackers and the line-of-sight of the laser beam. Most tracking instruments including star-trackers are rated for nulling capability, which can be fulfilled to much greater accuracy than it can be measured. Measurement of angle to within 10 arc seconds of itself

requires a fairly high quality angle measuring device. Knowledge of satellite location (presumed known) can be used to compute the angle between the local vertical (or normal) and the star-trackers; hence the error angle can be determined. All angles must be known to somewhat better accuracy than the desired 10 arc second measurement; this is not a straightforward exercise considering the constraints of power, weight and volume.

For space flights involving significant vehicle maneuvering, changes in the star field may necessitate more than one pair of star references, with associated complication. Nonpowered (or nearly so) orbital satellites may continuously track stars near the pole of the orbit.

The navigation problem invariably involves the use of a computer, either on-board or ground-based. An airborne computer may typically occupy 15,000 cm^3 (approximately 1/2 cubic foot), weigh about 65 kgm, and require at least 10 watts of power.

A ground-based computer would alleviate the computer size impact, but would introduce additional telemetry requirements which would restrict operation to those regions where continuous telemetry were available, and could introduce the need for telemetry volume which may be beyond the capability of the system, or which might require additional hardware; in any event, the logistics would be further complicated by an order of magnitude.

Then there is the matter of the star-tracker itself. This (or its equivalent) must be on-board, and must have a precision angle measuring device associated with it. Typical star-trackers have volumes of the order of 10,000 to 15,000 cm^3 (1/3 to 1/2 cubic foot), and two are required. Weight would be expected to be typical of optical equipment, and power is probably nominal. Detailed estimates are difficult because such precision equipment is not readily available off the shelf, but is custom-designed to take advantage of whatever flexibility the systems can offer.

TABLE 5-3

SCORING THE CANDIDATE SYSTEMS

FOR EACH EVALUATION CRITERION

Criterion	Weighting Factor	Differential Scoring	
		Laser	Radar
1. Accuracy	35	0	5
2. Data Rate	15	0	4
3. Power	4	4	0
4. Weight	3	0	2
5. Volume	2	0	2
6. Life	8	0	0
a. Shelf (1)			
b. Standby (2)			
c. Operating (5)		0	0
7. Availability	3	0	0
8. Performance Potential	3		
a. Theoretical (2)		0	0
b. Probable (1)		0	0
9. Other Capabilities	3	1	0
10. Environmental	4	0	2
a. Transmission (2)			
b. Target (2)		0	
11. Safety	2	0	1
12. Calibration	1	0	0
13. Requirements on Satellites	17		
a. Pointing Angle (2)		0	1
b. Attitude Data		0	8
c. Angular Rate (1)		0	0
d. Thermal (2)		0	0
e. Telemetry (1)		0	0
f. Storage (1)		0	0
g. Supplementary (1)			
Total:	100	5	25
		Net Score 0	20*

*The winner.

In summary, the requirement of 10 arc seconds in knowledge of pointing angle introduces sizing problems (power, weight and volume) which are comparable with the remainder of the system. While the problems are known to be substantial, it would be difficult to predict the impact on the system parameters more precisely without further examination. If the laser altimeter system is to be explored further, it is recommended that this problem be allocated a high priority.

Inasmuch as the principal impact of the laser altimeter attitude data requirement on the satellite has the most substantial impact on power, weight and volume, the weighting factors for these three items are reassigned as indicated in Table 5-3. Four points from power, two points from weight, and one point from volume are added to the initial two points assigned to attitude data.

Eight points (out of the nine available) are allocated to the radar altimeter, which has no need for attitude information if the pointing angle is less than 0.3°.

5.6 SELECTION OF AN ALTIMETER SYSTEM

A tabulation of the scoring places the candidate radar altimeter system 20 points ahead of the candidate laser altimeter system, as shown in Table 5-3.

Although many qualifying considerations enter into the scoring, the net result qualitatively has a high confidence level. The study indicates that the candidate radar altimeter system has a substantially greater prospect of meeting geodetic requirements than does the candidate laser altimeter system; the latter may indeed be capable of meeting the requirements also, but probably not quite as readily. This does not

imply that the radar altimeter system is well-defined, clean-cut, and does not have any problems; on the contrary, the study has uncovered many substantive problems. Many of the problems have been dealt with in the course of the study; others have been judged to be manageable.

5.7 SUMMARY AND CONCLUSION

The systems analysis study indicates:

a. Both candidate altimeter systems are capable of providing some useful geodetic data (such as accuracy of 0.5 meter).

b. Neither candidate system is yet capable of meeting all the geodetic requirements (such as 0.1 meter accuracy).

c. The candidate radar altimeter system is better able to meet geodetic requirements than the candidate laser altimeter system.

Therefore the conclusion of this study is the selection of the radar altimeter.

SEA SURFACE

APPENDICES

REFERENCES

BIBLIOGRAPHY

APPENDIX S–A

SEA SURFACE CHARACTERISTICS AND EFFECTS ON SPACE ALTIMETRY – GENERAL CONSIDERATIONS

(H.W. Marsh)

A.1 INTRODUCTION

For simplicity of discussion, waves can be considered in two categories: (1) wind-driven waves and (2) nonwind-driven waves. Basically, ocean waves can be treated as random surface perturbations. However, statistical studies in these areas should be extended beyond simple power spectral analyses to include such things as descriptions of the size of the geographical areas within which waves of a given type and amplitude occur. These details can be used in connection with discussions of beam spot size and system integration times necessary to deduce mean sea level from measurements to the wave-roughened sea if sea state is assumed constant over the measurement area.

The following paragraphs discuss applicable background material.

A.2 BACKGROUND

The sea surface changes with time and, at any instant, is irregular on a scale that extends from the microscopic upward to dimensions that are significant fractions of the ocean extents. The time and space changes are unpredictable in the long run, although definite laws govern the rates of change and hence permit some extrapolation from a (complete) set of present observations.

Altitude measurements over the sea are influenced by the shape and character of the surface in two general ways: (1) the altimeter signal (echo) will be degraded by surface motion and irregularity and (2) the observed altitude will be relative to an instantaneous and transient surface, which is not the desired "local mean sea level." Quantitative

assessment of these effects can be aided by a descriptive account of the sea surface.

Strictly, the physical sea surface should be regarded as an air-water interface, representing a region of rapid but not discontinuous transition from air to water. There is spray in the air and there are bubbles in the water. Nevertheless, the main effects to be expected concerning reflection and scattering of electromagnetic energy can be described using a mathematical model of a surface (infinitely thin interface). This surface is given by the instantaneous elevation, z, above msl, at each point (x,y) on the mean surface, at each instant of time. The elevation z is best known through its statistics, which are averages over time and space. Of central importance is the power spectrum, $B^2(\omega)$, which distributes the energy of the waves over frequency $\omega = 2\pi\gamma$. The energy is proportional to the mean square elevation (variance) and hence

$$\langle z^2 \rangle = \int_0^\infty B^2(\omega)\, d\omega .$$

A schematic representation of the power spectrum is displayed in Figure A-1, which is copied from Kinsman[1]. Another statistic is the wave number spectrum, $A^2(k)$, which distributes energy over the wave number, $k = 2\pi/\gamma$, γ being the wavelength. We have (for isotropic seas)

$$\langle z^2 \rangle = \int_0^\infty A^2(k)\, dk .$$

There is a classical relation for water waves in deep water (the dispersion equation):

$$\omega^2 = gk + \gamma k^3,$$

where g is the acceleration of gravity and γ the specific surface tension. Figure A-2 relates ω and k according to this equation, using $g = 980$ cm sec^{-2} and $\gamma = 74$ cgs units (clear water).

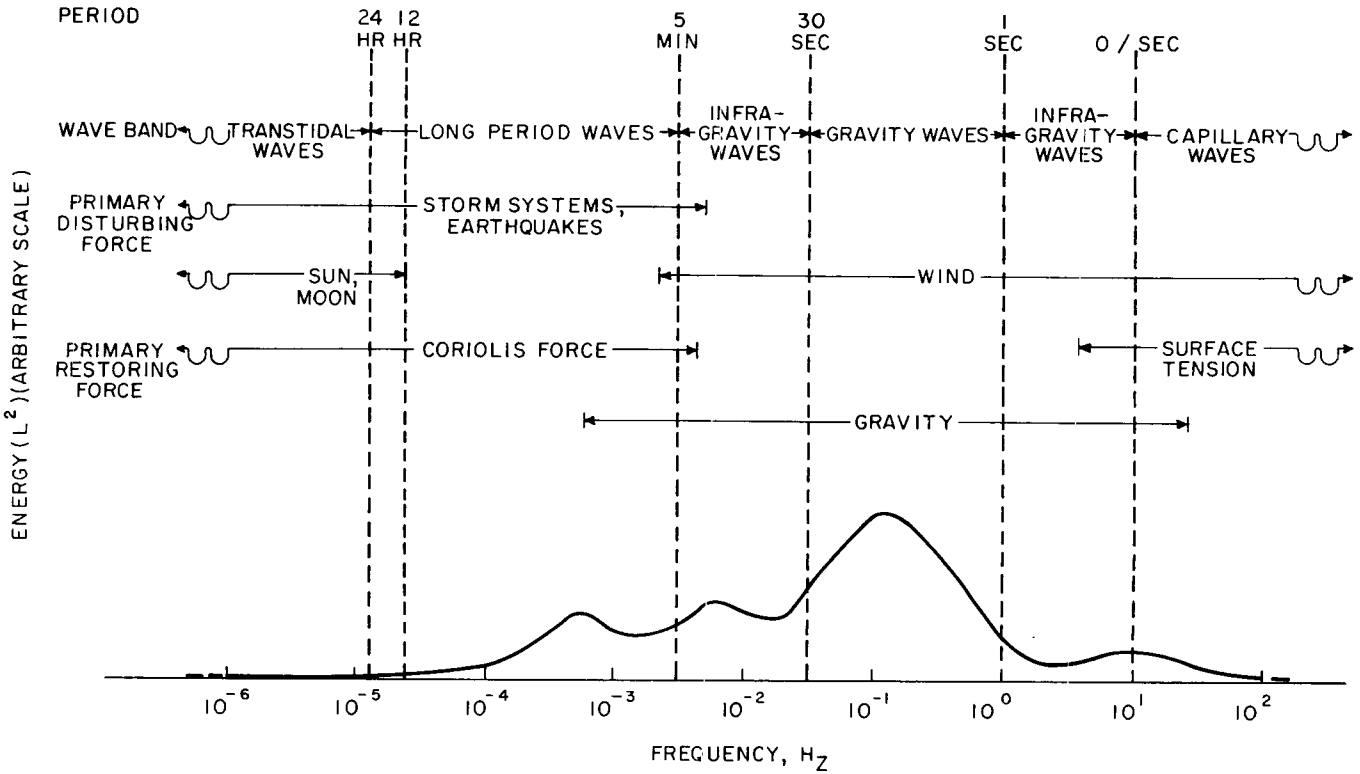

Figure A-1 Schematic Representation of the Energy Spectrum of the Surface Waves of the Oceans (After Kinsman)

For present purposes, it is convenient to divide the waves into two categories: wind-driven and nonwind-driven. An example of the relation of frequency vs. wavelength for the former is shown in Figure A-2. The latter includes very long swell, tides, and currents. A discussion of the wind wave spectra is discussed by Marsh and Mellen.[2] Generally, these waves change rapidly, have significant slopes, and are dominated by local conditions. They will have the greatest effect upon altimetry. The larger waves have pronounced geographical patterns and change relatively slowly.[3] The slopes are probably negligibly small and the elevations are probably less than 1 meter. Thus, the long waves contribute to a true geopotential surface. The altimetry measurement of the long waves may be very useful for study of tides and currents, although the geodesy problem requires averaging out the time variations. A knowledge of long wave patterns could be useful for hindcast corrections to observed altitudes or for forecasting to optimize orbits and sampling rates. This latter point is emphasized by Frey et al[4] in connection with the inevitable aliasing of sampled data.

From the foregoing discussion, it is assumed that wind waves present the central problem that can be addressed directly. The study of such waves is expected to contribute to selection of system parameters such as beamwidth and pulse length and power, but not to data reduction. Nevertheless, an analysis of return echo shape could reveal the local wave character and at least assist in data editing.

Frey[4] examines these parameters by interpreting existing radar backscatter data. A more detailed examination from a slightly different but related viewpoint can be used to optimize the parameters. This latter viewpoint identifies and counts the small facets that are favorably oriented to reflect energy back to the receiver; it has been used to interpret sun glitter patterns[5] and for various analytical purposes.[6] Under the assumption of Gaussian statistics, the A-crossing theory of Rice[7] can be generalized and the density of glitter points computed from rms wave slope and rms wave curvature. Thus, Marsh and Kuo[8] estimate a density

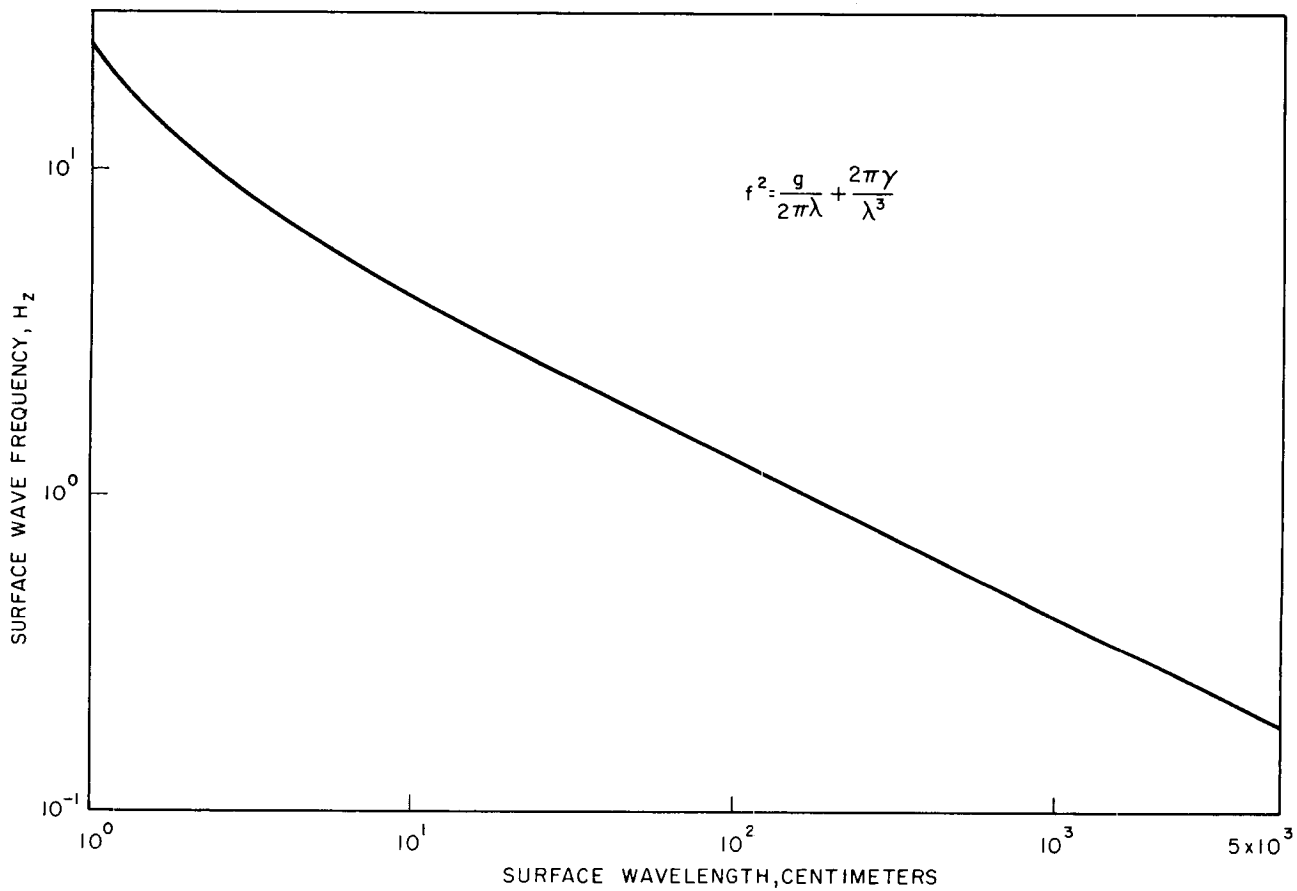

Figure A-2 Wavelength vs. Frequency (Deep Water Waves)

of $3/m^2$ at a wind speed of 12 knots, for nearly normal incidence. A better estimate can be made from the wave number spectrum, $A^2(k)$.

For power calculations, the analysis of Frey[4] provides a point of departure, which is supported by the Raytheon laser measurements over sea[9] and Electro-Optical Systems laser measurements over disturbed water in a tank[10].

APPENDIX S–B

SEA SURFACE VARIABLES AND PULSE DISTORTION

(R. Halvorsen/H.W. Marsh)

B.1 DISTRIBUTION OF SEA STATE

Sea surface variations will effect altimeter results so a knowledge of the seasonal and geographic distribution of wave heights is useful. Therefore, a brief compilation of wave distribution was made. Basic data were obtained from "Ocean Wave Statistics", by Hogben and Lumb, Her Majesty's Stationery Office, London. Figures B-1 and B-2 and Table B-1 indicate median wave height (in meters) for geographic locations by season and are for all wind directions. It will be noted that there are large ocean areas where information is lacking. Interpolation (guided by a knowledge of meteorological conditions) can be used to fill the blank areas where data is not available from other sources.

B.2 SEA WAVE DISTORTION OF ALTIMETER PULSES

Some of the altimeter measurements will have permanent value; others will be of interest only for their statistical contributions. In either case, the irreducible error of individual measurements is important. When the sea is smooth, the altimeter pulses are reflected with little or with correctable distortion. Where the wind is blowing, the sea is irregular and there is no well defined local elevation. Experiments with the glitter pattern of the sun show that reflections will occur from many wave facets, which are inclined so as to reflect specularly back toward the source. Each reflection will have a travel time depending on its elevation and inclination, and the total reflected pulse will be a composite of these individual reflections.

The earliest return will come from the highest facet of the sea. The pulse intensity will then grow as more facets are illuminated. When

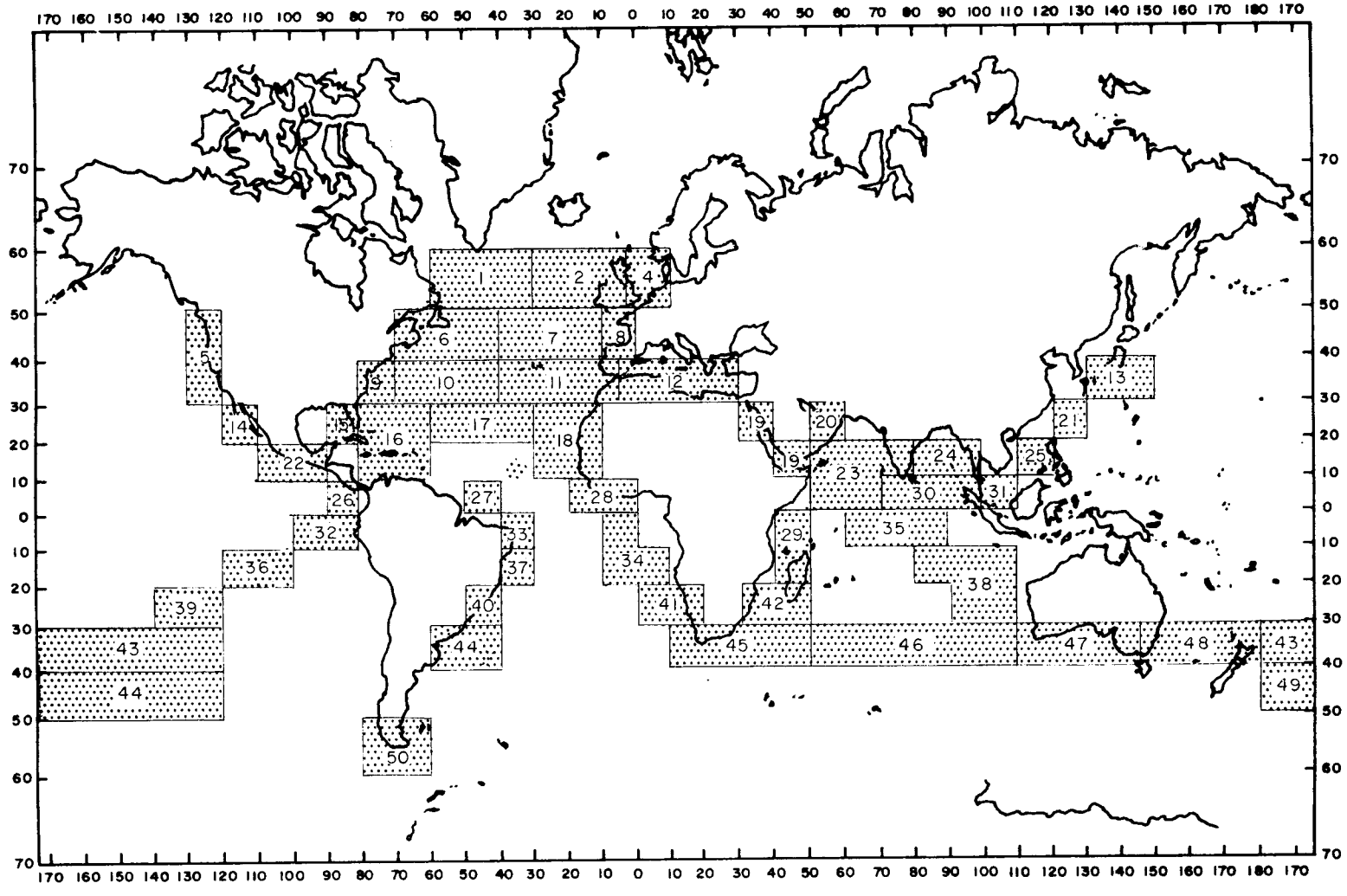

Figure B-1 Grouping of Marsden Squares into Areas

TABLE B-1

SEASONAL GEOGRAPHIC DISTRIBUTION OF

MEDIAN WAVE HEIGHT (METERS)

AREA	DEC-FEB	MARCH-MAY	JUNE-AUG	SEPT-NOV
1	2.0	1.5	1.0	2.0
2	2.0	1.5	1.5	2.0
3	1.5	1.0	1.0	1.0
4	1.5	1.0	1.0	1.0
5	2.0	1.5	1.0	1.5
6	2.0	1.5	1.0	1.5
7	3.0	2.0	1.0	1.5
8	2.0	1.5	1.0	1.5
9	1.5	1.0	1.0	1.0
10	2.0	1.5	1.0	1.5
11	1.5	1.5	1.0	1.0
12	1.0	1.0	0.5	1.0
13	1.5	1.0	1.0	1.0
14	0.5	1.0	1.0	1.0
15	1.0	1.0	0.5	1.0
16	1.5	1.0	1.0	1.0
17	1.0	1.0	1.0	1.0
18	1.0	1.0	1.0	1.0
19	1.0	0.5	0.5	0.5
20	0.5	0.25	0.5	0.5
21	1.5	1.5	1.0	1.5
22	0.5	0.5	1.0	1.0
23	1.0	0.5	1.5	0.5
24	0.5	0.5	1.0	0.5
25	1.5	0.5	1.0	1.5

TABLE B-1

SEASONAL GEOGRAPHIC DISTRIBUTION OF

MEDIAN WAVE HEIGHT (METERS)

(Continued)

AREA	DEC-FEB	MARCH-MAY	JUNE-AUG	SEPT-NOV
26	0.5	0.5	1.0	1.0
27	1.5	1.5	1.0	1.0
28	0.5	0.5	1.0	0.5
29	0.5	1.0	1.0	1.0
30	1.0	1.0	1.0	1.0
31	1.0	0.5	0.5	0.5
32	1.0	1.0	1.0	1.0
33	1.0	1.0	1.5	1.0
34	1.0	1.0	1.0	1.0
35	1.0	1.0	1.0	1.0
36	1.0	1.0	1.5	0.5
37	1.0	1.0	1.0	1.0
38	1.5	1.5	2.0	1.5
39	1.0	1.5	1.5	1.5
40	1.0	1.0	1.0	1.0
41	1.5	1.5	1.5	1.5
42	1.0	1.0	1.5	1.5
43	1.5	1.5	2.0	1.5
44	1.0	1.0	1.5	1.5
45	1.5	1.5	1.5	1.5
46	1.5	1.5	2.0	1.5
47	1.5	2.0	2.0	2.0
48	1.5	1.5	1.5	1.5
49	1.5	2.0	2.0	1.5
50	1.0	1.0	1.5	1.5

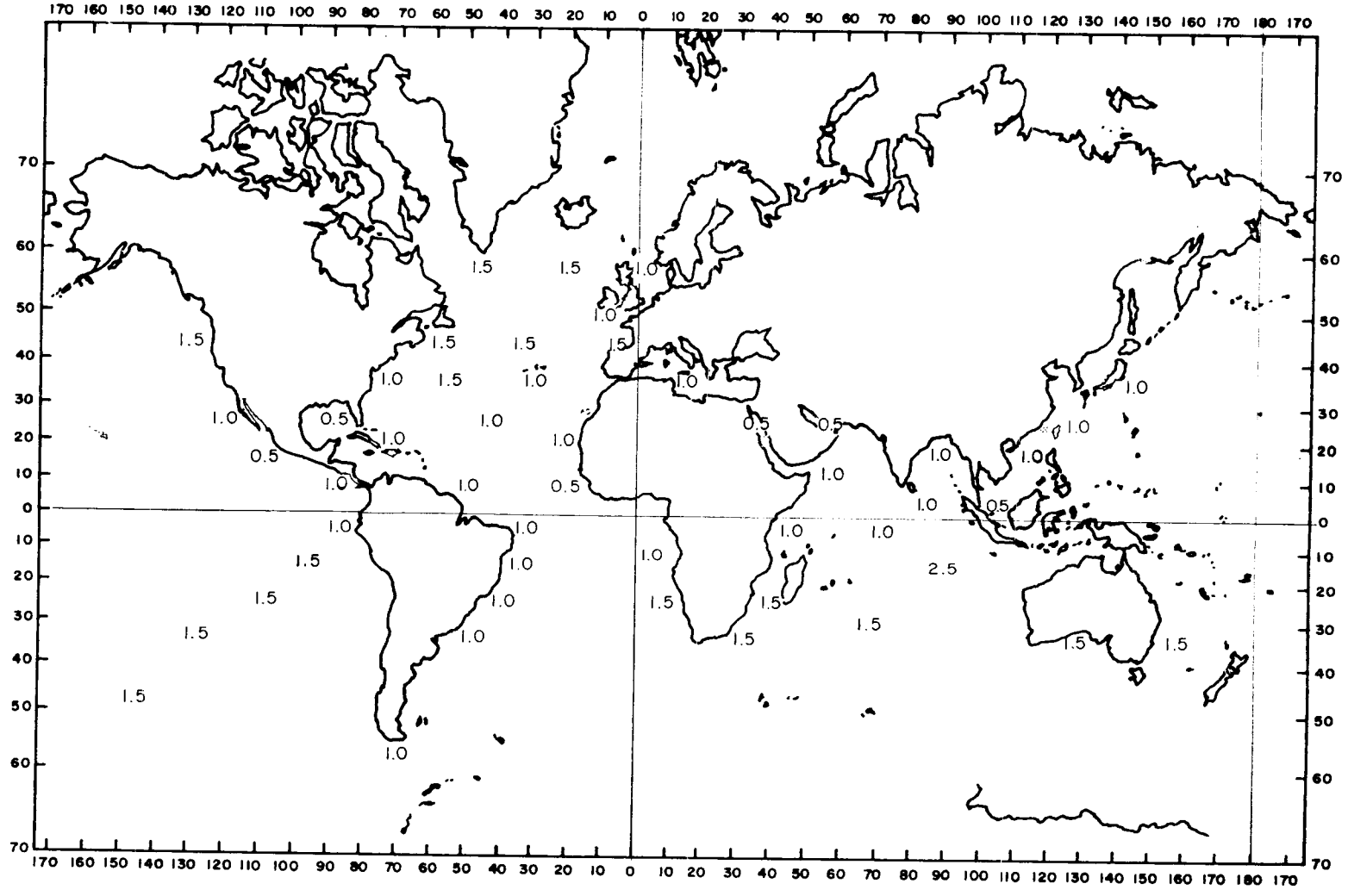

Figure B-2 Median Wave Height (Meters), All Seasons

the wave troughs are illuminated, the time dispersal of individual returns will be 2H/c, H being the peak crest to trough wave height and c the speed of light.

If the altimeter beam width is appreciable, the total return will be elongated because the edges of the beam reach the sea at greater distances than the center. Thus, for reasonable radar beams, the pulse elongation due to sea state will be negligible compared with the beam width effect. However, the distribution of returns over wave height will determine the character of the leading edge of a radar pulse and that of most of a laser pulse. If leading edge tracking is employed, there will be a bias toward too short an altitude; if the centroid of the return is timed, there may be a bias if the distribution of facets is not symmetric.

A guide in estimating the times of individual returns could be obtained from wave profiles recorded at sea. A few such have been obtained, using stereo-photography, but sufficient data of this type are not presently available. An alternate guide can be obtained using other measured statistics of the sea surface, of which the most applicable are the frequency spectra. These are measured from the time history of waves at a point, using a wave staff or similar device. The sea surface elevation from its mean may be approximated by the Fourier representation

$$z(x,y,t) = \int_0^{\infty} \int_0^{2\pi} S(k,a) \cos(\omega t - kx\cos\alpha - ky\sin\alpha + \theta)\, k\, dk\, d\alpha \qquad \text{(B-1)}$$

where ω is the radian frequency of waves of length $2\pi/k$, with fronts perpendicular to the line making the angle α with the x-axis, and θ is a random phase angle. For the gravity waves of interest here,

$$\omega^2 = gk, \qquad \text{(B-2)}$$

g being the acceleration of gravity. Using Equation (B-2), the spectrum S can be expressed alternatively as a wave number or frequency spectrum. If it were known, the dynamic sea surface could be calculated by inverting Equation (B-1). Being a two-dimensional problem, this is not practicable for computation; in addition, the available frequency spectra

yield only S^2 averaged over all directions α. However, a one-dimensional representation is feasible, and may be expected to exhibit many of the features of a vertical section of the surface. Such a representation was studied for use in a study of radar pulses using fast Fourier transform simulation.

This simulation used the frequency power spectrum according to Pierson and Moskowitz[11] in the form

$$A^2(\omega) = (\alpha g^2/\omega^5) \exp(-\beta\omega_o{}^4/\omega^4), \text{ where} \quad \text{(B-3)}$$

α, β are dimensionless constants:

$$\alpha = 8.1 \times 10^{-3}; \beta = 0.74,$$

$\omega_o = g/u$; u = wind speed (at 20 meters altitude) and g is the acceleration of gravity. The surface elevation is obtained by Fourier transformation of

$$B(k) \exp i\theta = A(\omega)(d\omega/dk)^{1/2} \exp i\theta \quad \text{(B-4)}$$

in which θ is a random variable. A 1024 point Fast Fourier Transform produced 1024 values of surface elevation (see Figure J-2 on page R-J-4) from which a histogram of horizontal facets was prepared, and is shown in Figure J-1 on page R-J-2. The elevation scale for these figures is proportional to the square of the wind speed as shown in Table B-2.

TABLE B-2

SCALE VALUES FOR FACET ELEVATION

Wind Speed (m/s)	Unit of Elevation (m)	Unit of Distance (m)	Modal Wavelength (m)
5	0.25	.22	23
10	1.0	.89	91
15	2.25	2.0	200
20	4.0	3.6	370

The modal wavelength shown in the table corresponds to the wave number k_o for which the power spectrum is maximum. The Fourier transformation was taken with a wave number interval of $k_o/10$.

B.3 INFLUENCE OF TIDAL FREQUENCIES ON SAMPLE RATE

While it was initially felt that other requirements would determine the sample rate, an analysis of the requirements imposed by tidal frequencies was deemed advisable. The purpose of this investigation was to determine a sample rate which would avoid any significant aliasing by tidal frequencies.

Munk and Cartwright[12] have analyzed 50 years of hourly tidal records taken at Honolulu. These records were chosen for analysis because they were taken on an oceanic island which is relatively free from shallow water effects. They found tidal frequencies above 3 cpd to be negligible and, therefore, chose a sample rate of 8 per day to be on the safe side in avoiding aliasing. Theoretical predictions for deep water (Neumann & Pierson)[13] are in general agreement with their observations.

If we consider the tides as a time series, this would require a time rate sample of 8 per day in approximately the same vicinity (within 1600 km of each other) to avoid aliasing that would be significant in the deep ocean basins. Another viewpoint is to treat the tide as a progressive wave traveling around the earth. Consider the wave to be stationary for the relatively brief time required for a satellite to pass over it, then a spatial sample rate of one for each 5000 km of satellite traverse would be sufficient if we base our sample rate on the work of Munk and Cartwright in the deep water environment.

All of the above is based on the assumption that deep water will be used to determine the shape of the geoid. The picture is altered slightly if data from shelf areas are to be used in determining the shape of the geoid. So called terrestrially generated components are introduced by bottom friction and interference from reflected waves. Frequencies up to the 6th harmonic of the semi-diurnal can be significant (see Figure B-3)

and would require time sample rates of 1 per hour and in close geographic proximity and a spatial sample rate of 1 for each 1600 km of satellite traverse.

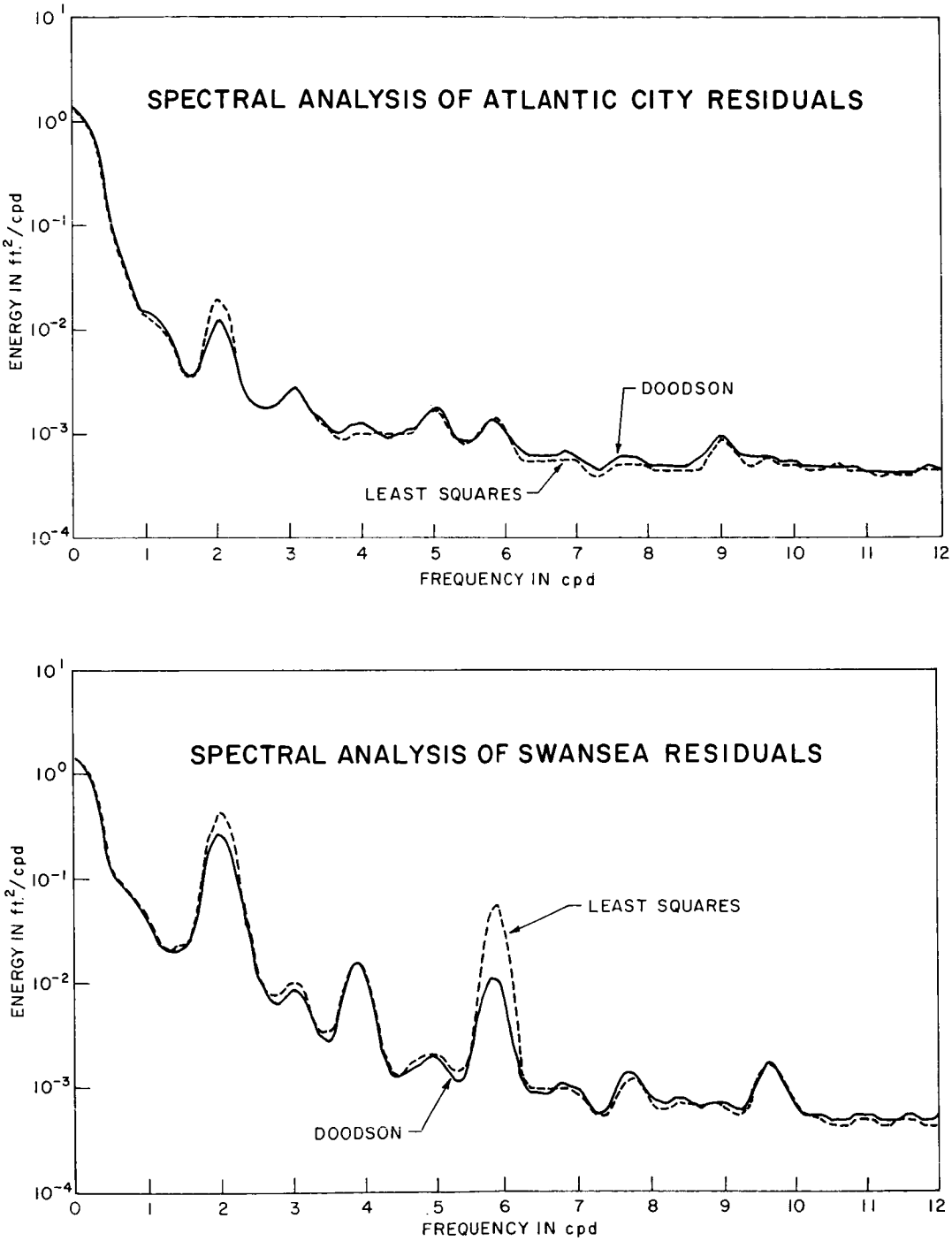

Figure B-3 Tidal Harnomics (After Zetler and Lennon)

SEA SURFACE REFERENCES

1. Kinsman, B., "Wind Waves," Prentice Hall, Inc., Englewood Cliffs, N.J., (1965).

2. Marsh, H.W. and Mellen, R.H., "Spectra of the Dynamic Sea Surface," Report under Contract No. Nonr 3353(00), Office of Naval Research, (1 October 1965).

3. Bigelow, H.B. and Edmondson, W.T., "Wind Waves at Sea, Breakers, and Surf," USNHO Pub. No. 602, (1952).

4. Frey, E.J., Harrington, J.V., and Von Arx, W.S., "A Study of Satellite Altimetry for Geophysical and Oceanographic Measurement," M.I.T.

5. Cos, C.S. and Munk, W., "Slopes of the Sea Surface Deduced from Photography of Sun Glitter," Bull. Scripps Inst. Oceanography 6, 401, (1956).

6. Martin, J.J., "Estimated Numbers of Multipaths," IDA Research Paper P-173 (March 1965).

7. Rice, S.O., "Mathematical Analysis of Random Noise," B.S.T.J. 23 and 24.

8. Marsh, H.W. and Kuo, E.Y.T., "Further Results on Sound Scattering by the Sea Surface," Report on Contract No. N140(70024)76964B (1 October 1965).

9. Raytheon SISD, Final Report, "Study and Design of a Spaceborne Laser Altimeter System, I," Contract No. NAS 8-21013 (28 February 1967).

10. Electro-Optical Systems, Inc., Final Report, "Surface Evaluation and Definition (SUEDE) Program," Contract No. NOw 66-059-C (13 December 1966).

11. Pierson, Willard S. Jr., and Moskowitz, Lionel, "A Proposed Spectral Form for Fully Developed Wind Seas Based on the Similarity Theorem of S.A. Kitaigorodskii," JGR December 15, 1954 Vol. 69 #24.

12. Munk and Cartwright, "Tidal Spectroscopy and Prediction," from Proceedings of the Symposium in Tidal Instrumentation and Prediction of Tides," Paris, May 3-7, 1965.

13. Neumann and Pierson, "Principals of Physical Oceanography," pp. 235-298.

SEA SURFACE BIBLIOGRAPHY

1. Hill, M.N., ed., "The Sea - Vol. I," Physical Oceanography, Interscience Publishers, pp. 567-801 (1962).

2. Kamon, B.V., "Continental Shelf Waves and the Effects of Atmospheric Pressure and Wind Stress on Sea Level," J. Geophys. Res. 71, (12), 2883-2893 (June 1966).

3. Katz, E.J., "The Low Frequency Components of the Spectrum of Wind Generated Waves, J. Marine Res. 19, (2) pp. 57-69.

4. Mandelbaum, H., "Variation of a Rotary Tidal Current with Moon age," J. Geophys. Res. 67, (1) 249-269 (January 1962).

5. Munk, Snodgrass, and Tucker, "Spectra of Low Frequency Ocean Waves," Bull. Scripps Instit. Oceanggraphy 7, (4) pp. 283-362 (1959).

6. Saur, J.F.T., "The Variation of Monthly Mean Sea Level at Six Stations in the Eastern North Pacific Ocean," J. Geophys. Res. 67, (7), pp. 2781-2790 (July 1962).

7. Sverdrup, Johnson, and Fleming, The Oceans, Prentice-Hall, Inc., pp. 400-761 (1942).

8. Walden, H., "Methods of Swell Forecasting," Proceedings of the Symposium on the Behavior of Ships in a Seaway, Netherlands Ship Model Basin - Wagenigen, pp. 427-438 (1957).

9. Wiegel, R.L., "Oceanographic Engineering," Prentice-Hall, Inc., pp. 299-339 (1964).

10. WHOI, "Oceanography from Space," Reference 65-10 (April 1965).

11. DuCastel, F. and Spizzichino, A., Ann. Telecomm. 14, pp. 33-40 (1959).

12. Beckmann, P. and Spizzichino, A., "The Scattering of Electromagnetic Waves from Rough Surfaces," The Macmillan Col, New York, N.Y. (1963).

13. Marsh, H.W., "Some Stochastic Structures for Modeling Underwater Sound," Report under Contract No. Nonr 3353(00), Office of Naval Research (20 May 1966).

GEODETIC REQUIREMENTS

APPENDICES

REFERENCES

BIBLIOGRAPHY

APPENDIX G—A

CALIBRATION

Calibration of a satellite altimeter can be easy or difficult depending on the rms error allowable in tracking facilities available, the measurement schedule, etc. At present, there is not enough information about the altimeter characteristics available to allow anything but a listing of feasible methods of calibration.

1. Fixed Mount Method - The transmit-receive equipment can be mounted at the top of one hill and a suitable reflector mounted at the top of another. Distances of 50 - 60 or even 100 km can be gotten without too much trouble. Tropospheric refraction error should be negligible for radio waves. They should be less than a decimeter for light waves unless multiple reflection techniques are used. All radiation not caught by the receiver must, of course, be directed so that it is neither a nuisance nor a danger to those not concerned with the experiment. Multipath problems may be severe for the radio altimeter.

2. Both laser and radio altimeters can be calibrated by mounting them in aircraft and flying over reflectors either natural (lake or seacoast) or artificial (cubic-corner reflectors). The airplane must either be tracked precisely during flight or, if reflectors are used on land, the ground photographed from the air at short intervals. Adequate marked control must be available on the ground, but these markers may also do as altimeter markers.

Since tracking position rms errors must be 1/3 to 1/10 the sought-for altimeter errors, optical ground tracking may be essential. Five to 10 km. measurement distance may be the most that can be expected by this method, as compared to the 50 - 100 km distance between hilltops.

3. Electronic and optical instruments for use in satellites can be made surprisingly sturdy. There is always the possibility, however, that the instrument has been disturbed enough during launch to affect the measurements. Calibration after launch is therefore usually advisable and sometimes necessary. Further, calibration after launch can be done under conditions almost the same as those in which the altimeter will make its workaday measurements. Finally, calibration at intervals during the life of the altimeter lets one detect and allow for secular (drift) or periodic variations in instrument.

Considering the kind of experiment to be run, calibration by measurement to special surface markers is not recommended. The best procedure is measurement of height above a lake or near-coast sea area while tracking with a complete set of tracking equipment i.e., enough equipment to give a fix on the satellite. With either SECOR or camera set, the satellite altitude can be fixed to ±0.5 to ±1.0 meters or, with care, to ± 0.2 meters. Height of the water surface can be determined with the same rms error.

Altimeter location can be found using only one tracking instrument, but this method introduces orbit theory and hence a bias whose size cannot be found from the theory itself.

Different methods for calibrating both radar and laser altimeters must be used even in doing the calibration with the altimeter in orbit. This is because the area irradiated by the radar altimeter is so large that the target sometimes cannot be made large enough to eliminate boundary problems without at the same time forcing the instrument to incompletely average over permanent surface variations. For example, the water level in Lake Geneva (Switzerland) is known with respect to European Datum to within a meter, certainly. Hence, it would be suitable as a target for calibration of an altimeter whose used irradiation area (uia) is less than at most half the shortest dimension of the lake, and preferably a third or less. A uia greater than this will probably mean that the return signal is contaminated by radiation reflected

from solid surfaces whose geometric relation to the lake surface cannot be established. Similarly, measurements of sea level off the Maine coast near the Bay of Fundy would be satisfactory if contamination by land features could be avoided.

Note that the calibration procedure will undoubtedly have to provide for the possibility that the measured height is a function of sea state.

APPENDIX G–B

SAMPLING

A satellite altimeter makes height measurements at specified (not necessarily equal) intervals of time. Through ground observations of satellite position and through orbital theory the times of measurement can be exchanged for locations from which the measurements were made. Since the measurements contain random errors and since the surface being measured varies rather randomly in height, it has become common to lapse into statistical jargon and speak of the measurements as samples. I will refer to them as samples to retain a common language with other chapters which use sample for measurement.

If the surface being measured were reasonably permanent, it would be satisfactorily defined if the location of the altimeter, the measurement, and the directions of measurement were specified (but see below for further comment on this point). The satellite designer would then have considerable freedom in specifying the times of measurement. But in the case of our problem it is the ocean surface that is measured, and this surface is far from permanent (in shape). On the other hand, our immediate problem is to define not the instantaneous, physical surface but an average, theoretical surface called mean sea level. The instantaneous surface is still of interest, but not of primary interest. We shall try to take advantage of this circumstance to avoid having to specify either sample time or sample location.

In the following section on sampling density we shall look for the simplest solution by assuming that the surface does not change. In the succeeding section on sampling rate we then see how a changing surface changes our sampling solution.

B.1 SAMPLE DENSITY

The surface we are trying to define, that is, whose coordinates we want to find, is assumed to be constant in time, so that every measurement from the same point in space in the same direction will yield the same value plus or minus the error in the measurement. We assume, further, that the surface is adequately specified by a set of surface spherical or rectangular harmonics of degree n and order m. If we select rectangular harmonics as the more demanding form,

$$h(x,y) = \sum_{i=1}^{I} \sum_{j=1}^{J} A_{ij} \exp\left[i(\omega_1 + \omega_2 y)\right] ,$$

a minimum of $(2I + 1)(2J + 1)$ measurements are needed. As long as these are at approximately equal intervals, their exact location does not matter, and hence the sample density can be specified rather than sample location.

Since neither height measurement nor altimeter location are exact, we increase the number of measurements in the hope that height and location errors will thereby average to negligible quantities. If a single height measurement has a σ of $\pm \sigma_h$, n measurements of the same height have a σ of $\sigma_h/\sqrt{n}$ (see Henriksen (1967)[10] for caution in this regard). To do the job correctly, the repeated measurements would have to be between the same points, or at least to the same point on the surface. Because we assumed that the surface was adequately expressed as a truncated series of harmonics with a specified number of terms, the conditions are formally satisfied by any reasonably uniform sampling density or overlay of uniform minimum densities. The result for a real surface will be that higher-degree (short wave length) surface variations will be treated as if they were random height variations. This can cause a small bias but, since short-wave length variations were assumed unimportant, an insignificant one.

Satellite location errors also affect the results, but not in a reasonable (easily handled) manner. We first classify the errors,

according to their direction, as tangent, normal, and binormal or, in the space-engineer's jargon, along-track, down, and cross-track. We further classify them, according to their source, as theory error and tracking error. Theory errors occur because the mathematical description (including computation) is incomplete and, even if complete, wrong. Theory errors cannot be expected to average to zero. They can be expected to correlate strongly with unmeasured surface variations and so be correctable. Further discussion of this point is not practicable here, but one way of dealing with theory errors is to shorten the length of orbital segment that theory must handle. Fortunately, such shortening also diminishes tracking errors. Tracking errors occur because the satellite location is first determined by observation and then by theoretical interpolation between observations. Since most observations give only one or two coordinates of a satellite, the lack of a full complement must be made up from theory. This makes it difficult to give a complete description of tracking errors separately from theory errors. We shall not go into these difficulties here. It is enough to note that the tracking error at any point is approximately the tracking error of the closest observation, increased by the deterioration of the orbit used in carrying the location forward.

One of the three directional components of the tracking error, that along the normal, is the most important, since it is close to the direction of the height measurement. Tracking errors in the other two directions are unimportant because, while they are of the same order of magnitude as the error along the normal, the rate of change of surface height in these directions (projected on the surface, of course) is extremely small. Placing tracking stations closer together has the effect therefore of (1) increasing the number of observations and (2) decreasing the effect of the orbit on the tracking error. Increasing the number of measurements (that is, raising the sampling density) will of course tend somewhat to average out the tracking errors but has little favorable effect on the theory error and could conceivably aggravate it.

In this connection we may note that one of the theory errors is the error in location of each tracking station. This particular error is not random; it cannot be removed by any statistical hanky-panky. It can be and is being diminished by conventional geodetic means and through earth satellites as intermediaries. Full discussion of this point here is not appropriate. If we denote the tracking sampling density by σ_T and ignore the effects of systematic errors on the total error, we can write, for the approximate variance in a coefficient, thus:

$$\sigma^2_{A_{ij}} = \frac{\sigma_h^2 + \sigma_r^2}{2n_M}$$

where n_M is the number of measurements made in an area $(L_1 \times L_2)/(2I + 1)(2J + 1)$, and L_1, L_2 are the linear (surface) extent of the surface variation being studied. The total number of measurements is therefore

$$N = (2I + 1)(2JM) \cdot 2n_m \quad ,$$

$$n_m = 2\sigma^2_{A_{ij}} / (\sigma_n^2 + \sigma_m^2) \quad .$$

In discussing the sampling density, I have assumed that the instrument is actually an altimeter - that is, it measures the distance from the instrument perpendicularly onto the surface below and that there is a one-one correspondence between altimeter location and surface point. As long as we are concerned with an everywhere convex surface like the geoid, no difficulty arises and the surface model is the envelope of the family of spheres with center on the orbit and radius equal to the altitude. If the surface profile is concave, however, the envelope and hence the altitudes do not determine the surface profile. Recovery of the surface profile from altimeter readings may therefore require knowledge not only of the time of earliest return (of signal) but also of the signal shape.

Another point that must be considered in determining sample density is that the required uniform density may be obtainable only at the cost of greatly increased density in some areas. If the location of samples cannot be completely controlled, the distribution of samples per unit area becomes chancy. If a minimum number per unit area is specified or if the geometric distribution of samples is specified (which is almost the same thing), the total number of samples will have to be increased until the probability of getting the specified minimum density is high enough. The consequence will be that some unit areas will have a higher-than-specified density. This point is further discussed in Appendix G-C.

Finally, it is obvious that a uniform sampling density in a completely unknown area will at least be satisfactory and may be optimum. But if we already know or suspect something about the topography, then the sampling density should be changed so that we get a most efficient density distribution based on what we know. Simply, we want to concentrate our measurements where surface heights vary rapidly and make few measurements where surface heights change only little. A satisfactory first step is to look at the bottom topography and make the density along a surface profile proportional to the average slope along the corresponding bottom section.

B.2 SAMPLE RATE

Sample density can be specified for a time-invariant surface, and sample rate is then arbitrary (or at least can be manipulated to suit the instrument design). The ocean surface, which is what we are really measuring, is not time invariant. If we were concerned primarily with the instantaneous surface, we would have to either make our measurements at such a rate that surface change during the measurement set is negligible or find a relation between measurements made at different times and places. The first alternative is out as far as satellite altimetry is concerned at present. This leaves the second alternative. Since our primary concern is not with the instantaneous but with the average surface, need we concern ourselves with the second alternative? Yes;

because unless we know something about the time-distance variation in surface we cannot trust the average that we deduce and, furthermore, cannot go back later from the average surface to find out what the instantaneous surface parameters may be. In looking at the sampling density problem, we found that it was not necessary to specify sample location if we specified sample density properly within the area of interest. (Mathematically the two types of specification are equivalent; practically they are not.) We hope that an analogous situation exists if we go from a time-invariant to a time-variant surface, that is, that we can specify sample rates rather than sample times. We also hope that the transition will not destroy our sample density estimates but will only cause a simple modification of them. In other words, we look for a simple relation between the instantaneous surface and the average surface as a function of time.

To begin, we catalog the temporal variations according to (1) period, (2) cause, and (3) amplitude. Any such classification is of course artificial. The water surface knows no classifications, so that when we isolate certain numbers as descriptive, we subjectively distort the true situation. This means that our classification, especially of phenomena in the still largely unexplored oceans, must be used with caution and the understanding that it has been affected by subjective opinions about how things ought to be. With this reservation the data given in Table B-1 are presented for use in estimating sample rates. Also to be remembered is that the values given are typical and not limiting or average. Ocean surface conditions vary too much and we have too few data on them to allow them to be represented adequately by one or two parameters.

Items 1 through 4 in the Table B-1 can be considered secular as far as a 1 to 10 year lifetime altimetry project is concerned. Hence averaging will not remove these effects, nor do we wish to do so. Item 5 is a tidal variation in the sea level and would have to be averaged over a 19 year to 40 year period. Its amplitude of 0.4 mm is so low that

TABLE B-1

PRINCIPAL TIME VARIATIONS IN SEA SURFACE HEIGHT ABOVE A REFERENCE SURFACE

	PERIOD	AMPLITUDE	CAUSE
	(years)	(meters)	
1.	----	-25,000	Permanent water loss
2.	0.001**	----	Land rise
3.	5×10^4	-200	Glacier formation during Pleistocene
4.	5×10^4	+120	Subsequent glacier melting
5.	18.6	0.0004	Tide (nodal)
6.	----	2.0	Air pressure
7.	1	0.2	Air pressure (static)
8.	1	0.2	Temperature
9.	1	0.2	Salinity
10.	1	----	Air pressure (dynamic)
11.	1	0.1	Mass transport
12.	1.2	0.005	Polar motion
13.	0.25	0.03	Tide (solar semi-annual)
14.	0.08	0.03	Tide (lunar monthly)
15.	0.04	0.06	Tide (lunar fortnitely)
	(seconds)		
16.	4300	0.5	Tide (lunar semi-diurnal)
17.	4300	0.25	Tide (solar semi-diurnal)
18.	3000	1	Seiche
19.	900	1	Tsunami
		(30)	*
20.	30	3	Swell
21.	10	5	Wind wave

* at coast
** rate in m/yr.

it could not be picked up by any altimeter we are considering. Item 6 is a variation whose period we do not know. It is a dimple in the water surface caused by an air-pressure high of long duration. Seasonal air pressure variations of this kind cause level variations of about 0.2 meters, but the longer-persisting pressure anomalies cause correspondingly greater surface distortion. If we were sure of the shape and period of the variation, we could correspondingly specify the number and frequency of measurements to be added over and above those needed to measure a completely static surface. As it is, we are not sure of these characteristics. We can reasonably assume, however, that the period is not less than 10 years. We can therefore treat the phenomenon by first computing the sample density n required if it were permanent and getting the sampling rate as 2n/P. In the present case a reasonable least value for P is 2 years. To avoid introducing an artificial correlation with seasonal variations, we should increase the sampling rate somewhat. How much to increase the rate will depend on (1) the required rms error, (2) the total sampling time, and (3) other minor factors.

Items 7 through 12 represent variations with approximately 1 year periods. Except for the last of these, the variations are rather directly related to the seasons, while the last is caused by the Chandlerian motion. This means that we can expect the Chandlerian motion variation to be moderately constant in amplitude and eventually to be predictable from the measurement of the motion, while the seasonal variations cannot be expected to have the same constancy of amplitude. Increasing the sampling rate would therefore be of less use than leaving the rate constant and increasing the time span of the measurements.

(In the discussion of sampling rate, the rate is assumed given as so many measurements per unit of time, and the unit is either year or second. This provides values which can easily be turned into power requirements, etc. In getting the geodetic and geophysical phenomena measured, however, it would obviously be desirable to get the sampling rate as the total number of measurements divided by the lifetime of the

satellite, with the satellite lifetime left dependent on the aims of the project. I think that enough information is now available on altimeter characteristics, etc., that either way of expressing sampling rate can be converted into the other. During the early stages of this project such information was not available and a choice had to be made.)

Items 13 and following can be thought of as high-frequency variations compared to those preceding. Tidal variations (in the open sea, of course) are reasonably regular in frequency; and, if they are sampled at a given point with a period 5/2 that of the highest frequency present, with appreciable amplitude, can be accounted for. The highest frequency given in Table B-2 is 3/day, approximately. Raytheon's Marine Research Laboratory (1968)[11] cites a frequency of 3 cycles per day as adequate for central Pacific variations. This would put the sampling rate at 8 per day, with an equivalent spatial sampling density of 1 per 5000 km. In using these figures for sampling rates in connection with tides, however, two points must be very thoroughly understood. (1) The quoted spatial density would obtain if tidal variations had a spatial distribution (wavelength and amplitude) corresponding to the temporal distribution. But maps of cotidal lines in the oceans show that such correspondence does not exist. Hence the removal of tidal variations from altimetry measurements will mean taking a time average at every sampling point in those places where we do not know enough about the tides to estimate the wave length. (2) Wavelength and frequency of tidal variations cannot be correlated in the open ocean by a simple relation. It is also true, however, that wavelength estimates can be made in large areas with an error smaller than would be significant in averaging the tidal variations. The total number of samples n_T is therefore not the product of the number of samples n_S needed for the time-variant surface by the number n_t of times a point must be sampled. It is instead the sum of the number of samples needed for the time-invariant surface plus $(n_t - 1)$ times the number of points needed to define the shortest wavelength component. Since the timing rms error is negligible this need not be taken into account.

TABLE B-2

LIST OF PRINCIPAL TIDES

FREQUENCIES AND AMPLITUDES

TYPE	FREQUENCY (n/day)	AMPLITUDE (cm.)
Syzygy	1.8×10^{-6}	$\ll 0.1$
Saros	1.5×10^{-4}	
Nodal (L) Cycle	1.5×10^{-4}	
Apsidal (L) Cycle	3.3×10^{-4}	
Annual (S)	3.4×10^{-3}	0.2
Semi-Annual (S)	1.1×10^{-2}	1.2
Monthly (L)	3.6×10^{-2}	3
Semi-Monthly (L)	7.4×10^{-2}	5.7
Diurnal		
Lunar	0.9	13
Solar	0.98	3
Luni-solar	1.	15
Semi-diurnal		
Lunar Elliptical	1.9	6.8
Lunar	1.9	3.4
Solar	2.	6.8
Luni-solar	2.	4.1
Terdiurnal		
Lunar	2.9	0.7

L = Lunar

S = Solar

Seiches have some of the properties of tides in that they have recognizable wavelength-height-frequency characteristics. They are more complex than waves, however. Since their frequency and wavelength parameters are related to the dimensions of the basin, it is recommended that the frequency and wavelength be computed, where necessary, for the area in question and that the number of samples in that area be increased accordingly.

Tsunamis are transient phenomena, and take on large amplitudes only near the coasts. Data contaminated by tsunamis near coasts can be identified by comparison with coastal surface observations and other outside data. Those data contaminated by presence of tsunamis in the open ocean can be corrected by comparing data over the same general area spaced several days or more apart. Since the width of tsunamis is on the order of 200 km , a sampling density of 1 measurement per 5000 km^2 would be satisfactory for a stationary wave.

APPENDIX G–C

SAMPLE SCHEDULING

The stated problem is to determine msl over as large a portion of the earth as possible. It can easily be shown that msl under land areas cannot be found by altimetric measurements on land. It can also be shown, albeit with some difficulty, that the geoid can in theory be determined under land from a knowledge of the geoid on the oceans. Since it can also be shown that there is a wide and probably insurmountable gap separating theory from what can actually be done, and since the geoid in ocean areas is almost as difficult to determine precisely as it is under land areas, the sea-geoid cannot be pushed too far inland.

The point of this moralizing is to justify the assumption that most emphasis should be placed on finding msl per se, at least to start with. After we have gotten a reasonable amount of knowledge of msl, we can look into the problem of finding mathematical functions for the geoid that can be used in land areas. The assumption is necessary because the sampling distribution function can be quite different according to the purpose to which the samples are to be applied.

N_H = Number of measurements per unit area

The unit area in this case is taken arbitrarily as 10^4 km^2. Then

$$N_H = f(\lambda, \phi).$$

We assume first that

$N_H = 0$ if $P[\lambda, \phi]$ is on land.

N_H = constant otherwise.

(This restriction will be slightly relaxed later to allow measurements on lake and shore areas.) We assume next that a knowledge of msl in ocean areas is wanted to the same resolution and accuracy as on land. Of course our knowledge of the geoid varies in different areas. It is quite detailed in Europe, Japan, and parts of the United States, for example. It is almost unknown (to us) except for the lowest harmonic components in Africa, much of South America, Asia, etc.

If we are ambitious and select the best land geoidal representations, as a goal for msl measurement on land, it turns out that the greatest lower bound (glb) for areas over which an average height may be given is approximately 10^4 km^2. That is, if average msl heights are found for 100 x 100 km sq adjoining disjoint areas over the ocean surface, the consequent msl representation will have the same details as are found in well mapped geoidal undulations in Europe or Japan.

If we are more conservative in our planning and choose, for example, the Australian geoid as a model, the glb becomes approximately 10^5 km^2 or 300 x 300 km squares. Finally, if we are willing to limit ourselves to a geoid over the oceans which can connect Fischer's geoid (see Figure C-1), the glb is about 3.0 x 10^6 km^2 or 550 x 550 km square.

The minimum number of points per unit area that can be allowed is 3, with 4 preferable and 5 or 6 desirable. The pattern of measurements corresponding to each is

3

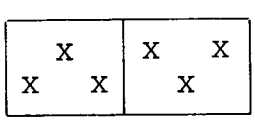

5

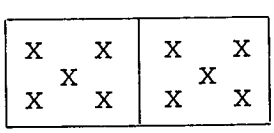

4

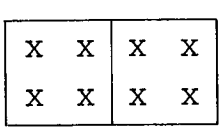

6

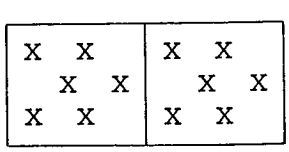

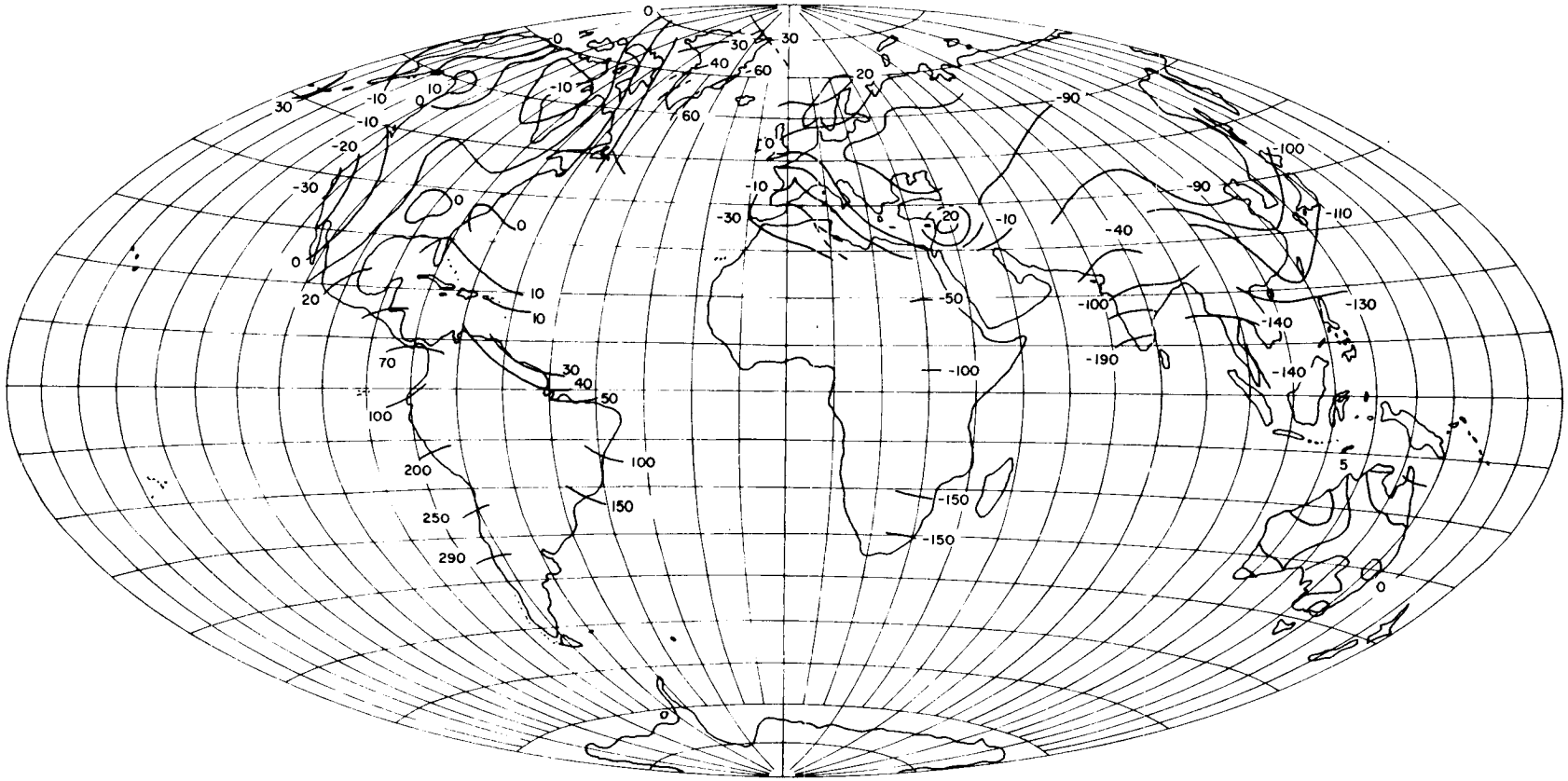

Figure C-1 Fischer's Geoid (1967)

If these patterns cannot be maintained (if the distribution of measurements within a unit area is random), a larger number of measurements per unit square must be made to give reasonable (67%) probability that the arrangement of the samples is adequate. To get by random sampling an arrangement which approximates that of 4 planned samples, 7 samples must be taken.

Assuming an inclination at which the satellite samples over about 50% of the available water surface, about 16,000 unit areas must be sampled. With scheduled sampling, this requires about 65,000 measurements; with random sampling, about 10^5 measurements if fine (short wave length) detail is to be mapped. This drops to 6500 or 10,000 if we are conservative and to 2000 or 4000 if we are ultra-conservative.

If measurements must be severely rationed, a good plan would be to make N_H a function of λ, ϕ such that

$$N_H = k \frac{dH_G(\lambda,\phi)}{d\theta}$$

where θ is the true anomaly. The value of $dH/d\theta$ must be estimated from the (scanty) gravimetric and bathymetric measurements at sea. Another possibility would be to concentrate on a few critical areas.

APPENDIX G–D

ALTIMETER SPECIFICATIONS

Preliminary specifications on altimeter characteristics are given below. They are derived only with ultimate geodetic performance in mind and must be modified as required by oceanological considerations.

D.1 ALTIMETER HEIGHT

The height H_a of the altimeter above the reference sphere or spheroid does not appear to be geodetically significant except in its relation to the distance between traces on successive revolutions of the altimeter measurement path. Figure D-1 is a graph of the approximate separation in degrees at the equator of successive traces as a function of altitude. For the range of altitudes we are considering (50 km to 2000 km) the trace separation varies between approximately $22^{\circ}.5$ (2300 km) and 35° (3850 km) at the equator. A separation of exactly $22^{\circ}.5$ would cause a retrace of the same path, which is undesirable. Precession of the plane of orbit (unless the inclination is 90°) will increase or decrease this by from about 5° per day for 0° inclination down to 0° per day at $\pm 90^{\circ}$ inclination. If particular small areas are of interest, it seems best to arrange the spacing so that the area is intensively and sequentially covered, which implies heights between 50 km and 300 km or around 1800 km, which would give close spacing every 1.5 days, or around 32 km, which would return to the close spacing every day. Vernier adjustment of spacing would be done through selection of the inclination. If the oceanic areas as a whole are to be measured, the principal consideration is to arrange the spacings so that the time interval between traversal of the same area is as long as possible. Given a long enough functioning life of the altimeter, the spacing is arbitrary within wide limits. These limits are, however, affected also by the smallest geoidal wave length to be detected or measured. We will want to select a spacing which will give as few redundant

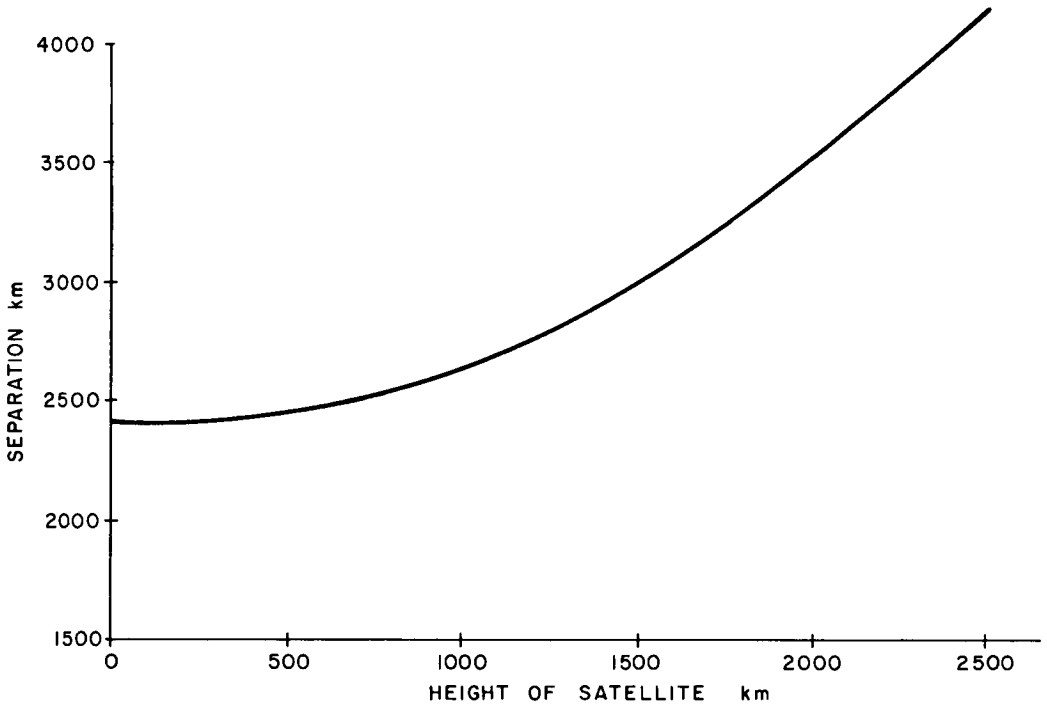

Figure D-1 Separation of Successive Traces of Subsatellite Point

measurements within a given wave length as possible. Since the choice of trace separations is reasonably wide, no detailed examination of this point will be made at present. Later, when alternative orbit parameters have been chosen, orbital calculations will be made to find the actual spacings to be expected. Parameters can then be varied until a suitable spacing is found. (Note that trace separation decreases with satellite latitude. This will have to be compensated by decreasing the number of measurements correspondingly).

Since trace separation does not appear to be critical if a long lifetime is expected, other factors more critical must be considered. The principal non-geodetic factors are: (a) measurement accuracy, (b) altimeter lifetime, and (c) rocket capabilities. The factors will be considered in that order.

a. Three major and partially conflicting considerations enter. First, the smaller H_S, the greater the returned signal strength. Second,

the smaller H_S, the less is the difference between measured height and true height likely to be. Third, the smaller H_S, the smaller is the radius of the sphere within which the satellite can usefully be tracked. It is desirable to have the satellite as low as possible to maximize the returned signal strength while minimizing the geometric ranging errors, but also to have the satellite for as long a distance as possible within tracking distance of a station (especially when the satellite is over the ocean). (Here also the question of trace separation enters, since the separation should be chosen to best fit, other things equal, the tracking station distribution.)

b. The lifetime of a satellite depends almost entirely on the distance of closest approach of the satellite to the earth's surface. Shape, mass, and rotation of the satellite are also influences, but they can be considered of secondary importance except for very large and light satellites and at times close to death. Of the many formulae proposed for computing a satellite's life span, the following was selected for its convenience.

$$t = t_1 + \frac{F(h_1) - F(h)}{k}$$

where k is a constant involving shape, weight, density, and diameter of the satellite and F(h) is a function of the height involving the atmosphere's characteristics:

$$F(h) = \frac{H}{2\sqrt{nr_i}}\left(\frac{1}{P_i} - \frac{1}{P_o}\right)$$

where P_i is the density at h = i, r is the radius vector, and H is the scale height of the atmosphere.

If we require that (1) the satellite have a lifetime of at least 365 days and that (2) during this time the altitude decrease per day be not more than 1 meter (the laser rms error), the minimum altitude is somewhat over 800 km. This minimum altitude can be reduced if we require only that non-computable altitude decrease be not more than 1 meter per day. The minimum altitude then becomes less than 600 km.

c. The question of rocket capabilities is closely connected with other questions such as rocket availability, etc. These questions will not be taken up at present.

In summary, the limits on satellite height seem to be between about 800 km (set by drag) and 2000 km (set by trace separation), with the lower limit favored by signal considerations and the upper by tracking considerations.

D.2 ORBIT INCLINATION

As mentioned in Paragraph D.1 previously, the trace separation wanted is a factor in selecting orbit inclination. More important, however, may be (1) the ratio of ocean to land area and (2) the percentage of cloud cover. Table D-1 shows the ratio of ocean area to land area that will be accessible to the altimeter as a function of orbital plane inclination. The ratios range, as would be expected, from a maximum of about 3 1/2 at zero inclination to about 2 1/4 at 90° inclination.

TABLE D-1

RATIO OF OCEAN TO LAND AREA COVERAGE AS FUNCTION OF ORBITAL PLANE INCLINATION

Inclination (Deg)	Ratio of Ocean to Land Coverage
0	3.64
30	2.88
60	2.75
90	2.25

It is assumed that the following water or ice should be regarded as land:

1. All water or ice within 15° of the two poles;
2. All channels through river deltas, particularly that at the mouth of the Amazon;
3. Inland lakes, including Lake Victoria.

(Based on Reference 23.)

But an equatorial orbit is out of the question if geodetic information of sufficient value to justify the project is wanted. Between the ratios at higher inclinations the difference is not as large. Hence the water/land ratio does not play an important role in deciding on inclinations unless (1) no way exists for operating the altimeter only over ocean areas and the total number of measurements must be very severely rationed, or (2) the data must be garnered in the minimum of time.

The percentage of cloud cover to be expected is certainly important if a laser altimeter is used and if no method for making measurements only through tolerably clear sky is incorporated. If a cloud/no-cloud discriminator is provided, the cloud cover percentage is still important because it will determine the relative number of measurements made in various regions. Measurements will, for a project of reasonable duration, be very unequally distributed over the ocean surfaces, with clear sky areas having low measurement density. This leads either to a false picture of the geoid or to commitment of the data analysis portion of the project to an elaborate scheme for weighting that may be of dubious usefulness.

If a radar altimeter is employed the percentage of sky cover has much less significance as far as measurability of the surface is concerned. But sea areas with a high percentage of cloud cover are also likely to be areas where the surface is much disturbed by waves, and hence the data recovered from such areas must be given a disproportionate amount of attention during the data analysis. I think that a safe maxim is to stay away as much as possible from cloudy areas regardless of the type of altimeter, but to relax this restriction considerably for radio wave altimeters if this is desirable and as little as possible for optical altimeters.

Table D-2 gives the occurrence of three categories of cloud cover for 4 different orbit-plane inclinations. It shows that inclinations outside $\pm 60^{\circ}$ are much less desirable than those inside. The tabular

TABLE D-2

% OF TOTAL SKY COVER

Entries in the table indicate the % of the total ground surface that has the stated sky cover, at each inclination.

Inclination \ % of total sky cover in the area	0-50%	50-75%	>75%
0^{o}	40%	56%	4%
30^{o}	41%	56%	3%
60%	31%	51%	18%
90^{o}	27%	47%	26%

NOTE: The amount of cloud cover and the amount and magnitude of surface wind-waves are probably correlated.
Computed from charts in Reference 24.

values are averages over a full year; more detailed planning of the observation sequence in northern and southern hemispheres as functions of the seasons could push these limits higher. In any case, a certain amount of study of cloud conditions in specific areas after selection of preliminary orbital parameters will be useful.

D. 3 ECCENTRICITY

No perfectly spherical orbit is possible either in theory or in fact. Neither, however, does there seem to be any justification for a deliberately elliptical orbit. Design of an elliptical orbit whose perigees occur over regions where precise altitudes are to be measured and whose apogee regions occur in the neighborhood of tracking station is not possible. A reasonably circular (low eccentricity) orbit whose mean altitude satisfies the conditions stated in Paragraph D.1 is therefore considered the best that can be required or used.

D. 4 ARGUMENT OF PERIGEE

Specification of this value for a nearly circular orbit is not useful.

D. 5 REMAINING PARAMETERS

Until a reasonably definite schedule of observations can be drawn up, approximate launch dates set, etc., the question of what value to specify for the longitude of the node cannot be settled. Its importance in a project using a long-lived altimeter (lifetime greater than 2 years) is small anyway. The same is true of the parameter σ_o, the mean anomaly at epoch.

APPENDIX G-E

DIMENSIONS OF SURFACE VARIATIONS

The geometric properties of a surface are defined by giving the coordinates of surface points in a convenient reference system. The surfaces of the earth, the sea, and the geoid are conveniently defined in a reference system in which one family of reference surfaces is a family of spheres or spheroids. One of the physical surface coordinates is then always small and always close to what is measured by the geodesist. Analytic descriptions of the physical surface are then conveniently expressed in terms of Legendre or Lamé series. Deviations of the physical surface from the reference surface are the sums of terms of higher and higher frequencies, just as when Fourier series are used with plane reference surfaces.

It has become convenient to speak of the wavelength of a feature or perturbation because Legendre series are built up on a wavelength kind of progression of terms. This way of speaking must be used cautiously if it is extended to characterizing features for numerical use. To avoid some of the difficulties introduced by speaking of the wavelength of a feature, the concept of feature width is introduced. The width is perhaps no more adequate for description than wavelength; very few features can be well described by only one or two numbers. The width does give a better visualization of the feature and cannot be plugged into a Legendre series by accident.

As shown in Figure E-1, the width of a feature is the distance (along the sphere) between the projections onto the sphere of those points which lie half way between maximum and minimum distance from the sphere. Since a feature is never two-dimensional, it will have two widths at least. In fact, it will usually be very irregular and its boundaries must be defined in order for the width to have meaning.

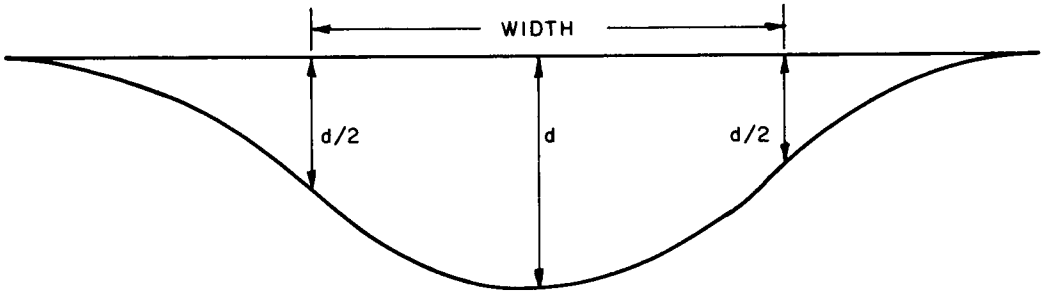

Figure E-1 Definition of 3 dB Width of Undulation

APPENDIX G-F

GEOIDAL UNDULATIONS

In making preliminary estimates of the size of geoidal undulations resulting from local geological features, we used merely the peak values and widths of observed gravity anomalies in the area. Since most of the anomalies were along a section, the computed geoidal height and width would be less dependable than if areal anomalies had been available. At this stage precise geoidal undulation size is not particularly important. It is used only for estimating sample densities, which may be off by a factor of 2 or 3 from the ultimately selected densities.

For more precise estimation for future planning, three methods are being studied. The first is to represent the ocean bottom feature by a simple geometric figure for which moments of inertia, I, can be easily computed. MacCullagh's formula

$$V = \frac{k^2 M}{r}\left[1 + \frac{1}{2r^2 M}\left(I_1 + I_2 + I_3 - 3I_{rr}\right)\right]$$

is then applied to find the potential V at a distance r from the feature's center of gravity (I_{rr} is the moment of inertia about r). If the direction vector of r with respect to I_j is $\vec{d}$, then

$$I_{rr} = \vec{d} \cdot I \cdot \vec{d}$$

where I is the inertial tensor made up of I_j and the cross moments I_{jk}. The cross moments I_{jk} will be zero if I_j are computed about the principal axes.

It seems as if many features of interest can be well represented either by a rectangular parallelopiped or by the frustrum of a right circular cone (see Figure F-1). The potential of a frustrum is the

(a) Rectangular Parallelopiped

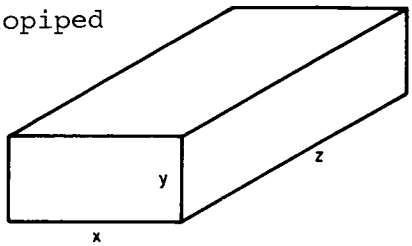

$$I_1 = \frac{m}{48}(y^2 + z^2)$$

$$I_2 = \frac{m}{48}(z^2 + x^2)$$

$$I_3 = \frac{m}{48}(x^2 + y^2)$$

(b) Right Circular Cone

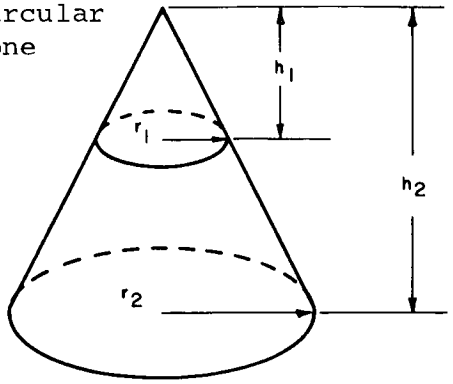

$$I_1 = \frac{3m}{20}\left[r^2 + \left(\frac{h}{2}\right)^2\right]$$

$$I_2 = \frac{3m}{20}\left[r^2 + \left(\frac{h}{2}\right)^2\right]$$

$$I_3 = \frac{3m}{10} r^2$$

Figure F-1 Standard Figures Approximating Geological Features

difference in potential from the two cones with radii r_1 and r_2. The potential from more complicated features can be built up by combining parallelopipeds of various dimensions. MacCullagh's formula works best when r is large compared to the dimensions of the feature. A second method which is more adaptable to complicated features and which works in the usual case that the geoid surface point is close to the disturbing feature is to use numerical integration. One integration is avoided by starting with the formula for the potential of a thin rod:

$$V_r = k^2 \sigma \, \ell n \left[\frac{\sqrt{(x - x_c)^2 + (y - y_c)^2 + (z - z_{c1})^2} + (z - z_{c1})}{\sqrt{(x - x_c)^2 + (y - y_c)^2 + (z - z_{c2})^2} + (z - z_{c2})} \right] .$$

The rod is parallel to the z-axis with end points at z_{c1} and z_{c2} and with density σ. The total potential at (x,y,z) from a body made up of these thin rods is then

$$V = \int_{x_c} \int_{y_c} V_r \, dy \, dx.$$

(z_{c1} and z_{c2} will of course be functions of x_{c1} y_c).

The third method can be used only when gravity values are available over an area. We then use Stokes' formula and numerical integration. A detailed gravimetric study of a seamount is shown in Figure F-2. A geoid could be constructed from the data on which the chart is based, but the result would be erroneous because we would be ignoring contributions from nearby, unknown gravity anomalies.

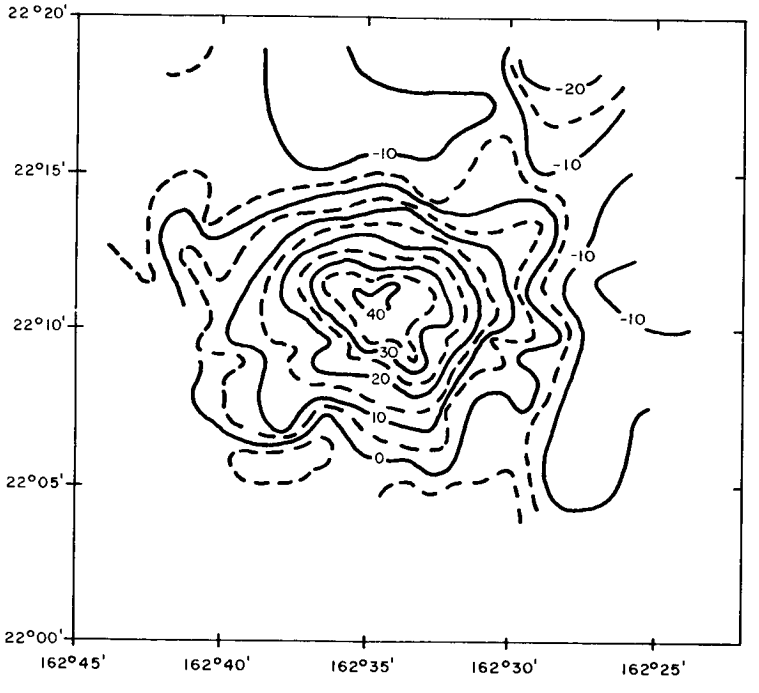

Figure F-2 Gravity Anomaly over Chautaugua Seamount (in mgal)[26]

APPENDIX G–G

TIMING

Time enters the altitude measurement procedure in three ways. First, it is used in determining the distance travelled by the radiation pulse. If the timing rms error is σ_t, the range rms error is

$$\sigma_d = c\sigma_t/2.$$

If σ_d is 1 meter, σ_t must be 0.6×10^{-8} or less. The second way it enters is in the determination of the location of the altimeter at time of measurement. The greatest velocity of the altimeter is along the orbit tangent and is less than 8×10^3 m/sec. A 1 meter rms error therefore requires a timing error of less than 1.3×10^{-4} second. Normal and binormal velocities are less than the tangent velocity by a factor of more than 10^3 for a reasonably circular orbit. Since for msl and geoid determination location errors in the tangent and binormal directions may be hundreds of meters without changing the msl or geoid height measurably, the timing error noted is perfectly adequate. The third way time enters into measurement is in scheduling the sample locations. A properly carried out experiment will specify as closely as possible the times and locations of measurements. Perhaps this can be done satisfactorily by specifying times at which the altimeter footprint enters an area, the time at which it leaves, and the sampling rate between. (See elsewhere for discussions of relation between sample rate and sample density). In any case, it seems unnecessary to specify sampling locations to better than ±1000 meters, at best, which is equivalent to specifying time of not better than $\pm 1.3 \times 10^{-1}$ second.

At present, the technology of time measurement allows the above error requirements to be satisfied without any difficulty. The 0.6×10^{-8} second requirement for σ_t is a requirement on short term stability, and short term stabilities of 1 part in 10^9 are routine for crystal oscillators. That is, we do not need the time per se here, but only the

time interval. As for the second requirement of 1.3×10^{-4} second, clocks with a long-term stability of 5×10^{-10} are by now standard. Assuming a time check once per day, the time error will be less than 0.5×10^{-4}.

APPENDIX G–H

ASTRO–GEODETIC GEOID

The astro-geodetic geoid height h_1^2 is computed from the total deflection ζ of the vertical and from the distance between deflection points by the formula

$$h_1^2 = \int_1^2 (\tan \zeta)\, ds.$$

The error ϵ_h is the result of errors from several sources, the most important of which are (1) the measurement of ζ and (2) the finite distance ΔS between stations. First-order astro-positions combined with first order geodetic positions give deflection errors ϵ_ζ within ± 0.5." We shall assume that ΔS is small enough that the error ϵ_I contributed by deflection variation within the ΔS intervals is less than $k \tan \zeta$. Total height variance ϵ_h^2 in a distance S is then satisfactorily estimated, for the purposes of this study, by

$$\epsilon_h^2 = \sum_j \frac{(\Delta S_j^2 (\Delta \zeta_j)^2 + k^2 \zeta_j^2)}{S} .$$

Figure H-1 shows the density μ of astro-geodetic stations in the areas of primary, long-arc triangulation. We estimate ΔS from this by

$$\Delta S \simeq 10^2/\sqrt{\mu} .$$

Figure C-1 shows the geoid along major primary long arcs. The errors in the indicated geoid heights can be derived from this.

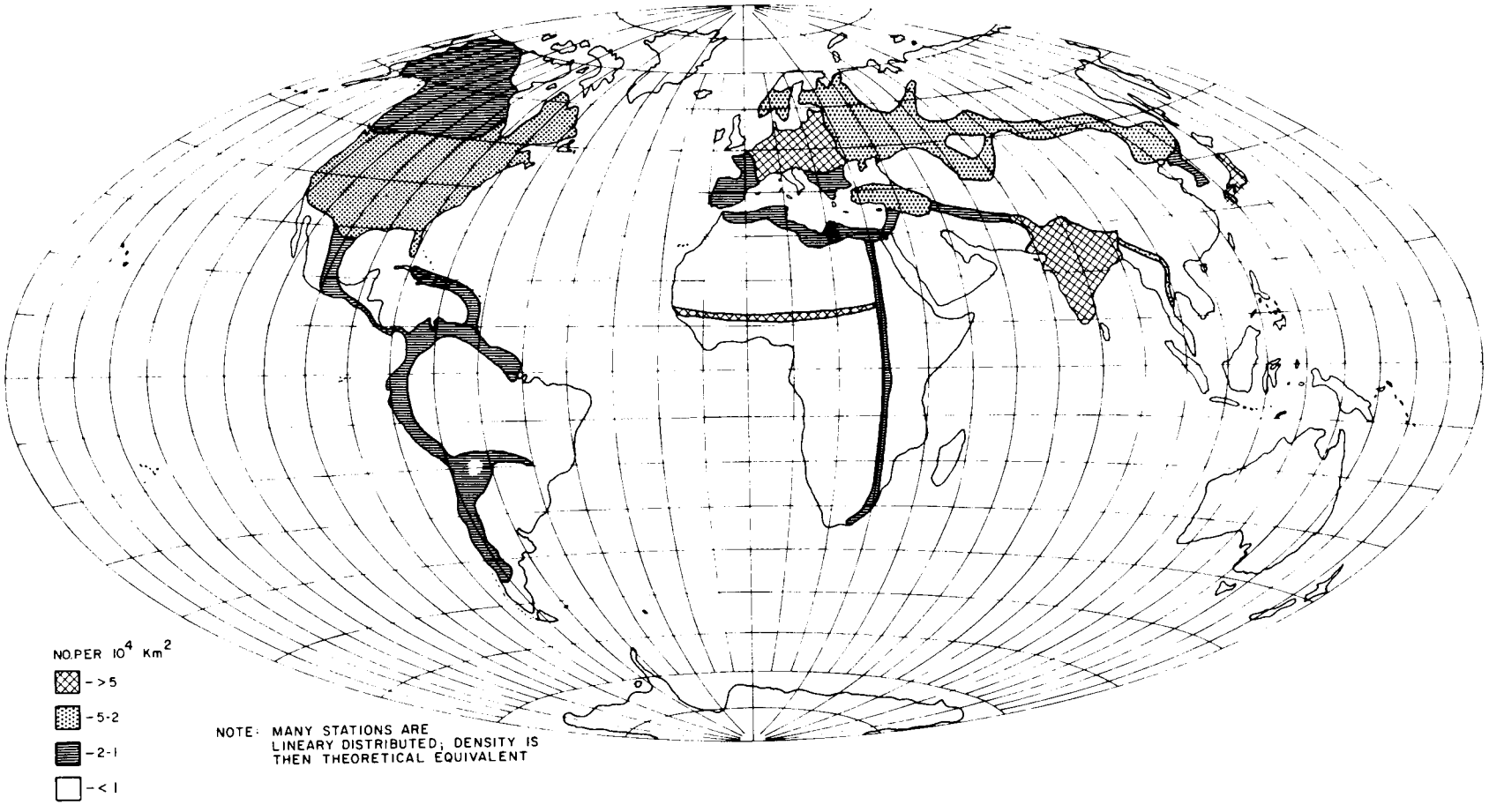

Figure H-1 Astro Station Density

APPENDIX G-I

SATELLITE GEOIDS

Since verification in 1958 of the Krassovsky ellipsoid dimensions from satellite tracking data, considerable work has been done on finding by similar means the less-pronounced wrinkles in the geoid. It is difficult often to compare the results of different workers because different reference systems are frequently used.

While comparison of geoids referred to spheroids or ellipsoids of the same shape does give a fast start toward finding out what is going on in satellite geophysics, a more leisurely pace afterwards shows that many factors must be considered if a true idea of the situation is to be developed. One of these factors is the way in which the tracking stations themselves are accounted for in the computations. Many, if not most, of the tracking stations whose data are used in a solution are connected to a common reference system only thru the orbital equations. This means that the values for the gravity potential coefficients are correlated strongly with the assumptions made in assigning coordinates to the tracking stations. A more homogeneous set of tracking-station coordinates may be found by using an altimeter to define the geoid (or msl).

As an indication of the discrepancies between geoid approximations found from satellite data, Figures I-1 and I-2 may be compared. The first is from Izsak (1964)[12]; the second from TRANET data (1966)[13]. A further comparison showing the change introduced by using a different spheroid as reference is gotten from Figure I-3 based on data from SAO (1967)[14]. Note that while the general features agree, such as the pair of eyes bracketing Central America or the high off Cape of Good Hope, there is considerable difference in values and in the figure at

non-extremal points. This is the sort of difference that satellite altimetry can resolve. A 15-meter height error would still allow us to differentiate between the 1964 and 1966 geoid approximations and a 5 meter to differentiate between the 1966 and 1967 geoid approximations.

The two later geoid approximations were computed by direct solution of the equation for the geoid.

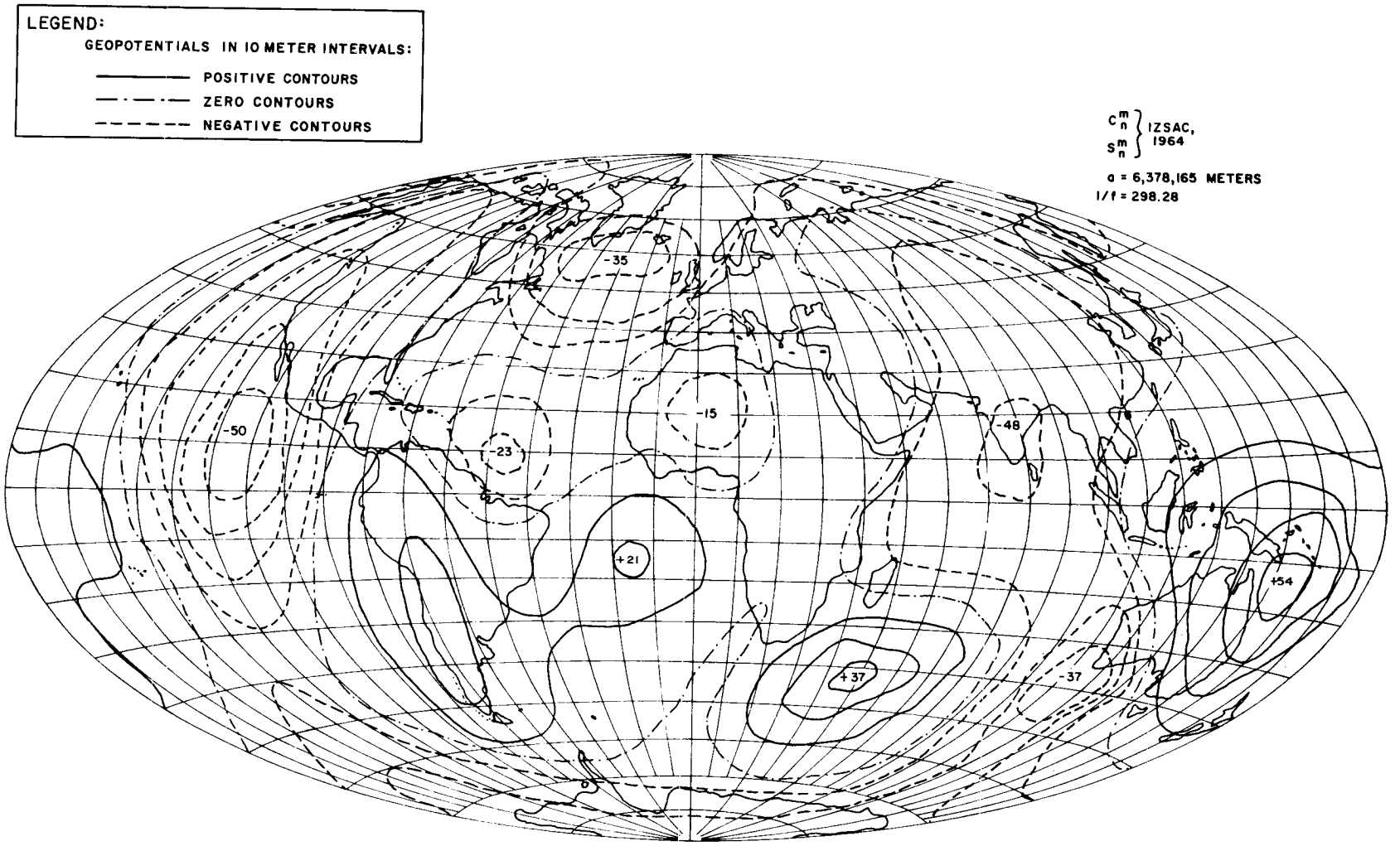

Figure I-1 Geoid, after Izsak (1964)

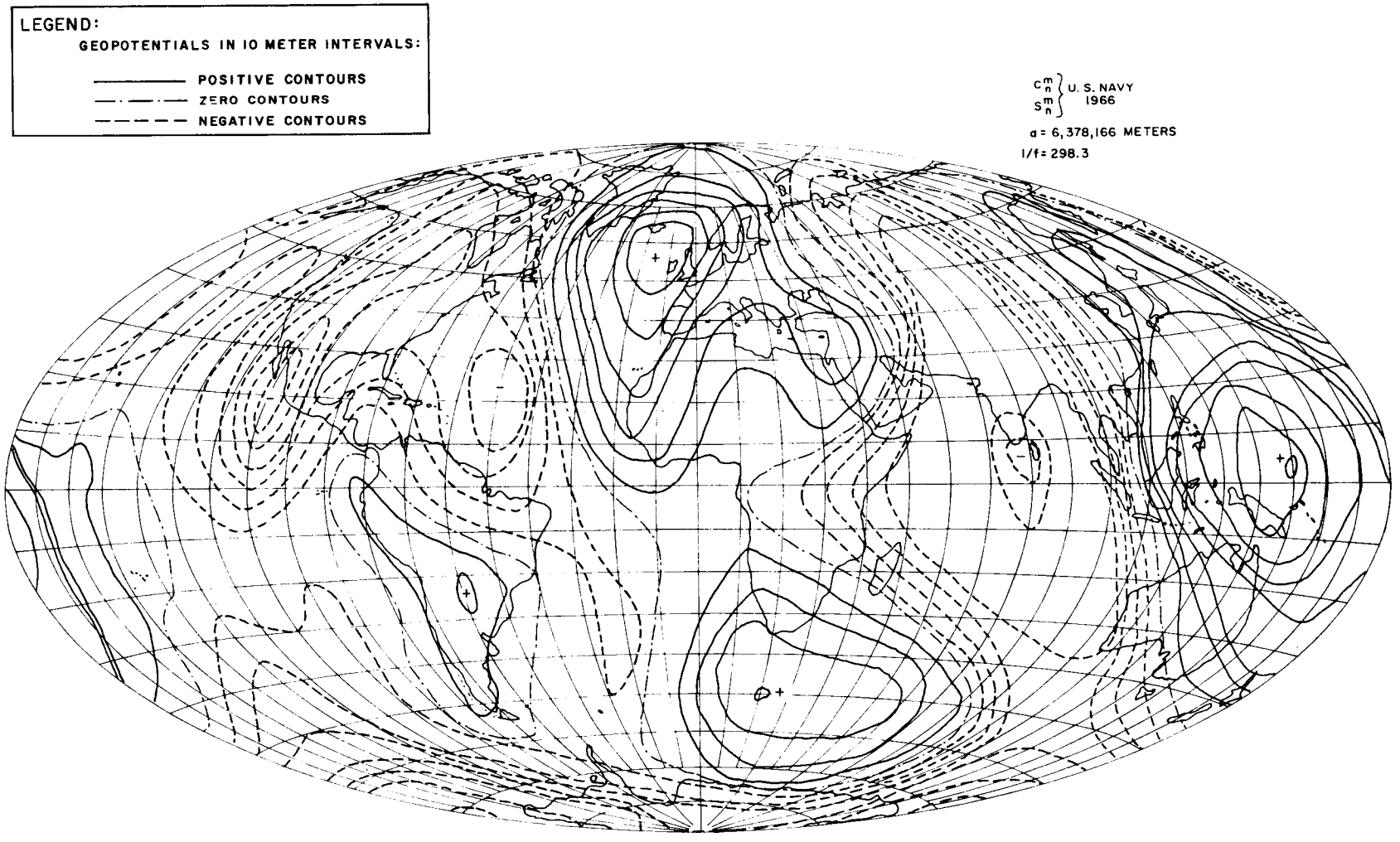

Figure I-2 Geoid, TRANET Data (1966)

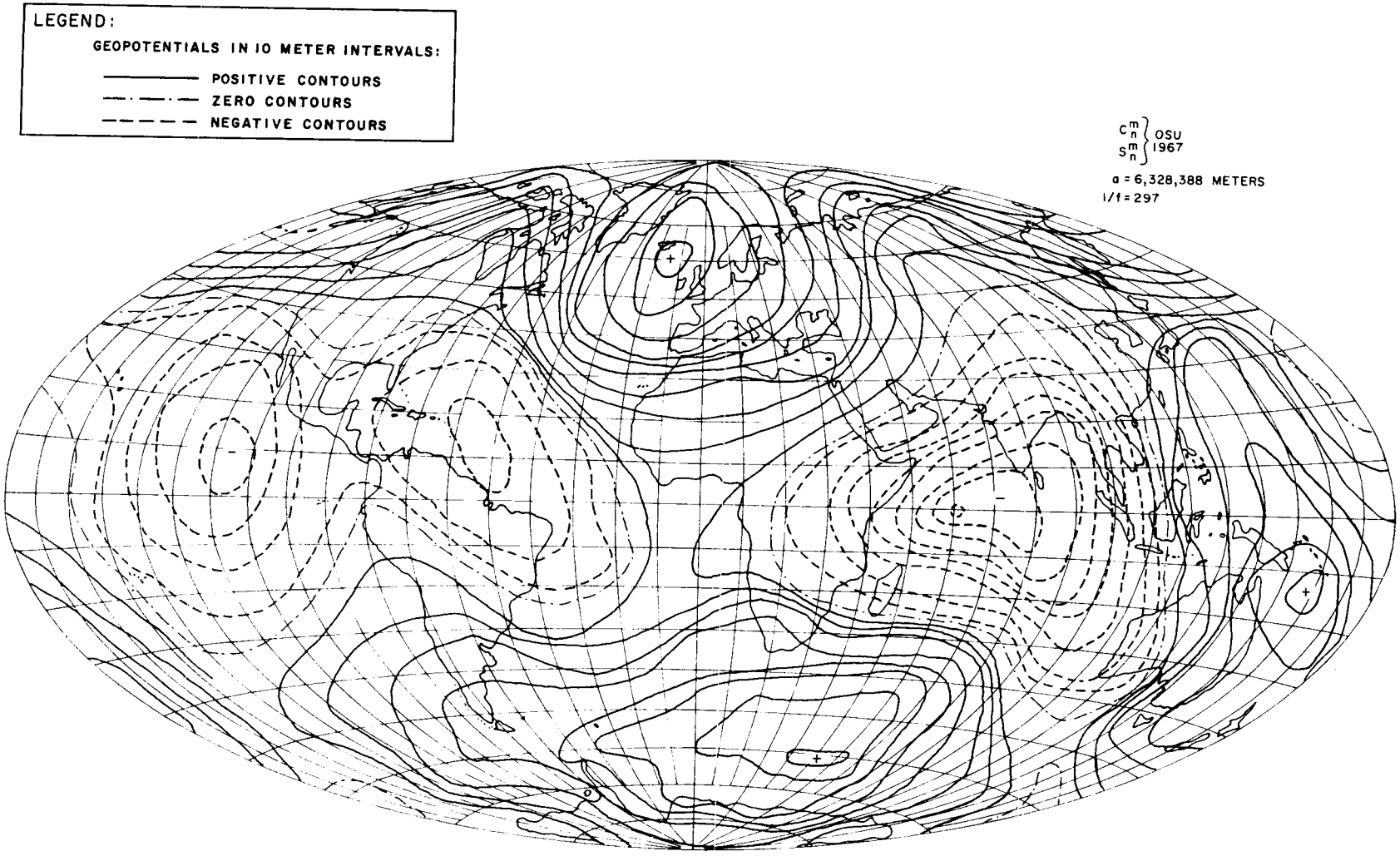

Figure I-3 Geoid, SAO Data (1967)

GEODETIC REFERENCES

1. Kinsman, B., Wind Waves, Prentice-Hall Inc., Englewood Cliffs, New Jersey, 1965

2. Scheidegger, A. E., Principles of Geodynamics (2nd ed.),Springer-Verlag, Berlin, pp. 70-98, 1962

3. Von Arx, W. S., "Level-surface Profiles Across the Puerto Rico Trench", Science 154: 1651-1654, 1966

4. Menard, H. W., Marine Geology of the Pacific, McGraw-Hill Book Co., New York, New York, 1964

5. Shepard, F., Submarine Geology (2nd ed.), Harper and Row, Publ., New York, New York, 1963

6. Schimke, G. R. and Bufe, C. G., "Geophysical Description of a Pacific Ocean Seamount", J.G.R. 73(2): 559-570, 1968

7. Anonymous, Marine Science Affairs, House Document 79, (90th U.S. Congress) Chapter 7, 1967

8. Henriksen, S. W., Personal Memorandum of March, 1968

9. Bjerhammar, A., Private Communication

10. Henriksen, S. W., "Application of Probability Limit Theorems to Measurements", Photogrammetria 22: 5-11, 1967

11. Marine Research Laboratories Technical Report for April 1968 on Satellite Altimetry, Internal Memorandum, SISD, Raytheon, Sudbury, Mass., 1968

12. Izsak, I. G., "Tesseral Harmonics of the Geopotential and Corrections to Station Coordinates", J. Geoph. Res. 69(12): 2621-2630, 1964

13. Anderle, R.J., "Geodetic Parameters Set NWL-5E-6 Based on Doppler Satellite Observations," in "Use of Artificial Satellites from Geodesy - II," (G. Veis, editor), Athens, Greece, 1966.

14. Gaposchkin, E., "Tesseral Ha monic Coefficients and Station Coordinates from the Dynamic Method," Smithsonian A. Obs. Special Report 200 (C. Lundquist and G. Veis, ed.), Volume 2, p. 105, 1966.

GEODETIC REFERENCES
(CONTINUED)

15. Bychkow, Livenel and Selivalof, "Change of Distribution of Wind Waves and Swell Elements in the Tropical Atlantic", Oceanology 5(3): 27-33, 1965

16. Doodson, A. T., "Mean Sea Level and Geodesy", Bull. Geod. 55: 69-88, 1960

17. Rossiter, "Long-term Variations in Sea Level", The Sea, (M. Hill, ed.), Interscience Publ., New York, pp. 590-610, 1962

18. Fairbridge, R., Physics of the Earth, Vol. 4, p. 99, Pergamon Press, London, 1961

19. Fedorov, K., "Equatorial Seiches", Oceanology 5(1): 37-39, 1965

20. Zaytsey, G., "Features of Long-Period Variations of Level and Salinity in the North Caspian Sea", Oceanology 5(2): 69, 1965

21. Rice, D., "Geoidal Section in the U.S.", Bull. Geod. 65: 243, 1962

22. Fischer, I., Technical Report No. 62, Army Map Service, Washington, D.C., 1967

23. Shepard, F., Submarine Geology (2nd ed.), Harper and Row, Publ., New York, New York, 1963

24. Menard, H W., Marine Geology of the Pacific, McGraw-Hill Book Co., New York, New York, 1964

25. Stommel, H., "Varieties of Oceanographic Experience", Science 139: 572-575, 1963

26. Schimke, G. R. and Bufe, C. G., "Geophysical Description of a Pacific Ocean Seamount", J.G.R. 73(2): 559-570, 1968

27. Defant, A., Physical Oceanography Vol. 1, Pergamon Press, N. Y., 1961

28. Roden, G., J. Geoph. Res. 65: 2809, 1960

29. Stommel, H., The Gulf Stream, Univ. of California Press, Berkeley, 1965

GEODETIC REFERENCES
(CONTINUED)

30. Litzin, E. and Pattulo, J., J. Geophys. Res. 66: 845, 1961

31. Newton, C., J. Geophys. Res. 66: 853, 1961

32. Fuglister, F., Progress in Oceanography, Vol. 1, Pergamon Press, London, 1963

33. Anonymous, Marine Science Affairs, House Document 79 (90th U.S. Congress) Chapter 7, 1967

34. Wooster, W., and Reid, J., in The Sea, Vol. 2, pp. 253-280, M. Hill, Editor, Interscience Press, N.Y., 1963

GEODETIC BIBLIOGRAPHY

1. Scheidegger, A. E., Principles of Geodynamics (2nd ed.), Springer-Verlag, Berlin, pp. 70-98, 1962

2. Arx, W. S. von, "Applications of the Gyropendulum, "The Sea," (M. Hill, ed.), Interscience, New York, 1962

3. Baker, C. and Ruppe, H., "Satellite Vehicles," Handbook of Astronautical Engineering, (H. Koelle, ed.), McGraw-Hill Book Co., New York, Chapter 24, pp. 52-53, 1961

4. El'yasberg, P., Theory of Flight of Artificial Satellites, (NASA transl. 1967), pp. 241-245, 1965

5. Arx, W. S. von, "Level-surface Profiles Across the Puerto Rico Trench", Science 154: 1651-1654, 1966

6. Fischer, I., "Present Astro-geodetic Geoid", Bull. Geod. 61: 245-265, 1961

7. Knauss, J., "Equatorial Current Systems", The Sea, (M. Hill, ed.), Interscience Press, New York, 1962

8. Platzman, G. and Rao, D., "Free Oscillations of Lake Erie", Studies in Oceanography 1964, U. of Washington Press, pp. 359-382, 1964

9. Kinsman, B., Wind Waves, Prentice-Hall Inc., Englewood Cliffs, New Jersey, 1965

10. U. S. Naval Oceanographic Office, Atlases of Sea and Swell Charts, H. O. 799B, C, D, E, G, 10712A U. S. Superintendent of Documents, Washington, D. C.

11. Sverdrup, H., Johnson, M., Fleming, R., The Oceans, Prentice-Hall Inc., Englewood Cliffs, New Jersey, 1942

12. Anonymous, Space Planners Guide, U. S. Air Force Systems Command, 1965

13. Munk, W. and Zetler, B., "Deep-Sea Tides: A Program", Science 158: 884-887, 1967

GEODETIC BIBLIOGRAPHY
(CONTINUED)

14. Marine Research Laboratories Technical Report for April 1968 on Satellite Altimetry, Internal Memorandum, SISD, Raytheon, Sudbury, Mass., 1968

15. Henriksen, S. W., "Application of Probability Limit Theorems to Measurements", Photogrammetria 22: 5-11, 1967

16. Bjerhammar, A., Private Communication

17. Izsak, I. G., "Tesseral Harmonics of the Geopotential and Corrections to Station Coordinates", J. Geoph. Res. 69(12): 2621-2630, 1964

18. Gaposchkin, E., "Tesseral Harmonic Coefficients and Station Coordinates from the Dynamic Method", Smithsonian A. Obs. Special Report 200 (C. Lundquist and G. Veis, ed.), Volume 2, p. 105, 1966

19. Henriksen, S. W., Personal Memorandum of March 1968

20. Shepard, F. and Dill, R., Submarine Canyons and Other Sea Valleys, Rand McNally Co., Chicago, Illinois, 1966

APPENDICES

REFERENCES

APPENDIX L-A

ATMOSPHERIC ERROR

The measurement of the range is based on the time interval between the transmitter pulse and the receiver pulse multiplied by the speed of light. The speed of light is dependent on the transmission medium and therefore changes when the atmosphere changes density.

In order to determine to what extent the atmospheric density changes affect the accuracy we have performed an analysis of the change of the speed of light by atmospheric density variations.

The basic equation for the measured range is:

$$R = \frac{c_o \, t}{2n} \qquad \text{(A-1)}$$

where:

c_o = speed of light in vacuum, = 299792.5 km/s
n = refractive index
t = round trip travel time

From the above formula we find by differentiating and setting n = 1, that:

$$\frac{dR}{R} \simeq - \, dn \qquad \text{(A-2)}$$

This formula shows that the index of refraction has to be known to better than one part in 10^6 to obtain an accuracy of 1 meter for a 1000 km range measurement.

A.1 AVERAGE REFRACTIVE INDEX

If the refractive index is not constant along the measuring path, the average value which has to be used in the basic range Equation (A-2) is:

$$n_{avg} = \frac{1}{R} \int_{s=0}^{s=R} n(s)\, ds \qquad \text{(A-3)}$$

The refractive index depends on the composition of the air, temperature, pressure, and in the ionosphere on the free electron density.

A.2 LOWER ATMOSPHERE

The following formula may be used to calculate the effect of the lower atmosphere on refractive index:[9]

$$n = 1 + \frac{\left(2876.04 + 3 \times \frac{16.288}{\lambda^2} + 5 \times \frac{0.136}{\lambda^4}\right) \times 10^{-7}}{1 + \alpha t} \times \frac{p}{760} - \frac{5.5 \times 10^{-8}}{1 + \alpha t} \times e \qquad \text{(A-4)}$$

where:

λ = wavelength in microns

p = barometric pressure, in mm Hg

α = expansion coefficient of gases, $\alpha = 0.003661$

t = temperature, in ^{o}C

e = partial pressure of water vapor, in mm Hg

The formula is accurate to $\pm 2 \times 10^{-7}$ over a temperature range of $-40^{o}C$ to $+50^{o}C$ and a pressure range of 400 to 800 mm Hg.

For $\lambda = .7\mu$ the formula is

$$n = 1 + \frac{298.02\ 10^{-6}}{1 + \alpha t} \times \frac{p}{760} \qquad \text{(A-5)}$$

The term containing e may be neglected, considering that e is in the order of 10 mm Hg and therefore:

$$\frac{5.5 \times 10^{-8}\ e}{1 + \alpha t} = \frac{5.5 \times 10^{-7}}{1} << 10^{-5}$$

As an approximation, the atmosphere is divided into layers where p and t are assumed constant. Equation (A-3) can then be written in the following form:

$$n = \frac{1}{R} \sum n_i R_i \qquad \text{(A-6)}$$

The following values have been calculated, taking the averages of summer and winter conditions:[10]

R_1: 0 to 5 km	$t_1 = -3.4^{\circ}C$	$p_1 = 580$ mm Hg
R_2: 5 to 10 km	$t_2 = -33^{\circ}C$	$p_2 = 300$ mm Hg

Using Equation (A-5):

$$n_1 = 1.0002315$$

$$n_2 = 1.0001342$$

With increasing height, p decreases further and n approaches 1 (one), contributing less than 10^{-6} to Equation (A-3).

A.3 IONOSPHERE

The refractive index in the ionosphere is given by the equation:[11]

$$n^2 = 1 - \frac{\omega_p^2}{\omega\ (\omega \pm \omega_B)} \qquad \text{(A-7)}$$

where ω_p is the plasma frequency

$$\omega_p = \frac{n_o\ e^2}{m\ \epsilon_o} \qquad \text{(A-8)}$$

and ω_B is the frequency of precession of the free electrons in a magnetic field

$$\omega_B = \frac{e\ B_o}{m} \qquad \text{(A-9)}$$

where:

ω = laser frequency, $\omega = 2\pi c/\lambda = 2.72\ 10^{15}$ Hz

n_o = density of free electrons; typical value for the ionosphere is 10^{12} electrons per m^3.

e = charge of an electron = 1.602×10^{-19} As

m = mass of an electron = 9.11×10^{-31} kg

ϵ_o = dielectric constant = 8.854×10^{-12} As/Vm

B_o = magnetic field of earth, typical value 0.3 gauss.

Typical values for ω_p and ω_B are with the above numbers:

$\omega_p \tilde{=}$ 54 MHz

$\omega_B \tilde{=}$ 6 MHz

With Equation (A-7), we obtain:

$$n^2 = 1 - \frac{(5.4 \times 10^7)^2}{2.72 \times 10^{15}\ (2.72 \times 10^{15} \pm 6 \times 10^6)}$$

$$n^2 = 1 - 3.87 \times 10^{-16}$$

and

$$n = 1 - 1.935\ 10^{-16}$$

The influence of the ionosphere on the refractive index is negligible.

A.4 CALCULATION OF THE AVERAGE REFRACTIVE INDEX

The layers in which the atmosphere has been divided are:

0 to 5 km:	$R_1 = 5$ km	$n_1 = 1.0002315$
5 to 10 km:	$R_2 = 5$ km	$n_2 = 1.0001342$
10 to 1000 km:	$R_3 = 990$ km	$n_3 = 1.0000000$

We obtain with Equation (A-6):

$$n_{avg} = \frac{1}{1000} (5 \times 1.0002315 + 5 \times 1.0001342 + 990)$$

$$n_{avg} = 1.0000018$$

The average speed of light along the measuring path is therefore:

$$C_{avg} = \frac{C_o}{n_{avg}} = \frac{299792.5}{1.0000018}$$

$$C_{avg} = 299791.96 \text{ km/sec}$$

This means that if the clock frequency is based on the speed of light in vacuum, a bias will be present of 2 parts in 10^6 in the range measurements. This is about 2 meters for a 1000-km orbit.

A.5 VARIATIONS OF THE REFRACTIVE INDEX

With the total differential of Equations (A-5) and (A-6), the effect of varying atmospheric conditions can be estimated.

$$d_n = \sum \frac{R_i}{R} dn_i \qquad \text{(A-10)}$$

$$dn_i = \frac{\partial n_i}{\partial t} dt_i + \frac{\partial n_i}{\partial p} dp_i \qquad \text{(A-11)}$$

$$0 \text{ to } 5 \text{ km: } \frac{R_1}{R} dn_1 = - (.418 \times 10^{-8} dt_1) + .196 \times 10^{-8} dp_1$$

$$5 \text{ to } 10 \text{ km: } \frac{R_2}{R} dn_2 = - (.216 \times 10^{-8} dt_2) + .196 \times 10^{-8} dp_2$$

If we assume $\alpha t << 1$

Taking variations of pressure and temperature in the lower atmosphere equal to 3 times the difference between summer and winter values, we get

0 to 5 km: $\Delta t = \pm 20^{o}C$ $\Delta p = \pm 20$ mm Hg

5 to 10 km: $\Delta t = \pm 20^{o}C$ $\Delta p = \pm 20$ mm Hg

$$\frac{R_1}{R} \, dn_1 = \pm .084 \, 10^{-6} \pm .040 \, 10^{-6}$$

$$\frac{R_2}{R} \, dn_2 = \pm .044 \, 10^{-6} \pm .040 \, 10^{-6}$$

From this we may conclude that the variations in the atmospheric density introduce an error of 1.5 parts in 10^7, meaning that our measurement accuracy is 15 cm for a 1000 km orbit.

APPENDIX L-B

SEA STATE

In the section on error analysis the statement was made that the centroid of the pulse is independent of the shape of the transmitted pulse. The proof of this statement follows here.

If the transmitted pulse is gaussian in time, we have:

$$E_I(t) = \frac{e^{-t^2/2\sigma_3^2}}{\sqrt{2\sigma_3^2\pi}}$$

where

$E_I(t)$: Energy of the pulse as a function of time

t: The time variable

σ_3: Defines the pulse width

Using τ as a new time variable, the resultant pulse is the convolution of E_I and E_R:

$$\overline{E}_R(t) = \int_{-\infty}^{+\infty} E_I(\tau) E_R(t-\tau)\, d\tau$$

or, for convenience let

$$\overline{E}_R(t) = g(t)$$

$$E_I(t) = f(t)$$

$$E_R(t) = h(t)$$

Then

$$g(t) = \int_{-\infty}^{+\infty} f(\tau)h(t-\tau)d\tau$$

and the centroid is defined as

$$C = \frac{\int_{-\infty}^{+\infty} tg(t)\ dt}{\int_{-\infty}^{+\infty} g(t)\ dt}$$

The integrals can be simplified by a fourier transform in the "ω" plane

$$F(\omega) = \frac{1}{2\pi} \int f(\tau)e^{-i\omega\tau}d\tau$$

$$H(\omega) = \frac{1}{2\pi} \int h(\tau)e^{-i\omega\tau}d\tau$$

Then,

$$G(\omega) = 2\pi F(\omega)H(\omega)$$

and

$$G(\omega) = \int g(t)e^{-i\omega t}dt$$

or

$$G(\omega)\Big|_{\omega=0} = \int g(t)dt$$

Also,

$$G'(\omega)\Big|_{\omega=0} = -i\int tg(t)dt$$

Thus,

$$C = (i)\ \frac{G'(\omega)}{G(\omega)}\Big|_{\omega=0}$$

and

$$G'(\omega) = 2\pi[F(\omega)H'(\omega) + H(\omega)F'(\omega)]$$

$$G(\omega) = 2\pi F(\omega)H(\omega)$$

Then

$$C = i\left\{\frac{F(\omega)H'(\omega) + H(\omega)F'(\omega)}{F(\omega)H(\omega)}\right\}\Bigg|_{\omega=0}$$

$$\boxed{C = i\left.\frac{H'(\omega)}{H(\omega)}\right|_{\omega=0} + i\left.\frac{F'(\omega)}{F(\omega)}\right|_{\omega=0}}$$

Taking the second term

$$i\left.\frac{F'(\omega)}{F(\omega)}\right|_{\omega=0}$$

in which

$$F(\omega)\Big|_{\omega=0} = \int_{-\infty}^{+\infty} \frac{1}{\sqrt{2\pi\sigma_3^2}} e^{-t^2/2\sigma_3^2} e^{-i\omega t} dt\Bigg|_{\omega=0}$$

$$F(\omega) = \frac{1}{\sqrt{2\pi\sigma_3^2}} \int_{-\infty}^{+\infty} e^{-\frac{1}{2\sigma_3^2}\left[t^2 + 2\sigma_3^2 i\omega t\right]} dt$$

$$F(\omega) = \frac{1}{\sqrt{2\pi\sigma_3^2}} \int_{-\infty}^{+\infty} e^{-\frac{1}{2\sigma_3^2}\left\{\left[t + \sigma_3^2 i\omega\right]^2 - (\sigma_e i\omega)^2\right\}} dt$$

$$F(\omega)\Big|_{\omega=0} = \frac{1}{\sqrt{2\pi\sigma_3^2}} \int_{-\infty}^{+\infty} e^{-\frac{t^2}{2\sigma_3^2}} dt = 1$$

and

$$F'(\omega) = \frac{-i}{\sqrt{2\pi\sigma_3^2}} \int_{-\infty}^{+\infty} te^{-\frac{1}{2\sigma_3^2}\left[t^2 + 2\sigma_3^2 i\omega t\right]} dt$$

$$F'(\omega)\Big|_{\omega=0} = \frac{-i}{\sqrt{2\pi\sigma_3^2}} \int_{-\infty}^{+\infty} te^{-t^2/2\sigma_3^2} dt = 0$$

hence

$$i\,\frac{F'(\omega)}{F(\omega)} = \frac{0}{1} = 0$$

So that finally,

$$C = i\,\frac{H'(\omega)}{H(\omega)}\Big|_{\omega=0}$$

where

$$H(\omega) = \frac{1}{2\pi} \int_{-\infty}^{+\infty} H(t)e^{-i\omega t}dt$$

$$H'(\omega) = \frac{-i}{2\pi} \int_{-\infty}^{+\infty} th(t)e^{-i\omega t}dt$$

$$H(\omega)\Big|_{\omega=0} = \frac{1}{2\pi} \int_{-\infty}^{+\infty} h(t)\,dt$$

$$H'(\omega)_{\omega=0} = \frac{-i}{2\pi} \int_{-\infty}^{+\infty} th(t)\,dt$$

Then

$$C = \frac{\int_{-\infty}^{+\infty} th(t)\,dt}{\int_{-\infty}^{+\infty} h(t)\,dt}$$

C therefore depends only on the function h(t) rather than on the convolution g(t). This simplifies the calculation which can now be performed by computer. The computer program for calculating the centroid shift C3 as a function of wave height 2A, wave length L and phase P is given below. S1 and S2 are the σ points on the gaussian curves related to the intensity distribution across the beam and the intensity angle dependence of the return beam respectively.

```
8 PRINT "THE VALUES OF A,L,P,S1,S2 ARE?"
9 INPUT A,L,P,S1,S2
10 PRINT "THE FOLLOWING VALUES ARE IN METERS"
11 PRINT
12 PRINT "WAVE HEIGHT","WAVE LENGTH", "CENTROID SHIFT"
19 LET D = 100
20 LET P1 = 3.14159
21 LET P2 = P1/2
25 LET C1 = 3E8
30 LET R0 = .02
35 LET E0 = 1
45 LET K = R0*E0/(2*S1*S2)
50 LET G = .5*(2*P1*A/(L*S1))↑2
58 LET Q = R = 0
60 FOR M = 0 TO D
70 LET E = 0
80 LET Y = -2*M*A/D+A
90 FOR N = 0 TO 100
100 LET J = N
110 GO TO 145
120 LET J = -N
145 IF (A↑2-Y↑2)=0 THEN 153
150 LET X=(L/(2*P1))*(-ATN(Y/SQR(A↑2-Y↑2))+P+2*P1*J+P2)
152 GO TO 160
153 IF Y>0 THEN 155
154 GO TO 157
155 LET X = L*P/(2*P1)+L*J
156 GO TO 160
157 LET X = L/2+L*P/(2*P1)+L*J
160 LET W = EXP(-(X-L*P/P1)↑2/(2*S2↑2))
165 LET E2 = K*EXP(-G*(A↑2-Y↑2)/A↑2)*(EXP(-X↑2/(2*S2↑2))+W)
170 LET E = E2+E
180 IF (E2/E)<1E-5 THEN 220
190 IF J>0 THEN 120
200 NEXT N
220 LET Q = Q+E
230 LET R = R+(4*M*A/(C1*D))*E
240 NEXT M
250 LET C = R/Q
251 LET C3 = 1.5E8*(2*A/C1-C)
260 PRINT A,L,C3
300 END
```

LASER REFERENCES

1. Formation and Characteristics of Giant Pulses in Optical Masers. D.V. Missio and K.N. Seeber, ALTA FREQUENZA. N. Vol. XXXIV 1965, Pg. 69E-323.

2. Study and Design of a Spaceborne Laser Altimeter System. FINAL REPORT, Vol. I, Contract No. NAS8-21013.

3. Sea Echo at Laser Wavelength. A.V. Jelalian, Proceedings of the IEEE, Vol. 56, No. 5, May 1968, pg. 828.

4. Doppler Optical Navigator, FINAL REPORT, Contract No. AF33(615)-3892.

5. Slopes of the Sea Surface Deduced from Photographs of Sun Glitter, C. Cox and W. Munk, Bull. of the Scripps Institution of Oceanography of the Univ. of California, Vol. 6, No. 9, pg. 401-488.

6. Ocean Wave Statistics, N. Hogben, F.E. Lumb, Ministry of Technology, National Physical Laboratory, Her Majesty's Stationery Office, 1967.

7. "Transmission and Scattering of Infrared Radiation by Clouds," E.M.I. Report 1963.

8. Handbook of Military Infrared Technology, pp. 119-121.

9. Barrell, H. and Sears, J.E., The Refraction and Dispersion of Air for the Visible Spectrum, Phil. Trans. Royal Soc., London, Series A/1939, pp. 238.

10. Hodgman, Ch. D., Handbook of Chemistry and Physics, 34th Edition 1952-1953, pp. 2875.

11. Jackson, J.D., Classical Electrodynamics, 1962, pp. 226 to 229.

APPENDICES

REFERENCES

APPENDIX R–A

WAVEFORM ANALYSIS

A.1 RADAR-TO-EARTH GEOMETRY

The radar-to-earth geometry is shown in Figure A-1. A radar pulse of length $\hat{t}$ intercepts the sea surface at the vertical incidence point and spreads radially outward from this ground zero point. The following relationships hold for the small angle ($\hat{\theta}$) case:

$$\hat{h} = \frac{c\hat{t}}{2} = \frac{R_g^2}{2h^-} = \frac{\hat{\theta}^2 h^+}{2} = \text{pulse range or equivalent depth of penetration} \qquad \text{(A-1)}$$

$$\hat{\theta} = \frac{R_g}{h} = \sqrt{\frac{c\hat{t}}{h^+}} = \sqrt{\frac{2\hat{h}}{h^+}} = \text{half ground angle of pulse} \qquad \text{(A-2)}$$

$$\hat{t} = \frac{R_g}{2h^-} = \frac{2\hat{h}}{c} = \frac{\hat{\theta}^2 h^+}{c} = \text{transmitted pulse length} \qquad \text{(A-3)}$$

where:

h = satellite altitude

$h^+ = h(1+\frac{h}{r_e})$ = positive curved earth compensated altitude

$h^- = h(1-\frac{h}{r_e})$ = negative curved earth compensated altitude

r_e = radius of Earth

R_g = ground range to pulse edge

Also:

$$\hat{A} = \pi R_g^2 = \pi c h^- \hat{t} = 2\pi \hat{h} h^- = \pi h \hat{\theta} = \text{area of target circle} \qquad \text{(A-4)}$$

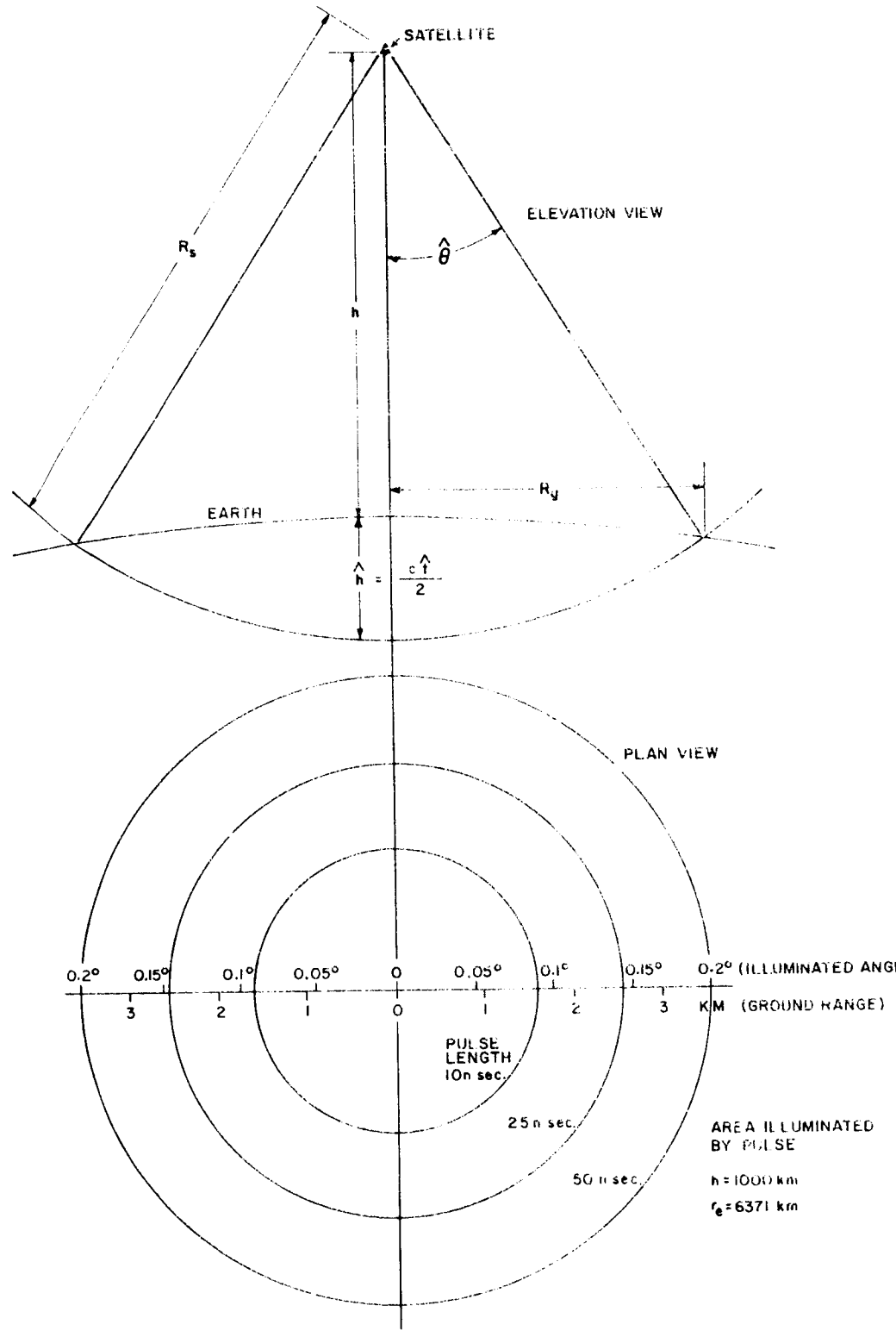

Figure A-1 Radar to Earth Geometry

The doppler bandwidth of the received signal, (f_d), depends on the radar frequency (f), pulse angular radius ($\hat{\theta}$), and vehicle orbital velocity (v_o), and to a slight degree the vertical component of sea-state velocities v_s; thus

$$f_d = \frac{2v_o f\hat{\theta}}{c} \pm \frac{2v_s f}{c} \qquad \text{(A-5)}$$

The relationships between angles, pulse time, and doppler frequency is shown in Figure A-2.

Values of v_o vs vehicle altitude are shown in Table A-1.

TABLE A-1

VALUES OF V_o vs VEHICLE ALTITUDE

h (km)	h (SM)	h (NM)	v_o (km/hr)	v_o (km sec)
800	496	432	26842	7.46
900	559	486	26657	7.41
1000	621	540	26475	7.36
1100	684	595	26300	7.31
1200	745	648	26128	7.26
1300	807	702	25960	7.21
1400	870	755	25790	7.16
1500	931	810	25622	7.12

For these altitudes and for a 50 ns pulse, doppler frequencies to about 1600 cps require consideration at X-band. These doppler frequencies are needed for estimating transmitter power requirements for phase tracking purposes.

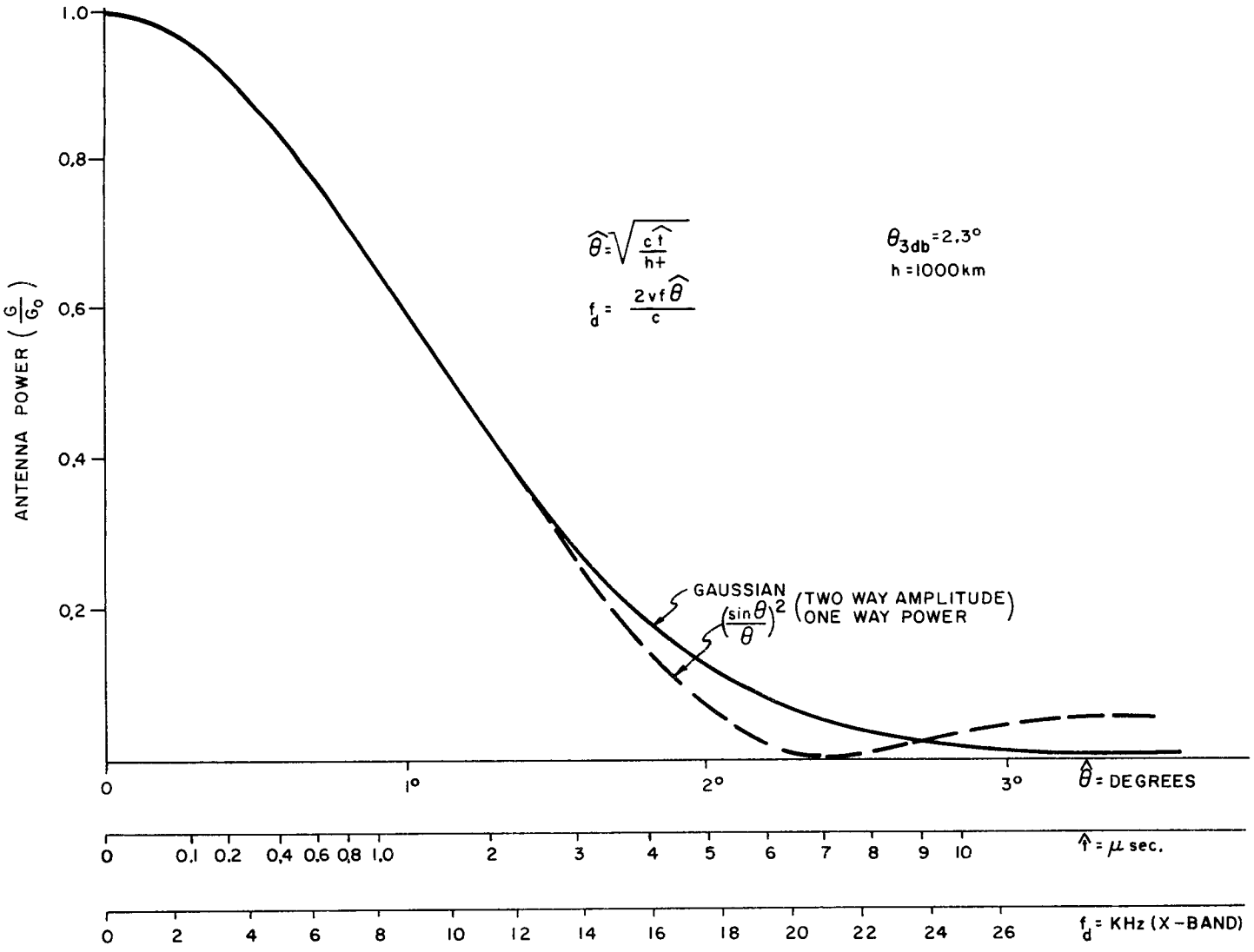

Figure A-2 Gaussian Antenna Pattern

A.2 RECEIVED WAVEFORMS FROM SEA SURFACE TARGETS

The sea-state free radar return signal waveform from the sea-surface can be obtained by integrating elemental returns over the target area as functions of antenna gain, reflection coefficients, and slant range vs time. If the power impulse response, or received waveform from a transmitter pulse of zero duration can first be obtained, then the return for any other transmitted pulse can be found by convolving the power impulse response on the transmitted power waveform.

The return from an elemental target area (dA) can be obtained from radar range equation parameters, thus

$$dP_r = \frac{P_t G^2 \lambda^2 (\sigma_o \, dA)}{(4\pi)^3 R_s^4} \qquad (A-6)$$

As a function of target element angle off vertical ($\hat{\theta}$) the terms may be grouped, thus:

$$dP_r(\hat{\theta}) = \frac{K \times G^2(\hat{\theta}, \phi) \; \sigma_o(\hat{\theta}) \; R_g dR_g d\phi}{R_s^4(\hat{\theta})} \qquad (A-7)$$

where:

K = angle independent terms

R_g = ground range of element from vertical ground zero

$\hat{\theta}$ = element angle off vertical $\approx \frac{R_g}{h}$

ϕ = element azimuth angle.

The plan view of Figure A-1 shows the geometry of a transmitted impulse striking ground zero then progressing radially outward describing successive concentric rings, each having elemental area $dA_o(\hat{\theta})$. By differentiating equation (A-4), this elemental area is found to be:

$$dA_o = \pi h\, d\hat{\theta} = \pi ch\, d\hat{t}; \text{ (area of elemental circle)}$$
$$= \text{constant} \qquad \text{(A-8)}$$

It can be seen from this equation that for a pulse of constant duration or elemental length ($d\hat{t}$) the elemental (or incremental) area (dA_o) is also constant. As the radius and circumference increases the radial element becomes correspondingly narrow, giving a resulting area which remains constant.

The impulse response is the return from these elemental circular target areas expressed as a function of time, i.e., by substituting from (A-2):

$$\hat{\theta} = \sqrt{\frac{c\hat{t}}{h}} \qquad \text{(A-9)}$$

Again collecting all angle independent parameters, including dA, into the constant K gives from (A-7):

$$\delta(\hat{\theta}) = \frac{K\, G^2(\hat{\theta})\, \sigma_o(\hat{\theta})}{R^4(\hat{\theta})} \quad ; \text{ (impulse response vs } \hat{\theta}) \qquad \text{(A-10)}$$

All three of the angle dependent parameters, namely $G^2(\hat{\theta})$, $\sigma_o(\hat{\theta})$, and $\frac{1}{R^4(\hat{\theta})}$, can be approximated to well within the accuracies required for this analysis by the gaussian forms:

$$G^2(\hat{\theta}) \approx \exp\left[-k_1\left(\frac{\hat{\theta}}{\theta_a}\right)^2\right]; \quad \text{see Figure A-2}$$

$$\sigma_o(\hat{\theta}) \approx \exp\left[-k_2\left(\frac{\hat{\theta}}{\theta_\sigma}\right)^2\right]; \quad \text{see Figure A-3}$$

$$P_R(\hat{\theta}) \approx \frac{1}{R^4(\hat{\theta})} \approx \exp\left[-k_3\left(\frac{\hat{\theta}}{\theta_r}\right)^2\right]; \quad \approx \cos^4(\theta) \text{ form.}$$

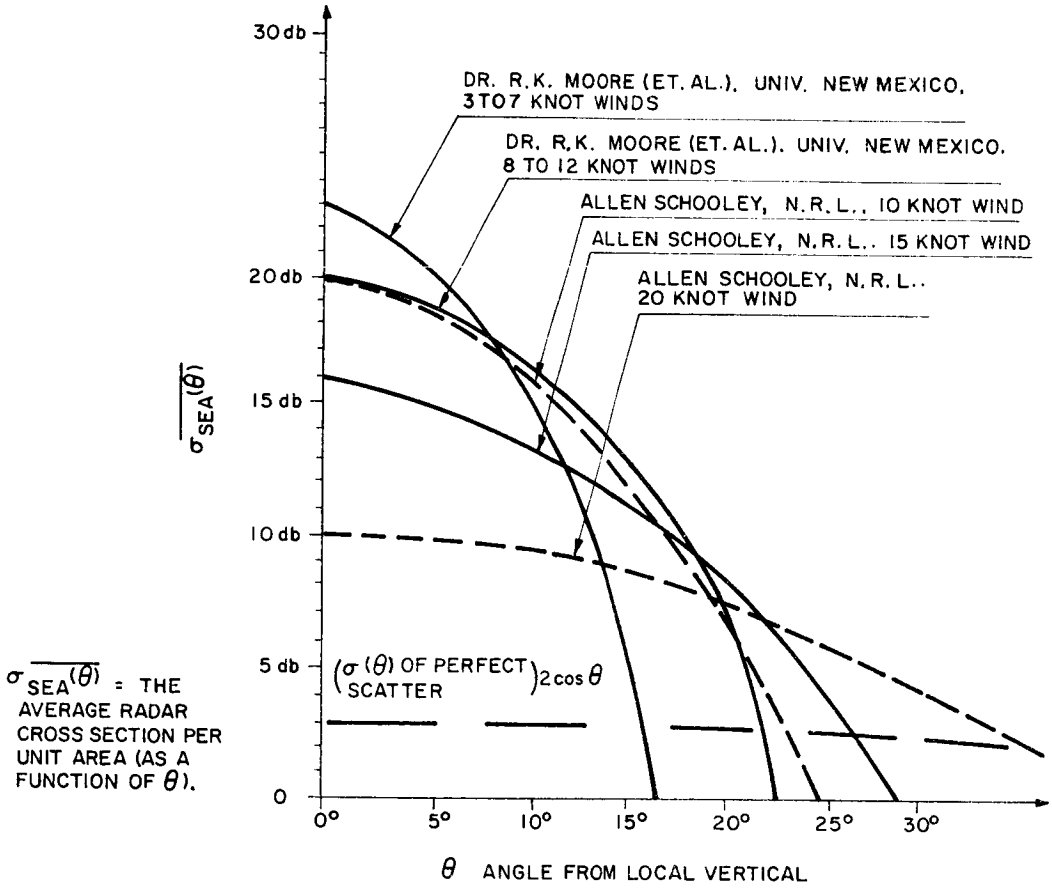

Figure A-3 Average Radar Cross Section Per Unit Area From Ocean Plotted as a Function of Angle of Incidence, θ[17].

The combined product term is again gaussian and can be written:

$$G_T(\hat{\theta}) \approx \exp\left[-k_T \left(\frac{\hat{\theta}}{\theta_T}\right)^2\right] \qquad \text{(A-11)}$$

where:

$$\frac{1}{\theta_T^2} = \frac{1}{\theta_a^2} + \frac{1}{\theta_\sigma^2} + \frac{1}{\theta_R^2} \qquad \text{(A-12)}$$

Now, substituting (A-9) into (A-11) to obtain the impulse response vs time gives:

$$\delta(\hat{\tau}) = K \exp\left(-\frac{k_T\, c\hat{\tau}}{\theta_T^2\, h}\right) \qquad \text{(A-13)}$$

If all θ's are defined with respect to 3 dB widths, the same as is commonly done for antenna beamwidths, then k_T can be evaluated vs θ_T^2 as 3 dB combined widths giving:

$$k_T = 2.77$$

Since only waveform is of interest here and absolute amplitude is irrelevant, the constant group parameter (K) can be equated to unity, giving a very simple form to the impulse response, thus,

$$\delta(\tau) = e^{-\left(\frac{2.77\ ct}{\theta_T^2\ h}\right)} = e^{-\frac{t}{\tau}} \quad ; \text{ impulse response} \qquad \text{(A-14)}$$

Where τ is the impulse response decay time constant given by:

$$\tau = \frac{\theta_T^2\ h}{2.77\ c} \quad ; \text{ impulse decay time constant.} \qquad \text{(A-15)}$$

It can be seen that the impulse response is a decaying exponential whose decay time constant depends on altitude (h) on antenna beamwidth (θ_a), and on reflection coefficient (σ_o), i.e., its 3 dB decay angle (θ_σ). Estimates can be made of the sensitivity of τ to the respective variables by use of the error form for (A-15) giving:

$$\frac{d\tau}{\tau} = \frac{dh}{h} = \frac{2d\theta_T}{\theta_T} \qquad \text{(A-16)}$$

Thus, a 1% change in altitude gives a 1% change in time constant, and a 1% change in beamwidth (θ_T) gives a 2% change in time constant. This form is used in the accuracy analysis (Section 4.4.1) to indicate the corresponding altitude errors which might be expected from changes in τ. In any event altitude errors are small when $\frac{\hat{t}}{\tau} \ll 1$, and can be corrected vs known altitude or σ_o changes to give negligible residual errors.

The problem of obtaining impulse responses is very much more complicated where the antenna beam is off vertical giving varying antenna gain around the elemental circle of integration. In this case, no simple analytic solution is apparent as was obtained for the symmetrical case just presented. Instead a computer program was set up in which incremental returns were integrated over the beamwidth to give the resulting impulse time function (see Section A.1).

It was found that for small off-vertical beam displacements the effect was an apparent change in impulse time constant. For larger displacements, initial amplitudes are reduced and maximums occur at times corresponding to the element intercept with the antenna center point or maximum gain point.

Corresponding satellite stabilization accuracy requirements are obtained on the basis of this off-vertical waveform analysis. Altitude errors are negligible for vertical angle displacements of 15% of the antenna beamwidth. Errors start to become significant at about 20% and climb rather rapidly as percent angular displacements become progressively large.

Further analysis of received waveforms from real transmitted pulses of extended duration can be made by resorting to network analogy. The sea surface can be considered to be replaced by a network having the same impulse response. Since the sea surface impulse response $[\delta(\hat{t})]$ was found to be a decaying exponential, it can be replaced by an RC low-pass filter having the same time constant. A low-pass filter of this form is known to act as an integrator to pulses which are short compared to the time constant. The sea surface can therefore be considered to be an integrator over the interval $\hat{t} << \tau$. Note that powers, not amplitudes, are convolved in this analysis.

On this basis the response of the clutter-free, sea-state free sea to a short rectangular pulse is seen to be a "ramp step", i.e., a ramp with an initial and final break occurring at the leading and trailing edge of the rectangular pulse, and the same waveform as would be obtained by integrating the rectangle. Waveforms are shown in Figure A-4. The effects of Rayleigh clutter and sea-state are discussed in Section A.9 as a separate consideration.

Similarly, the return from a short gaussian shaped transmitted pulse comes back as an error function waveform obtained from integrating the gaussian pulse. The eventual decay of the signal tails back toward zero occurs over the time constant τ and has long-time significance, such as determining prf rates when it is desired to have reasonably small amplitudes or decay to near zero-level before another waveform is initiated.

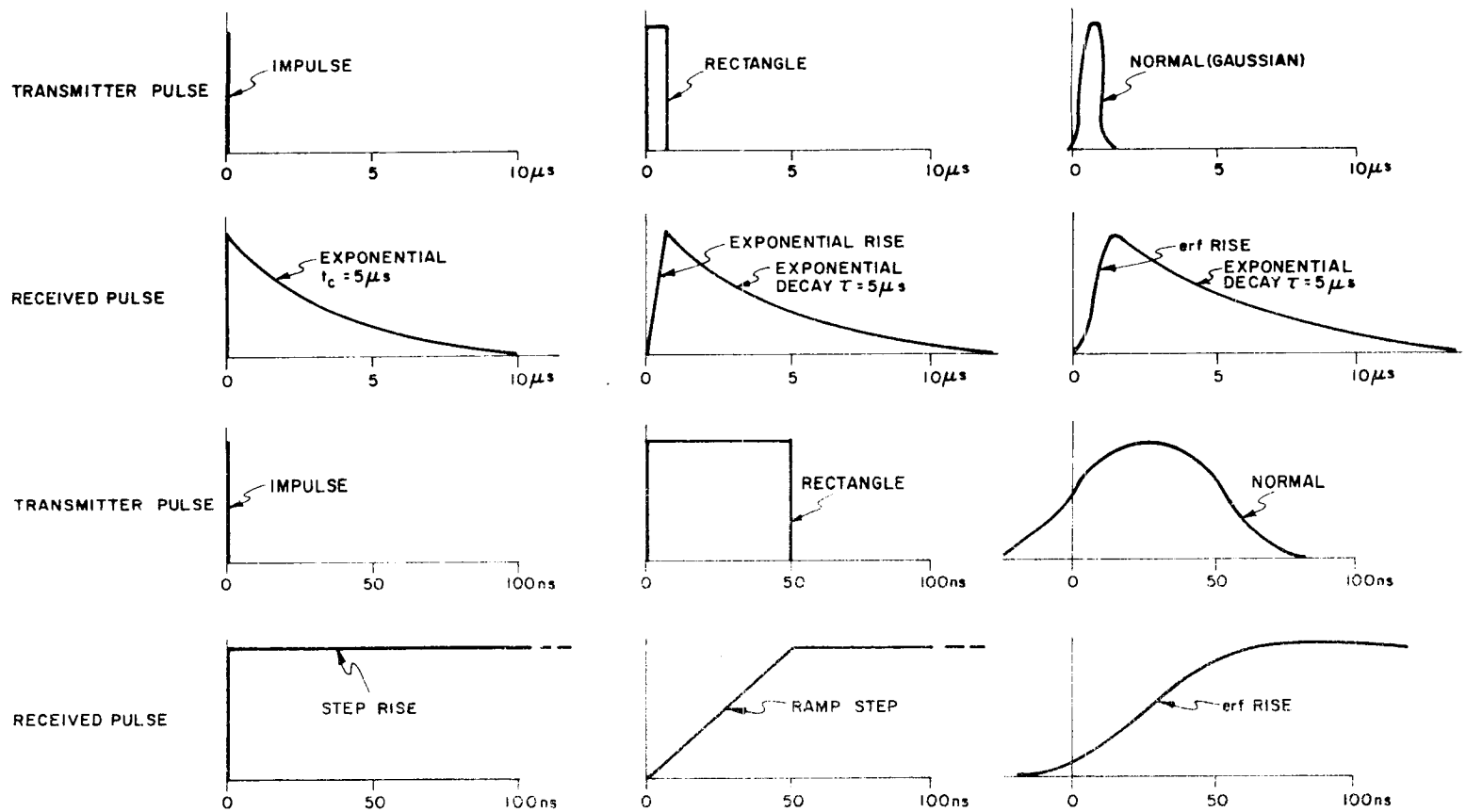

NOTE: The two top rows show pulse on a compressed time scale to emphasize overall pulse showing extended trailing edge decay.
The two bottom rows have an expanded time scale to show leading edge detail.

Figure A-4 Transmitted and Received Power Waveforms

The same analysis holds for the large antenna case except that in this case the decay time constant obtained from equation (A-15) is extremely short, possibly in the vicinity of 1 ns. By the corresponding network analogy the integrator time constant is now so short that $\hat{t} >> \tau$, instead of the opposite condition that held for the small antenna. Now the return signal is nearly unchanged by the sea surface target curvature giving almost no pulse stretching or integration.

Samples of returns from impulses and extended pulses are shown in Figure A-4 on time scales commensurate with both $\hat{t}$ and τ.

A.3 TRANSMITTER WAVEFORMS

Several candidate waveforms have been examined in selecting the waveform best suited to the particular geometry and accuracy requirements of our system. These waveforms initially classified as either continuous wave (cw) or the short pulse types.

The cw types include fmcw, noise modulated cw or multiple sine wave modulated cw. The primary objection of the cw type altimeters is the severe transmitter-receiver imposed isolation problem that becomes a gating item at the long ranges of the satellite borne altimeter where free space attenuations are very high. Rain and cloud backscatter must also be considered. Rain and cloud backscatter is integrated over the illuminated volume of the radar signal and is particularly large with cw waveforms, which generate backscatter contributions over the entire range whereever scatterers occur. Since the T-R isolation and backscatter problems are not readily resolved, the short pulse types seem more appropriate for the long range geometry involved.

The short pulse types may be classified under the headings of pulse-compression or simple pulse types. The pulse compression types include pseudo-random noise, pulse-code modulation forms with video compression, chirp waveforms with i-f compression, and a wide variety of forms combined with frequency or phase shift keying, pulse position, pulse duration, or pulse amplitude modulation forms.

The primary advantage of pulse compression over conventional pulse radar is the trade-off in duty cycle or pulse length vs pulse peak power with small loss in resolution or accuracy. For long range radars, transmitter energy is sometimes peak power limited so that improved S/N performance can be obtained only by increasing pulse length or prf. Increasing pulse length need not be accompanied by reduced spectral bandwidth if complex waveforms such as chirp or PRN codes are used where bandwidth is independent of pulse length.

The disadvantages of pulse compression are similar to the disadvantages of cw systems except in degree. They increase the T-R isolation problem and the backscatter problem, plus introducing a certain amount of complexity, weight and power which may be serious.

The possibility exists that pulse compression techniques can be developed which will be capable of extending transmitter duty cycles to near 50% thereby permitting the use of solid-state transmitters. If studies indicate that side lobe characteristics are not objectionable and if circuit complexity is not prohibitive, then pulse compression for this system is recommended.

High prf as an alternative to pulse compression, is limited by two factors: (1) range ambiguities and (2) pulse-to-pulse overlap between successive pulses when antenna broad beamwidths are employed. The range ambiguity problem is not serious since coarse altitude information is always available from tracking stations. This coarse altitude information would permit prf as high as 1 MHz or higher except for other prf considerations. The pulse-to-pulse overlap problem requires that pulses should not succeed each other at a rate greater than about two decay time constant (2τ) intervals. This constraint limits the prf to about 100,000 pps, the value which has been selected for this system.

The high prf system has other advantages. It makes possible the use of a coherent detector giving a linear output and constant waveforms independent of changes in signal-to-noise in the received signal. This linearity is an important accuracy consideration as will be shown later. At low prfs, lower than the doppler bandwidth, the phase of successive signals changes so rapidly that it becomes impossible to phase track. At 100 kHz however, good phase tracking is possible and detector errors can then be sharply reduced.

Furthermore, the use of the altitude-locked prf oscillator is aided by the high prf rate. Pulse-time discriminator errors are sampled at higher rates giving smaller per sample errors with better smoothing because of the much larger amount of error data processed.

The problem of transmitter-receiver isolation is eliminated by providing synchronized interlace of the transmit-received signals. Since the transmitter pulse is always generated at the positive-going axis-crossing of the prf oscillator sine wave, and since the pulse-time discriminator gate is generated at the negative-going axis crossing, then no interference can result since the transmitter is always off when the target echo signal is being received.

A pulse length has been selected that is long enough to give good sea-state immunity and short enough to give good accuracy. For good sea-state immunity the pulse length $(\frac{c\hat{t}}{2})$ should be longer than the expected wave heights by approximately a 3:1 ratio. This ratio allows extreme crest and trough altitudes to be accommodated on the linear ramp region. For 20 knot winds, wave heights of about 3 meters can be expected. A 50 ns pulse will accommodate about 7.6 m (25 ft) wave heights and provides a reasonable margin over the 3 meters expectation. On the other hand, the 50 ns pulse is short enough to give immunity to such time constant changing variables as altitude σ_o vs sea-state, and beam vertical pointing error. It provides a short (7.6 m) time base for good timing accuracy vs noise and it has a doppler bandwidth

over the pulse footprint angles small enough to permit adequate phase tracking in the coherence tracking circuit. The 50 ns pulse provides no overall accuracy limitation and on this basis, appears to meet system requirements.

A.4 PROCESSOR WAVEFORMS

The function of the processor as applied to this particular system is to modify the received signal waveform in a manner which defines a precise timing point on this waveform. The primary objective is to obtain timing accuracy. A final processed waveform is sought which will be as immune as possible to such waveform degrading effects as receiver noise, sea clutter, and sea state. It should also be as immune as possible to signal strength variations, to small waveform variations such as results from altitude changes or vertical misorientation of the antenna beam, and to component aging or instability variations.

For the idealized noise, clutter, and sea-state-free case from a square-law detector, the leading edge of the processor input signal waveform can be described as a ramp step, having a ramp length equal to the length of the transmitted rectangular pulse length. This extended ramp region has no precise timing point except for the two break points which are not suitable for range tracking. These breakpoints are also extremely sensitive to sea-state. Leading edge tracking therefore, as applied to the ramp step, does not provide accurate timing. A specific point on the leading edge must be defined or referenced by the processor.

The question of sea state immunity has been examined rather carefully and has been found to be contingent on the shift of the centroid of the sea state impulse response (see Appendix G) vs change in sea state and on the length of the leading edge ramp compared to wave height.

Literature search to date has yielded almost no information on the forms and variations to be expected in the electromagnetic impulse response (also called Green's function, the spreading function or the weighting function) at vertical incidence vs sea state. Of particular interest is the possible shift in centroid of this response function vs sea state. Information obtained from Raytheon's Marine Research Laboratory indicates nearly zero shift in centroid as sea state increases from zero to 20 knots wind, corresponding to the range of values over which white caps and spray effects can probably be ignored. On the hypothesis that the centroid does not shift, the zero axis crossing point also does not shift and tracking continues to be with respect to calm sea surface levels as though disturbances were not present. No bias shift upward or downward vs sea state occurs.

The second contingency requires that sea-state should not be so high that the impulse response does spread out over a peak-to-trough distance greater than the linear ramp region in the vicinity of the zero axis crossing point. A 50 ns ramp will accommodate wave heights of about 7.6 meters. Since mean waveheights seldom exceed 2.5 meters (see Figure A-5) it becomes evident that a very high percentage of data can be processed without significant error. In the rare cases where sea state is so high as to introduce possible error, it is possible to either eliminate this suspect data on the basis of signal strength information indicating rough sea, or to make appropriate corrections provided extensive measurements have been made to permit corrections to the desired accuracy.

A.5 DELAY DIFFERENCING

The process of obtaining the desired axis crossing waveform from the received ramp step is similar to two stage differentiation except that differentiation assumes infinitesimal delay whereas delay differencing assumes some finite, convenient delay. The first delay-differencing stage is introduced to take care of the integrating affect of the sea target and the second to obtain a doublet type waveform with

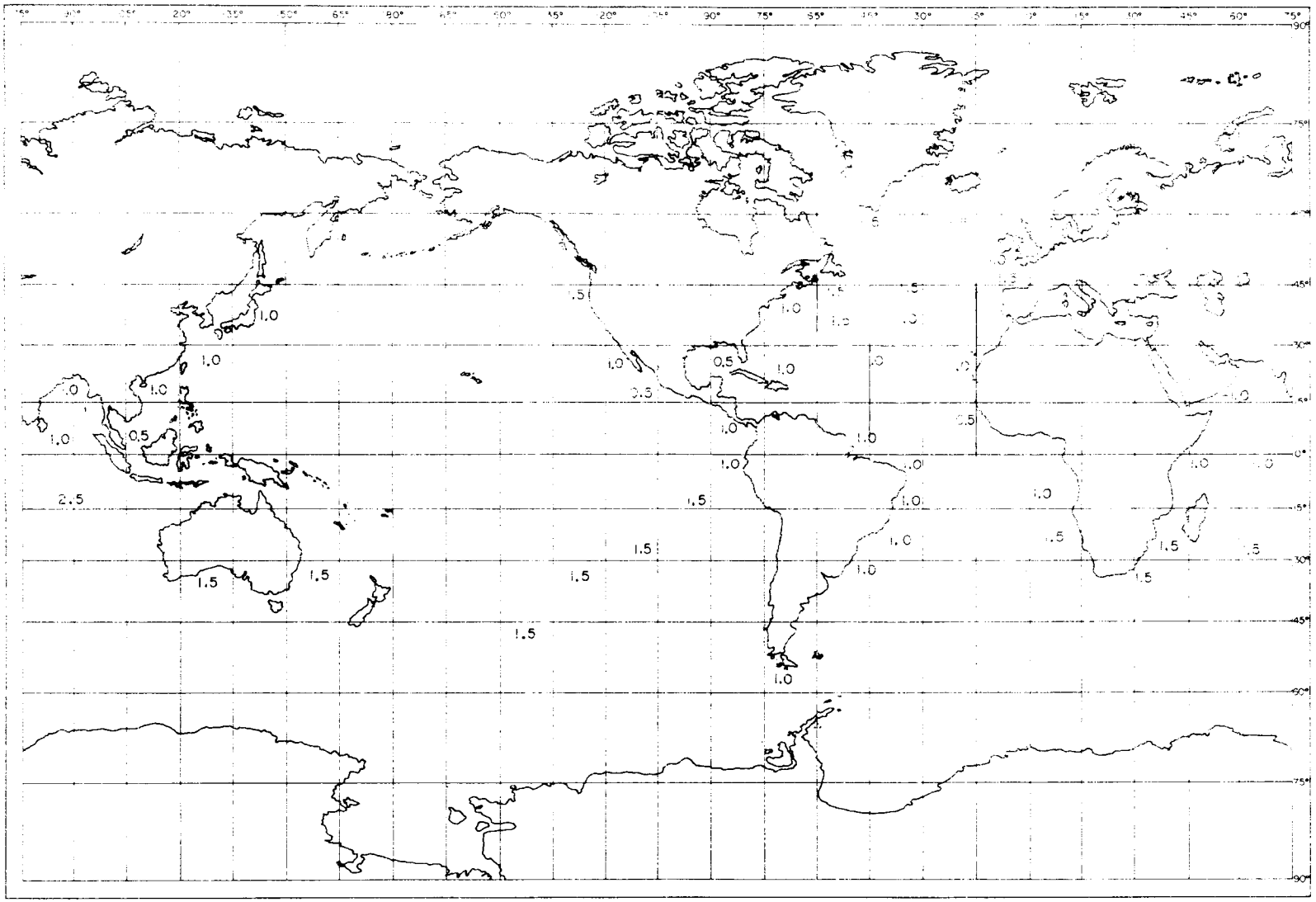

Figure A-5 Median Wave Height (Meters), All Seasons

the axis crossing center point positioned as desired for accurate timing. Straight differentiation is not entirely satisfactory since realistic RC differentiators yield undesirable waveform distortions and signal attenuations. Most of the differentiator objections can be avoided by delay differencing, i.e., subtracting an appropriately delayed signal from the undelayed counterpart. This delay differencing provides better waveform control and greater processing flexibility without the waveform and S/N degradation which is normally accompanied with differentiation.

Figure A-6 shows the idealized waveforms through the two-stage delay-differencing processor. It must be repeated that these are the waveforms which would be expected from sea-state-free, clutter-free, noise-free signals from a square-law detector when an ideal rectangular pulse is transmitted. Since the processor is a linear network (linear in the network sense in that separate signals do not interact to generate intermodulation products), then superposition holds and the final result can be obtained by handling the noise-free signals and the signal-free noise waveforms separately, then adding these separate outputs to obtain the combined output.

The top line of Figure A-6 shows the received ramp step with a delay inverted replica superimposed. This first stage delay differenced output yields the triangle waveform shown on the second line. The second-delay-differencing stage yields the doublet or discriminator-like waveform with the zero-axis crossing point centrally located giving the precise timing point as desired.

A.6 OPTIMUM PROCESSING

It may be appropriate at this point to discuss optimum processing relative to the processor just described. Optimization is usually with respect to some single consideration such as accuracy vs S/N only and may not be optimum in all other respects. Skolnik[1*] describes an optimum processor consisting of a matched filter followed by a differencing circuit. The matched filter optimizes the S/N ratio and the differencing gives an axis crossing waveform with optimum slope.

*Reference 1, Page 465

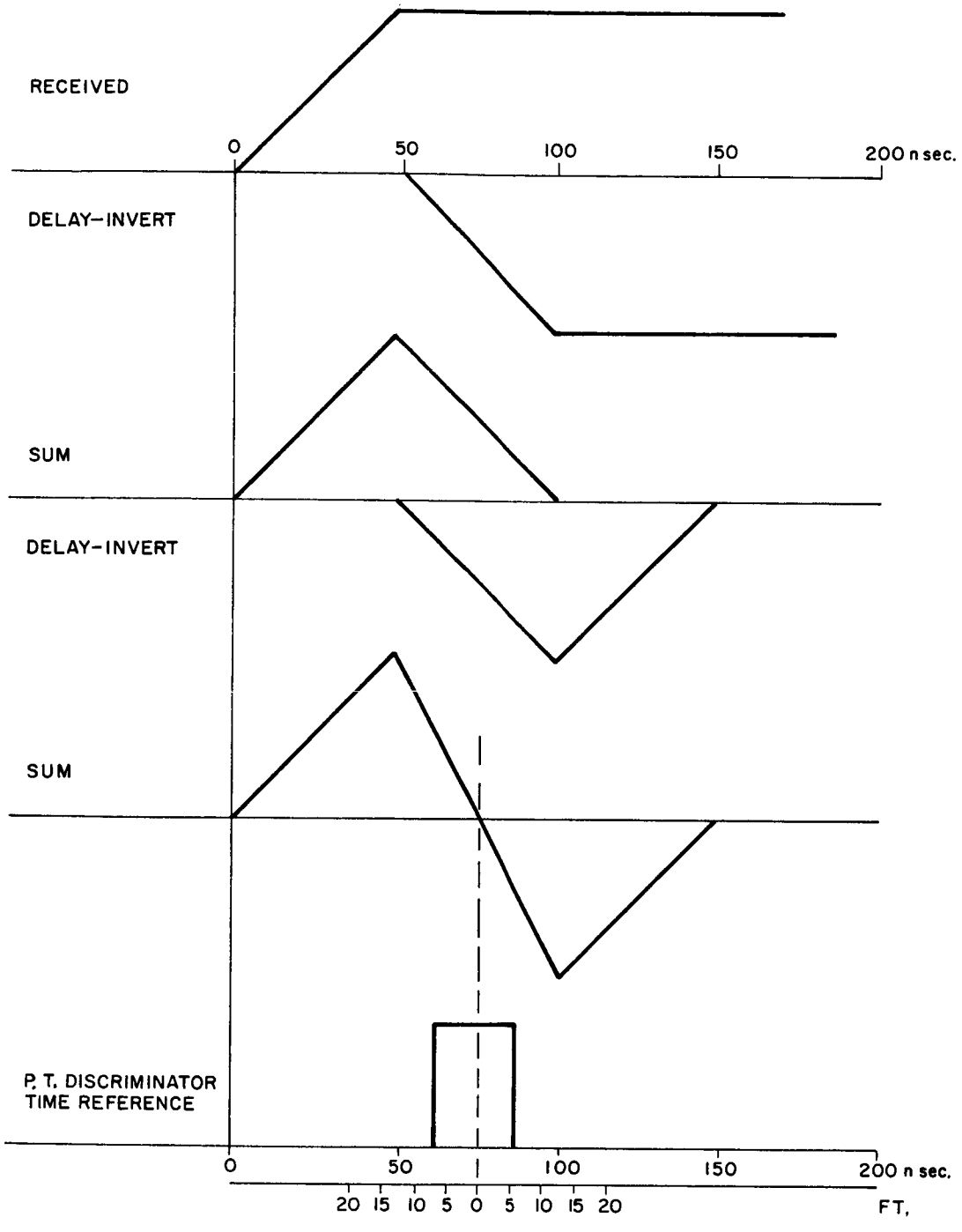

Figure A-6 Processor, Waveforms (Idealized, Noise and Clutter Free, using Square-Law Detector

The objection to this type processing for our system is that it integrates signal energy over the entire return pulse region including the long tails which are sensitive to time constant variations. It is preferable to use only information near the ramp step where maximum accuracy information is concentrated and where minimum waveform variation errors occur. The matched filter for the overall received waveform is not optimum except vs receiver noise. It is not optimum with respect to time constant variations.

An analysis of processor accuracy performance can be carried out by comparing the $f_o \sqrt{S/N}$ products before processing with the same product after processing. Optimum processing (matched-filter-differencing) maximizes this product but is approximately equaled in performance by the delay-differencing processor including the pulse-time discriminator gate used in our system. Matched filtering increases S/N ratios without greatly changing the cut-off frequency. On the other hand, the two stage delay differencing circuits give a waveform having much extended f_o but accompanied by some reduction in S/N ratio. The net result shows no great $f_o \sqrt{S/N}$ preference between the two processors, but does permit choice to be made on the basis of circuit simplicity, time constant and sea-state immunity considerations. The sea-state immunity consideration requires further discussion.

A.7 EFFECT OF SEA-STATE ON PROCESSOR WAVEFORMS

The effect of sea-state on the idealized processor waveform can be found by convolving the electromagnetic impulse response or spreading function of the sea-state on the idealized sea-state free waveform, as explained later in this section. Constraints imposed are that the electromagnetic impulse response be obtained at vertical incidence for a curvature-free sea surface. Also that the sea sample which reflects the electromagnetic impulse be large enough to eliminate nearly all pulse-to-pulse variation in response, i.e., infinitely large sample size is to be taken.

Convolution may appear intuitively plausible as an application of the principal of superposition. The reflected waveform from a transmitted impulse can be obtained by adding successively the separate responses from each element of the sea-state surface. The highest wave crests may be taken as the first element encountered by the impulse. The elemental response for high crests alone, taking into account curvatures of both the earth and beamwidth, will be found to have the same idealized doublet waveform that was previously described. The next highest crest element likewise gives the same doublet waveform but is delayed slightly by the altitude difference and weighted in amplitude according to expected signal strength at the element altitude. Continuing on to successive elements, delaying and adding each, yields the final desired waveform by the process of superposition or convolution.

The network analogy of sea-state can be represented as before by a network having the electromagnetic impulse response of sea-state. This sea-state network is taken to be in cascade with the previously obtained sea-state free surface network impulse analogy (the RC integrator). Combining both networks in cascade shows by network analogy that the effect of sea-state can be shown by convolving the sea-state impulse response on the idealized sea-state free waveform as was initially contended.

Figures A-7, A-8, and A-9 show the effects of sea-state on the final processed waveforms. Figure A-7 shows the hypothetical electromagnetic spread or impulse response obtained from Raytheon's Marine Research Laboratory (see Appendix R-G). In Figure A-7 the transmitted impulse wavefront can be thought of as arriving from the left, striking first the highest wave crests, then striking progressively more crests until maximum reflected amplitude is obtained at about the 2 meter altitude point where most crests appear (assuming 20 knot wind), then falling off in strength near calm sea level where maximum slopes occur giving a signal minima. A second maxima occurs at trough maxima depression level.

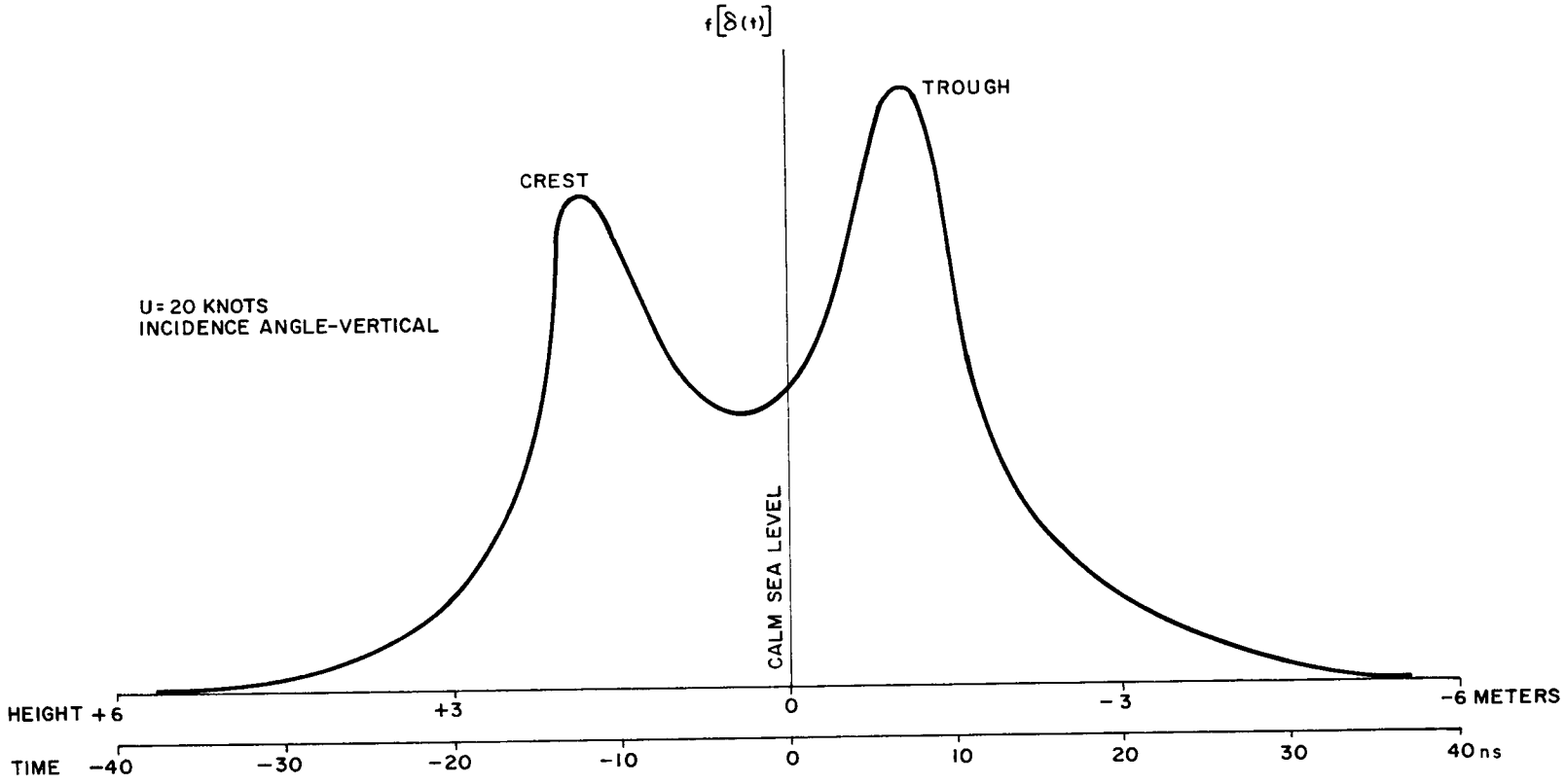

Figure A-7 Electromagnetic Spread Function of Sea-State (Impulse Response)

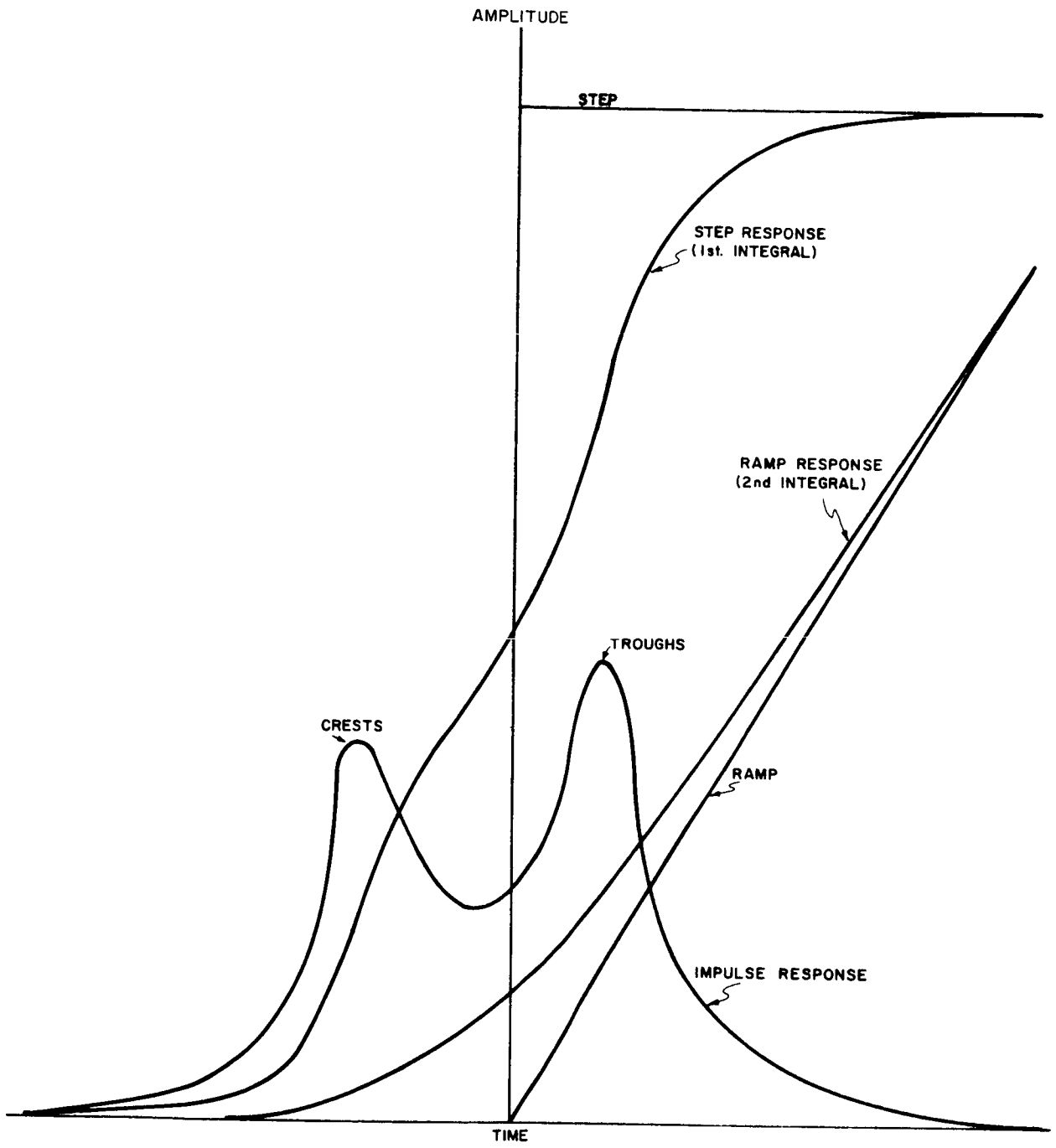

Figure A-8 Impulse, Step, and Ramp Response versus Sea-State

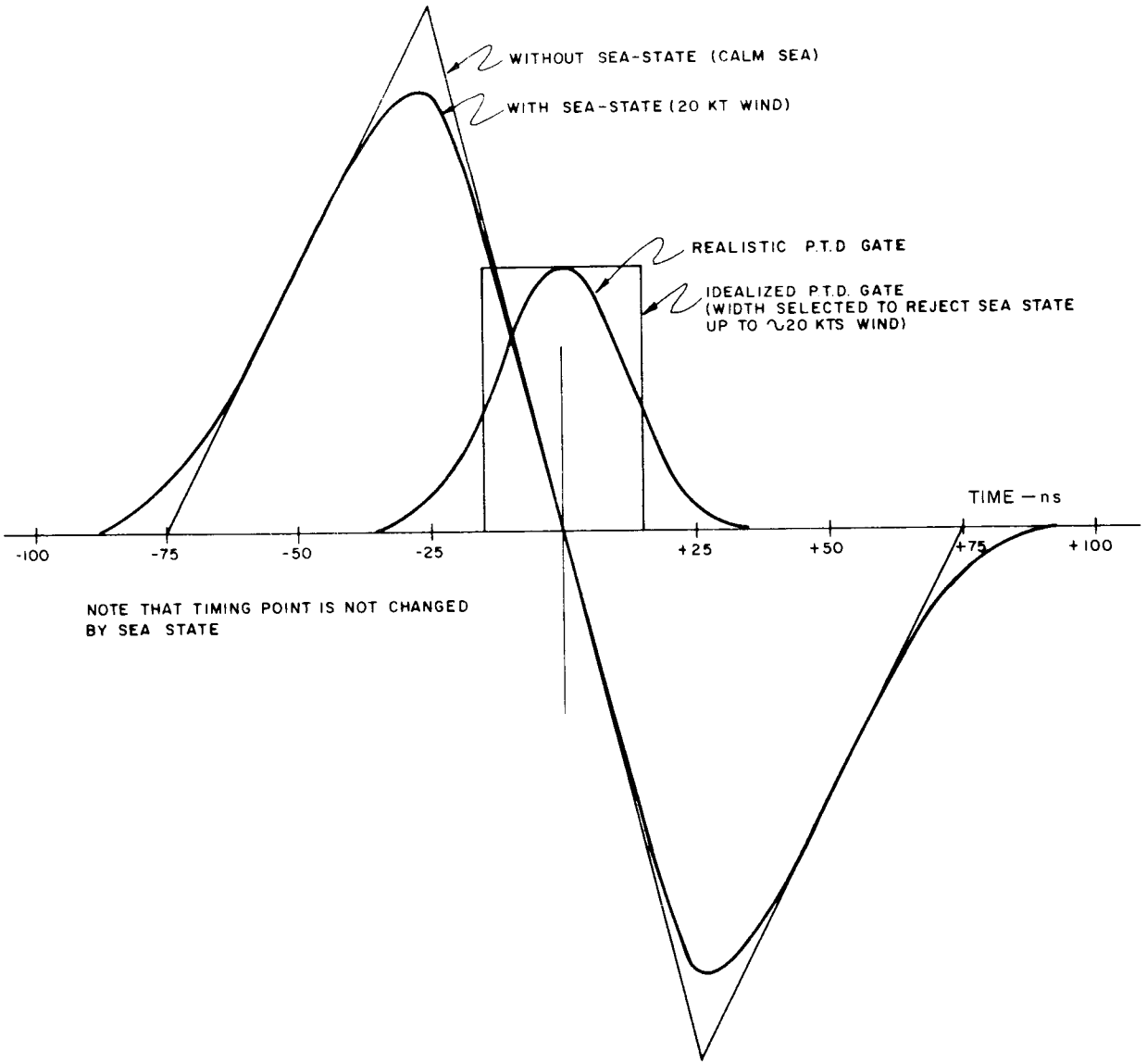

Figure A-9 Processor Output Wave with and without Sea-State

This maxima is somewhat higher than the crest maxima, indicating somewhat trochoidal or Stokes sea wave structure. The signal strength finally falls to zero as the deepest troughs are intercepted by the impulse at depths of about 5 meters.

This response is considered to be hypothetical since it has no experimental verification and since the response model was based on optical considerations which may be questioned at microwave frequencies.

It may be noticed that the impulse response is somewhat unsymmetrical about the calm sea reference line. However, the highest amplitude return signal maximum occurs from trough regions where displacements are somewhat less than was true for the crest side. The combined effect of amplitude times displacement is to give quite negligible shift in the centroid which gives the tracking point of the processed waveform. Estimates using this hypothetical response show about .03 meters shift in centroid away from the calm sea or msl for 20 knot wind waves. Only negligible tracking error is therefore expected in sea states up to 20 knots wind on the assumption that further investigations confirm the impulse response waveforms which are currently being studied.

Figure A-8 shows the result of convolving this response first on a step and then on a ramp. The step response is obtained by integrating the impulse response, after which the ramp response is then obtained by performing a second integration of the step response. It can be seen in Figure A-8 that the effect of sea state on the ideal ramp gives maximum departure from ideal near break points or within the dimensions of the sea wave spread and becomes small on extended linear regions away from breaks. Sea state immunity is therefore obtained by selecting a timing point on a straight ramp region well away from break points.

Figure A-9 shows the result of convolving the sea state function on the final idealized doublet waveform. As pointed out, very little change occurs along the linear regions away from break points. At the zero-axis crossing point the convolution integral can be written:

$$V_o(\tau) = \int_{-\infty}^{\infty} f(\tau-t)\ f\ [\delta(t)]\ dt\ ;\ (\tau = \text{scanning displacement} \tag{A-17}$$

It is convenient to locate the coordinate axis at the zero cross-over point. Then for $\tau = 0$:

$$V_o(0) = \int f(t)\ x\ f\ [\delta(t)]\ dt = \int mt\ x\ f[\delta(t)]\ dt \tag{A-18}$$

where:

$$f(t) = mt = \text{ramp equation vs time;}\quad m = \text{slope}$$
$$f[\delta(t)] = \text{sea state impulse response,} \tag{A-19}$$

but the centroid of the sea state function can be written as:

$$\tau_c = \int \frac{t\ x\ f\ [\delta(t)]\ dt}{A} = \text{centroid of sea state function.} \tag{A-20}$$

This function resembles the response $V_o(0)$ at $\tau = 0$ and can be written by comparison as:

$$V_o(0) = mA\tau_c, \tag{A-21}$$

which shows that the zero crossing point shifts with the centroid (τ_c) of the sea state function.

Figure A-9 shows a pulse-time discriminator pulse centered on the axis crossing point. If the ramp waveform is integrated over a gated region short enough to eliminate the breaks where sea state effects occur then sea state effects, except for the small shift in centroid, will give negligible errors in altitude readings.

A.8 EFFECT OF RECEIVER NOISE ON PROCESSOR WAVEFORMS

As discussed earlier, the effects of receiver noise can be analyzed independent of signal when linear circuits allowing super-position are used. The noise output can then be added to the noise-free signal to give the combined result. Receiver noise at the output of the synchronous detector will have gaussian distribution with zero mean and with the same bandwidth as the receiver. If this receiver noise is then passed through a low-pass processing or tracking filter the variance is reduced by the ratio of the noise bandwidth to the filter bandwidth. For example if 20 MHz bandwidth noise is passed through a 1 Hz filter the variance is reduced 73 dB, therefore, noise amplitudes are reduced by a factor of about 4500.

Signal waveforms at the processor input as examined on a pulse-to-pulse basis may be nearly obscured by noise. However in linear circuits the mean level of noise remains constant and is unaffected by randomness of the individual pulses. No analysis error is introduced by overlooking the per pulse randomness and looking only at the final filtered waveform.

On this basis the effect of noise can be visualized by assuming that many dB of noise filtering occurs prior to the processor, giving a gaussian distributed deviation with much reduced variance about the idealized mean of the final processed waveform. An analysis of noise effects is contained in the accuracy section. The discussion given here is intended only to show that receiver noise has a small effect on performance when long-integrating times, i.e., narrow bandwidth tracking filters, are used.

A.9 EFFECT OF SEA-CLUTTER ON PROCESSOR WAVEFORMS

Sea clutter results from the random vector addition of many target element contributions at the receiver input giving Rayleigh amplitude distribution to the detected signal waveforms. The signal output will

have the appearance of signal-plus-noise, the clutter portion being taken as the variance or noise power of the wave resulting from the random vector additions.

The sea clutter has some important differences to receiver noise however. The clutter waveforms are repetitive on a pulse-to-pulse basis because they are dependent on slowly changing geometry. The clutter waveforms do change, however, at doppler controlled rates as range to individual target elements change vs vehicle motion. The repetitive waveforms change shape most rapidly at the trailing edge corresponding to the outer edge of the target illuminated area where velocities and doppler frequencies are highest. Change is relatively slow at the leading edge where doppler frequencies approach zero at vertical incidence. It is this repetitive characteristic of the clutter noise that permits phase tracking and subsequent synchronous detection to be carried out.

A second difference between clutter and receiver noise is the constant signal-to-clutter ratio where signal is taken as the mean or dc component of power of the detected signal, and clutter is taken as the variance or ac component of power of the waveform. For Rayleigh amplitude distributions the resulting signal to clutter ratio is known to be constant and equal to $\pi/(4-\pi)$ or approximately 3.66.

Clutter fluctuations can be reduced by filtering in the same manner as noise except that the doppler bandwidth, instead of the receiver bandwidth, determines the smoothing ratio. Accuracy estimates are shown elsewhere. Estimates of processed signal-to-clutter ratios are given in Appendix R-B.

APPENDIX R–B

TRANSMITTER POWER REQUIREMENTS

Transmitter power requirements for this altimeter are based on accuracy considerations in receiver noise and clutter, and on phase tracking requirements for obtaining good coherent detection over the bandwidth of the doppler spectrum. The customary detection statistics problems are not applicable to this case since detection is not an objective. The accuracy and tracking requirements are dominant and are more demanding than the usual detection requirements.

Both the accuracy and the tracking problems can be solved by the straight forward networks approach. Signal-to-noise and signal-to-clutter ratios at the processor output are found by first obtaining the corresponding ratios at the inputs, then introducing the effects of the processor and integrators as cascade linear networks. The use of coherent detection permits the use of linear network analysis throughout.

B.1 ALTITUDE ACCURACY VS RECEIVER NOISE

The signal-to-noise ratio at the detector input can conveniently be found as a first sampling point in the network. This S/N ratio is obtained as an instantaneous function of time on a per pulse basis by using the conventional range equation form:

$$\left(\frac{\hat{S}}{N}\right)_{d_1} = \frac{\hat{P}_t G^2 \lambda^2 \sigma}{(4\pi)^3 h^4 K T_\epsilon B L_b L_a L_m} \quad ; \text{ General range equation form for S/N at detector input.} \qquad \text{(B-1)}$$

For the pulse length limited case such as ours where antenna gain can be considered to be essentially constant over the illuminated area of the short pulse, i.e., where $\hat{\theta} << \theta_a$, the target cross section equivalent area is given by:

$$\sigma = \sigma_o A_{ill} = \sigma_o \pi c \hat{t} h \; ; \quad \text{equivalent target cross-section} \qquad \text{(B-2)}$$

Substituting in (B-1) gives,

$$\left(\frac{\hat{S}}{N}\right)_{d_1} = \frac{\hat{P}_t G^2 \lambda^2 \pi \sigma_o c \hat{t}}{(4\pi)^3 h^3 K T_\epsilon B L_a L_m L_b} \; ; \quad \text{Instanteous signal-to-noise at detector input during each pulse.} \qquad \text{(B-3)}$$

This form is used for obtaining the signal-to-noise ratio at the end of the ramp step (assuming a rectangular pulse of length $\hat{t}$). Two cases will be considered; (1) a typical case where parameters are favorable, and (2) a worst case example where parameters are about as unfavorable as might be expected without disrupting performance.

The parameters assumed are shown below in Table B-1.

TABLE B-1

Parameter	Typical Value	Worst Case Value	Remarks
P_t	1 kW	1 kW	Assumed transmitter pulse peak power
G	38 dB	38 dB	.76 m antenna-uniforms illumination
λ	3 cm	3 cm	X-band, 10 GHz
σ_o	20 dB (10 knots wind)	10 dB (20 knots wind)	See Figure A-3, Page R-A-7
c	3×10^{10} cm/sec	3×10^{10} cm/sec	
$\hat{t}$	50 ns	50 ns	Transmitted pulse length assumed rectangular
$(4\pi)^3$			

TABLE B-1 (Continued)

Parameter	Typical Value	Worst Case Value	Remarks
h	1000 km	1300 km	
k	1.38×10^{-23}	1.38×10^{-23}	watts/^{o}k/Hertz bandwidth
T_{ϵ}	1690^{o}K	1830^{o}K	See note 1
B	20 MHz	20 MHz	See note 2
L_b	1	1	See note 3
L_a	1	1.5	See note 4
L_m	2	2	Microwave transmission losses

Note 1. The equivalent input temperature (T_{ϵ}) is used since antenna temperature (T_a) may be appreciably lower than standard room temperature ($T_o = 290^{o}$k) for an antenna directed vertically downward over the ocean. In this case much of the thermal energy is sky re-radiation energy and antenna temperature as low as 150^{o}K are typical.

The equivalent input temperature is given by:

$$T_{\epsilon} = T_a + T_r = T_a + (F-1)\ T_o \qquad \text{(B-4)}$$

Using:

$T_a = 150^{o}$K ; antenna temperature

F = 8 dB = 6.3 ratio; Receiver Noise Figure

$T_o = 290^{o}$K

Gives:

$T_{\epsilon} = 1690^{o}$K; typical input noise temperature

For worst case, the antenna temperature is assumed to be:

$T_a = T_o$

For which case: $T_{\epsilon} = FT_o = 1830^{o}$; worst case noise temperature

Note 2. The noise bandwidth of the receiver is taken as 20 MHz to match approximately the 50 ns transmitted pulse spectrum. The spectral bandwidth of the transmitted signal is unchanged by the sea surface which has essentially flat response over the spectral bandwidth of the signal.

Note 3. Bandpass mismatch loss in the receiver (L_b) is taken as unity (no mismatch loss). For the practical case assuming a gaussian shaped pulse into a single-tuned bandpass characteristic where $\hat{t}x\tilde{B}=1$, when both are measured at the exp $(-\frac{\pi}{4}) \approx 0.5$ power level, near perfect match is achieved and loss is negligible.

Note 4. Atmospheric loss (L_a) at vertical incidence is negligible at X-band under fair weather conditions. However, about 1.75 dB two-way loss is estimated for 10 mm per hour rain conditions. (See Barton[2])

Substitution of these parameters in equation (B-3) gives:

$$(S/N)_{dl} \approx 91 \text{ or } 19.6 \text{ dB; typical S/N at end of ramp.} \qquad \text{(B-5)}$$

Using the worst case parameters gives:

$$(S/N)_{dl} \approx 2.5 \text{ or } 4 \text{ dB; as worst case S/N at end of ramp.} \qquad \text{(B-6)}$$

These values can now be introduced into the accuracy form for a ramp waveform in noise. Applied to the ramp obtained at the processor output the axis crossing uncertainty can be written as

$$\sigma_t = \frac{\hat{t}}{2\sqrt{(S/N)_{pos}}} \quad ; \text{ timing error of axis crossing point in noise, on a single pulse basis} \qquad \text{(B-7)}$$

The factor 2 in the denominator results from the slope doubling effect of the doublet waveform which goes from maximum positive to maximum negative over the duration of the ramp ($\hat{t}$).

The S/N degrades somewhat in going through the processor. At each delay-differencing stage noise powers are approximately doubled since noise waveforms are delayed one pulse length and subtracted. Noise is essentially non-coherent after delays of 1/bw and therefore noise powers add. For two stages, noise power essentially quadruples giving:

$$(S/N)_{pol} = (1/4) \times (S/N)_{dl} \quad ; \text{ S/N at processor output per pulse.} \tag{B-8}$$

The effect of integration is to reduce the standard deviation by the square root of the number of samples integrated. The number of samples integrated is related to the prf and to integrator bandwidth by:

$$n_i \cong \frac{f_r}{2\ B_o} \quad ; \text{ no. of pulses integrated} \tag{B-9}$$

Assuming:

f_r = 100000 pps at 1000 km

$B_o = \frac{1}{2\pi\tau} = .16$

τ = 1 second

Gives:

n_i = 314160 pulses integrated (τ = 1 sec)

The accuracy equation (B-7) can be rewritten as:

$$\sigma_t = \frac{\hat{t}}{2\ \sqrt{(S/N)_i}} = \frac{\hat{t}}{2\ \sqrt{(S/N)_{pol} \times n_i}}$$ std deviation of axis crossing time after n_i pulses integrated. (B-10)

Substituting values given and converting to altitude uncertainty:

$$\sigma_{hn} = \frac{c\sigma_t}{2}$$ standard deviation of altitude (B-11)

Gives:

$$\sigma_{hn} = \frac{\hat{ct}}{4\sqrt{(S/N)_{dl} \times \frac{314160}{4}}}$$

or for the typical $(S/N)_{dl} = 144$

$$\sigma_{hn} = \frac{3.82}{\sqrt{91 \times \frac{314160}{4}}} \approx .0014 \text{ meters; altitude uncertainty vs. receiver noise} \qquad \text{(B-12)}$$

Using the worst case value for $(S/N)_{dl} = 2.5$

Gives:

σ_{hn} = .0086 meters; worst case altitude uncertainty.

Evidently from the standpoint of accuracy in receiver noise, the 1 kW transmitter power is excessive. However, the accuracy in clutter and the phase tracking requirements need to be evaluated.

B.2 ALTITUDE ACCURACY vs RAYLEIGH CLUTTER

Altitude accuracy in the presence of Rayleigh clutter can be evaluated by the same accuracy equation formulated for receiver noise in paragraph 4.4.1.1, except that new parameter definitions are now applicable.

$$\sigma_{hc} = \frac{\hat{ct}}{4\sqrt{(S/C)_i}} \quad ; \qquad \text{(B-13)}$$

where $(S/C)_i$ is the signal-to-clutter ratio after integration and is given by:

$$(S/C)_i = (S/C)_{dl} \times \frac{n_{ci}}{G_{cp}} \quad ; \text{ signal to clutter ratio after integration.} \qquad \text{(B-14)}$$

As explained in the accuracy analysis, $(S/C)_{dl}$ is the signal-to-clutter ratio at the end of the ramp or at $\hat{t}$ = 50 ns. The signal portion of the waveform is defined as the mean squared level, and the clutter portion is the variance. Therefore:

$$(S/C)_{dl} = \frac{\text{mean}^2}{P^2 - \text{mean}^2} = \frac{\pi}{4-\pi} = 3.66 \text{ (constant)} \qquad \text{(B-15)}$$

This S/C ratio holds for Rayleigh type signals regardless of amplitude. The number of samples integrated (n_{ci}) in the case of clutter depends on the doppler bandwidth, i.e., clutter bandwidth. The doppler bandwidth for a 50 ns pulse is about 1500 cps (see Figure A-2). Giving:

$$n_{ci} = \frac{1500 \times 2\pi\tau}{2} = 1500 \times \pi\tau = 4720 \text{ pulses integrated}$$

The clutter gain in the processor (G_{cp}) results from delay differencing in two stages as was discussed for noise. For clutter however, since clutter varies as signal amplitude varies, and since clutter at the timing crossover is the sum of one full amplitude and two half amplitude signals the clutter power is increased by $1 + (1/2)^2 + (1/2)^2 = 1.5$.

Substituting into (B-14) and (B-15) gives:

$$\sigma_{hc} = \frac{c\hat{t}}{4\sqrt{(S/C)_{dl} \times \frac{n_{ci}}{G_{cp}}}} = \frac{3.82}{\sqrt{3.66 \times \frac{4720}{1.5}}} = .035 \text{ meters altitude uncertainty vs clutter.}$$

This clutter error is seen to be independent of transmitter power level and of prf. It has been analyzed here because of its close analogy to the receiver noise case which does however depend on power level and prf.

B.3 PHASE-TRACKING ACCURACY vs TRANSMITTER POWER

The signal-to-noise ratio for phase tracking performance is evaluated in a similar manner. It is desired to know the phase tracking uncertainty resulting from noise in the tracking circuit. Since the doppler frequency being tracked has about 1500 Hz bandwidth it is evident that the tracking circuit must be at least this broad and will have approximately the same noise bandwidth. The number of noise samples integrated (n_{pi}) will then be:

$$n_{pi} \approx \frac{f_r}{2\ B_d} \approx \frac{100000}{2 \times 1500} \approx 33 \qquad \text{(B-16)}$$

The $(S/N)_{pt}$ for phase tracking will be:

$$(S/N)_{pt} = (S/N)_{dl} \times n_i = (S/N)_{dl} \times 33;\ \text{S/N at phase tracker output}$$

For worst case values $(S/N)_{dl}$ was taken as 4, giving:

$$(S/N)_{pt} = 4 \times 33 = 132 \qquad \text{(B-17)}$$

This S/N ratio can be converted to corresponding phase error or uncertainty by using:

$$\phi = wt$$

$$d_\phi = wdt$$

$$\sigma_\phi = w\sigma_t;\ \text{standard deviation of phase tracking angle.} \qquad \text{(B-18)}$$

where σ_t is the timing uncertainty vs. (S/N)

For a sinusoidal waveform in noise, the timing uncertainty is given by:

$$\sigma_t = \frac{1}{w\ \sqrt{S/N}} \qquad \text{(B-19)}$$

The corresponding phase error is, from (B-18):

$$\sigma_{\phi} = \frac{1}{\sqrt{S/N}} \qquad \text{(B-20)}$$

From (B-17) then

$$\sigma_{\phi} = \frac{1}{\sqrt{132}} = \frac{1}{11.5} \text{ radians} \approx 5^{o} \text{ phase tracking error.}$$

This 5^{o} of phase tracking uncertainty for worst case noise and for the highest clutter components at 1500 Hz can be considered satisfactory. It is this phase tracking requirement which appears to be the transmitter power limitation of the system and which dictates the 1 kW power level selected.

APPENDIX R–C

WAVEFORMS FROM NON–COHERENT DETECTORS

The use of non-coherent detectors is known to introduce waveform changes as a function of changes in signal-to-noise ratios. Use of agc does not help since both signal and noise are controlled simultaneously and ratios remain unchanged.

The approximate S/N power relationship for non-coherent detectors is given by:

$$\left(\frac{S}{N}\right)_{out} \approx \frac{\left(\frac{S}{N}\right)^2_{in}}{1 + \left(\frac{S}{N}\right)_{in}} \quad ; \quad \text{S/N power relation for non-coherent detector} \qquad \text{(C-1)}$$

The corresponding S/N amplitude relationship is:

$$\left(\frac{s}{\sigma_n}\right)_{out} = \frac{\left(\frac{s}{\sigma_n}\right)^2_{in}}{\sqrt{1 + \left(\frac{s}{\sigma_n}\right)^2_{in}}} = \frac{\left(\frac{s_{max}}{\sigma_n}_{in}\right)^2 \left(\frac{s_{in}}{s_{max}}\right)^2}{\sqrt{1 + \left(\frac{s_{max}}{\sigma_n\ in}\right)^2 \left(\frac{s_{in}}{s_{max}}\right)^2}} \qquad \text{(C-2)}$$

Letting $k = \left(\frac{s_{max}}{\sigma_n}\right)$; amplitude ratio at end of ramp,

Then:

$$\bar{s}_{out}(k, \bar{s}_{in}) = \frac{k^2 \bar{s}_{in}}{\sqrt{1 + k^2 \bar{s}^2_{in}}} \qquad \text{(C-3)}$$

Where:

$\bar{s}_{in}$ is the normalized input signal $\left(\frac{s_{in}}{s_{max}}\right)$

For the case $\bar{s}_{in} = 1$, Equation C-3 gives the final value $s_{out} = 1$.

$$\bar{s}_{out}(k, 1) = \frac{k^2}{\sqrt{1 + k^2}} \quad ; \qquad \text{final value at end of ramp.} \qquad \text{(C-4)}$$

The final normalized form going from $s_o = o$ to $s_o = 1$ for input $s_i = o$ to s_i can then be written (taking ratio of (C-3) to (C-4)):

$$s_o = s_i^2 \sqrt{\frac{1 + k^2}{1 + k^2 s_i^2}} \quad ; \quad \text{normalize amplitude relation between input and output} \qquad \text{(C-5)}$$

This expression gives the waveform of the output amplitude (s_o) with respect to the input amplitude (s_i) for a family of curves having varying signal-to-noise ratios k. Figure C-1 shows that output curves rise more abruptly for k large than for k small, introducing corresponding altitude errors when non-coherent detectors are used.

Power estimates (see Appendix R-B) show signal-to-noise power ratios varying from about 144 for typical conditions to about 4 for unfavorable conditions. For this range of values (not considered as maximum expected) the corresponding k varies between about 12 to 2. The corresponding altitude error from Figure C-1 is about 1.5 meters and more than can be tolerated for this system. A 10-fold increase in transmitter power would have reduced this error to about 0.5 meters but would still be large and would introduce serious power problems. Coherent processing which eliminates this error appears to be the best solution.

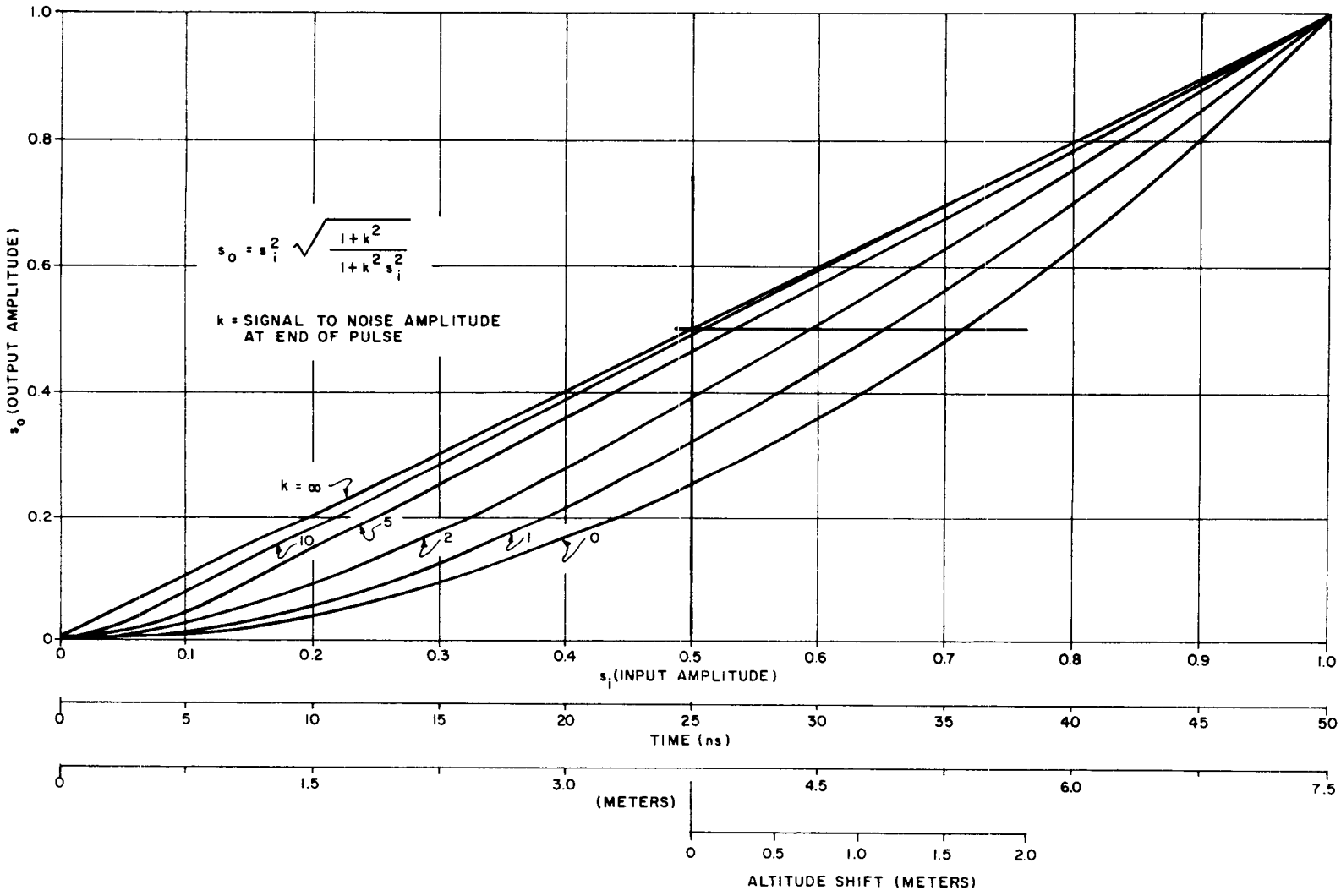

Figure C-1 Waveform Change in Non-Coherent Detector vs S/N Ratio at Input (Ramp Return from Rectangular Pulse)

APPENDIX R–D

ALTITUDE ERROR VS RECEIVED WAVEFORM TIME CONSTANT FOR A SQUARE–LAW DETECTOR

The received waveform is related to the impulse response from the sea surface. For the noise and clutter-free case the impulse response (see Figure A-4) is approximately a decaying exponential having a time constant which varies with respect to altitude, reflection coefficient and beam pointing angle. The corresponding altitude errors are analyzed in this appendix.

The ramp doublet waveform at the processor output is obtained by subtracting delayed replicas of the initial received rising exponential waveform. At the zero axis crossing point the ordinate is given by the ordinate of the rising exponential at time $3t_1$, minus 3 times its value at t_1 where t_1 is $\hat{t}/2$ or 1/2 pulse lengths from t_o.

Figure D-1 below shows the processed doublet as derived from the rising exponential, with the curvatures somewhat exaggerated to illustrate the effects on cross-over timing vs. changes in time constant (t_c).

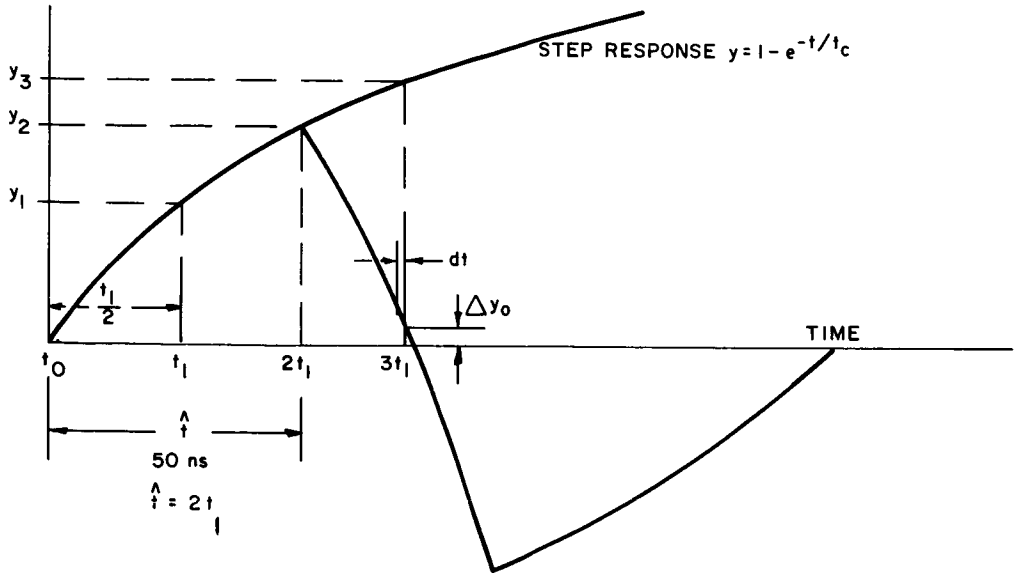

Figure D-1 Processed Doublet Waveform

The ordinate at the timing crossover point $(t - 3t_1)$ is given by:

$$\Delta y_o = y_3 - 3y_1$$

$$= \left(1 - e^{-\frac{3t_1}{t_c}}\right) - 3\left(1 - e^{-\frac{t_1}{t_c}}\right); \text{ by evaluating at corresponding t.}$$

(D-1)

By using the series expansion to three terms:

$$e^x \cong 1 + x + \frac{x^2}{2} \quad : \text{three term approximation form.} \tag{D-2}$$

gives:

$$\Delta y_o = 3\left(\frac{t_1}{t_c}\right)^2 \quad = \text{ordinate error resulting from exponential curvature (not straight line)} \tag{D-3}$$

The corresponding change in ordinate as time constant (t_c) varies is:

$$dy_o = 6\left(\frac{t_1}{t_c}\right)^2 \times \frac{dt_c}{t_c}; \text{ derivative vs } t_c \tag{D-4}$$

The resulting timing change is obtained from slope at crossover, thus:

$$\left(\frac{dy}{dt}\right)_o \approx \frac{y_2}{t_1} \approx \frac{1 - e^{-2\frac{t_1}{t_c}}}{t_1} \approx \frac{2\frac{t_1}{t_c}}{t_1} \tag{D-5}$$

Solving for dt:

$$dt = \frac{dy_o}{\left(\frac{dy}{dt}\right)_o} = \frac{6\left(\frac{t_1}{t_c}\right)^2 \times t_1 \times \frac{dt_c}{t_c}}{2\left(\frac{t_1}{t_c}\right)} = 3\left(\frac{t_1}{t_c}\right) \times t_1 \times \frac{dt_c}{t_c} \tag{D-6}$$

= axis crossing timing error

The corresponding altitude error is found from $\frac{dh}{dt} \approx \frac{R_1}{t_1}$

$$\frac{dh}{R_1} = \frac{dh}{\frac{ct_1}{2}} = \frac{dt}{t_1} = 3\left(\frac{t_1}{t_c}\right) \frac{dt_c}{t_c} \qquad \text{(D-7)}$$

for which

$$dh = \frac{ct_1}{2} \times 3 \frac{t_1}{t_c} \times \frac{dt_c}{t_c} \qquad \text{(D-8)}$$

assuming:

$t_1 = 25$ ns

$t_c = 5$ µs

$\frac{dt_c}{t_c} = 10\%$; worst possible variation in time constant

gives:

$dh = \frac{4.15 \times 3 \times 0.1}{200} = 0.0062$ meters altitude error for 10% change in time constant (t_c).

Summing by formula:

$$t_c = \sum_{1}^{M} t_i = \frac{2nh_1}{c} + (1 + 3 + 5 + n_1)\frac{\Delta h_1}{c} = \frac{2nh_1}{c} + n^2\frac{\Delta h_1}{c} \quad \text{(E-5)}$$

$$= \frac{2nh_1}{c}\left(1 + \frac{n\Delta h_1}{2h_1}\right) = \text{total counting time for n trips} \quad \text{(E-6)}$$

letting:

$$h_2 = h_1 + \Delta h$$

and:

$$\Delta h = n\Delta h_1$$

gives:

$$t_c = \frac{2n}{c}(h_2 - \Delta h)\left(1 + \frac{\Delta h}{2h_1}\right); \text{ total counting interval in terms of final altitude } h_2 \approx h_1. \quad \text{(E-7)}$$

Also, referenced to an indicated altitude (h_c) as for a fixed altitude case:

$$t_c = \frac{2n}{c}h_c; \text{total counting interval in terms of fixed altitude } h_c. \quad \text{(E-8)}$$

Solving the two last equations for final altitude (h_2) in terms of indicated altitude (h_c) gives by equating and solving for h_2:

$$h_2 = \frac{h_c}{1 + \frac{\Delta h}{2h_1}} + \Delta h \approx h_c\left(1 - \frac{\Delta h}{2h_1}\right) + \Delta h \approx h_c + \frac{\Delta h}{2} \quad \text{(E-9)}$$

Some approximations which appear to be insignificant have gone into this derivation. No consideration has been given to evaluating the magnitude of these approximations.

Corrections for vehicle path dynamics will possibly be made by ground based computers using nearly exact computational techniques. Under such circumstances it appears that final errors could be kept well under 0.03 meters.

APPENDIX R-F

RELATION BETWEEN ALTITUDE AND PRF

For the ambiguous prf used in this system, with transmit and received signals held interlaced by the use of a phase locked prf oscillator, the timing waveforms for the prf oscillator, the transmitter gate, the received waveform, and the pulse time discriminator reference pulses are shown in Figure F-1.

This diagram does not contain sufficient detail to illustrate the exact timing relationship between altitude and prf. Another diagram showing the effects of various system delays including atmospheric delay (t_a), receiver delay (t_r), and processor delay (t_p) is shown in Figure F-2.

From this figure, it can be seen that the total signal transmit time including atmospheric, receiver, and processor delays can be written as:

$$t_T = n_a t_1 + \frac{t_1}{2} \qquad \text{(F-1)}$$

$$\frac{t_1}{2} = t_o + t_d = t_o + t_a + t_r + t_p \qquad \text{(F-2)}$$

$$t_h = n_a t_1 + t_o = n_a t_1 + \frac{t_1}{2} - t_d = t_1\left(n_a + \frac{1}{2}\right) - t_d \qquad \text{(F-3)}$$

Also, using

$$t_1 = \frac{1}{f_r} \ ,$$

gives:

$$t_h = \frac{\left(n_a + \frac{1}{2}\right)}{f_r} - \left(t_a + t_r + t_p\right) \ . \qquad \text{(F-4)}$$

The corresponding altitude is:

$$h = \frac{ct_h}{2} = \frac{c}{2}\left(\frac{n_a + \frac{1}{2}}{f_r}\right) - \frac{c}{2}(t_d) \ . \qquad \text{(F-5)}$$

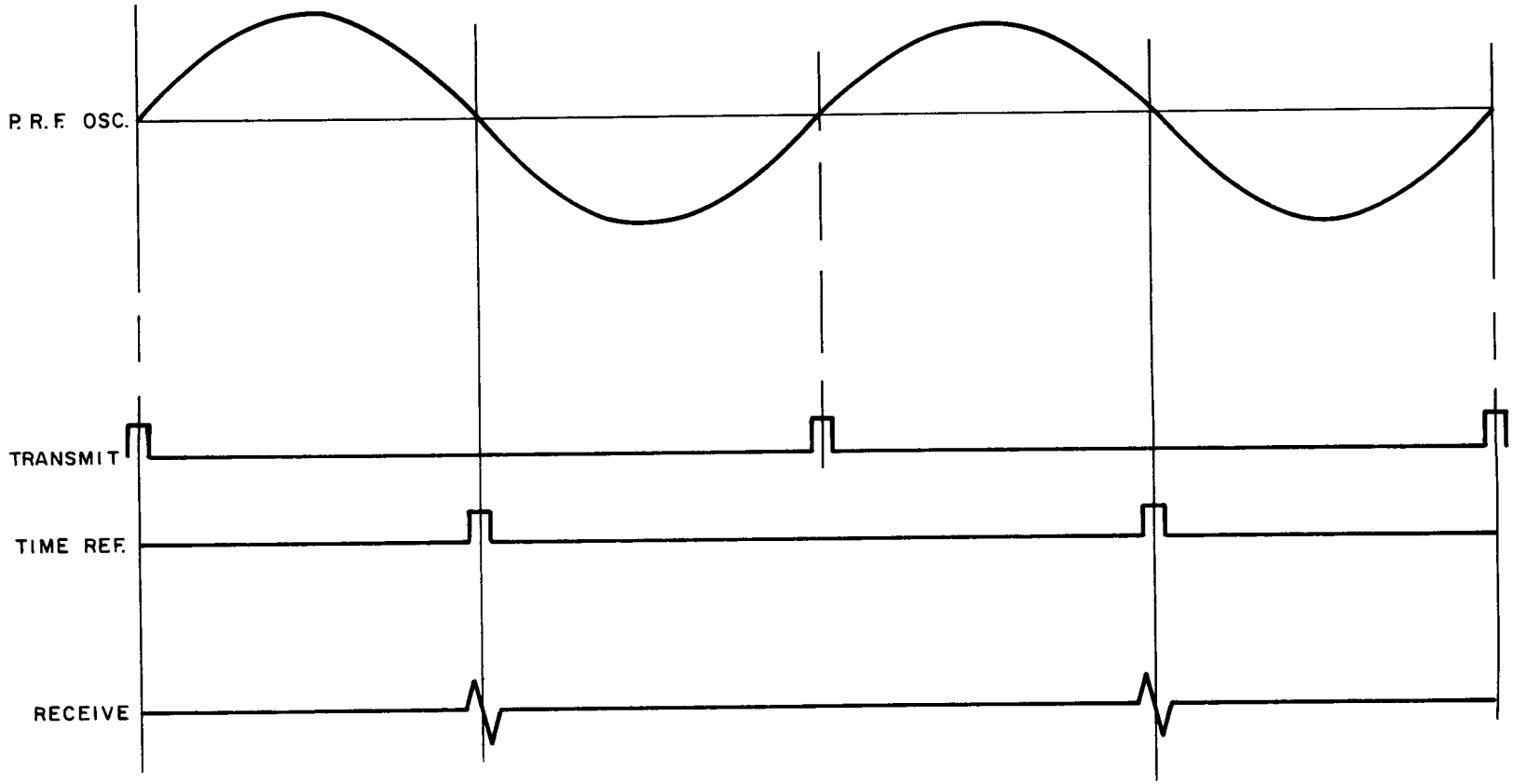

Figure F-1 Altitude Timing Waveforms

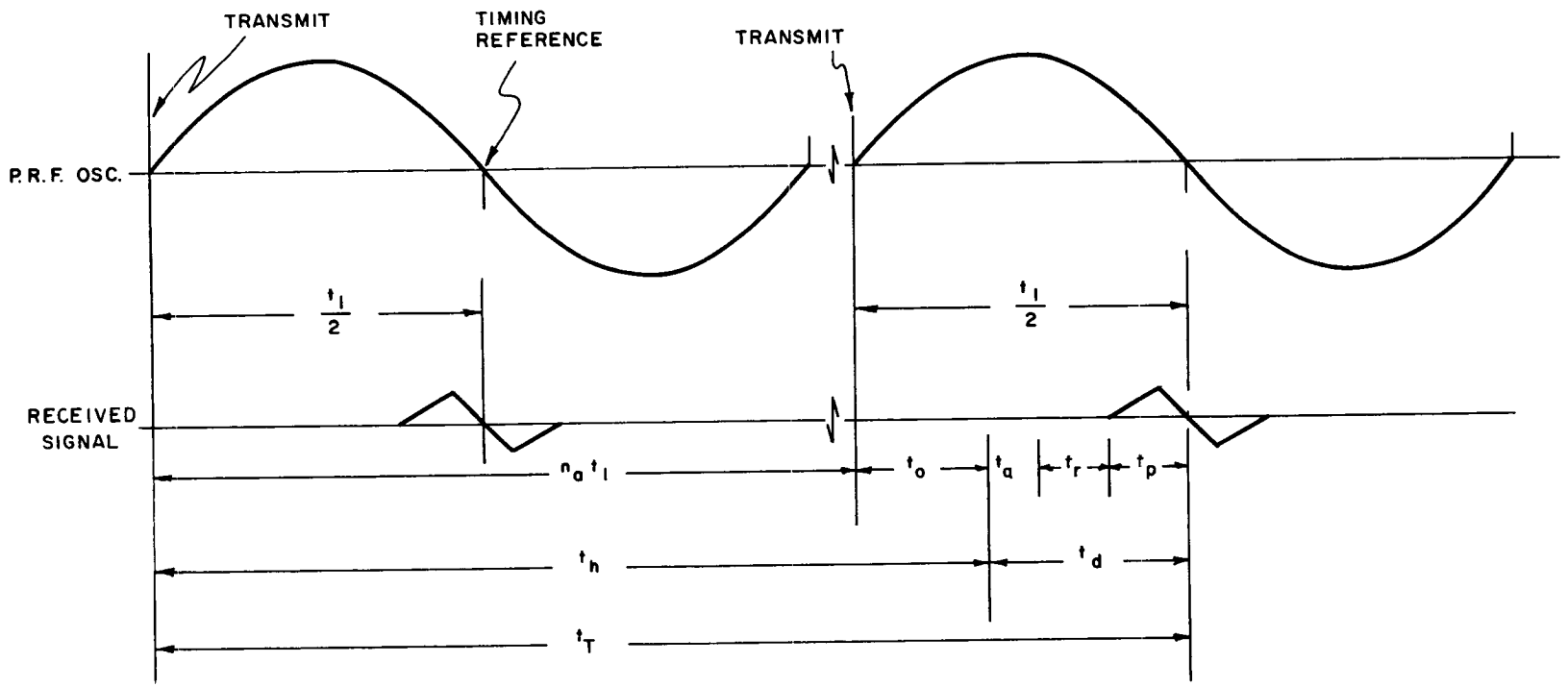

Figure F-2 PRF and Altitude Timing Waveforms

This is an exact relationship between altitude and prf. If a stable standard clock is used for counting altitude and if the clock frequency (f_c) is much higher than the prf, the ratio of frequencies is the same as the ratio of cycles counted over a timing interval, thus:

$$\frac{N_c}{N_r} = \frac{f_c}{f_r} \quad . \tag{F-6}$$

Substituting for f_r in the previous equation, gives:

$$h = \frac{c}{2}\left(\frac{N_c}{N_r}\right)\left(\frac{n_a + \frac{1}{2}}{f_c}\right) - \Delta h_d \quad . \tag{F-7}$$

This final form shows the relationship between altitude (h) and clock count (N_c) taken over an interval while a specified prf count (N_r) is being registered. The delay error (Δh_d) must be known from system calibrations in order to obtain the final corrected altitude.

APPENDIX R-G

COHERENCE DISTANCE OF BANDPASS NOISE VS. REFERENCE OSCILLATOR

The signal return from the sea surface has the same power spectrum as the transmitted signal since the sea surface is not frequency selective over the bandwidth of the signal spectrum. The phase spectrum, however, is randomized by the rough surface which has irregularities many wavelengths in depth.

Synchronous detection requires that the phase of the received signal be coherent with a reference sine wave source over an interval commensurate with a pulse length. The problem of determining coherence distance can be analyzed by examining the cross-correlation function (the coherence function) between this received bandpass signal and a stable sine wave signal.

The cross-correlation function $\phi(\tau)$ is obtained by convolving the signal spectrum on the sine wave spectrum, then taking the Fourier transform of the resultant spectrum. The signal spectrum is first obtained by multiplying the input signal spectrum by the receiver bandpass assuming a normal distribution function (gaussian like) transmitted pulse and a normal like (single tuned) receiver bandpass, then the signal spectrum will also be like a normal function. The two-sided spectra of the resulting signal, the reference oscillator, and the convolution of both are shown in Figure G-1.

The transform of this convolved result represents the waveform of the output from the synchronous detector. The high frequency terms at $\pm 2f_1$ will be removed by filtering, leaving only the low frequency term, obtained by transforming the normal function spectra centered at zero frequency.

This cross correlation function will also be a normal function whose width at $\exp(-\frac{\pi}{4})$ level will be the reciprocal of the spectra in Hertz also at the $\exp(-\frac{\pi}{4})$ level.

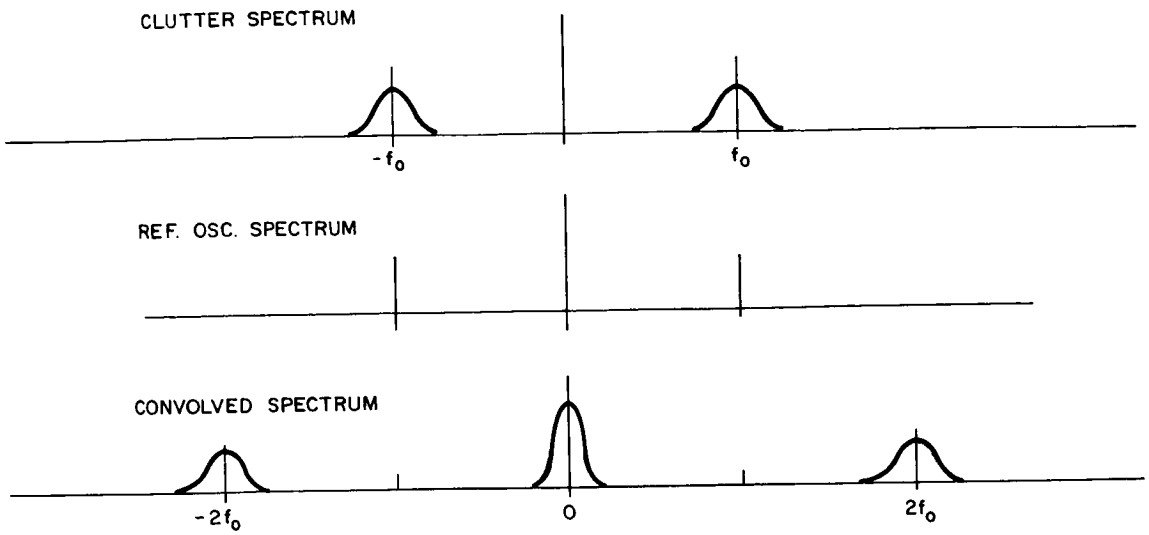

Figure G-1 Cross-Correlation Spectrum

Figure G-2 shows the corresponding pulses and spectra from the transmitter through the synchronous detector. The coherence function from the detector can be considered as the output for continuous bandpass noise or Rayleigh clutter signals. The output for the ramp step can be derived from this response. Analysis of the synchronous point vs. the received ramp shows that phase reference is at the point of maximum output and not at the initial up-break of the ramp. This phase referencing point gives best linear performance near the ramp center and beyond, where most accuracy information is concentrated. Conclusions are that the coherence region is adequate for good processing.

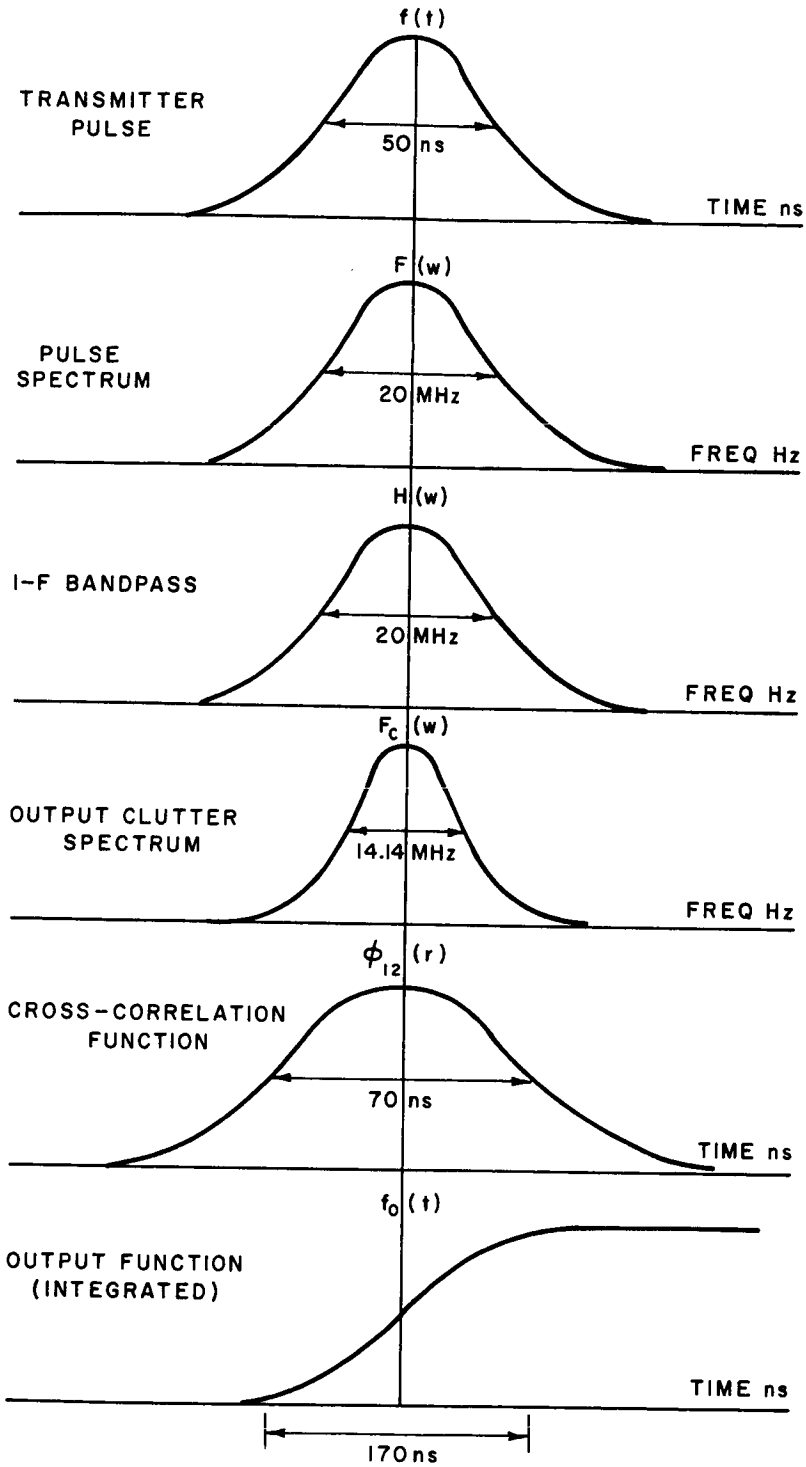

Figure G-2 Synchronous Detector Analysis

APPENDIX R-H

TROPOSPHERE REFRACTIVITY DELAY ERROR

The magnitude of errors caused by changes in troposphere refractivity is analyzed here. Data is taken from Barton[2] pg. 478, and from the Handbook of Geophysics chapter 9[2].

The apparent altitude is related to propagation velocity c by:

$$h = \int \frac{c\,dt}{2} = \frac{c_o}{2} \int \left(1 - \frac{N}{10^6}\right) dt \qquad \text{(H-1)}$$

where c_o is velocity in vacuum and N is refractivity as a function of time. Integrating gives:

$$h = h_o - \frac{c_o}{2} \int_o^t \frac{N(t)\,dt}{10^6} = h_o - \Delta h; \text{ N as a function of time} \qquad \text{(H-2)}$$

and since h_o is a constant error-free term it can be eliminated giving:

$$\Delta h = \int_o^h \frac{N(h)}{10^6}\,dh \; ; \quad \text{altitude delay vs N taken as a function of altitude.} \qquad \text{(H-3)}$$

From Barton pg. 479[2].

$N(h) = 313 \exp(-.14386h)$: h in km

Integrating for h = 1000 km gives

$$\Delta h = \frac{313}{.14386 \times 10^6} = 2.18 \text{ meters; altitude delay in troposphere (mean value)}$$

This delay can be subtracted out to give a corrected altitude reading. The variations about this mean delay are the important error terms. Data from Barton and from the Handbook of Geophysics indicate variation in N of about 100 or ± 50 in extreme cases. This extreme variation is related to corresponding altitude error by the same form. This extreme value probably represents at least two sigma (2σ) deviation giving a one

deviation value of

$\sigma = \pm .17$ meters

Further corrections based on known atmospheric information obtained from such sources as ships at sea, ground weather stations, weather satellites or from the satellite borne altimeter radiometer itself, should reduce this error by perhaps another factor of 2 indicating that it is not a serious error source.

APPENDIX R–I

GROUND CHECK OF SATELLITE OSCILLATOR FREQUENCY

For accurate altimetry with satellite processing, a timing oscillator is required having accuracies of 1 in 10^7 or better. Long time service aboard satellite requires that this accuracy be checked and adjusted versus ground based frequency standards.

Check of satellite-borne oscillator frequencies is complicated by the high velocity of the vehicle which introduces doppler shifts that must be taken into account.

One method of checking frequencies is to provide a highly accurate ground based oscillator operating at the desired oscillator frequency, then recording the doppler beat between the ground and satellite oscillators as the satellite passes the tangential or zero doppler angle.

If both oscillators are at precisely the same frequency the zero doppler position will occur when the satellite is precisely at the normal angle. If a frequency error exists however, the zero doppler angle shifts forward or backward from normal by an amount given by:*

$$\Delta\theta = \frac{c}{v}\frac{\Delta f}{f} \qquad \text{(I-1)}$$

where $\Delta\theta$ is angular displacement from normal (radians)

c = velocity of light

v = vehicle orbital velocity

$\frac{\Delta f}{f}$ = fractional difference in oscillator frequency.

For accuracy checks to 1 in 10^7, angular accuracy must be measured within

$$\Delta\theta = \frac{3\times10^5}{7} \times 10^{-7} = 4.28 \text{ milliradians} = .246 \text{ degrees}$$

This rather small angle can be accurately measured by recording the doppler beat pattern photographically to form a zone plate pattern as

* (See footnote on Page R-I-2)

is done with synthetic array side-looking radar. The zero doppler point can then be obtained by passing coherent light through the zone plate to give a highly resolved single line at the zero doppler angle.

If necessary, the normal angle to the satellite can be obtained by the same technique except that the ground station oscillator signal can be reflected or relayed to the satellite and return. Since no frequency difference can exist at normal, the zero doppler and zone plate zero will provide a true reference normal which can be photographed at the same time the other pattern is being recorded. Angular separation can be measured from the line separation of the two processed patterns.

---

*The doppler shift between the satellite oscillator frequency (f_s) and the received signal at the ground station will be:

$$f_d = f_s - f_r = \frac{v\theta}{c} f_s \quad : \quad v\theta = v_r = \text{component of radial velocity} \qquad \text{(I-2)}$$

The frequency difference between the ground and satellite oscillators will be:

$$\Delta f = f_s - f_g = \frac{v\theta}{c} f_s + (f_r - f_g) \qquad \text{(I-3)}$$

at the zero beat instant when $f_r = f_g$ then,

$$\frac{\Delta f}{f_s} = \frac{v\theta}{c} + 0 \qquad \text{(I-4)}$$

giving the relationship used in equation (I-1).

APPENDIX R–J

IMPULSE RESPONSE OF SEA STATE

Figure J-1 is a histogram of sea wave maxima and minima (facets) altitudes versus the calm sea reference level. This histogram was prepared by computer simulation as described in Appendix S-B. Related spectral data have been developed by Neumann, Pierson and others.[16] Scale values are shown in Table B-2 on page S-B-7; e.g., elevations in Figure J-1 are in meters, assuming fully developed waves at winds of 20 knots (10 m/s).

It can be observed that the facet density goes through two maxima, one corresponding to elevation of maximum crests to the right of zero, and the other corresponding to the elevation of the maximum troughs to the left of zero. For the twenty knot wind example these crest-to-trough maxima are separated by about 2.5 meters. Some crests and troughs are separated by greater or less distances but the probability of these other elevations decreases rather rapidly with departure from the maxima. Some few crests, for example, may occur at 3 meters above zero or calm sea level but almost none have greater elevations.

Of great importance to altimetry is the location of the centroid of this spread function (closely related to the electromagnetic impulse response). The centroid X_c is defined by $X_c = \frac{\Sigma xydx}{\Sigma ydx}$

where x = elevation (of points on ocean surface)

$y = y(x)$ = weighting or density of points (for each x)

This centroid has been estimated directly from the histogram by the relationship:

$$H_c = \frac{\Sigma h_i n_i}{\Sigma n_i} = \text{centroid elevation} \qquad \text{(J-1)}$$

where:

H_c = distance of centroid from zero or calm sea level

h_i = sample elevation

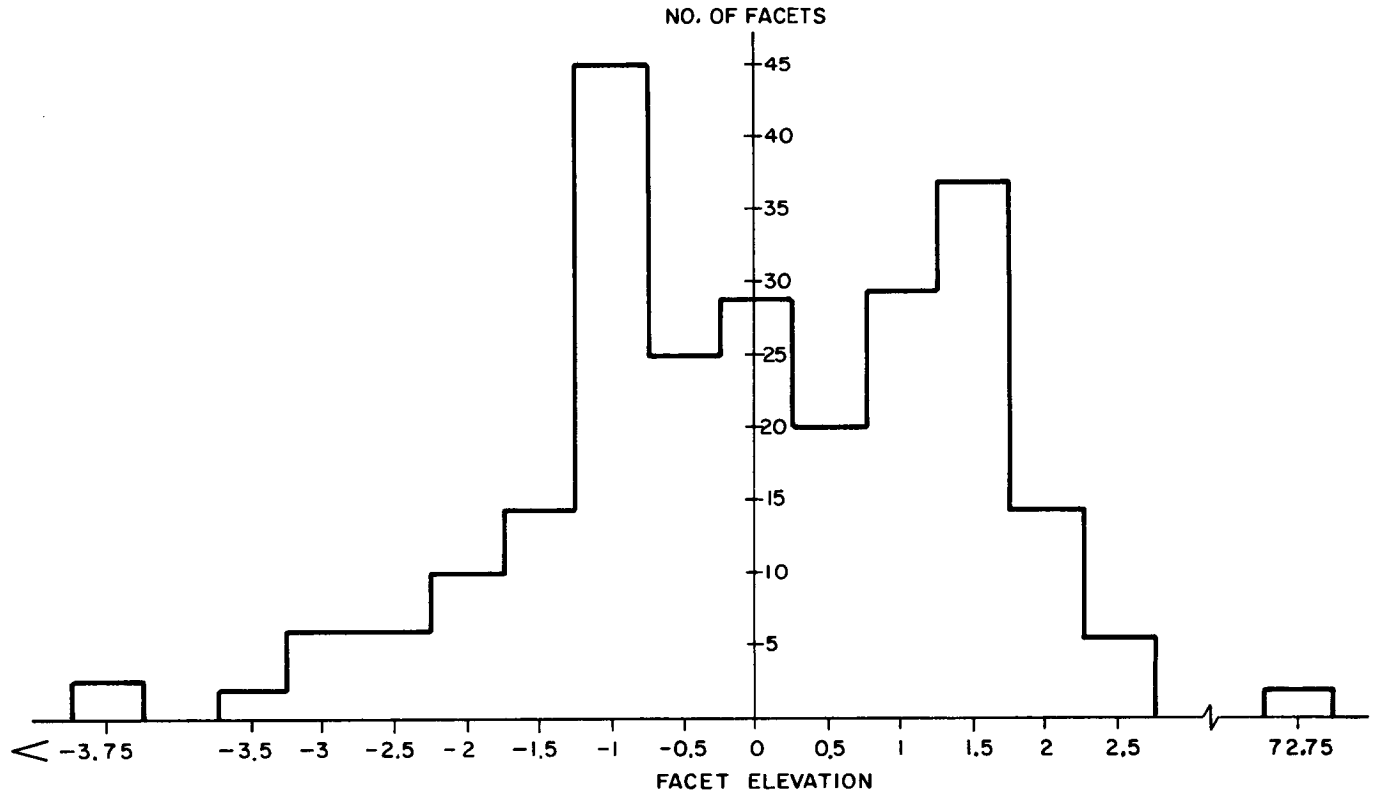

Figure J-1 Histogram of Facet Elevation

n_i = number of facets at h_i

A direct evaluation from the histogram by counting values gives:

H_c = -.0675 meters (toward troughs)

A similar evaluation was performed using the smoothed curves obtained from the histogram. Centroid data from this smoothed curve gave the smaller centroid elevation (depression) used in the error analysis section. Without further data there is no assurance that the smoothed data is any more accurate than the histogram data from which it was obtained.

Elevations vary almost as the square of wind velocities. Extension of centroid estimates can be made for other sea-state conditions by using the quadratic relationship.

Figure J-2 shows the computer simulated waveforms from which the histogram of Figure J-1 was obtained.

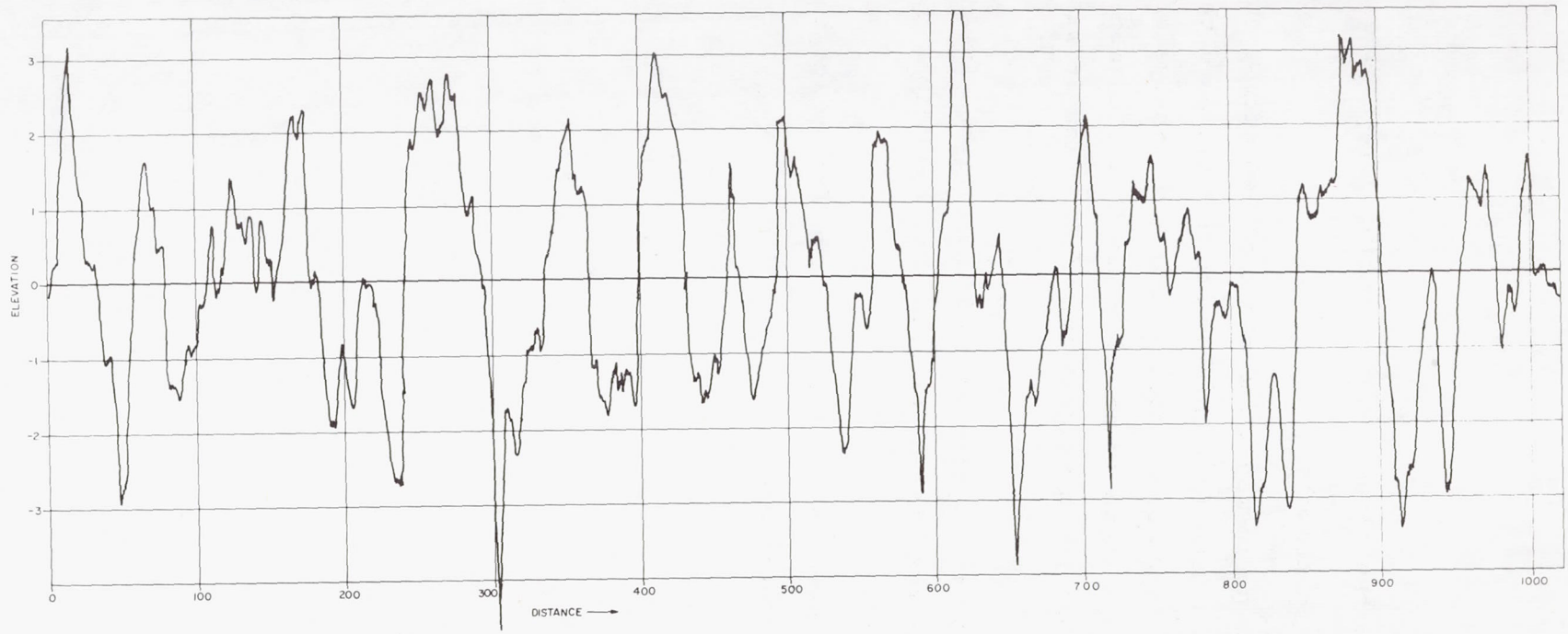

Figure J-2 Surface Elevation Based on 1024 Point Fast Fourier Transform

APPENDIX R-K

WAVEFORM VS. VERTICAL STABILIZATION OF ANTENNA BEAM

An analysis of waveforms vs. off-vertical beam displacement angles has been performed by computer. The problem is complicated by introduction of non-symmetry in signal return around the impulse circle as it spreads outward from the incident point. Integration around the spreading circle must take into account antenna gain at each point.

Figure (K-1) shows ground plane geometry for the off-vertical case.

By cosine-law: (see Figure)

$$R_b^2 = R_C^2 + R^2 - 2R_c R \cos \phi \qquad \text{(K-1)}$$

From satellite-to-ground geometry:

$$\theta_b = \frac{R_b}{h} = \text{angle of element area off beam center} \qquad \text{(K-2)}$$

$$\theta_v = \frac{R}{h} = \text{angle of element area off vertical} \qquad \text{(K-3)}$$

$$\theta_c = \frac{R_c}{h} = \text{angle of beam center off vertical} \qquad \text{(K-4)}$$

Substituting into the cosine law equation gives:

$$\theta_b^2 = \left(\frac{R_b}{h}\right)^2 = \left(\frac{R}{h}\right)^2 + \left(\frac{R_c}{h}\right)^2 - 2 \frac{R}{h} \frac{R_c}{h} \cos \phi \qquad \text{(K-5)}$$

$$= \theta_v^2 + \theta_c^2 - 2\theta_v \theta_c \cos \phi$$

The element angle θ_v is known vs. time thus:

$$\theta_v = \sqrt{\frac{ct}{h}} \qquad \text{(K-6)}$$

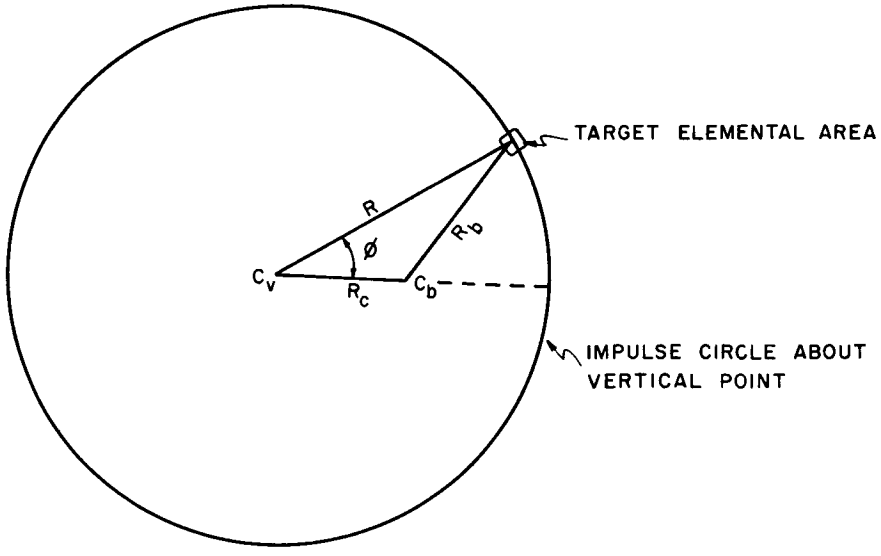

Figure K-1 Off-Vertical Geometry

C_v = Vertical Incidence Point (1st Contact)

C_b = Beam Center

R_c = Ground Displacement of Beam Center from Vertical Point C_v.

R_b = Ground Displacement of target element from Beam Center

R = Ground Displacement of target element from Vertical Point

ϕ = Angular Displacement of target element from Beam Center

Giving vs. time

$$\theta_b^2(t) = \frac{ct}{h} + \theta_c^2 - 2\theta_c\sqrt{\frac{ct}{h}}\cos\phi \qquad \text{(K-7)}$$

These relations permit a computer program to be specified vs. $\theta_b(t)$ and element angle ϕ. Plots have been obtained of received signal impulse response vs. beam off-vertical angle θ_c and are shown in Figure K-2.

The time scale has been compressed logrithmically to show detail in the first 100 ns of the pulse while retaining general curvature information out to 10 microseconds. The top curve for the vertical case (θ_c=0) would be the decaying exponential shown in Figure A-4. As the beam becomes progressively more mis-oriented with respect to vertical the impulse response becomes more flattened in the first 100 ns region, reaching optimum flatness for about 1^o mis-orientation. At this angle the target appears as an ideal integrator over the flat region extending out to about 500 ns. Very small altitude errors vs misorientation result because of the small change in waveform over the first 50 ns pulse duration.

At extreme mis-orientation such as 2^o and 3^o the signal amplitudes are much reduced at vertical but tend to increase as the pulse passes out toward the toe of the beam. Even at these extreme angles, the curves are flat during the first 50 ns of pulse length and should introduce very small errors from a waveform aspect. The reduction in amplitude is the major effect, and in extreme cases may introduce S/N errors.

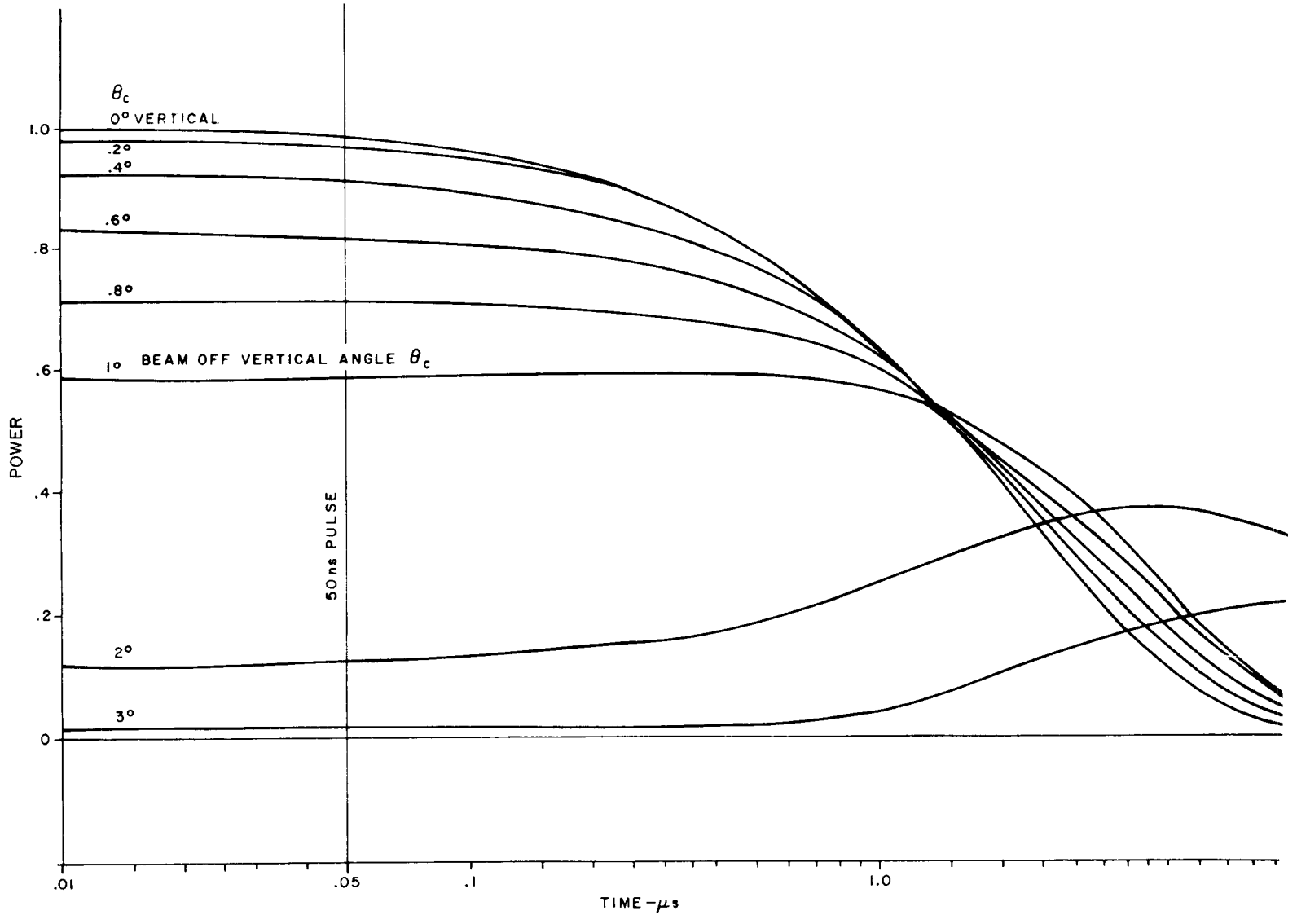

Figure K-2 Impulse Response vs. Beam Angle Off-Vertical (θ)

APPENDIX R-L

SOME RADAR SIGNAL PROCESSING CONSIDERATIONS FOR SPACE GEODESY ALTIMETERS

(David K. Barton, Author)

L.1 INTRODUCTION*

This Appendix describes some radar signal processing considerations associated with problems of radar altimetry from a spacecraft to the Earth's oceans. David K. Barton's approach begins with some ideal concepts which are the necessary steps used in building a more practical approach. These ideals consider infinitely short pulses, infinitely narrow antenna beamwidths and ideally matched transmitter waveforms versus receiver bandwidths and sea state spectra. In arriving at more practical solutions, S/N requirements for coherent versus non-coherent designs are discussed briefly. Some guidelines for practical system designs are presented.

The need for further data regarding impulse response is inferred in Paragraph L.4 and is discussed in Appendix R-G of this report. It may also be noted that the use of a variable, maybe adaptive, transmitted waveform which matches pulsewidth to sea state has been considered impractical at this time.

L.2 SUMMARY

The basic process of radar altitude measurement over a rough sea surface is investigated, and error estimates are made as a function of wave height and radar resolution. Applicability of Doppler processing and pulse compression is considered briefly. Measurements to a few

*Introduction by E. Weiss

a. Height distribution of projected surface area (also approximate power distribution for high angular resolution with impulse)

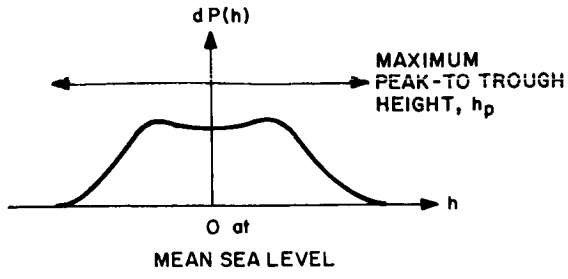

b. Average signal power envelope, $\tau c/2 \ll hp$, high angular resolution

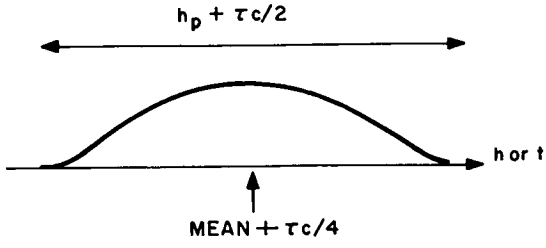

c. Average signal power envelope, $\tau c/2 > hp$, high angular resolution

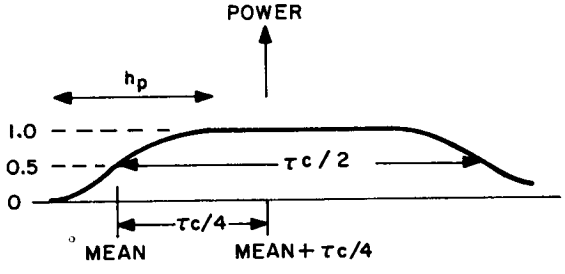

d. Illuminated area vs range for wide beam, smooth sea

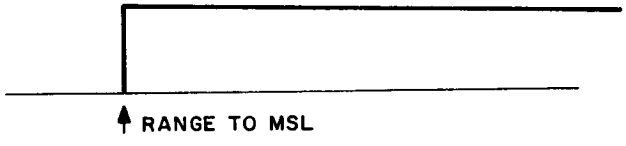

e. Average signal power envelope, $\tau c/2 > hp$, wide beam

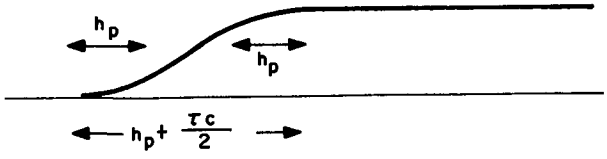

Figure L-1 Altimeter Signal Envelopes

percent of the peak wave height should be possible, if the distribution of radar cross section is close enough to the distribution of actual surface area.

L.3 IDEAL RADAR PROCESS

The most accurate radar for measurement of sea level would use a beam so narrow that small portions of each wave would be resolved and measured separately. With such a radar, transmitting a series of impulses, point-by-point measurements of height would be obtained over any desired line or area, and the height distribution of Figure L.1 could be obtained. Since the small areas represented by each point would be given equal weight, a simple averaging process would yield msl, regardless of shape and symmetry of the distribution or of reflectivity variations. Such very high resolution, which has been obtained in ground-based and low-altitude airborne equipment, is clearly unfeasible for satellite use.

L.4 REDUCED (BUT HIGH) ANGULAR RESOLUTION

As a first step toward a practical system, let us consider an angular resolution element which includes several complete waves in one dimension, with the height of each wave varying along the crest in the other dimension. The surface elements contributing to the total echo would then represent a fair sample of the height distribution, Figure L-1a. The echo power, averaged over a large number of observations, would be distributed in range in much the same way as Figure L-1a but the distribution might be distorted if the capillary wave structure were not rough enough to scatter power uniformly over an angular sector broader than the slope variation of the major waves. Hopefully, the distortion would be either small or symmetrical about msl.

The curve of Figure L-1a could not be considered a "waveform," because the echo power observed on any sweep would vary randomly, with no correlation between samples spaced by the impulse width. If a large number of sweeps were added (integrated), after square-law detection, Figure L-1a would be approximated, subject to residual noise and the distortion mentioned above.

L.5 HIGH ANGULAR RESOLUTION, RECTANGULAR PULSE

Now let us increase the pulsewidth to a more practical value. The average echo power envelope will be the convolution of the pulse waveform with Figure L-1a, shown in Figure L-1b for a short pulse and Figure L-1c for a long pulse. For a pulsewidth which exceeds the maximum wave height, the leading edge of the power envelope follows the integral of the height distribution. The derivative of the power envelope can be used to reproduce the distribution, and the 50 percent point on the leading edge of the power envelope indicates msl. Again, Figure L-1b and L-1c are not waveforms but mean values of an ensemble of random (exponentially-distributed) functions whose autocorrelation function drops linearly to zero over one pulsewidth. During the leading and trailing edges of each received pulse, more rapid fluctuations take place because the correlation time in those regions cannot exceed the amount of overlap between the pulse and the height distribution. The first derivative of each received pulse is a noiselike function whose autocorrelation function is an impulse, at least until it has passed through a receiver filter of finite bandwidth.

L.6 LOW ANGULAR RESOLUTION

Now we consider the echoes received from an antenna which illuminates a large area of the sea, such that the echoes from the edge of the beam are delayed by several pulsewidths. The functions of Figure L-1a - L-1c are now convolved with a step function which decays only slightly during a period equal to the pulsewidth, Figure L-1d. Figure L-1e shows the resulting signal power envelope, approximately following the integral of Figure L-1c. The only recognizable feature of this envelope is the half-power point on the leading edge, which occurs when the center of the pulse coincides with msl. The autocorrelation function of each received waveform in this envelope is that of the transmitted pulse, and the autocorrelation function of its first derivative is an impulse, modified by the receiving filter weighting function.

L.7 PROCESSING AND MEASUREMENT

The envelope functions of Figure L-1 and the autocorrelation functions of the waveforms which contribute to each envelope, dictate the possible processing methods. Considering Figure L-1e, we can expect to measure the time of the half-power point on the leading edge with an accuracy which depends on the slope, the number of independent waveforms averaged, and the signal-to-thermal-noise ratio. The ratio of fluctuation power to mean power at each point in the signal waveform is fixed by the exponential distribution.

The slope is maximized by reducing pulsewidth toward zero, but this degrades S/N ratio. The optimum accuracy is obtained when the receiver is approximately matched to the transmitted pulse, and the width of the resulting radar response function is approximately matched to the width of the height distribution ($B\tau \tilde{=} 1$, $\tau c \tilde{=} h_p$). Figure L-2 shows the resulting signal and noise envelopes and functions. A block diagram is shown in Figure L-3. The gates are used to sample and weight a large number of waveforms, producing a null when the center gate is aligned with the half-power point of the signal envelope. The average output, averaged over a sufficiently long period, is independent of any constant noise level because the gates have equal positive and negative weighting. The location of the center null is independent of signal amplitude because the double weighting of the center gate balances the single weighting of the last gate for any signal. The two end gates are made longer than the center gate to minimize the errors from noise and signal fluctuation. The center gate will contribute the major noise error, because it takes only one sample of noise and signal on each waveform (each repetition period). The constant noise level will apply for single-pulse S/N ratios $< < 1$. Note that the triple gate is approximately the derivative of a conventional split gate, with the two end gates spread in time to average more noise and signal samples.

a. Height distribution

b. Transmitted pulse

c. Radar response to point target

d. Average signal power envelope for high angular resolution

e. Leading edge of signal power envelope for wide beam

f. Signal and noise power envelope

g. Leading-edge gate function, to be applied to square-law detected output

h. Discriminator response, voltage vs displacement of gate

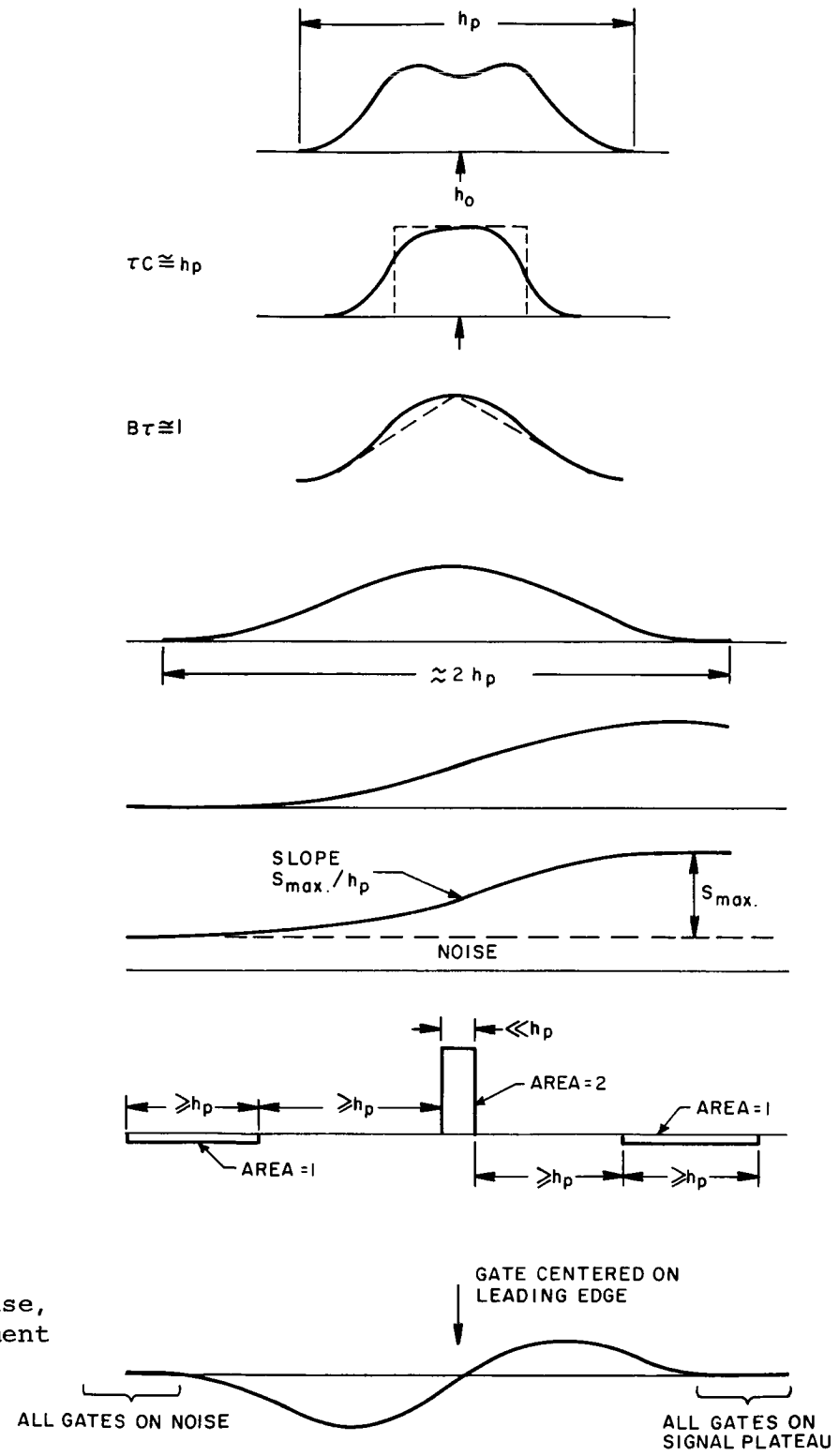

Figure L-2 Measurement Process Functions

L.8 ERROR ANALYSIS

In the absence of thermal noise, there will be an error caused by signal fluctuation. Each detected sample will contribute to the mean, and will also have a random component whose rms value equals the mean. The sum of n_ϵ independent samples will have a mean value S_{max} proportional to n_ϵ, and a standard deviation proportional to $\sqrt{n_\epsilon}$. Thus, the ratio of mean signal to rms random signal after averaging n_ϵ independent samples will equal $\sqrt{n_\epsilon}$, and the corresponding rms height error component will be $\approx h_p \sqrt{n_\epsilon}$. The number of independent samples available per second will be proportional to the square root of the range resolution width. For example, if the radar response is matched to h_p, as in Figure L-2 the surface within a radius

$$r \tilde{=} \sqrt{2\, h_o\, h_p}$$

will contribute to the echo, and the effective width of the Doppler spectrum will be

$$\Delta f \tilde{=} \frac{2\, v\, r}{\lambda\, h_o} = \frac{2\, v}{\lambda} \sqrt{\frac{2\, h_p}{h_o}}$$

The number of independent samples gathered per second for a satellite velocity v = 7000 m/sec at an altitude $h_o = 1.5 \times 10^6$ m with a radar wavelength $\lambda = 0.03$ m and a peak wave height $h_p = 6$ m will be

$$n_\epsilon \tilde{=} \Delta f \tilde{=} \frac{2 \times 7000}{0.03} \sqrt{\frac{2 \times 6}{1.5 \times 10^6}} = 1320$$

The minimum rms error caused by signal fluctuation for the matched system, will be

$$\sigma_h \tilde{=} \frac{h_p}{\sqrt{n_\epsilon}} \tilde{=} \frac{6}{\sqrt{1320}} = 0.16 \text{ m}$$

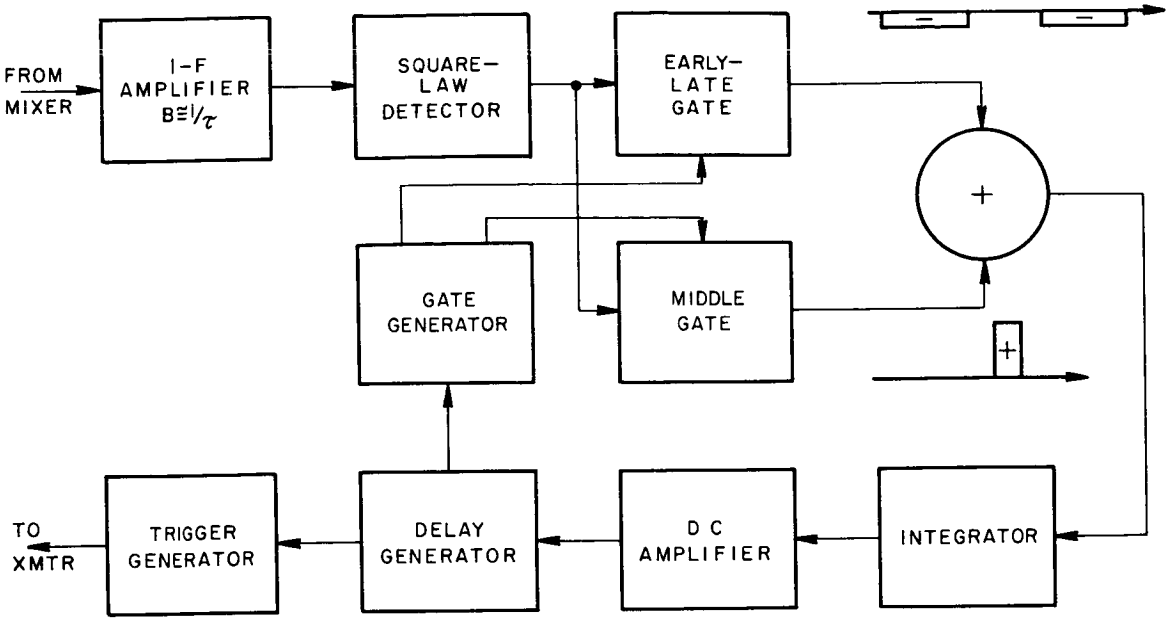

Figure L-3 Block Diagram of Leading-Edge Tracker

for an average taken over one second (7000 m travel over the surface) with at least 1320 incoherent samples.

The thermal noise error can be calculated approximately from

$$\sigma_h \tilde{=} \frac{2\, h_p}{(S/N)\sqrt{n}} \qquad (S/N \ll 1$$

where S/N is the maximum signal-to-noise power ratio per pulse and n is the number of pulses averaged. In one second, $n = f_r$, the pulse repetition frequency. For example, if S/N = 0.1, we must use f_r = 560 kHz to hold $\sigma_h < 0.16$ m. This suggests that a higher S/N ratio is required for high accuracy, leading to distortion of the S + N envelope function in the detector. For $\sigma_h \tilde{=} 1$ m, f_r = 16 kHz would be sufficient, using the matched system. If the pulse is broadened beyond h_p and bandwidth is matched to pulsewidth, the slope will be decreased (as the leading edge of Figure L-2e is broadened). The Doppler spread and n_ϵ will also increase, n_ϵ varying with the square root of τ. Fluctuation error will

increase approximately with the 3/4 power of pulsewidth. Thermal noise error will remain essentially constant, as long as $S/N < 1$, and will then increase as the square root of pulsewidth for very long pulses (where $\sqrt{S/N}$ appears in the denominator).

L.9 COHERENT PROCESSING

The difficulty in obtaining adequate S/N ratio with the pulsewidth matched to wave height leads to consideration of coherent processing. As long as the predetection bandwidth B_c exceeds the Doppler spread Δ_f, there will be a gain in effective S/N ratio and no significant reduction in n_ϵ. The envelope functions shown in Figures L-1 and L-2, however, do not apply after coherent detection. This is because the phase becomes decorrelated after approximately one pulsewidth (and its first derivative has an impulse as its autocorrelation function). Hence, if we are to locate the half-power point of the signal envelope, we must use two phase detectors with independent reference signals, one gated at the midpoint of the leading edge and the second in the region of maximum response. Because the phase detector output is a linear function of signal voltage, the weighting ratio of the central gate should be 1.4 to 1 rather than 2 to 1, compared to the end gates.

The accuracy attainable with a matched system should be in the order of

$$\sigma_h \simeq \frac{2\,h_p}{\sqrt{(S/N)_c\, B_c\, t_o}} = \frac{2\,h_p}{\sqrt{E/N_o}} \qquad (S/N_c) > 1$$

where $(S/N)_c$ is the signal-to-noise ratio after Doppler filtering to the bandwidth $B_c > 1320$ Hz, t_o is the observation interval, and E/N_o is the energy ratio in that interval. The error has a lower limit of 0.16 m in one second (set by signal fluctuation, see Paragraph L.8). As the pulse is broadened, the error will increase approximately as the square root of pulsewidth. For $(S/N)_c < 10$, there may be an appreciable error caused by phase noise in the reference signal to the coherent detector.

L.10 PULSE COMPRESSION

As an alternative to Doppler processing, pulse compression offers a second means of narrowing the radar resolution cell without sacrificing signal energy or using excessive peak power. Ideally, the compressed pulse would have all the desirable characteristics of a narrow rectangular pulse of increased peak power, so that thermal noise limitations could be avoided with a pulse matched to the wave height distribution. In practice, however, the integrated power in all sidelobes beyond the main response will be added to the signal during the leading edge, causing a shift of this waveform toward the left (Figure L-2e). This shift may not be entirely predictable, since the sidelobe response may extend well beyond the flat portion of the widebeam antenna response. Even with this possible error, pulse compression should definitely be considered.

L.11 CONCLUSIONS

a. Extraction of data on altitude above msl is possible in a widebeam radar system using leading-edge ranging techniques.

b. The leading-edge differentiation could be performed by averaging the received signal and noise power in gates, to avoid large values of the time derivatives of individual waveforms.

c. For best accuracy, the radar receiver should be matched to the pulse spectrum, and the resulting range response matched to the wave height distribution. A large number of noncoherent samples should be averaged to minimize effects of signal fluctuation.

d. Doppler processing or pulse compression can be used to reduce peak power requirements, but the details of instrumentation must take into account the random nature of the signal and the effects of the long signal envelope.

e. Accuracies approaching three percent of the peak wave height should be approached, if the S/N ratio and number of samples are sufficient, and if the detector characteristics can be controlled and calibrated.

f. Since the radar of limited angular resolution must average the altitude above a surface weighted in accordance with radar reflectivity, an additional error of a few percent may be caused by differing asymmetries in distributions of surface height and cross section.

APPENDIX R–M

SYSTEM REQUIREMENTS VS ANTENNA DIAMETER

Antenna diameter recommendations reflect considerations of such factors as antenna mounting convenience and attitude stabilization accuracy requirements, both of which favor small antennas, as opposed to system power requirements, which favor larger antennas.

Tradeoffs in transmitter peak power, system power and antenna attitude stabilization requirements versus antenna size are shown in Figure M-1. The proposed .75m (2.5 ft.) diameter antenna implies a structually mounted slotted array and 0.3 degrees attitude stabilization accuracy. Pulse peak transmitter power of 1 kW and a total system power of 200 W are also assumed.

Pulse peak power decreases as the fourth power of antenna diameter. Corresponding total altimeter system power decreases at a slower rate partly because of receiver, processor, and altitude counting, storage power requirements (which remain unchanged), and also because of transmitter, modulator, and source power requirements that vary more slowly than radiated power requirements.

Increasing antenna diameter from 2.5 ft. to 5 ft. reduces total altimeter system power from 200 W to about 70 W. With an 8 ft. diameter antenna, system power is about 40 W.

The larger antenna diameters can be obtained either by using satellites that are structurally larger, or by resorting to folded, collapsible, or furlable designs that are basically more complex, heavier, and larger in volume than the proposed antenna. They should be considered feasible, however, especially if system power considerations indicate such a need.

Still further power reductions might be achieved at the cost of slight degradation in altitude accuracy. Some substantial saving may be possible by using less phase tracking power than has been recommended, giving somewhat increased clutter error. Since this clutter error is presently rather small, further power reductions may be possible while introducing almost negligible degradation in overall accuracy. More extensive analysis would be necessary to estimate more precisely the power reduction that might be tolerated for phase tracking.

Further work on power reduction is indicated during the hardware design phase, when satellite system constraints (such as power and attitude stabilization) are brought into focus.

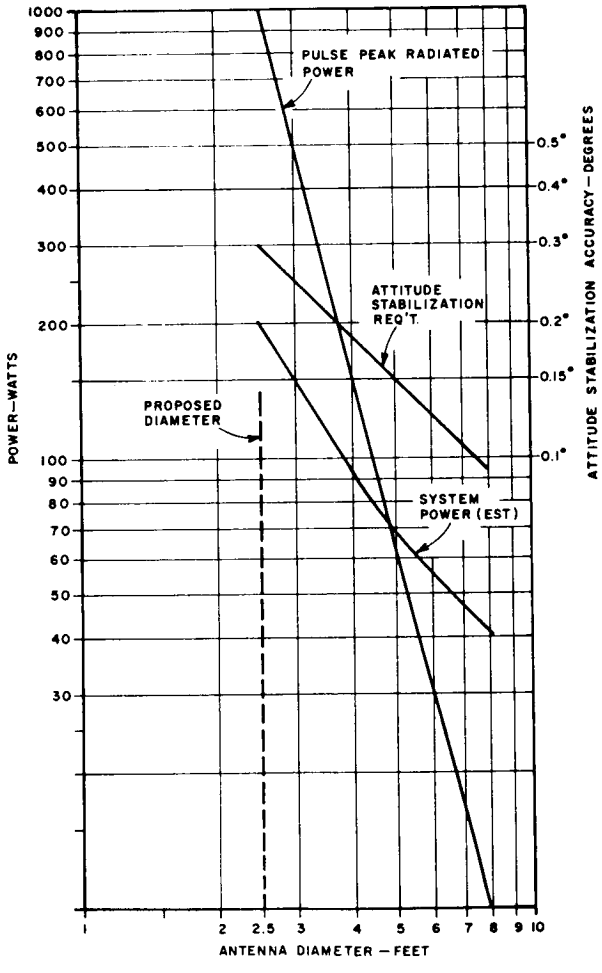

Figure M-1 Tradeoffs in Transmitter Peak Power, System Power and Antenna Attitude Stabilization Requirements vs Antenna Size

RADAR REFERENCES

1. M. Skolnik: Introduction to Radar Systems.McGraw-Hill Co.,Inc.,1962.

2. D. Barton: Radar System Analysis. Prentice-Hall, Inc., 1965.

3. Frey, Harrington & Von Arx: A Study of Satellite Altimetry for Geophysical and Oceanographic Measurement.

4. S. Valley: Handbook of Geophysics and Space Environments, Air Force Cambridge Research Laboratories. McGraw-Hill Co.,Inc.,1965.

5. Report on Nanosecond Pulse Propagation Over Line-of-Sight Paths TM-IERTM-ITSA92: October 1967. Institute for Environmental Research, Institute for Telecommunications Science, Boulder, Colorado.

6. F.T. Barath: Microwave Radiometry and Applications to Oceanography. Woods Hole Oceanographic Institute, Reference No. 65-10, 1965, Woods Hole, Massachusetts.

7. W. Conway and A. Mardon: Microwave Radiometers for Ocean and Weather Measurements. Ibid.

8. R.K. Moore and C.S. Williams, Jr.: Radar Terrain Return at Near Vertical Incidence, Proc. IRE Vol. 45, pg. 228, February 1957.

9. Marsh: Sea Wave Distortion of Altimeter Pulses. Marine Research Lab., Submarine Signal Division, Raytheon Co., 1968.

10. C. Cook and M. Bernfeld: Radar Signals. Academic Press, 1967.

11. F. C. MacDonald: Radar Sea Clutter and Ocean Wave Spectra (Prentice-Hall Inc. Englewood Cliffs, New Jersey)., 1960.

12. E.M.I. Electronics, Report #DP1025: Radar Sea Clutter. Astia Document 328919 Hayes, Middlesex England, August 1961

13. Auburn Research Foundation: The Study of Radar Reflectivity of Sea Water at Vertical Incidence. Auburn University,June 1962.

RADAR REFERENCES (CONTINUED)

14. E.A. Wolff: A Review of Theories and Measurements of Radar Ground Return.
Astia Document 235972. Airforce Cambridge Research Center, Bedford, Massachusetts, February 1960.

15. Space Geodesy Altimetry Study: Monthly Progress Report for May 1968; NASA Contract NASW-1709.

16. B. Kinsman: Wind Waves. Prentice-Hall, Inc., 1965.

17. T. W. Godbey: Oceanographic Satellite Radar Altimeter and Wind Sea Sensor, in Oceanography from Space, Ref. No. 65-10, Woods Hole Oceanographic Institution, Woods Hole, Mass.; April, 1965